



University  
of Glasgow

Lewis, Emily Elizabeth Louise (2016) *Modelling the mesenchymal stem cell niche in vitro using magnetic nanoparticles*. PhD thesis.

<http://theses.gla.ac.uk/7243/>

Copyright and moral rights for this thesis are retained by the author

A copy can be downloaded for personal non-commercial research or study

This thesis cannot be reproduced or quoted extensively from without first obtaining permission in writing from the Author

The content must not be changed in any way or sold commercially in any format or medium without the formal permission of the Author

When referring to this work, full bibliographic details including the author, title, awarding institution and date of the thesis must be given

# **MODELLING THE MESENCHYMAL STEM CELL NICHE *IN VITRO* USING MAGNETIC NANOPARTICLES**

Emily Elizabeth Louise Lewis

(MChem, MRes)



University  
of Glasgow

**Submitted in fulfilment of requirements for the degree of Doctor of Philosophy  
(PhD)**

**Centre for Cell Engineering  
Institute of Molecular, Cell and Systems Biology  
School of Medical, Veterinary and Life Sciences  
University of Glasgow  
Glasgow, G12 8QQ  
January 2016**

## Abstract

Mesenchymal stem cells (MSCs) are multipotent stem cells residing within the bone marrow, with the ability to differentiate into cells of mesodermic origin (e.g. bone, cartilage and fat). These cells also possess extensive immunomodulatory and wound healing properties. Therefore, MSCs have multiple applications in the field of regenerative medicine. However, present day culturing techniques, encourage a loss of multipotency and limit the availability of true MSCs, for research and clinical use. A culturing technique, which is able to sustain multipotent and quiescent MSCs, is therefore required for future use.

MSCs reside within a unique microenvironment in the bone marrow, termed the niche, which protects and regulates stem cell homeostasis. The niche environment controls maintenance, proliferation and differentiation of the stem cells. Current research is focused on the creation of an *in vitro* niche model, to study the regulatory mechanisms, which govern stem cell fate. The majority of existing models use traditional two-dimensional (2D) techniques. However, stem cells cultured by this method are known to lose potency and spontaneously differentiate into undesired cell types. These issues are caused by 2D *in vitro* niche models lacking the complexity and the three-dimensional (3D) nature, of the native *in vivo* niche. Therefore, in the last few years, research has moved away from 2D models, towards creating 3D *in vitro* niche models.

This project aimed to develop a novel, bio-responsive *in vitro* 3D MSC niche model. The methodology adopted the use of magnetic nanoparticle loaded MSCs, which were levitated using an external magnetic field, to form multicellular spheroids which were subsequently located within a Type I collagen gel. The MSCs within the spheroid niche model exhibited native niche behaviour (retention of multipotency and quiescence). Furthermore, in the presence of a wound, the model accelerated the wound healing process. The MSCs directionally migrated out of the niche towards the wound site and start differentiating into the local resident cell type. Further investigation, identified IL-6 as a potential MSC migratory signal in this bio-response.

# Table of Contents

<b>Abstract.....</b>	<b>2</b>
<b>List of Tables.....</b>	<b>8</b>
<b>List of Figures .....</b>	<b>9</b>
<b>Acknowledgement.....</b>	<b>12</b>
<b>Author’s Declaration.....</b>	<b>13</b>
<b>Abstract and Publications .....</b>	<b>14</b>
<b>Conference Proceedings .....</b>	<b>14</b>
<b>Definitions/Abbreviations.....</b>	<b>15</b>
<b>1 General Introduction:.....</b>	<b>19</b>
<b>1.1 Stem Cells.....</b>	<b>19</b>
<b>1.2 Mesenchymal Stem Cells.....</b>	<b>23</b>
1.2.1 MSC Characteristic Properties .....	25
1.2.2 Immunomodulatory Properties .....	28
<b>1.3 MSCs in Regenerative Medicine .....</b>	<b>30</b>
<b>1.4 Stem cell niche.....</b>	<b>33</b>
1.4.1 Cellular Communication.....	36
1.4.2 Cell cycle.....	37
1.4.3 MSC migration from the niche.....	38
<b>1.5 Exploitation of the stem cell niche .....</b>	<b>40</b>
<b>1.6 <i>In vitro</i> studies of the stem cell niche .....</b>	<b>42</b>
1.6.1 Two-dimensional stem cell niche models.....	42
1.6.2 Three-dimensional stem cell multicellular spheroid niche models.....	44
<b>1.7 <i>In vivo</i> studies of the stem cell niche .....</b>	<b>51</b>
<b>1.8 Magnetic Nanoparticles .....</b>	<b>51</b>
1.8.1 Cellular uptake and intracellular processing of mNPs.....	53
1.8.2 Nanotoxicology .....	54
<b>1.9 Aims and Objectives .....</b>	<b>55</b>
<b>2 Materials and methods .....</b>	<b>59</b>

<b>2.1</b>	<b>Cell Culture Solutions</b> .....	<b>62</b>
<b>2.2</b>	<b>Cell Culture</b> .....	<b>64</b>
2.2.1	General Protocol .....	64
2.2.2	Bone Marrow extraction .....	64
2.2.3	CD271 positive selection from bone marrow extracts .....	65
<b>2.3</b>	<b>Cell Culturing Methods</b> .....	<b>65</b>
2.3.1	Optimising Magnetic Nanoparticle Uptake into Cells.....	65
2.3.2	Type I collagen gel formation.....	66
2.3.3	Monolayer Culture .....	66
2.3.4	Spheroid Culture .....	67
<b>2.4</b>	<b>Statistical Analysis</b> .....	<b>67</b>
<b>2.5</b>	<b>Research colleagues</b> .....	<b>67</b>
<b>3</b>	<b>The Development of an <i>In vitro</i> Mesenchymal Stem Cell Niche Model</b> .....	<b>70</b>
<b>3.1</b>	<b>Introduction</b> .....	<b>70</b>
3.1.1	The Bone Marrow Niche Microenvironment.....	70
3.1.2	3D <i>In Vitro</i> Bone Marrow Niche Models.....	70
<b>3.2</b>	<b>Objectives</b> .....	<b>72</b>
<b>3.3</b>	<b>Materials and Methods</b> .....	<b>73</b>
3.3.1	Cell culture and Magnetic Nanoparticle Incubation .....	73
3.3.2	Magnetic Nanoparticle Uptake into MSCs.....	73
3.3.3	Observing Cells via Fluorescence Microscopy .....	74
3.3.4	Rheology analysis of the gels .....	76
3.3.5	Induced differentiation of MSCs via osteogenesis and adipogenesis .....	76
3.3.6	RNA isolation .....	78
3.3.7	Fluidigm preparation.....	79
<b>3.4</b>	<b>Results</b> .....	<b>83</b>
3.4.1	Niche Model Development: Stage 1 .....	83
	Optimising the mNPs Loading Conditions of the MSCs. ....	83
3.4.2	Niche Model Development: Stage 2 .....	88
	Assessing mNP Retention Within MSCs Following Trypsinisation.....	88
3.4.3	Niche Model Development: Stage 3 .....	91
	Assessing mNP-loaded MSC Response to an External Magnetic Field in Monolayer. ....	91
3.4.4	Niche Model Development: Stage 4: .....	92

Assessing mNP-loaded MSC Viability and Phenotype in Monolayer Culture and 3D Spheroid Culture. ....	92
3.4.5 Niche Model Development: Stage 5 .....	98
Assessing the Formation of a MSC Spheroid Within a Collagen Gel. ....	98
3.4.6 Niche Model Development: Stage 6 .....	104
Assessing the Collagen Gel Stiffness (with and without spheroids). ....	104
3.4.7 Niche Model Development: Stage 7 .....	107
Assessing MSC Proliferation and Cell Cycle Gene Expression in Monolayer and Spheroid Culture Systems. ....	107
3.4.8 Niche Model Development: Stage 8 .....	111
Assessing MSC Differentiation Potential in Monolayer and Spheroid Culture Systems. ....	111
<b>3.5 Discussion.....</b>	<b>114</b>
3.5.1 Niche Model Development: Stage 1 .....	114
Optimising the mNPs Loading Conditions of the MSCs. ....	114
3.5.2 Niche Model Development: Stage 2 .....	115
Assessing mNP Retention Within MSCs Following Trypsinisation.....	115
3.5.3 Niche Model Development: Stage 3 .....	117
Assessing mNP-loaded MSC Response to an External Magnetic Field in Monolayer. ....	117
3.5.4 Niche Model Development: Stage 4: .....	119
Assessing mNP-loaded MSC Viability and Phenotype in Monolayer Culture and 3D Spheroid Culture. ....	119
3.5.5 Niche Model Development: Stage 5 .....	122
Assessing the Formation of a MSC Spheroid Within a Collagen Gel. ....	122
3.5.6 Niche Model Development: Stage 6 .....	123
Verifying the Collagen Gel Stiffness (with and without spheroids). ....	123
3.5.7 Niche Model Development: Stage 7 .....	125
Assessing MSC Proliferation and Cell Cycle Gene Expression in Monolayer and Spheroid Culture Systems. ....	125
3.5.8 Niche Model Development: Stage 8 .....	129
Assessing MSC Differentiation Properties in Monolayer and Spheroid Culture Systems. ....	129

3.6	<b>Summary .....</b>	<b>131</b>
<b>4</b>	<b>MSC Spheroid Niche Model Response to Wound Healing .....</b>	<b>134</b>
4.1	<b>General Introduction .....</b>	<b>134</b>
4.2	<b>Objectives.....</b>	<b>135</b>
4.3	<b>Materials and Methods.....</b>	<b>137</b>
4.3.1	Time-lapse assessment of wound healing assays.....	137
4.3.2	Assessing MSC migration from a spheroid niche in response to an artificial wound. ....	137
4.3.3	MSC differentiation assessment post migration from the spheroid niche to wound site.....	138
4.4	<b>Results.....</b>	<b>142</b>
4.4.1	Time-lapse assessment of wound healing assays.....	142
4.4.2	Assessing MSC migration from a spheroid niche, in response to an artificial wound. ....	144
4.4.3	MSC differentiation assessment post migration from spheroid niche to wound site.....	149
4.5	<b>Discussion.....</b>	<b>156</b>
4.5.1	Time lapse assessment of wound healing assays. ....	156
4.5.2	Assessing MSC migration from a spheroid niche in response to an artificial wound	158
4.5.3	MSC differentiation assessment post migration from spheroid niche to wound site.....	162
4.6	<b>Summary .....</b>	<b>165</b>
<b>5</b>	<b>Assessment of paracrine cell signalling within the induced MSC spheroid niche .</b>	<b>168</b>
5.1	<b>General Introduction .....</b>	<b>168</b>
5.2	<b>Objectives.....</b>	<b>169</b>
5.3	<b>Materials and Methods.....</b>	<b>171</b>
5.3.1	Cytokine Analysis .....	171
5.3.2	IL-6 Addition assay .....	172
5.4	<b>Results.....</b>	<b>173</b>
5.4.1	Identification of cytokine secretion from scratched models.....	173
5.4.2	MSC niche model response to IL-6. ....	174
5.5	<b>Discussion.....</b>	<b>177</b>

5.5.1	Identification of cytokine secretion from scratched models.....	177
5.5.2	MSC niche model response to IL-6. ....	179
<b>5.6</b>	<b>Summary .....</b>	<b>182</b>
<b>6</b>	<b>Concluding remarks: MSC <i>in vitro</i> niche model .....</b>	<b>184</b>
<b>6.1</b>	<b>General Discussion.....</b>	<b>184</b>
<b>6.2</b>	<b><i>In vitro</i> niche models compared to <i>in vivo</i> niche behaviours .....</b>	<b>185</b>
<b>6.3</b>	<b>Applications of the MSC spheroid niche model.....</b>	<b>186</b>
6.3.1	MSC regulation within the niche.....	186
6.3.2	Creation of a MSC bank.....	188
6.3.3	Modelling disease states.....	188
6.3.4	Scar healing .....	190
6.3.5	Aging of the MSC niche .....	190
6.3.6	Pharmacology Assessments.....	191
<b>6.4</b>	<b>Conclusion .....</b>	<b>193</b>
6.4.1	Recommendation for Future work .....	194
	<b>References: .....</b>	<b>195</b>

## List of Tables

Table 1-1: Characterisation of stem cells with regard to their potency (differentiation potential). .....	20
Table 1-2: The MSC immunophenotype Profile. ....	26
Table 2-1: A List of materials reagents and suppliers used throughout all experiments.....	59
Table 3-1: Thermal cycle conditions used on each sample prior to Fluidigm analysis. ....	79
Table 3-2: Fluidigm primers designed for human genes. ....	80
Table 4-1: Fluidigm primers designed for human genes. ....	139
Table 5-1: Functional classes of selected cytokines. ....	168

## List of Figures

Figure 1-1: Stem cell classification indicating direction of stem cell differentiation potential. ....	21
Figure 1-2: Mesenchymal Stem Cell differentiation. ....	23
Figure 1-3: Schematic diagram of the location of the MSC niche within bone marrow. ....	25
Figure 1-4: Diagram highlighting the immunosuppressive properties of MSCs....	28
Figure 1-5: MSCs examples used in cell therapy and tissue engineering. ....	30
Figure 1-6: Conceptual model of a stem cell niche. ....	34
Figure 1-7: Diagram depicting cell cycle.....	37
Figure 1-8: Mesenchymal stem cell roles in each stage of the wound healing process over time. ....	39
Figure 1-9: Issues to be assessed for successful application of stem cells within regenerative medicine. ....	42
Figure 1-10: Diagram depicting various 3D culturing techniques.....	50
Figure 1-11: Schematic diagram of a partially functionalised mNP. ....	52
Figure 3-1: Schematic diagram of the fluorescent mNPs employed in the project. ....	73
Figure 3-2: Timeline of experimental procedure used to induce differentiation in MSCs with osteogenic and adipogenic media. ....	77
Figure 3-3: Graph of mNP uptake within MSCs analysed using ICP-MS.....	84
Figure 3-4a: Representative fluorescence images of MSCs incubated with mNPs in the presence or absence of a magnetic field. ....	86
Figure 3-4b: Quantitative analysis of the complete immunofluorescent images from Figure 3-3a demonstrating mNP uptake into MSCs. ....	87
Figure 3-5: Representative TEM images of MSCs incubated with mNPs. ....	88
Figure 3-6a: Fluorescence images of MSCs with and without mNPs (for 15, 30 and 60 minutes) following trypsinisation and re-seeding.....	89
Figure 3-6b: Quantitative analysis of complete fluorescent images with and without mNPs (for 15, 30 and 60 minutes) following trypsinisation and re-seeding. ....	90
Figure 3-7: Representative light microscopy image of mNPs residing within MSCs, under optimised pre-loading conditions, following 30 minutes incubation. ....	90

Figure 3-8: Schematic diagram of 6 well plate design with the magnet beneath the well.....	91
Figure 3-9: Monolayer culture of mNP-loaded MSCs cultured for up to 14 days.	93
Figure 3-10: Schematic diagram of 6 well plate design for MSC spheroid formation, with the magnet above the well. ....	94
Figure 3-11: Spheroid culture of MSCs with mNPs incubated for up to 14 days. .	95
Figure 3-12: Quantitative analysis of data collected from immuno-fluorescent images depicted in Figure 3-9 and Figure 3-11, which compared monolayer and spheroid culture conditions. ....	96
Figure 3-13: Box plot depicting the size distribution of a sample of MSC spheroids produced in this thesis. ....	97
Figure 3-14: TEM images of cross-sectioned spheroids highlighting areas between MSCs.....	97
Figure 3-15: Schematic diagram of one of the wells in the 24 well plate design with the magnet below the well.....	98
Figure 3-16: Representative viability images of control MSCs incorporated within a collagen gel.....	99
Figure 3-17: Representative viability images of MSCs pre-loaded with mNPs and incorporated within a collagen gel. ....	100
Figure 3-18: Schematic diagram showing the MSC viability within the gel. ....	100
Figure 3-19: Representative cytoskeleton images of control MSCs incorporated within a collagen gel. ....	101
Figure 3-20: Representative cytoskeleton images of MSCs pre-loaded with mNPs and incorporated within a collagen gel.....	102
Figure 3-21: Schematic diagram showing the MSC cell distribution within the gel. ....	103
Figure 3-22: Schematic diagram of MSC spheroids transplanted into a collagen gel. ....	104
Figure 3-23: Stiffness of collagen gels, with and without spheroids. ....	106
Figure 3-24: Analysis of MSC proliferation via BrdU incorporation within a monolayer and spheroid culture system. ....	108
Figure 3-25: Gene expression analysis of key cell cycle genes from MSCs extracted from spheroid cultures.....	110
Figure 3-26: Outgrowth of MSC monolayer from MSC spheroids. ....	112

Figure 3-27: Microscopy images of induced MSCs with osteogenic and adipogenic media. ....	113
Figure 3-28: Schematic diagram of magnetic field distribution from 350 mT magnet.....	118
Figure 3-29: Table and graph depicting cyclins and cyclin dependent kinase expression involved during the different phases of the MSC cell cycle. ....	126
Figure 4-1: Light microscopy time lapse images assessing the wound healing process.....	143
Figure 4-2: Fibroblast viability assessed over 24 hours, in the presence or absence of a scratch.....	144
Figure 4-3: MSC spheroid niche co-cultured with control (unscratched) fibroblast monolayers assessed over 3 days. ....	145
Figure 4-4: MSC migration from the spheroid niche when co-cultured with scratched fibroblast monolayers, assessed over 3 days. ....	147
Figure 4-5: Wound healing assay assessing the presence of MSC niche models. ....	151
Figure 4-6: High magnification images of MSCs migrating towards a scratched osteoblast monolayer expressing phosphorylated RUNX-2 after 3 days. ....	152
Figure 4-7: Heat map depicting MSC gene expression profiles extracted from the spheroid niche model.....	154
Figure 4-8: Gene expression analysis of MSCs extracted from the spheroid niche model after co-culture with an unscratched and scratched osteoblast monolayer. ....	155
Figure 4-9: Simplified diagram of Notch signalling pathway. ....	160
Figure 4-10: Illustration of MSC migration and homing <i>in vivo</i> . ....	161
Figure 5-1: Quantitative analysis of cytokines secreted, from unscratched and scratched osteoblast monolayer after, 3 hours, 12 hours, 24 hours and 72 hours. ....	173
Figure 5-2: Quantitative analysis of cytokines secreted, from unscratched and scratched fibroblast monolayer after, 3 hours, 12 hours, 24 hours and 72 hours. ....	174
Figure 5-3: Niche model response to IL-6 addition over time.....	176
Figure 5-4: Diagram demonstrating the bone remodelling process. ....	177
Figure 5-5: IL-6 signalling via the gp130/JAK/STAT pathway. ....	180

## Acknowledgement

First of all, I would like to thank my supervisors, Catherine Berry and Matthew Dalby. I would like to take this opportunity to express my sincerest gratitude to Catherine for all the help and positive encouragement over the past three years. I will look back at my time in Glasgow with so many fond memories, which will be mainly down to the fantastic opportunities she has given me. I would also like to thank Matt for all the invaluable help towards the end of the project. Also, I would personally like to thank Helen Wheadon for giving up her precious time to help me with the fluidigm protocol and data collection.

Secondly, I would like to thank all my immediate family, my mother for reading and re-reading this document for grammatical errors (I know my grammar is appalling) and my father for all the phone calls over the 3 years. Your persistent encouragement, support and faith in my ability have kept me going throughout this period. I would like to thank my husband Timothy for understanding what this project has meant to me and for putting up with my fluctuating mood swings!

Thirdly, I would like to thank anyone who has helped me along the way; all help was always very much appreciated and never taken for granted.

## **Author's Declaration**

I hereby declare that the research reported within this thesis is my own work, unless otherwise stated, and that at the time of submission is not being considered elsewhere for any other academic qualification.

Emily Lewis

4th January 2016

## Abstract and Publications

Publications authored by the candidate on conducted research relating to this thesis.

Lewis EEL, Child HW, Hursthouse AS, Stirling D, Mullen M, Paterson D, McCully M, Berry CC: The Influence of Particle Size and Static Magnetic Fields on the Uptake of Magnetic Nanoparticles into Three Dimensional Cell-Seeded Collagen Gel Cultures. *Journal of Biomedical Materials Research Part B: Applied Biomaterials*. (2014)

## Conference Proceedings

**2013 TCES** “Modelling the mesenchymal stem cell niche *in vitro* using magnetic nanoparticles”. Cardiff, UK (poster presentation)

**2013 DTC in Proteomic and Cell Technologies Symposium** “Modelling the mesenchymal stem cell niche *in vitro* using magnetic nanoparticles”. Glasgow, UK (oral presentation)

**2014 TCES** “Development of mesenchymal stem cell niche *in vitro* using magnetic nanoparticles”. Newcastle, UK (poster presentation - runner up for best poster competition)

**2015 Stem cells: from basic research to bioprocessing** “Novel 3D bio-responsive mesenchymal stem cell niche model”. London, UK (oral presentation)

## Definitions/Abbreviations

2D	Two-dimensional
3D	Three-dimensional
µg	Microgram
µL	Microlitre
mL	Millilitre
α-MEM	Alpha minimal essential media
ANOVA	Analysis of variance
BMP	Bone morphogenetic protein
BrdU	5-bromo-2-deoxyuridine
BSA	Bovine serum albumin
CCL	Chemokine ligand
CCN	Cyclin
CDK	Cyclin dependent kinase
CDKI	Cyclin dependent kinase inhibitor
CNS	Central nervous system
cDNA	cDNA complementary deoxyribose nucleic acid
CO <sub>2</sub>	carbon dioxide
cRNA	complementary ribonucleic acid
CXCR	chemokine receptor
CXCL12	stromal-derived factor-1
DAPI	4'-6-Diamidino-2-phenylindole
DAMPs	damaged or associated molecule patterns
DC	Dendritic cells
DMEM	Dulbecco's modified eagle medium
DNA	deoxyribose nucleic acid
ECM	extracellular matrix
EDTA	ethylenediaminetetraacetic acid
EGF	Epidermal growth factor
ESC	embryonic stem cell
FBS	foetal bovine serum
FAK	focal adhesion kinase

FITC	fluorescein isothiocyanate
g	acceleration due to gravity
G'	elastic modulus
G''	viscous modulus
G <sub>0</sub>	quiescent phase
G <sub>1</sub>	GAP phase 1
G <sub>2</sub>	GAP phase 2
HEPES	4-(2-hydroxyethyl)-1-piperazineethanesulfonic acid
HFSCs	hair follicle stem cells
HGF	Hepatocyte growth factor
HIMF	hypoxia-induced mitogenic factor
HSC	hematopoietic stem cell
h-TERTs	Infinity telomerase-immortalised primary human fibroblasts
Hz	Hertz
ICP-MS	inductively coupled plasma-mass spectrometry
IDO	indoleamine 2,3-dioxygenase
IGF-1	insulin-like growth factor-1
IL-6	interleukin-6
INF- $\gamma$	interferon gamma
iPSC	induced pluripotent stem cell
IV	Intravenously
KCl	potassium chloride
kPa	Kilopascal
kV	kilovolt
Mols	Mols
M phase	mitosis phase
MHC	major histocompatibility complex
MMP	matrix metalloproteinase
mNP	magnetic nanoparticle
MuSCs	muscle stem cells
MS	multiple sclerosis
MSC	mesenchymal stem cell

MRI	magnetic resonance imaging
mT	Militesla
NaCl	sodium chloride
NaOH	sodium hydroxide
NK	natural killer
NP	Nanoparticle
PBS	phosphate buffered saline
PCR	polymerase chain reaction
PDGF	platelet-derived growth factor
PEA	poly(ester amide)
PEG	polyethylene glycol
PGE2	prostaglandin E2
PI3K	phosphoinositide 3-kinase
PPAR- $\gamma$	peroxisome proliferator-activated receptor-gamma
PPRs	pattern recognition receptors
p-value	probability value
Rb	retinoblastoma protein
RNA	ribonucleic acid
R point	restriction point
Rpm	revolutions per minute
SDS	sodium dodecyl sulphate
S-phase	synthesis-phase
SPIO	superparamagnetic iron oxide
TEM	transmission electron microscopy
TGF- $\beta$ 1	transforming growth factor beta 1
TNF	tumour necrosis factor
VEGF	vascular endothelial growth factor

# CHAPTER 1

# 1 General Introduction:

## 1.1 Stem Cells

At the turn of the 20<sup>th</sup> Century, scientists recognised that during foetus development, certain cell types became the building blocks of life, which were able to differentiate into various tissue cell types. In 1908, at the annual Congress of the Haematologic Society in Berlin, Alexander A. Maximov first proposed the term stem cell (Loya, 2014). Maximov hypothesised blood cells originated from only one cell type and he suggested the local environment impacted on the differentiation capability of these cells (Friedenstein, 1989). The term 'stem cell' helped to describe these experimental observations, by comparing the process to the stem of a tree, giving rise to numerous branches. However, it was only in the 1960s, when McCulloch and Till studied mouse haematopoiesis, the researchers were able to unravel the potential properties of these stem cells (Till and McCulloch, 1961). The researchers discovered that transplanting spleens into irradiated mice formed cell colonies which were able to self-renew and differentiate into other cell types (Becker et al., 1963).

Since the 1960's, stem cell research has intensified, in order to better understand, as well as harness, two highly desirable and unique properties; self-renewal and differentiation (Slack, 2012). Self-renewal allows the proliferation and generation of daughter stem cells, which possess the same properties as the parent stem cell. Conversely, stem cells are also able to differentiate and generate daughter cells with different characteristics, which become more specialised and form distinct tissue types. However, whilst these differentiated daughter cells (termed progenitor cells) have multi-lineage differentiation potential, they have limited self-renewal capabilities.

Stem cells are categorised by their ability to differentiate, termed 'potency'. When an egg is fertilised (zygote), totipotent stem cells are created in the first few divisions. These totipotent stem cells have the potential to recreate all extra-embryonic and embryonic cell types, making them the most versatile type of stem cell (McClure and Schubiger, 2007). Following further cell division and proliferation, these cells form a blastocyst, a structure comprising an inner mass

## Chapter 1 - Introduction

of pluripotent stem cells, which will form the embryo, and a rich source of embryonic stem cells (ESCs). These pluripotent cells are restricted to forming the three germ layers: ectoderm, endoderm and mesoderm. The endoderm layer forms the gastrointestinal tract and lungs of the foetus, whilst the mesoderm layer forms the muscle, bone and blood system, and the ectoderm layer develops into the epidermal and nervous system. ESCs become even more specialised as the foetus develops, creating a hierarchy of stem cell potency; multipotent, oligopotent and unipotent stem cells (Table 1-1 and Figure 1-1) (Lin et al., 2013). Adult stem cells are also known as somatic stem cells and encompass all multipotent, oligopotent and unipotent stem cells (Slack, 2012). Adult stem cells have a more restricted differentiation ability and are only able to differentiate into a limited number of different cell types.

**Table 1-1: Characterisation of stem cells with regard to their potency (differentiation potential).**

Stem cell type	Characteristic	Example
Totipotent	Differentiate into all embryonic and extra-embryonic cell types.	Cells of the zygote.
Pluripotent	Differentiate into all three germ layers.	Embryonic stem cells and adult stem cells.
Multipotent	Differentiate into limited number of cell types.	Adult stem cells e.g. mesenchymal stem cells.
Oligopotent	Differentiate into one or two cell types.	Adult stem cells e.g. lymphoid stem cells.
Unipotent	Differentiate into one cell type.	Adult stem cells e.g. spermatogonial stem cells.

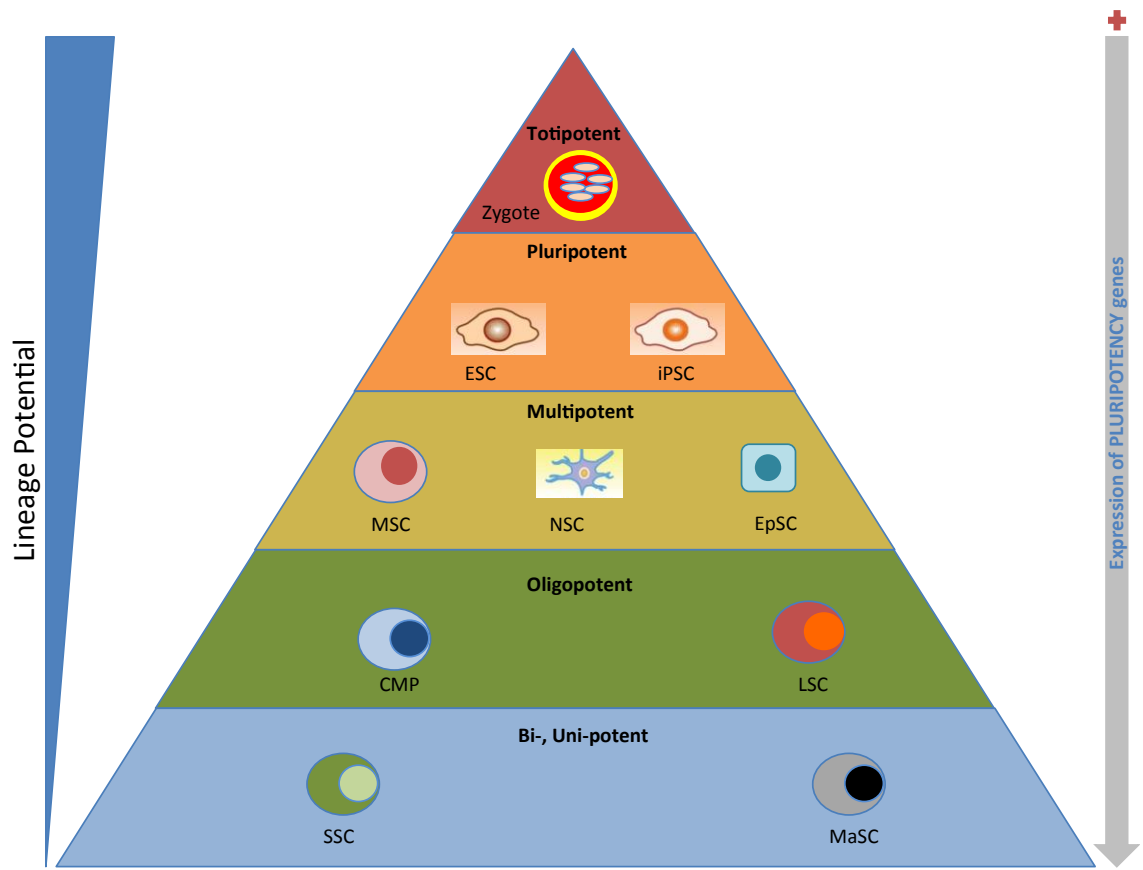


**Figure 1-1: Stem cell classification indicating direction of stem cell differentiation potential. Embryonic stem cell (ESC), induced pluripotent stem cell (iPSC), mesenchymal stem cell (MSC), neural stem cell (NSC), epithelial stem cell (EpSC), common myeloid progenitor (CMP), lymphoid stem cell (LSC), spermatogonial stem cells (SSC) and mammary stem cells (MaSC) (Adapted from (Lin et al., 2013).**

Multipotent stem cells are only capable of differentiating into a limited number of cells, which are closely related to the stem cell. For example, haematopoietic stem cells (HSCs) are able to differentiate into all of the blood's cellular components including platelets, red blood cells and white blood cells. Whereas, oligopotent stem cells are only able to differentiate into one or two mature cells types. An example of oligopotent stem cells are lymphoid stem cells, which are able to create some blood cells including B and T cells, but are not able to differentiate into red blood cells.

Unipotent stem cells have the ability to self-renewal, but have the lowest differentiation capability, because they are only able to differentiate into a single cell type. For example, spermatogonial stem cells, which reside within the testes are only able to differentiate into spermatozoa.

## Chapter 1 - Introduction

Pluripotent stem cells, such as ESCs, have a wide differentiation capacity compared to other stem cell types. Another advantage of ESCs is their ability to indefinitely self-renew *in vivo*, as well as retain an undifferentiated state, which are easily maintained *ex vivo* (Barker and de Beaufort, 2013). However, there is ethical and political controversy regarding the use of human ESCs in regenerative medicine, as it involves the destruction of embryos (Lo and Parham, 2009). Furthermore, evidence has shown ESCs induce an immune response by the host which may lead to rejection and failure of the transplant (English and Wood, 2011).

In 2006, Yamanaka et al., overcame these ethical issues by creating the first induced pluripotent stem cells (iPSCs) from adult mouse fibroblasts. These cells possessed similar properties to ESCs, without the associated ethical issues. The somatic cells were reprogrammed by the introduction of 4 transcription factors (Oct4, Sox2, c-Myc and Klf4) increasing their capability of expansive differentiation and self-renewal *in vitro* (Takahashi and Yamanaka, 2006). As the genome of somatic cells had been altered to create iPSCs, they are known to be less immunogenic upon transplantation into the original host, compared to the use of ESCs (Zhao et al., 2011). Therefore, iPSCs may provide patient specific somatic cells, which may model their disease to assess the effects of drug interactions *ex vivo* (Yu and Thomson, 2014). Although the use of iPSCs alleviates the ethical issues of using ESCs, there are still challenges when implanting iPSCs, which have been identified by Wan et al., (Wan et al., 2012). These concerns include the introduction of viral vectors, which alter the genome leading to the possible creation of tumourigenic cells. At present, the use of iPSCs are considered unsafe for clinical trials, until such time as the oncogenic and immunogenic problems have been resolved (Damdimopoulou et al., 2015).

Unfortunately, both ESCs and iPSCs produce teratomas (tumours) upon *in vivo* implantation, within the host organism. The teratomas are benign tumours consisting of various tissues from all three germ layers and exhibit rapid growth formation (Zhang et al., 2008). These tumours have been known to consist of organs, teeth, hair, muscle, cartilage, and bone tissue (Turgut and Lu, 2007). Therefore, stem cell research has shifted focus towards the use of adult derived

## Chapter 1 - Introduction

stem cells, which alleviate the issues associated with ESCs and iPSCs (Barker and de Beaufort, 2013).

### 1.2 Mesenchymal Stem Cells

In 1974, Friedenstein et al., isolated and identified stem cells, which he called colony forming unit fibroblasts (Friedenstein et al., 1974). In 1991, Caplan renamed the cells MSCs, due to their ability to differentiate into cells of mesoderm origin (mesenchymal tissue) including; adipocytes (fat), chondrocytes (cartilage) and osteocytes (bone) (Figure 1-2) (Caplan, 1991).

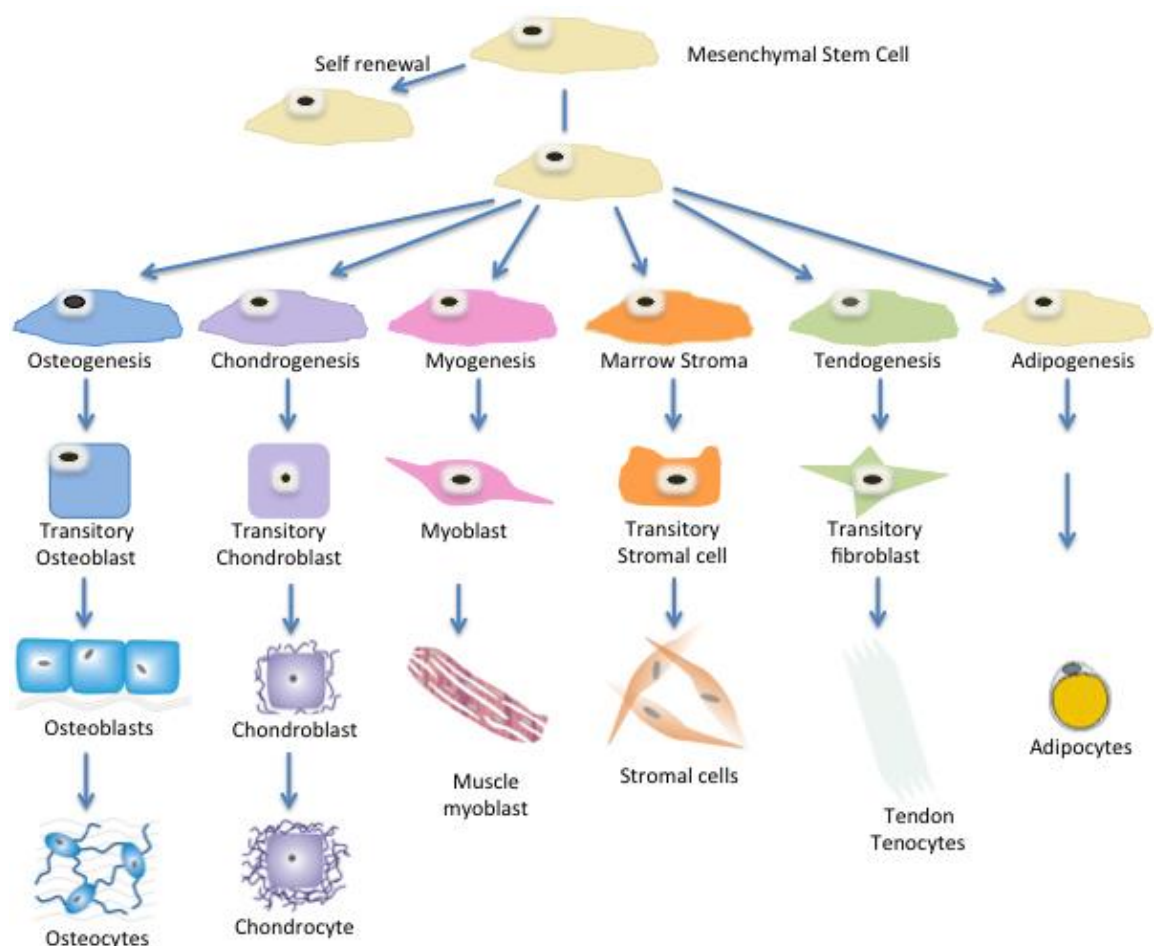


**Figure 1-2: Mesenchymal Stem Cell differentiation.** MSCs are capable of self-renewal and differentiation into cells of the mesoderm lineage. (Adapted from (Caplan and Bruder, 2001)).

MSCs have been discovered within bone, skeletal muscle, cartilage, fibroblasts and haematopoiesis-supporting stroma (Bianco et al., 2013). MSCs have also been found and isolated from other tissue sources, including adipose tissue, umbilical cord and Wharton's jelly (Ragni et al., 2013). Most MSCs are commonly

## Chapter 1 - Introduction

isolated from the bone marrow, even though these cells only make up 0.01% of the total bone marrow population. However, they are easily cultured *ex vivo*, due to their excellent adherent properties to tissue culture plastic (Maltman et al., 2011). MSCs, obtained from bone marrow and adipose tissues, are known as “adult” MSCs. These adult MSCs have a limited differentiation capacity compared to “young” MSCs from an umbilical cord, and studies have also shown the differentiation potential of “adult” MSCs decreases with age (Ragni et al., 2013).

Within the bone marrow, MSCs are known to reside in a microenvironment, termed the niche. Two distinct niche areas have been identified, the sinusoidal niche and the endosteal niche; both are critical to MSC survival and growth. Recent evidence has found MSCs residing on the outer surface of sinusoids (blood vessels in bone marrow) and have been described as a subset of perivascular cells (see Figure 1-3). The sinusoids are formed during the organogenesis of bone and are part of the perivascular stromal compartment in the bone (Bianco et al., 2013). All MSCs are pericytes and are known to interact with endothelial cells, which allow the stem cells to react to injury/inflammation, within a localised area (Sorrell et al., 2009).

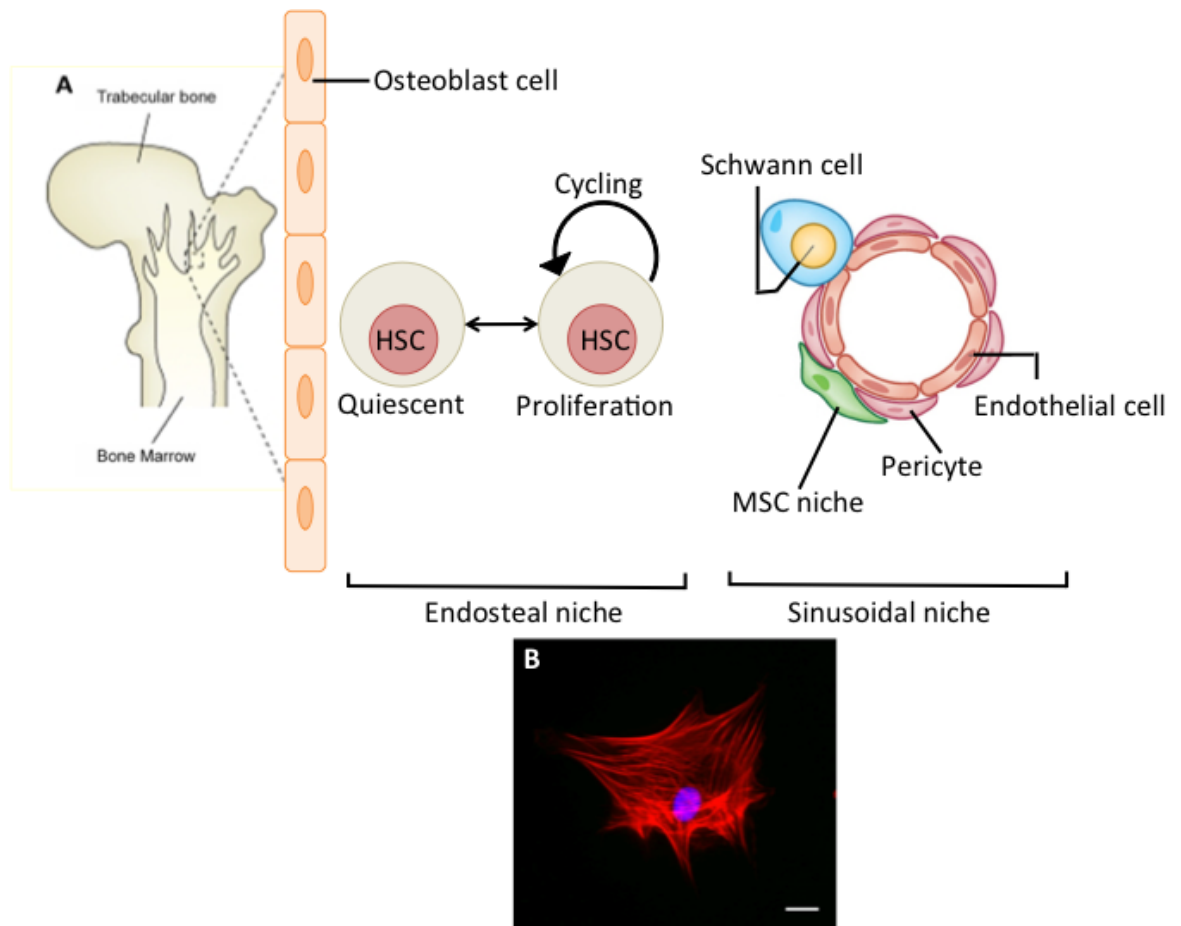


**Figure 1-3: Schematic diagram of the location of the MSC niche within bone marrow.** (A) Indicates the location of MSCs within trabecular bone marrow, by the sinusoidal capillaries (sinusoidal niche) and the inner bone lining (endosteal niche). Adapted from (Ehninger and Trumpp, 2011) (B) Immunofluorescence image of a MSC (personal image). Red = actin, blue = nucleus, 40x objective, scale bar = 20  $\mu\text{m}$ .

### 1.2.1 MSC Characteristic Properties

Characterising MSCs has proved challenging. In 2005, the International Society for Cellular Therapy (ISCT) suggested the acronym MSC might encompass multipotent mesenchymal stromal cells, because they possess similar biological activities to the stem cells, but do not meet all stem cell activity criteria (Horwitz et al., 2005). The ISCT meeting identified some data lacked evidence of MSCs retaining their multipotency properties in unfractionated plastic-adherent cells (Horwitz et al., 2005). Currently, there is no consistent nomenclature or definition of MSCs however, the ISCT proposed a set of minimal criteria to characterise MSCs, as MSCs may express different cell surface markers depending on their location within the body. For example, adipose derived MSCs may express Cluster of Differentiation-90 (CD90) and only change to CD105, (commonly referred as endoglin-an angiogenic marker) when they adhere to

## Chapter 1 - Introduction

tissue culture plastic (Keating, 2012). In 2006, the ISCT committee identified three main criteria to characterise MSCs, which are as follows: (a) MSCs must be able to adhere to plastic when cultured in standard conditions, (b) MSCs must express CD105, CD73 and CD90, and lack CD45, CD34, CD14 or CD11b, CD79alpha or CD19 and HLA-DR surface molecules expression and (c) MSCs must be able to differentiate *in vitro* into the following cell types, osteoblasts, adipocytes and chondrocytes (Dominici et al., 2006).

MSCs reside within a heterogeneous cell population and demonstrate a diverse range of morphologies, physiologies and surface antigen expression. Therefore, MSCs are identified using a combination of these characteristics. *In vivo*, MSC function and cell phenotype have been identified by their expression of growth factor receptors, protein cytokines, extracellular matrix proteins and adhesion molecules. The scientific community have decided MSCs used in research should not express haematopoietic or endothelial cell lineage markers such as CD11b, CD14, CD31, CD33, CD34, CD133 and CD45 or co-stimulatory molecules CD80, CD86 and CD40. However, it has been widely accepted that all MSCs express STRO-1 and CD271 (Casado-Díaz et al., 2011). A detailed list of generically accepted MSC markers, providing an immunophenotypic profile, is depicted in Table 1-2.

**Table 1-2: The MSC Immunophenotype Profile.**

**A comprehensive list, description and role for each MSC cluster of differentiation (CD). Positive (+) and negative (-) indicate the protein expression for MSC classification. (Adapted from (Casado-Díaz et al., 2011)).**

Immunophenotype	Description	Role
CD11 <sup>-</sup>	A component of various integrin's	Mediates leukocyte adhesion
CD14 <sup>-</sup>	Human gene	Expressed by macrophages
CD18 <sup>-</sup>	Integrin	Cell adhesion and cell-surface signalling
CD31 <sup>-</sup> (PECAM-1)	Type I integral membrane glycoprotein	Platelet endothelial cell adhesion molecule-1
CD34 <sup>-</sup>	Cell surface glycoprotein	Cell-cell adhesion molecule
CD40 <sup>-</sup>	Co-stimulatory protein	Expressed by endothelial cells
CD45 <sup>-</sup>	Type I trans-membrane protein	Expressed by differentiated

## Chapter 1 - Introduction

		haematopoietic cells
CD56 <sup>-</sup> (NCAM)	Single trans-membrane glycoprotein	Neural cell adhesion molecule
CD80 <sup>-</sup>	Co-stimulatory molecule	Signals T cell activation and survival
CD86 <sup>-</sup>	Co-stimulatory molecule	Signals T cell activation and survival
MHC-II <sup>-</sup>	Cell surface molecule	Mediates interactions of leukocytes
CD29 <sup>+</sup>	Integrin	Cell adhesion
CD44 <sup>+</sup>	Cell-surface glycoprotein	Cell-cell interactions, cell adhesion and migration
CD54 <sup>+</sup> (ICAM-1)	Intercellular adhesion molecule	Plays role in inflammation, immune responses and in intracellular signalling events
CD71 <sup>+</sup> (TfR1)	Transferrin receptor	Mediates uptake of transferrin-iron complexes
CD73 <sup>+</sup> (5'-NT)	Enzyme	Converts AMP to adenosine
CD90 <sup>+</sup> (Thy-1)	Glycosylated membrane protein	Thought to play role in cell-cell and cell-matrix interactions
CD105 <sup>+</sup> (Endoglin)	Type I membrane glycoprotein	Plays role in angiogenesis
CD106 <sup>+</sup> (VCAM-1)	Vascular cell adhesion molecule	Cell adhesion molecule
CD120a <sup>+</sup> (TNFR)	Tumour necrosis factor receptor	Cooperates with an adaptor protein determining cell response e.g. inflammation
CD124 <sup>+</sup>	Type I cytokine receptor	Regulates IgE antibody production in B cells
CD166 <sup>+</sup> (ALCAM)	Type I trans-membrane glycoprotein	Mediates adhesion interactions
CD271 <sup>+</sup>	Low affinity nerve growth factor receptor	Stimulates neuronal cells to survive and differentiate
MHC-I <sup>+</sup>	Cell surface molecule	Mediates cellular immunity
STRO-1 <sup>+</sup>	Cell surface antigen	
Nestin <sup>+</sup>	Type VI intermediate filament protein	Used in assessing cell proliferation and migration

## 1.2.2 Immunomodulatory Properties

MSCs are classed as non-immunogenic, and therefore do not cause an immune response upon implantation. As described above, MSCs are characterised as CD40<sup>-</sup>, major histocompatibility complex-II (MHC-II<sup>-</sup>), CD80<sup>-</sup> and CD86<sup>-</sup>, but are MHC-I<sup>+</sup>. The lack of immune response may occur because the MSCs do not possess these co-stimulatory molecules, even though the cells are MHC-I<sup>+</sup>, which may activate T cells (Ozawa et al., 2008, Uccelli et al., 2008, Sohni and Verfaillie, 2013). The MSCs respond to both the adaptive and innate immune systems by suppressing T cells and dendritic cell (DC) maturation, decreasing B cell activation and proliferation (Figure 1-4).

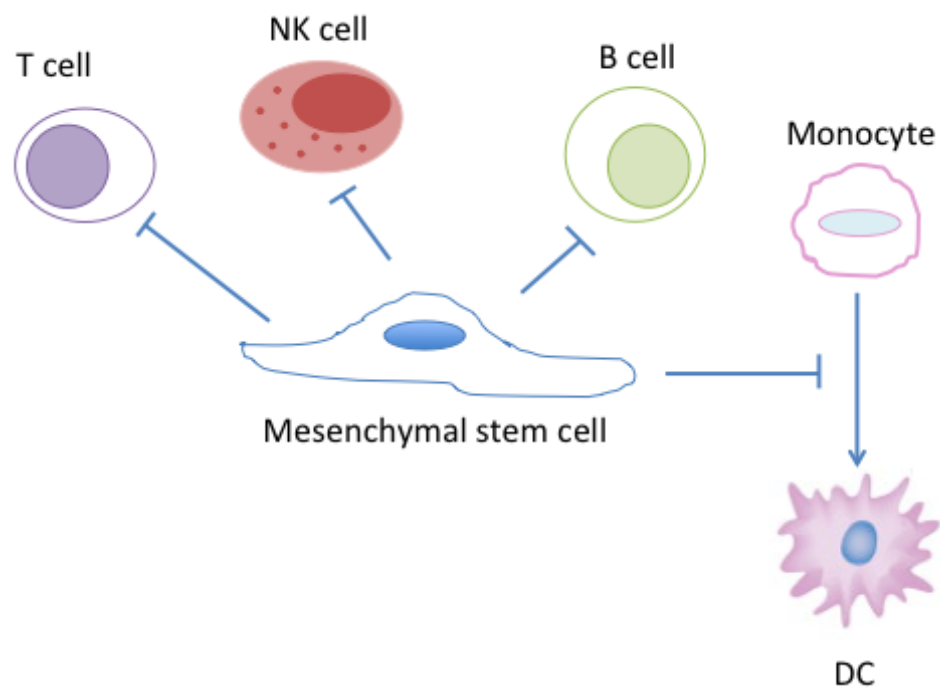


**Figure 1-4: Diagram highlighting the immunosuppressive properties of MSCs. MSCs inhibit proliferation of T cells, natural killer (NK) cells and B cells. Additionally, MSC's prevent the differentiation of monocytes into dendritic cells (DCs). (Adapted from (Gebler et al.)).**

MSCs play an active role in disrupting the innate immune system. DCs express MHC-I and MHC-II, as well as co-stimulatory factors. MSCs have been shown to reduce the expression of MHC-I, CD11c, CD63 and co-stimulatory molecules on DCs, thus impeding their antigen expression on the cell surface. MSCs are known to inhibit the production of DCs, by affecting the maturation process of monocytes, which turn into DCs, as well as inhibiting the production of tumour-necrosis factor (TNF) in DCs (Jiang et al., 2005, Ramasamy et al., 2007, Aggarwal

## Chapter 1 - Introduction

and Pittenger, 2005). The combination of all these factors causes a reduction in the pro-inflammatory effects of the DCs.

NK cells are cytotoxic lymphocytes and MSCs have been shown to down regulate expression of certain activating receptors (NKp30 and NKG2D) in resting NK cells (Spaggiari et al., 2006). Therefore, this process reduces the cytotoxic activity and target-cell killing by NK cells. Interferon gamma (INF- $\gamma$ ) is a cytokine produced from NK cells. In the presence of high concentration of INF- $\gamma$ , MSCs are protected from NK cell mediated lysis, which may inhibit NK cell function. Furthermore, MSCs have displayed the ability to disrupt the neutrophil process, by slowing down the respiratory burst, after the neutrophils have bound to bacteria (Raffaghello et al., 2008).

During the adaptive immunity process, MSCs inhibit T cell proliferation by supporting their survival, thus over stimulating T cells through the T cell receptor, which then undergo activation-induced cell death (Benvenuto et al., 2007). Reduced T cell proliferation instigates a decrease in INF- $\gamma$  production, which in turn alters the state of the cells from a pro-inflammatory to an anti-inflammatory state. Additionally, MSCs aid the generation and proliferation of regulatory T cells, which suppress the immune system by releasing HLA-G5 (Selmani et al., 2008).

Research conducted *in vitro* indicates MSCs inhibit B cell proliferation and differentiation, which is involved in antibody production, by turning B cells into antibody-secreting cells (Corcione et al., 2006). It has been suggested B cells respond to T cells activity and therefore, B cells may be affected by the inhibition of T cell function by MSCs.

Therefore, the immunomodulatory properties of MSCs indicate their potential use as a universal donor by reducing the hosts' immune response and therefore, the MSCs have great potential in treating a large number of immune and non-immune diseases.

### 1.3 MSCs in Regenerative Medicine

Over the past 15 years there has been a gradual emergence of interest in the field of regenerative medicine. Regenerative medicine heralds a promising future, focusing on the regeneration and replacement of cells, tissues and organs to restore functionality, using the body's own repair mechanisms. Previously, cell and tissue regeneration has been achieved by using either cell therapy based treatments and/or tissue engineering, combining engineered scaffolds, cells and biomolecules, to stimulate regeneration of the defective area with a view to producing functional tissues (Liu et al., 2007). The advent of stem cell research has led researchers to develop exciting new approaches to improve these advancements, and increase their applications in biomedical science (Liao et al., 2008). The potential use of MSCs in cell therapies and tissue engineering has been steadily gaining momentum, due to their diverse range of properties, as highlighted in Figure 1-5.

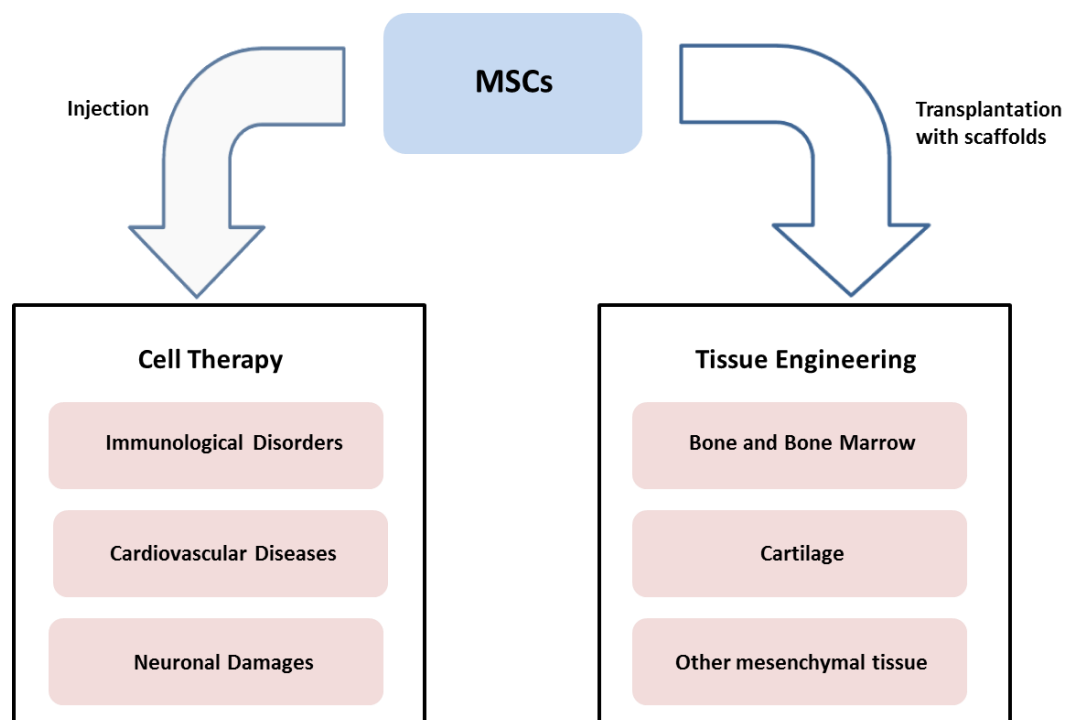


**Figure 1-5: MSCs examples used in cell therapy and tissue engineering.** Diagram of potential MSC uses in cell therapy and tissue engineering. (Adapted from (Kagami et al., 2011)).

When MSCs are used in cellular therapy, the cells are either intravenously (IV) delivered through the patient's drip system or directly injected into the defective site. The self-renewal and differentiation capacity of MSCs have also

## Chapter 1 - Introduction

shown potential clinical use in regenerating damaged tissue in the musculoskeletal system. Recent *in vivo* studies have demonstrated the self-renewal properties of transplanted MSCs. These transplanted MSCs were able to create a miniature bone organ, which allowed the establishment of haematopoiesis from the host animal (Sacchetti et al., 2007). Using MSCs in this way may help patients suffering from large bone defects (trauma as well as skeletal abnormalities), maxillofacial injuries, osteoarthritis, bone loss (osteoporosis) or atrophic non-union fractures (where the bone will not heal without intervention). Bone autografts are currently the gold standard for augmenting bone in non-healing bone fractures. However, when this method fails (due to problems of altered osteogenic properties at the donor site or when the risk outweighs the benefits of the bone graft), cell based therapies using MSCs are a viable alternative (Gómez-Barrena et al., 2015). This method involves transplanting MSCs incorporated in scaffolds to accelerate bone formation during the repair and regeneration process. A further potential use for MSCs is in the repair of damaged oral bone and subsequent tooth loss, which costs the US \$5-6 billion/year in surgical treatments (Fischer et al., 2011). Current dental treatments have not always been successful and have resulted in long recovery times and increased resource costs.

Therefore, instead of creating and implanting replacement materials, research has invested in the development of new functional tissue, leading to the generation of a natural system of *in situ* tissue repair, with the implantation of MSCs within the patient (Kon et al., 2012). For example, a patient suffering from osteoarthritis also has cartilage degeneration, which may lead to knee and hip replacements. Alternative regenerative medicine treatments, such as using tissue engineering and stem cells, may eliminate the need for knee or hip replacements and improve the patient's quality of life. A clinical trial intra-articularly injected MSCs into patients suffering from osteoarthritis in the knee. The researchers found improved knee joint function, reduced pain sensation, as well as regenerating hyaline-like articular cartilage (Jo et al., 2014). Jo et al., suggested the improved knee function and regeneration of hyaline-like articular cartilage may be due to MSCs differentiating into chondrocytes and secreting paracrine signals, as they induce chondrocyte proliferation and ECM synthesis.

## Chapter 1 - Introduction

MSCs excellent immunosuppressive and immunomodulatory properties have led to the suggestion that the harnessing of these effects may treat autoimmune diseases such as multiple sclerosis (MS). The use of cell therapies in the treatment of autoimmune diseases has developed from the idea of rebuilding damaged immune-regulatory networks, by the creation of a group of memory cells, which would be able to react to environmental pathogens (Dazzi and Krampera, 2011). A mouse study conducted by Karussis et al., used a chronic autoimmune encephalomyelitis (EAE) model, to investigate MS (Karussis et al., 2008). The researchers intravenously administrated MSCs into the mice and found the cells induced neuroprotection, maintaining the axons in the central nervous system (CNS). Furthermore, the MSCs were shown to differentiate into cells of neural-glial lineage. In other studies, MSCs immunomodulating properties were shown to successfully down regulate the clinical manifestations of MS in the EAE model (Zappia et al., 2005). MSCs inhibit the autoimmune attack of the CNS, thus reducing damage to the axons and limiting the effects of MS (Gerdoni et al., 2007).

Other potential uses for MSC-based regenerative medicine therapies, include Parkinson's disease, spinal cord injury and cardiovascular repair. Parkinson's disease is a neurodegenerative disease, which attacks the dopaminergic neurons. Currently, there are no treatments for Parkinson's disease to stop or reverse this process. Animal models studying Parkinson's disease have shown MSCs protect and regenerate damaged DA neurons (Glavaski-Joksimovic and Bohn, 2013).

MSCs have shown promise in aiding recovery following spinal cord injury, by secreting neurotrophic molecules to reduce the glial cyst, thus leading to neuroprotection in the damaged area (Boido et al., 2014). A study using dogs with spinal cord injuries, found MSCs directly remyelinated numerous axons in the damaged area after transplantation (Lee et al., 2011b). Moreover, MSCs used in cell therapy have been shown to aid cardiovascular repair by secreting pro-angiogenic and cardioprotective paracrine molecules (Williams et al., 2013). Williams et al., intra-myocardially injected MSCs into pigs suffering from myocardial infarction and found progressive reduction in infarct size post injection.

## Chapter 1 - Introduction

MSCs have potential within regenerative medicine by exploiting MSC self-renewal and differentiation capabilities, in repairing and restoring functionality to a wide range of tissues (bone, cartilage and cardiovascular). However, there have been failures with MSCs engrafting into the target area. In pre-clinical and clinical studies, MSCs are most commonly delivered systemically by intravenous injection (IV). Following the introduction into the host, MSCs have been found to congregate in pulmonary vasculature due to the pulmonary first-pass effect, rather than the MSCs reaching the target area (Lee et al., 2009, Lin et al., 2014, Fischer et al., 2009). Therefore, studies have shown treatment using MSCs have been inefficient or of limited effect in the treatment, because the MSCs tend to accumulate in the lungs (Kean et al., 2009). Additionally, there have reports on the efficacy of the administration in the timing of MSCs injections. A study conducted by Cho et al., compared single and multiple injections of MSCs into pigs to induce the adaptive immune system (Cho et al., 2008). The single injections did not induce the immune system however, multiple injections into the same site led to detectable antibody production levels. Therefore, these problems need to be addressed, before MSC therapy may be utilised as a favourable treatment.

### 1.4 Stem cell niche

At present, there has been limited *in vivo* research into the MSC niche, which is known to provide cues that control MSC self-renewal and differentiation. As discussed earlier, recent evidence suggests part of the MSC bone marrow niche is located in the perivascular areas and pericytes (contractile cells associated with endothelial cells) aid the niche *in situ* (Zhao et al., 2014a, Mitsiadis et al., 2007). The niche nurtures the stem cells, as well as controlling homeostasis, through a process of complex molecular events (Mitsiadis et al., 2007, Laine et al., 2012). For example, the niche sustains the stem cell population, by assessing whether the cells are active or quiescent (Joddar and Ito, 2013), and protects stem cells from over stimulation, preventing differentiation and apoptosis (cell death) (Weber and Calvi, 2010). Researchers have suggested the niche also protects stem cells from multiple gene mutations (creating cancer cells) by maintaining the stem cells in a quiescent state as well as possessing a low metabolic rate (Gattazzo et al., 2014). Recently, studies have shown the major

## Chapter 1 - Introduction

purpose of the niche is to anchor stem cells *via* membrane proteins to either the surrounding environment, such as extracellular matrix (ECM), or allow cells to adhere to each other (Joddar and Ito, 2013). The interactions between stem cells, the ECM and the resident niche cells are regulated by these adhesion molecules (Lane et al., 2014). For example, these membrane proteins attaching the niche to the ECM are exposed to the surrounding environment and are influenced by the physical properties (bulk stiffness) of the ECM. Examples have shown these physicals properties activate intracellular pathways within the stem cells in the niche thus, influencing stem cell fate (Watt and Huck, 2013, Swift et al., 2013).

The fate of the stem cells within the niche is influenced by several factors including cell-cell interactions, cell-surrounding environment interactions and soluble factors (e.g. growth factors and cytokines), as illustrated in Figure 1-6 (Higuchi et al., 2012). The stem cell niche microenvironment consists of stem cells, differentiating progenitors, non-stem support cells and ECM, all of which regulate stem cell fate and differentiation. Signals from soluble and surface-bound factors, along with mechanical properties of the surrounding environment and cell-cell connections, are integrated within the niche (Rasi Ghaemi et al., 2013).

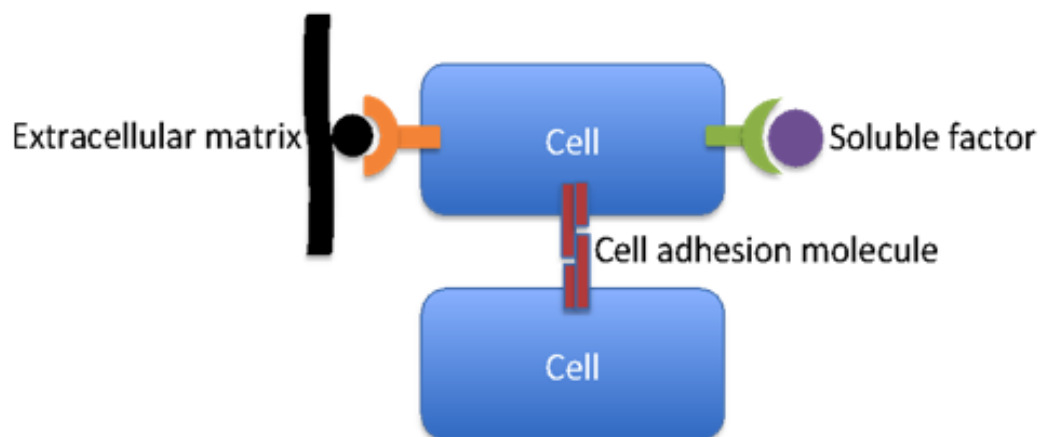


**Figure 1-6: Conceptual model of a stem cell niche.**  
(Adapted from (Joddar and Ito, 2013))

The niche has an organised structure, which permits cell-fate decisions and allows key signalling between stem cells and the surrounding environment. Moore and Lemischka identified three main categories of a mammalian stem cell

## Chapter 1 - Introduction

niche: 1) anatomical organisation of cells within the niche, 2) integrated positive and negative feedback signalling, and 3) shared intercellular signalling pathways between stem cells and supporting cells (Moore and Lemischka, 2006).

Stem cell proliferation may be controlled by these positive and negative feedback systems. Research has suggested maintaining stem cell supply is controlled by feedback mechanisms from progenitor cells, as well as from the autocrine and paracrine systems (Ema and Suda, 2012). A recent study showed the location of the stem cell in the niche influenced cell behaviour (Rompolas et al., 2013). Rompolas et al., were able to predict fates of stem cells (i.e. whether stem cells remain uncommitted, generate precursors or committed to differentiating) by the position of the stem cell within the hair follicle niche. The researchers identified stem cells in the upper half of the bulge remained quiescent whereas, cells in the compartment, which becomes the new hair germ became committed to differentiation. This vital niche homeostasis and control of stem cell fate creates a dynamic system, dictated by cell-cell communication (signals), both within the niche and the external environment.

The ECM is known to directly and indirectly play a role in the maintenance of the stem cell niche. Biochemical, physical, structural, and mechanical properties of the ECM composition are able to regulate stem cell fate by permitting signals to travel through the ECM and interact directly with the stem cells (Gattazzo et al., 2014). Additionally, the ECM creates biochemical gradients by directly binding to growth factors, which in turn creates a pool of biofactors ready for release.

The stem cells in the niche respond to metabolic, inflammatory and hormonal cues released from the surrounding area (Kiel et al., 2005, Chen et al., 2014). Additionally, the niche cells fate and decisions are affected by temperature fluctuations, shear forces and chemical signals from the external environment (Chen et al., 2009b, Dong et al., 2009). The MSCs niche has been shown to respond to growth spurts, skeletal tissue damage and infection to repair bone, cartilage and tendons (e.g. a broken bone or a slipped disc).

### 1.4.1 Cellular Communication

Due to the limited research conducted on the MSC niche *in vivo*, whilst some evidence exists for the structure and cellular components, the exact location is still ambiguous. However, there have been extensive investigations into the HSC niche, which also resides within the bone marrow environment and MSCs are known to support the HSC niche. Studies have shown parts of the HSC niche and the MSC niche occupy the same perivascular regions within bone marrow. Therefore, information concerning signalling, ECM interaction and molecular pathways found within the HSC niche, may possess similarities compared to the MSC niche.

Although there are dissimilarities between the different types of the stem cell niche, there are key similarities between the individual stem cell niches. For example, there are common key signalling pathways (e.g. Wnt/ $\beta$ -catenin, Notch and Hedgehog), which have been identified. Additionally, there are common “support” cells, which lend critical support to stem cells, (e.g. osteoblasts for HSCs and pericytes for MSCs) and communicate with each other through cell surface receptors, gap junctions and soluble factors. As well as possessing these properties, the niche must allow for intercellular adhesion to permit signals to communicate between the stem cells (Roeder et al., 2011).

Integrins are important in the interaction between the ECM and stem cells, and are key in the adhesion, anchorage and homing of stem cells. Integrins are transmembrane receptors, which attach the cytoskeleton of the cell to specific proteins in the ECM. Also, integrins are known to directly activate stem cell self-renewal and proliferation, *via* their interaction with focal adhesion kinase (FAK) and phosphoinositide 3-kinase (PI3K) (Legate et al., 2009, Buitenhuis, 2011).

The biophysical properties of the extracellular environment have been shown to affect stem cell behaviour. Compression of the ECM by neighbouring cells, alter the stiffness; stem cells can accommodate this change by regulating their internal cytoskeletal tension through a mechanism termed mechanotransduction. This mechanism generates isometric tension within the cytoskeleton thus maintaining cell shape. Cell geometry and cytoskeletal

## Chapter 1 - Introduction

organisation are regulated by specific mechanotransduction pathways (Ras/MAPK, PI3K/Akt, RhoA/ROCK, Wnt/ $\beta$ -catenin and TGF- $\beta$ ) and YAP/TAZ transcription factors (Halder et al., 2012, Dupont et al., 2011, Sun et al., 2012).

### 1.4.2 Cell cycle

In the absence of regeneration cues, MSCs maintain a quiescent (resting) state within the niche, which reduces the generation of genetic defects (Rasi Ghaemi et al., 2013). MSCs remain in this quiescent state, indicating the cells have not been activated in the cell cycle process. There are four phases/segments of the cell cycle, with  $G_0$  reflecting the quiescent state (Figure 1-7).

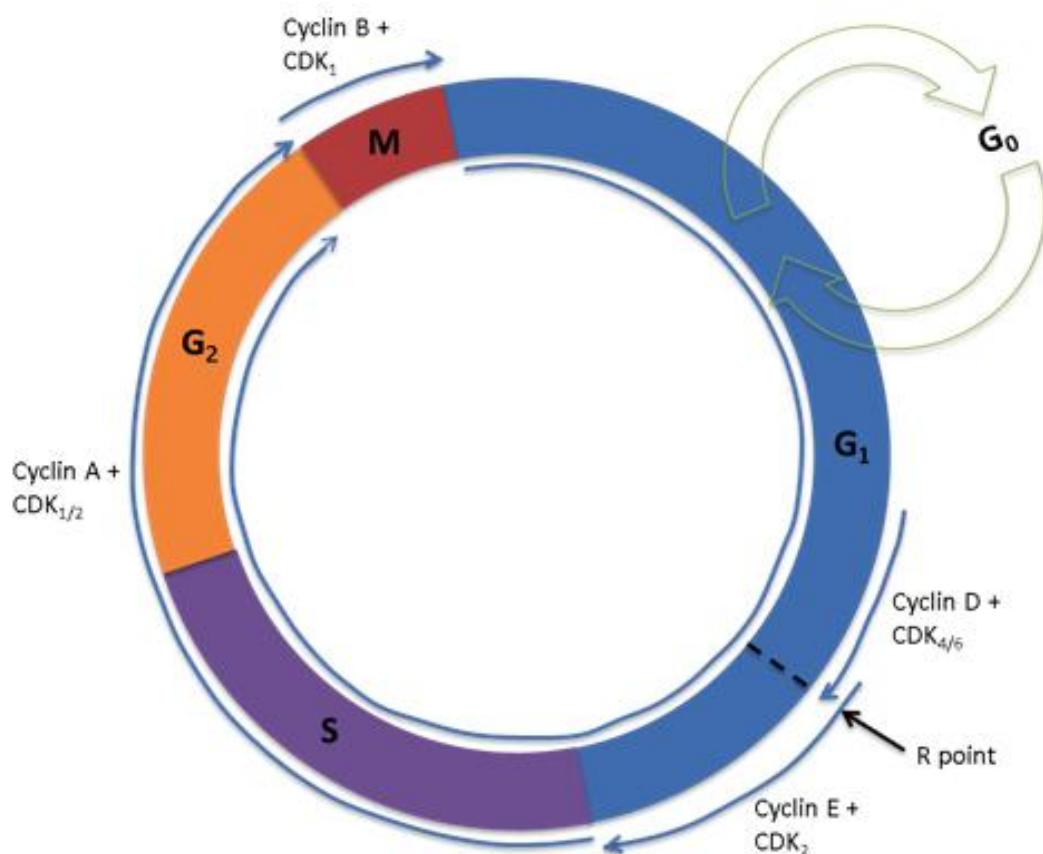


**Figure 1-7: Diagram depicting cell cycle.**

The phases of cell cycle regulation;  $G_0$  indicates MSC quiescent state. A dividing MSC passes through a series of stages described as the cell cycle. There are two gap phases ( $G_1$  and  $G_2$ ); an S (for synthesis) phase, when the genetic material is duplicated; and an M phase, in which mitosis separates the genetic material and the cell divides. (Taken from (Matsumoto and Nakayama, 2013))

These cell cycle phases are highly regulated, particularly with the progression from Gap 1 ( $G_1$ ) to synthesis (S) phase and from Gap 2 ( $G_2$ ) to Mitosis (M) phase. Each stage of the cell cycle is governed by pairs of cyclins and cyclin-dependent

## Chapter 1 - Introduction

kinases (CDKs) (Orford and Scadden, 2008). Progression through  $G_1$  phase depends upon the cyclin D-CDK4 or CDK6 complex. The cycle subsequently requires the presence of the cyclin E-CDK2 complex to pass from the  $G_1$  to S phase. Moreover, the progression from  $G_2$  to M phase depends upon the presence of cyclins A and B with CDK1 complexes (Matsumoto and Nakayama, 2013). Intrinsic and extrinsic signals must stimulate the cell to allow progression through the  $G_1$  phase to enter the cell cycle. Once progression has travelled beyond the restriction (R) point, the cell no longer requires external stimulation to enter the cell cycle. In the absence of intrinsic and extrinsic signals, the MSCs in the niche are known to exit the cell cycle during the  $G_1$  phase and enter a quiescent ( $G_0$ ) stage (Orford and Scadden, 2008).

Mitosis is governed and regulated by the transcription factor E2F, which is key to the activation of cell cycle progression. Retinoblastoma proteins (Rb) may be phosphorylated by cyclin-CDK complexes, which in turn activate E2F, *via* the inhibition of the Rb (Matsumoto and Nakayama, 2013). Additionally, CDK inhibitors (CKIs) are members of either Ink4 or Cip/Kip families, which negatively regulate cell cycle progression. Inhibitors of CDK4/CDK6 belong to the Ink4 group whereas, members of the Cip/Kip family directly inhibit CDK2 in the late  $G_1$  phase (Orford and Scadden, 2008).

Stem cells divide to produce daughter cells, either through symmetric or asymmetric cell division, to replace cells undergoing differentiation. Symmetric cell division produces either two differentiating cells or two stem cells. Whereas, asymmetric cell division produces one stem cell and one differentiating cell (Rasi Ghaemi et al., 2013). The positioning of a daughter stem cell in the niche is dependent upon exposure to external environmental cues.

### **1.4.3 MSC migration from the niche**

MSCs have an active role in tissue repair. Studies have shown MSCs migrate towards sites of injury, inflammation and tumours (Shi et al., 2012). The processes involved in normal wound healing require a series of complex events, progressing from initial bleeding to inflammation, cell migration, proliferation,

## Chapter 1 - Introduction

re-epithelisation and finally remodelling of the ECM. The three main stages of the wound healing process have been identified as inflammation, proliferation and remodelling (Maxson et al., 2012). The inflammatory phase occurs within the first three days, after which the proliferation stage is initiated and may continue for 2 weeks. This stage is followed by the remodelling phase, which may continue for a few years to allow the wound to fully heal. MSCs are involved within all three stages of wound healing and tissue repair, as shown in Figure 1-8.

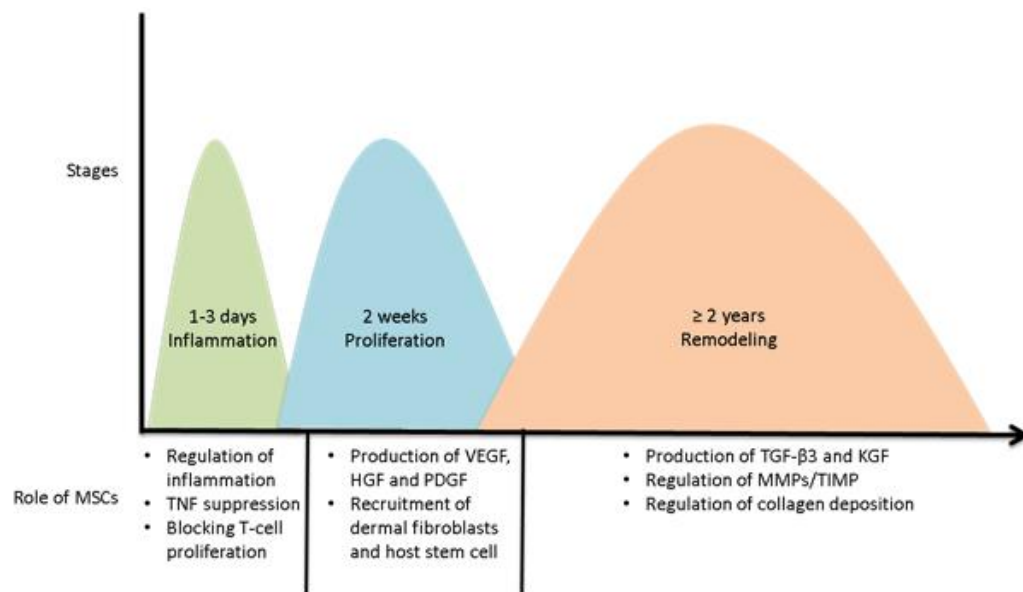


**Figure 1-8: Mesenchymal stem cell roles in each stage of the wound healing process over time.**  
(Taken from (Maxson et al., 2012))

Inflammation or injury causes cellular release of cytokines, which stimulate the recruitment of MSCs. These cytokines include TNF- $\alpha$ , IFN- $\gamma$ , interleukin-6 (IL-6) or hypoxia-induced mitogenic factor (HIMF) (Yagi et al., 2012). Inflammation and injury sites contain high levels of cytokines, following the activation of Natural Killer (NK) cells and T cells secreting TNF- $\alpha$  and IFN- $\gamma$ . MSCs are stimulated by the detection of IFN- $\gamma$  to produce indoleamine 2,3-dioxygenase (IDO), which inhibits proliferation of activated T or NK cells. Additionally, injury leads to the maturation of DCs, which initiate T cell responses, although MSCs have also been shown to disrupt the DC maturation process. The release of prostaglandin E2 (PGE2) and IL-6 cytokines from MSCs controls DC maturation, leading to T cell suppression. Furthermore, MSCs are able to suppress T cells *via* the NF $\kappa$ B pathway (Yagi et al., 2012). The initial stage of injury causes MSCs to secrete

## Chapter 1 - Introduction

anti-inflammatory cytokines IL-10 and IL-4 (Maxson et al., 2012). MSCs possess the chemokine receptor (CXCR4) and stromal-derived factor-1 (CXCL12), which are activated by inflammation or injury and are key to the migration of the cells to the injury site. Furthermore, it has been reported MSCs migrate following the activation of other chemokine receptors including CCR1, CCR4, CCR7, CCR9, and CCR10, CXCR5 and CXCR6 (Sohni and Verfaillie, 2013).

Local cellular responses to injury/inflammation are regulated *via* the paracrine signalling from the MSCs, whilst differentiation of the MSCs aids tissue repair. Research has shown an improvement in tissue repair by the differentiation and paracrine signalling from MSCs (Sasaki et al., 2008, Chen et al., 2008). Cytokines released during injury cause immune modulators to be secreted from MSCs (e.g. platelet-derived growth factor (PDGF-AB), insulin-like growth factor 1 (IGF-1), hepatocyte growth factor (HGF), epidermal growth factor (EGF), chemokine ligand 5 (CCL5)) (Maxson et al., 2012). Paracrine signalling from MSCs has been shown to affect the regulation of cell survival, proliferation, migration and gene expression of various cell types. These cell types include endothelial cells, keratinocytes and fibroblasts (Hocking and Gibran, 2010). The soluble factors released from MSCs stimulate proliferation and migration of other cell types to enhance and accelerate wound healing. Additionally, MSCs secrete growth factors, including vascular endothelial growth factor (VEGF) and HGF through paracrine signalling, which reduces scar tissue and maintains the balance of transforming growth factor- $\beta$ 1 (TGF- $\beta$ 1) and TGF- $\beta$ 3 (Ennis et al., 2013). Therefore, MSCs have been found to accelerate damaged tissue repair by their active involvement in all three stages of the wound healing process.

### **1.5 Exploitation of the stem cell niche**

Over the past decade, the scientific community has recognised the huge potential of the exploitation of the niche in the development of novel therapeutics, in particular the field of regenerative medicine (Mason and Dunnill, 2008). The use of stem cells has revolutionised cell therapies however, there are still issues related to their clinical use. Particular problems occur with low viability upon *in vivo* transplantation and the possibility of the manifestation of unfavoured behaviours, by differentiating into undesired cell types. Further

## Chapter 1 - Introduction

research is necessary to understand the underlying mechanisms controlling stem cell homeostasis in the niche and utilise this knowledge to advance novel therapeutics and aid damaged tissue repair.

Further understanding of cell-cell communication in the niche, may allow researchers to mimic the regulation observed within the niche, allowing control over MSC fate (i.e. either promoting self-renewal or driving MSCs towards a specific cell lineage) (Wagers, 2012). Understanding the behaviour of MSCs in the niche environment, under normal and pathological conditions, will allow important exploration of their therapeutic potential in various clinical applications (Samadikuchaksaraei et al., 2014). If MSCs were able to be manipulated *in vitro*, it would potentially provide two important sources of cells. Firstly, it would allow the promotion of MSCs self-renewal, thus promoting the expansion of MSC numbers for experiments or transplantation use in clinic. Secondly, it would allow the direction of MSCs to become certain cell types, for example, bone forming osteoblasts, which may be used in clinical treatments of various bone conditions.

Therefore, an important research area has emerged over the past few years to focus on the design of *ex vivo* stem cell niche models to study and mimic this special microenvironment. Lane et al., have suggested in the future, niche stem cells will be directly targeted by a combination of various factors (e.g. small biomolecules), which may be applied at different stages of treatment (Lane et al., 2014). This treatment would allow the patient's own stem cells to regenerate damaged tissue, without *ex vivo* cell expansion and differentiation as shown in Figure 1-9 (Lane et al., 2014).

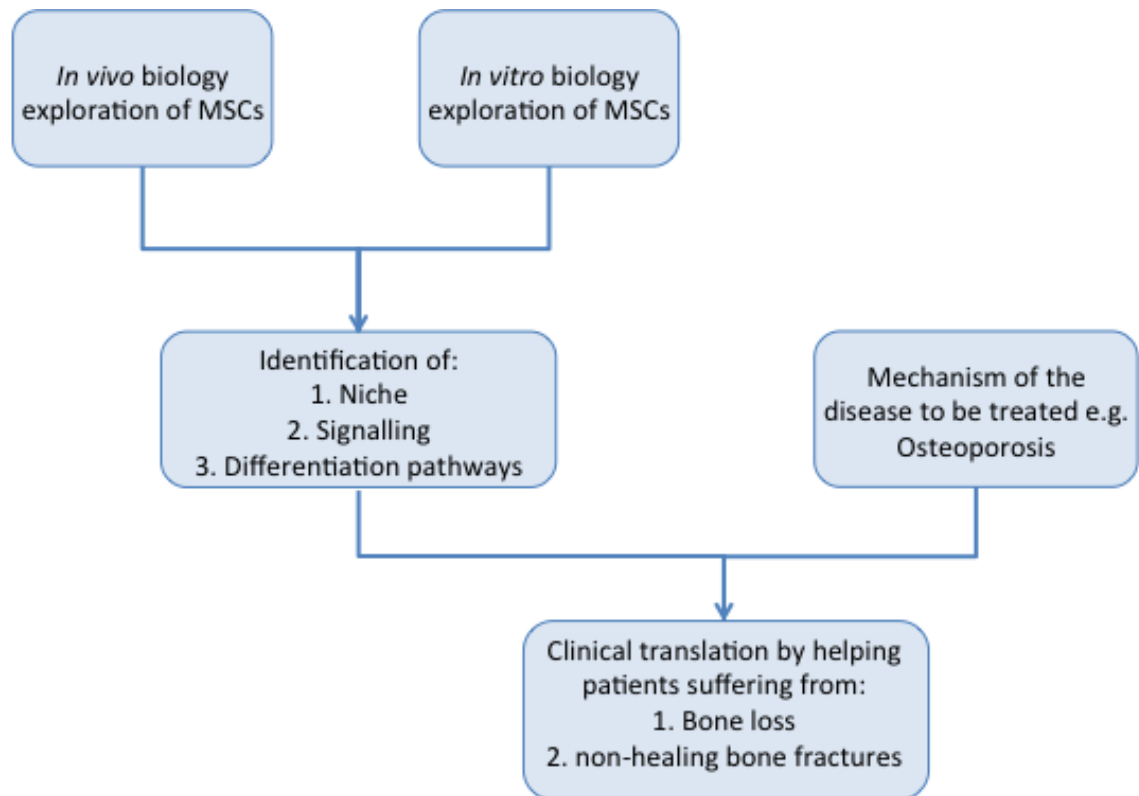


Figure 1-9: Issues to be assessed for successful application of stem cells within regenerative medicine. (Adapted from (Samadikuchaksaraei et al., 2014)).

## 1.6 *In vitro* studies of the stem cell niche

The development of *in vitro* models of the MSC niche will enhance our understanding of the communication mechanisms between MSCs and the surrounding environment. To date, researchers have mainly developed two-dimensional (2D) monolayer models. However, these 2D models provide poor representations of the true MSC niche due to the lack of ECM and three-dimensional (3D) environment, therefore limit extrapolation to the *in vivo* situation. Furthermore, MSCs spontaneously differentiate in monolayer culture over a short incubation period (Baer et al., 2010). Therefore, research is shifting towards the development of three-dimensional (3D) *in vitro* niche models, which are more complex and better mimic the *in vivo* niche environment (Cheng et al., 2012).

### 1.6.1 Two-dimensional stem cell niche models

*In vitro* MSC niche studies have been performed using 2D substrates to maintain stem cell self-renewal or drive down a specific differentiation pathway. Studies

## Chapter 1 - Introduction

have tried to replicate the niche by using ECM components, soluble factors and manipulating the physicochemical environment. For example, mimicking the niche by culturing on 2D substrates or scaffolds may be achieved by coating the surface with ligands or ECM proteins, immobilising growth factors or applying oxygen gradients. Furthermore, altering the stiffness of the substrate/scaffold itself or imprinting relevant topographies on the surface prior to cell attachment can also more closely mimic the *in vivo* niche (Dalby et al., 2007, McMurray et al., 2011, Dellatore et al., 2008).

As previously discussed, cell-cell communication is important in modulating stem cell behaviour within the niche. To this end, researchers have designed *in vitro* environments to improve the understanding of cell-cell and cell-substrate interactions. Recently, for example, Kim and Kino-oka used polyamidoamine dendrimer (highly branched cascade polymer) immobilised surfaces on polystyrene substrates in the presence of feeder cells, to examine the mechanisms of iPSCs in cell-cell and cell-substrate interactions (Kim and Kino-oka, 2014). The researchers altered the cell-cell and cell-substrate interactions, by increasing the dendrimer density on the substrate and they were able to identify key signalling pathways and transcription factors in self-renewal and cell differentiation (Kim and Kino-oka, 2014).

Research has been conducted to study the physicochemical properties of the MSC stem cell niche by exploring the mechanical properties of the ECM. Altering the stiffness of the material is known to guide MSCs down various differentiation lineages, such as neurogenesis, chondrogenesis and osteogenesis. The pioneering study by Engler & Discher showed the importance of substrate stiffness on MSC differentiation (Engler et al., 2006). Their study showed MSCs seeded on polyacrylamide gels of varying stiffness's (0.1, 1, 11, and 34 kPa) caused neurogenic, myogenic and osteogenic differentiation. Furthermore, Wen et al., found matrix porosity did not induce adipose stromal cell differentiation, but was directly dependent on substrate stiffness (Wen et al., 2014). Additionally, Zhao et al., cultured MSCs directly onto hydrogels of varying stiffness and found the physicochemical properties of the surrounding area were important factors in stem cell differentiation (Zhao et al., 2014b).

## Chapter 1 - Introduction

Zhang and Kilian demonstrated MSC cell shape was also extremely important in maintaining stem cell quiescence, an important facet of MSC behaviour in the niche (Zhang and Kilian, 2013). They were able to control MSC proliferation and maintenance through imprinting nanotopographies on the surface of substrates. The resultant topography directed MSC spreading, focal adhesion formation and cell morphology, thus creating low cytoskeleton tension, which in turn promoted low actomyosin contractility leading to MSC quiescence. Alternatively, nanotopographies may be used to increase stem cell spreading and thus induce osteogenic differentiation (Dalby et al., 2007).

In summary, whilst a great deal of useful information regarding MSC behaviour has been identified through using 2D cell culture models, this technique is too simplistic to aid the description of the full complexity of the special microenvironment. Culturing stem cells in 2D has led to unnatural niche cell morphologies and different functionality compared to the *in vivo* cells. Studies have shown vast differences between cells cultured within a 3D and 2D environment, concerning cell-cell and cell-matrix interactions (Griffith and Swartz, 2006). Furthermore, differences have been shown between cell morphology and receptor expression between the two culturing methods. A study, which investigated non-malignant and malignant epithelial cells, found enormous phenotypic differences between the cells being cultured in 2D and 3D models (Weaver et al., 1997). There were no phenotypic differences between the two cell types, when they were cultured two dimensionally however, the 3D culture assay showed phenotypic discrimination. The researchers found the non-malignant cells formed polarised, growth arrested alveolar structures and the malignant cells produced disordered proliferative amorphous structures (Weaver et al., 1997). Therefore, currently there is a drive to create 3D *in vitro* niche models, which may allow for greater similarity to cellular behaviour and characteristic expression of the *in vivo* MSC niche.

### **1.6.2 Three-dimensional stem cell multicellular spheroid niche models**

Research of *in vitro* 3D cell culture modelling is in its exploratory phase. Table 1-3 summarises current cell research utilising 3D spheroid models.

## Chapter 1 - Introduction

**Table 1-3: Table summarises current studies into 3D spheroid modelling.**

Cell Type	Year	Method	Results	Conclusion	Reference
Ovarian cancer cells	2015	Aggregation by hanging drop	<ul style="list-style-type: none"> <li>- Tightly packed spheroids</li> <li>- Observed cell-cell interaction</li> <li>- High viability</li> <li>- Higher resistance to cis-platin compared to 2D models</li> </ul>	System may be used to: <ul style="list-style-type: none"> <li>- Improve knowledge of ovarian cancer spheroid biology</li> <li>- Perform preclinical drug sensitivity assays</li> </ul>	(Raghavan et al., 2015)
Colon carcinoma cells and breast cancer cells	2015	Aggregation on PVA coated PDMS microfluidic device	<ul style="list-style-type: none"> <li>- Model used to screen anticancer drugs</li> <li>- Varied drug dosages and spheroid size</li> <li>- Found drug susceptibility was lower with increasing tumour size</li> <li>- Spheroids exhibited higher resistance to the drugs compared to 2D cultures</li> </ul>	System may be used to: <ul style="list-style-type: none"> <li>- Screen the anticancer candidates with increased reliability and physiologic accuracy</li> <li>- model drug cytotoxicity</li> <li>- Analyse signalling pathways in drug screening</li> </ul>	(Chen et al., 2015)
MSCs	2015	Self-aggregation with media containing methyl cellulose	<ul style="list-style-type: none"> <li>- Dedifferentiated MSCs in spheroids</li> <li>- Identified Oct4, Nanog and Sox2 levels in 3D MSCs were lower than ESCs</li> <li>- Found 3D MSCs did not reach pluripotency but underwent lineage-restricted dedifferentiation</li> <li>- Identified balanced autophagy as a main mechanism for dedifferentiation</li> </ul>	<ul style="list-style-type: none"> <li>- Mimicked features of blastema formation with MSC spheroids</li> <li>- Model important in improving the understanding of tissue dedifferentiation and regeneration</li> </ul>	(Pennock et al., 2015)
MSCs	2013	Aggregation by membranes made of chitosan or chitosan and hyaluronan (HA)	<ul style="list-style-type: none"> <li>- Up-regulation of N-Cadherin</li> <li>- Increased expression of Wnt genes/ proteins and substrate-dependent cell fate</li> <li>- Identified activated signalling pathways (ERK1/2 or Smad2/3)</li> </ul>	3D platform may be used to: <ul style="list-style-type: none"> <li>- Examine the role of Wnt signalling in controlling MSC fate</li> <li>- Study stem cell behaviour in various environments</li> </ul>	(Hsu and Huang, 2013)

## Chapter 1 - Introduction

			<ul style="list-style-type: none"> <li>- Controlled Wnt signalling by varying the density of HA on chitosan</li> </ul>		
Osteosarcoma cells and breast adenocarcinoma cells	2014	Cells aggregated on agarose-coated plates and then embedded into collagen gels	<ul style="list-style-type: none"> <li>- Largest osteosarcoma spheroids in stiffest gel</li> <li>- Largest adenocarcinoma spheroids in softer gels</li> <li>- Found metabolically active ring of cells on the periphery and non-viable cells in the core</li> <li>- Identified expansile nanoparticles as better delivery of anti-cancer drug compared to bolus delivery</li> </ul>	<p>Created a 3D biomimetic culture platform to:</p> <ul style="list-style-type: none"> <li>- Study basic cancer cell behaviour</li> <li>- Evaluate new anticancer drugs, plus delivery of new anticancer drugs</li> </ul>	(Charoen et al., 2014)
HepG2 cells	2015	Chemically aggregated with NaIO <sub>4</sub> and acrylic acid-modified chitosan (chitosan-AA). Then embedded in hydrogels	<ul style="list-style-type: none"> <li>- Pre-aggregation group produced spheroids in 1 day compared to several days in control group</li> <li>- Spheroids formed in the pre-aggregation group were bigger than control group</li> <li>- Cells in the pre-aggregation group grew and proliferated faster compared to control group</li> </ul>	<ul style="list-style-type: none"> <li>- Developed a new inter-cellular linker- chitosan-AA</li> <li>- Improved cell-cell interaction in pre-aggregated group</li> </ul>	(Liu et al., 2015)
Colorectal cancer cells and fibroblasts	2015	Cells aggregated on agarose-coated plates	<p>Increased fibroblast proliferation and migration in co-cultured spheroids compared to single cancer cell type spheroids</p> <p>Increased fibronectin and EGFR but decreased laminin, <math>\beta</math>-catenin, E-cadherin and type I collagen expression in co-cultured spheroids</p>	<ul style="list-style-type: none"> <li>- Co-culture model mimicked the epithelial-mesenchymal transition state of <i>in vivo</i> tumours in early metastasis</li> </ul>	(Kim et al., 2015)

## Chapter 1 - Introduction

			compared to single cancer cell type spheroids		
Mouse dental papilla cells	2014	Aggregated on low-attachment culture plates	<ul style="list-style-type: none"> <li>- Significantly increased osteoblastic marker gene expression and mineralized nodule formation in spheroids compared to 2D cultures</li> <li>- Identified a proliferating cell-dense peripheral zone and a hypoxic/ apoptotic cell-sparse core zone</li> </ul>	<ul style="list-style-type: none"> <li>- Created an effective formation of homogeneous spheroid colonies and high throughput method</li> <li>- However, the spheroids were small</li> </ul>	(Yamamoto et al., 2014)
MSCs	2012	Forced aggregation and either embedded with gelatin microparticles or left alone	<ul style="list-style-type: none"> <li>- No differences in spheroid size or cell morphology</li> <li>- No differences in cellular spatial organisation</li> <li>- Increased spheroid stiffness with embedded microparticles</li> </ul>	<ul style="list-style-type: none"> <li>- Model may allow the delivery of growth factors in a controlled manner</li> <li>- Microparticles may modulate MSCs physiology to direct cell fate</li> </ul>	(Baraniak et al., 2012)
Fibroblasts, myoblasts and ESCs	2007	Cell aggregation by biotinylation and avidin cross-linking	<ul style="list-style-type: none"> <li>- Aggregate formation was dependent on concentration</li> <li>- Increased aggregation rate of modified ESCs compared to unmodified ESCs</li> <li>- Greater differentiation capacity of engineered ESCs compared to natural ESCs</li> </ul>	<ul style="list-style-type: none"> <li>- Aggregation methodology may be transferred to improve the complexity of other <i>in vitro</i> 3-D spheroid models</li> </ul>	(De Bank et al., 2007)

## Chapter 1 - Introduction

There are various techniques available to create 3D cell culture models and each one has their own advantages and disadvantages. These techniques include forced floating, hanging drop multicellular spheroids, agitation/spheroids, matrices/scaffolds and microfluidic devices (Breslin and O'Driscoll, 2013). There are difficulties creating a realistic *in vitro* niche, because cells need to be encouraged to congregate together, in isolation from the surrounding environment. Most recently, researchers have focused on generating simple 3D models by creating multicellular spheroid structures of stem cells.

The forced floating method allows the cells to congregate together using a non-adhesive substrate material with high nutrient culture media. However, this technique does have limitations, as it takes several days for the aggregates to form and there are issues with the mass production of the spheroids. For example, Cheng et al., used chitosan-coated substrates and formed aggregates with adipose-derived stem cells over 7 days (Cheng et al., 2012). Even though the stem cells expressed high multipotent markers, this method is inefficient because it is labour intensive, as the substrates require non-adhesive coatings.

An alternative method of creating multicellular spheroids is *via* the hanging drop technique. Cells are held in suspension in growth media and then inverted, which suspends the cells in media droplets, forcing the cells to accumulate at the tip of the liquid-air interface. This method has high reproducibility however, it is labour intensive and spheroids are very fragile and fall apart very easily. Therefore, this technique to produce spheroids is impractical for longer-term studies. Bartosh et al., used the hanging drop technique to create 3D MSC spheroids, but the technique was laborious and it took 4 days for the cell aggregates to form (Bartosh et al., 2010).

Another way to create 3D cell cultures is to use mechanical agitation, such as bioreactors or rotational spinning flasks. There are some issues associated with using this technique, as it requires specialised equipment and the cells are exposed to unnatural shear forces within the spinning flasks. Gerlach et al., used a bioreactor system with adipose-derived stem cells and created adipose-like tissue (Gerlach et al., 2012). Also, Alimperti et al., cultured MSCs within spinning flasks to form cell aggregates (Alimperti et al., 2014). However, this

## Chapter 1 - Introduction

method of culturing MSC spheroids requires the use of expensive specialised bioreactors.

One-way to improve the complexity of 3D *in vitro* models involves using a scaffold-based system thus, creating a more realistic *in vitro* environment. A recent study conducted by Souza et al., successfully suspended spheroids in hydrogels using a quick and cost effective method (Souza et al., 2010). They preloaded glioblastoma cells with magnetic iron oxide nanoparticles and placed them in a hydrogel in the presence of an external magnetic field. Even though the cells contain mNPs, studies have shown their incorporation does not affect natural cellular responses (Qin et al., 2013).

MSCs cultured *in vitro* within any of the above 3D spheroids exhibit more realistic and natural cellular characteristics. Therefore, using 3D culture methods provides an excellent environment to probe cell-cell and cell-matrix interactions. For example, MSC spheroids have allowed the intricate study of intercellular adhesion proteins N-cadherin and cadherin-7 (Oberlender and Tuan, 1994, Kim and Rajagopalan, 2010). Close observations of cadherins in a realistic 3D niche model may allow the study of important differentiation pathways associated with cell-cell and cell-matrix interactions (Bratt-Leal et al., 2011). In addition, signalling pathways in MSCs linked to chondrogenesis and osteogenesis have been studied, using 3D MSC spheroids which showed activation of SMAD2/3, ERK1/2, Wnt genes and  $\beta$ -catenin upon differentiation (Hsu and Huang, 2013). Furthermore, studies of MSCs 3D spheroids have demonstrated high multipotency, with cells retaining their stem cell properties far better compared to 2D monolayer culture (Shen et al., 2013). For example, MSC spheroids have shown greater differentiation capabilities by the expression of similar osteogenic and adipogenic markers, compared to conventional 2D culture methods (Baraniak and McDevitt, 2012). Additional studies have found MSC spheroids exhibit significantly greater differentiation capacity, compared to MSCs cultured in the 2D monolayer technique (Huang et al., 2011, Wang et al., 2009). The shift from 2D cultures to 3D spheroids increases the complexity of the environment thus, improving the cellular characteristics observed within an organism Figure 1-10.

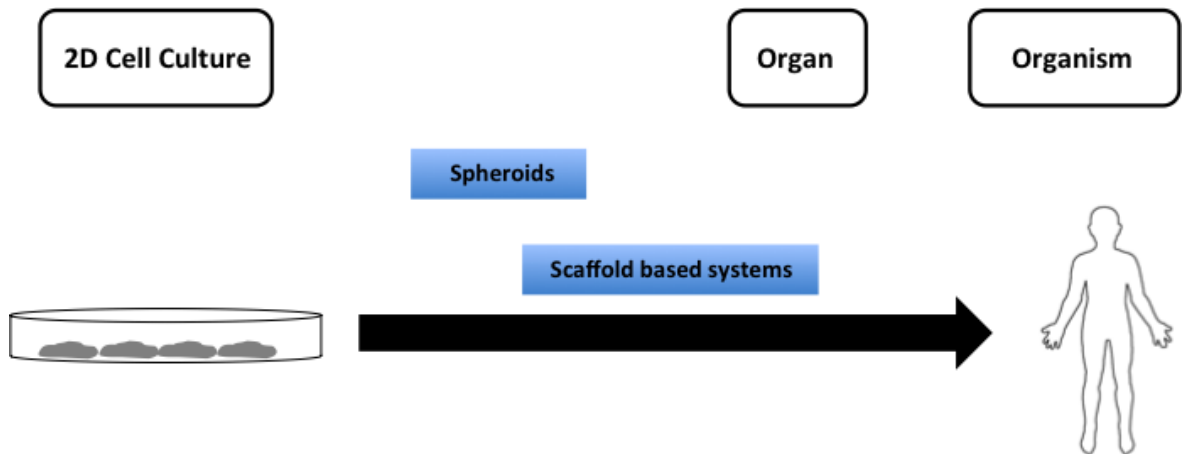


**Figure 1-10: Diagram depicting various 3D culturing techniques.**  
(Adapted from (Page et al., 2013)).

ECM proteins are commonly used to build scaffolds in 3D culture models. Collagen is an ECM protein and the most prevalent protein in the body, making up approximately 25-35% of the total body protein content (Higuchi et al., 2012). Additionally, collagen has been found to be the main component of connective tissue. There are various different types of collagen however, collagen Type I has been found to be the most abundant type, as well as the main constituent of bone, bone marrow, skin and tendons (Campbell and Wicha, 1988, Higuchi et al., 2012). The physical properties of collagen change depending on temperature, due to its thermo-sensitive properties. Collagen has low critical solution temperature properties, allowing it to dissolve in aqueous solutions at low temperatures and stiffen to a gel at  $-37^{\circ}\text{C}$ . The adhesion of MSCs with collagen Type I has shown to involve integrin  $\alpha 1\beta 1$  and  $\alpha 2\beta 1$  receptors on the cell surface (Higuchi et al., 2013).

Research has shown various deficiencies using *in vitro* 3D models. These include fluctuations in the matrix derived from biological specimens, which may lead to unrepeatable and inconsistent experimental data (Tibbitt and Anseth, 2009). Another weakness using 3D models is the increased cost of reproducing large scale and high throughput assays, compared to existing 2D monolayer models, particularly in the drug development industry (Gurski L. et al., 2010). Furthermore, some research has shown a wide variation in size of the spheroids within the same well, which leads to non-uniform results (Wilson and McDevitt, 2013). Also, 3D spheroids show a lack of vascularisation in the model, which is pivotal for assessing drug delivery, in comparison to the *in vivo* environment

(Edmondson et al., 2014). Nevertheless, using collagen Type I within an *in vitro* MSC 3D niche model would provide a realistic *ex vivo* model which mimics the *in vivo* environment.

## 1.7 *In vivo* studies of the stem cell niche

Studying the stem cell niche *in vivo* would provide the most relevant information about the native niche environment within the organism. Unfortunately, research conducted on the MSC niche has been extremely limited due to their low abundance in the bone marrow and diverse range of cell surface marker expression (Shiozawa et al., 2008). However, other stem cell niches have been investigated *in vivo* and has allowed the identification of certain stem cell behaviours, which would not have been determined using *in vitro* models. For example, Rodgers et al., identified two distinct phases ( $G_{Alert}$  and  $G_0$ ) within the quiescent state in the cell cycle of muscle stem cell niche in mice (Rodgers et al., 2014). Using this particular model, the authors were able to confirm the regulatory mechanisms, which were previously suggested with *in vitro* models. Furthermore, the model showed the transition between the two phases was important in stem cell positioning is crucial in determining cell location and allows a rapid response to injury and also plays an active role in niche homeostasis.

Using *in vivo* models has allowed the extensive study of stem cell niche cycling states, identifying active and quiescent phases (Morrison and Scadden, 2014). For example, Kurth et al., detected slow cycling MSCs within the synovium knee joint in injured mice (Kurth et al., 2011). Furthermore, *in vivo* analysis of stem cells in their natural environment has allowed the identification of Wnt signalling functionality in hair follicle stem cells within mice (Lien et al., 2014). This *in vivo* model established T cell factor 3/4 proteins were able to suppress Wnt target genes, as well as perform an active role in stem cell fate.

## 1.8 Magnetic Nanoparticles

During the last decade extensive research has been conducted using magnetic nanoparticles (mNPs) within biomedicine (Berry, 2009). These nanoparticles may

## Chapter 1 - Introduction

be synthesised from magnetic elements such as iron oxide, nickel and cobalt. However, all clinical studies currently use iron oxide as the core metal, as it has high biocompatibility (inertness in the human body) and may be easily manufactured using standard chemical methods. Due to their high reactivity, the core of the nanoparticle is usually coated with either a natural or synthetic biocompatible material, which improves the nanoparticle stability and also confers stealth properties for *in vivo* use (i.e. to evade the reticuloendothelial system). The majority of these mNP coatings are created from polymers such as dextran and polyethylene glycol (PEG), as well as fatty acids. The mNPs may be further functionalised by combining them with target specific cell-targeting ligands or antibodies, as well as tags such as fluorescent dyes, providing both particle monitoring, plus high biological affinity, as shown in Figure 1-11.

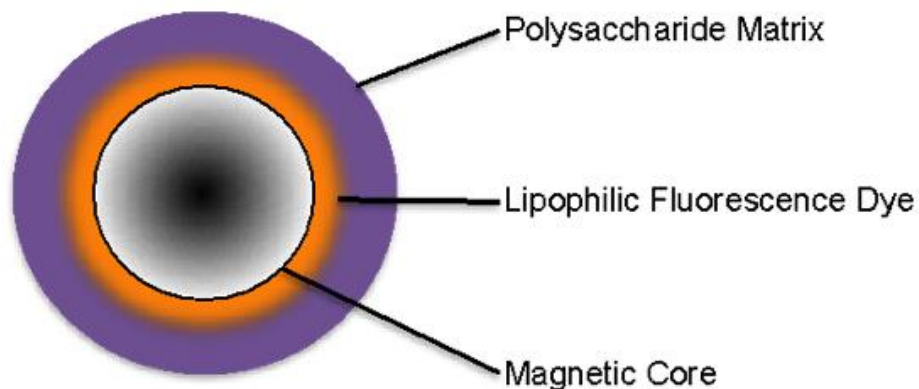


**Figure 1-11: Schematic diagram of a partially functionalised mNP.**  
(Adapted from (Chemicell, 2015)).

There have been issues associated with using mNPs *in vivo*, particularly with their bio-distribution and low tissue specificity within the body. Therefore, there are particular parameters which need to be considered before mNPs may be applied *in vivo*, (e.g. pharmacokinetics, passive targeting and direct targeting) (Prijic and Sersa, 2011). External magnetic fields may be used to increase target specificity and direct the mNPs to a desired location. Furthermore, direct targeting has shown to be improved by the addition of specific antibodies on the mNPs, which causes them to accumulate in the desired tissue (Leuschner et al., 2006).

Iron oxide mNPs consist of a magnetite ( $\text{Fe}_3\text{O}_4$ ) or maghemite ( $\gamma\text{-Fe}_2\text{O}_3$ ) core, and their sub-micron size confers unique thermal, chemical and magnetic properties,

## Chapter 1 - Introduction

which are distinct from the bulk material and therefore makes them excellent diagnostic and therapeutic tools. Furthermore, the particles benefit from their use as contrast agents in magnetic resonance imaging (MRI), because they are inherently trackable (Chang et al., 2013). MNPs have been applied to both *in vitro* and *in vivo* settings, as they respond rapidly to a magnetic field. For example, mNPs have been used in numerous biological applications, ranging from detecting biomolecules in magnetic cell selection, to inducing hyperthermia in malignant cancer tumours (Sun et al., 2008, Chen et al., 2009a, Dejardin et al., 2011). Additionally, cells have been tracked and cell migration has been observed *via* the cellular uptake of mNPs using microscopy and MRI. Fluorescence microscopy has been used to easily observe the mNPs, which have been tagged with a fluorescence probe (Berry, 2009).

### 1.8.1 Cellular uptake and intracellular processing of mNPs

The majority of biomedical applications using mNPs, including MSC spheroid generation, require nanoparticle (NP) ingestion by the cell. Several factors are known to influence cellular uptake, including NP size shape and charge (Chithrani et al., 2006). For example, Chithrani and Chan, demonstrated rod-shaped nanoparticles had a slower rate of cellular uptake compared to spherical nanoparticles (Chithrani and Chan, 2007). The mNPs are uptaken into cells *via* endocytosis, whereby the mNPs are transported into the cell body (Sahay et al., 2010).

Endocytosis may be further sub categorised into either (a) phagocytosis; large particles up to 20  $\mu\text{m}$  are engulfed into the cell, (b) pinocytosis/fluid phase uptake; particles are enveloped by fluids and solutes, transported through the cell membrane and thus absorbed into the cell or (c) receptor mediated endocytosis by either clathrin or caveolin. The exact endocytosis pathway used to uptake mNPs into cells is dependent upon the surface chemistry, size, charge and shape of the NP. Researchers have suggested nanoparticles smaller than 200 nm are endocytosed *via* clathrin vesicles whereas particles between 200 and 1000 nm are engulfed through caveolin-mediated endocytosis (Kelf et al., 2010).

## Chapter 1 - Introduction

MNP cellular uptake may be increased by the application of an external magnetic field. In a method termed 'magnetofection', studies have shown mNP uptake may be increased by culturing cells above an external magnetic field. Zhang et al., applied an external magnetic field to cancer cells in the presence of magnetic, mesoporous silica nanoparticles and observed a 2-fold higher efficiency rate of mNP cellular uptake compared to cells only exposed to mNPs (Liu et al., 2012, Zhang et al., 2010). Essentially, the external magnetic field accelerated the sedimentation of the mNPs on the surface of the cells thus making the mNPs more readily available for endocytosis. Furthermore, Dejardin et al., observed cellular uptake of mNPs was significantly enhanced in the presence of an external magnetic field over an exposure period of 1, 5, 30 and 60 minutes (Dejardin et al., 2011).

### 1.8.2 Nanotoxicology

Studying the niche *in vitro* requires the cells in this environment to behave and possess the same characteristics as the true native niche *in vivo*. Therefore, the internalisation of mNPs must not have a detrimental effect on the intracellular or intercellular mechanisms, as this may provide a misinterpretation of MSC behaviour. Excessive iron ions are known to form oxygen radicals within cells and tissue, causing peroxidative damage to the surrounding area *via* the Fenton reaction. Therefore, the long-term cytotoxic effects of these mNPs require further study.

Shin et al., assessed HeLa cells exposed to a static external magnetic field whilst containing ferromagnetic mNPs (Shin et al., 2012). The researchers found the internalisation mNPs within the cells did not affect morphology or deform the cytoskeleton network, which plays an important role in adhesion and division. Furthermore, cell viability was not affected by the presence of the mNPs within the cells compared to control cells.

Soenen et al., studied the cytotoxic effects of iron oxide mNPs on neural progenitor cells, rat pheochromocytoma cells and human endothelial cells (Soenen et al., 2011). The researchers assessed cell morphology, cell proliferation, induction of reactive oxygen species, cell homeostasis, viability

## Chapter 1 - Introduction

and functionality. Cell morphology was affected at high mNPs concentrations (600 µg/mL) however, at concentrations of 300 µg/mL there were no significant differences in cell surface area compared to the controls. Additionally, focal adhesions, cell cycle progression or cell proliferation were not affected at the 300 µg/mL concentration of mNPs. All the mNPs concentrations used during these experiments did not induce acute cytotoxic effects however, there was a requirement of long-term monitoring of the effects of internalised mNPs in cells.

MSCs incubated with iron oxide mNPs were assessed in both *in vitro* and *in vivo* for cell viability, proliferation, migration and cell homing (Xu et al., 2012). Migration and cell homing of MSCs were monitored in an *in vivo* mouse model and assessed on their ability to migrate and home towards a site of inflammation. The cells containing the mNPs exhibited the same responses as the control cells. The cells containing the mNPs were able to transmigrate to site of inflammation, suggesting that the mNPs did not affect MSC phenotype. Additionally, they found the viability and proliferation of the MSCs were not affected by the incorporation of the mNPs.

Furthermore, Qin et al., showed that adipose-derived stem cells, containing iron oxide mNPs, demonstrated similar cell viability, cell cycle, apoptosis and differentiation capacity compared to non-labelled cells (Qin et al., 2013). The researchers assessed the cells *in vivo* by MRI for 4-8 weeks and found cells migrated to ischemic tissues, thus the cells exhibited native *in vivo* behaviour, without any cytotoxic effects.

The creation of an *in vitro* niche in an *ex vivo* environment, requires the retention of the mNPs within the cells, to form the levitated spheroid, at least until the cells have formed their own cell-cell integrin binding and stabilised the spheroid.

### 1.9 Aims and Objectives

As previously stated in Chapter 1 section 1.6.1, there are numerous issues associated with developing a relevant *in vitro* MSC niche environment. However, the use of a 3D MSC multicellular spheroid may alleviate these problems. A

## Chapter 1 - Introduction

technique whereby cells containing mNPs can be levitated *via* an external magnetic field to form cell spheroids may be adapted to create a MSC niche *ex vivo*. Due to the magnetic properties exhibited by the mNPs, 3D MSC niches created in this way, have the potential to be monitored both *in vitro* (if fluorescently tagged) and *in vivo via* MRI following transplantation. Furthermore, MSC spheroids have shown they are may be easily manipulated using an external magnetic field suggesting, once implanted *in vivo* the spheroids may be moved to a desired location (Kyrtatos et al., 2009). Also, cellular responses within this implanted spheroid niche may be closely observed by tracking the stem cells using MRI.

The MSC niche is known to control stem cell fate by either promoting self-renewal or directing the stem cells to differentiate. Therefore, unravelling the processes and mechanisms within this specialised microenvironment, may enable direct manipulation of the stem cells, to either maintain self-renewal or drive specific differentiation. Enabling artificial control of MSC fate will aid current therapeutic treatments, particularly in the field of tissue regeneration, to create a bank of stem cells or required differentiated cells. Current *in vitro* niche models are too simplistic and do not represent the native niche environment and MSCs are known to differentiate into undesired and unspecific cells.

The aim of this thesis is to create a physiologically relevant 3D biomimetic *in vitro* MSC niche model, using mNPs and collagen gels, which will assess MSC functionality and behaviour. The following objectives will need to be met to achieve the aim.

### 1. Development of a 3D MSC niche model *in vitro* using mNPs.

- Verify mNP uptake into MSCs, *via* an external static field.
- Assess MSC spheroid formation *via* magnetic levitation.

## Chapter 1 - Introduction

- Compare MSC phenotype and quiescence in 3D spheroids with corresponding 2D culture.
- Assess MSC spheroid model in collagen gels to create a more realistic niche model.

### 2. Assess MSC functional behaviour within the 3D spheroid niche model.

- Compare MSC niche model migration response in the presence and absence of an artificial wound.
- Assess differentiation capabilities of MSC niche model in a scratch wound assay.

### 3. Identify MSC migratory signals in the 3D niche model.

- Determine cytokine release profile from an osteoblast and fibroblast scratch wound assay.
- Assess MSC migratory response in the 3D niche model following exposure to specific cytokines.

# CHAPTER 2

## 2 Materials and methods

**Table 2-1: A List of materials reagents and suppliers used throughout all experiments. (\*Preparation methods of solutions are described in detail in Section 2.1).**

Materials/Reagents	Supplier(s)
<b>1. Cells</b>	
Human bone marrow MSCs	Promocell GmbH, Germany and Southern General Hospital, UK
Infinity telomerase-immortalised primary human fibroblasts (h-TERT-BJ1)	Clontech Laboratories Inc., USA
Human primary osteoblast cells	Promocell GmbH, Germany
<b>2. Nanoparticles</b>	
200 nm sized mNPs coated in polydimethylamine (PEA)	Chemicell GmbH, Germany
200 nm sized mNPs coated in PEA-FITC tag	Chemicell GmbH, Germany
<b>3. Cell Culture</b>	
Dulbeccos modified eagle medium (DMEM)	Sigma-Aldrich, UK
Medium 199	Sigma-Aldrich, UK
Foetal bovine serum (FBS)	Sigma-Aldrich, UK
Penicillin-streptomycin	Sigma-Aldrich, UK
MEM Non-essential amino acids	Sigma-Aldrich, UK
L-glutamine 200 mM	Invitrogen, UK
Sodium pyruvate	Life Technologies, UK
Ascorbate-2-phosphate	Sigma-Aldrich, UK
Dexamethasone	Sigma-Aldrich, UK
Insulin	Sigma-Aldrich, UK
Indomethacin	Sigma-Aldrich, UK
Isobutylmethylxanthine	Sigma-Aldrich, UK
Trypsin	Sigma-Aldrich, UK
Versene*	In house
Trypsin/versene solution*	In house
Sodium Chloride (NaCl)	VWR Chemicals, UK

## Chapter 2 - Material and Methods

Potassium Chloride (KCl)	VWR Chemicals, UK
Glucose	Fisher Scientific, UK
HEPES	Fisher Scientific, UK
Ethylenediaminetetraacetic acid (EDTA)	Sigma-Aldrich, UK
Phenol Red solution 0.5%	Sigma-Aldrich, UK
HEPES solution	In house
EasySep™ Human CD271 Selection Kit	StemCell Technologies, France
Ficoll-Paque™ PREMIUM	GE Healthcare, UK
Rat Tail Collagen Type I, > 2 mg/mL	First Link Ltd., UK
10X MEM	First Link Ltd., UK
0.1 M sodium hydroxide (NaOH)	Sigma-Aldrich, UK
<b>4. Electron Microscopy</b>	
Gluteraldehyde (25% aq pure, EM Grade)	Sigma-Aldrich, UK
Sodium cacodylate	Agar Scientific Ltd, UK
Osmuim tetroxide	Agar Scientific Ltd, UK
Aqueous uranyl acetate	Agar Scientific Ltd, UK
Ethanol	VWR Chemicals, UK
Methanol	VWR Chemicals, UK
Propylene oxide	VWR Chemicals, UK
Epon resin araldite (812 Kit E202)	TAAB Lab Equipment Ltd UK
Uranyl acetate	Sigma-Aldrich, UK
Reynolds lead citrate	Agar Scientific Ltd, UK
<b>5. Cell Staining</b>	
PBS	Sigma-Aldrich, UK
Formaldehyde (38%)	Fisher Scientific, UK
Sucrose	Fisher Scientific, UK
Magnesium Chloride ((MgCl <sub>2</sub> ) hexahydrate)	VWR Chemicals, UK
Triton X	Sigma-Aldrich, UK
BSA	Sigma-Aldrich, UK
LIVE/DEAD® Viability/Cytotoxicity kit	Invitrogen, UK
anti-BrdU antibody kit	GE Healthcare, UK
Rhodamine-phalloidin	Invitrogen, UK

## Chapter 2 - Material and Methods

Vectashield-DAPI	Vector laboratories, USA
Primary antibodies	Abcam, UK and Santa Cruz biotechnologies, USA
Biotinylated secondary antibodies	Vector laboratories, USA
Unbiotinylated secondary antibodies-Texas Red	Vector laboratories, USA
Streptavidin-FITC/Texas Red	Vector laboratories, USA
0.5% Tween 20 in PBS*	In house
Tween 20	Sigma-Aldrich, UK
Oil Red O	Sigma-Aldrich, UK
Triethyl phosphate	Sigma-Aldrich, UK
Mayer Haematoxylin solution	Sigma-Aldrich, UK
<b>6. ICP-MS</b>	
RIPA buffer*	In house
TRIZMA® base	Sigma-Aldrich, UK
Sodium deoxycholate	Sigma-Aldrich, UK
Sodium dodecyl sulfate (SDS (1%))	VWR Chemicals, UK
<i>aqua regia</i> *	In house
Concentrated nitric acid	VWR Chemicals, UK
Concentrated hydrochloric acid	Fisher Scientific, UK
<b>7. RNA Isolation</b>	
TRIzol	Life Technologies, UK
Chloroform	Sigma Aldrich, UK
Glycoblu	Ambion, UK
Isopropanol	Sigma Aldrich, UK
RNase free water	Qiagen, UK
RNeasy micro kit	Qiagen, UK
Primers	Eurofins Genomics, Luxembourg
SuperScript III Reverse Transcriptase	Invitrogen, UK
2x TaqMan PreAmp Master Mix	Applied Biosystems, UK
2x SsoFast EvaGreen Supermix	Bio-Rad
RNaseOUT Recombinant RNase inhibitor	Invitrogen, UK
DNA suspension buffer	Life Technologies, UK
Exonuclease I Reaction Buffer	New England Biolabs, UK

Exonuclease	New England Biolabs, UK
BioMark, 20x DNA Binding Dye sample loading reagent	Fluidigm Corporation, USA
<b>8. Cytokine analysis</b>	
Pro Human Cytokine Group I, 5-plex Assay Kit	Bio-Rad, UK
Human IL-6 full length protein	Abcam, UK

## 2.1 Cell Culture Solutions

### Modified alpha-MEM (stem cell growth media)

DMEM	500 mL
FBS	50 mL
Penicillin-streptomycin	10 mL
MEM non-essential amino acids	5 mL
Sodium pyruvate	5 mL

### Modified DMEM (standard growth media)

DMEM	400 mL
Medium 199	100 mL
FBS	50 mL
Penicillin-streptomycin	10 mL
L-glutamine 200 mM	5 mL
Sodium pyruvate	5 mL

### Versene

Water	1000 mL
NaCl	8 g
KCl	0.4 g
Glucose	1 g
HEPES	2.38 g
EDTA	0.2 g
0.5% phenol red	2 mL
Adjusted to pH 7.5	

### Trypsin/versene solution

Versene (In house solution)	20 mL
Trypsin	0.5 mL

## Chapter 2 - Material and Methods

**PBS solution**

PBS	1 tablet
Water	200 mL

**Cell Fixation buffer**

PBS solution	90 mL
Formaldehyde (38%)	10 mL
Sucrose	2 g

**Cell Permeability buffer**

PBS solution	100 mL
Sucrose	10.3 g
NaCl	0.292 g
MgCl <sub>2</sub> hexahydrate	0.06 g
HEPES	0.476 g
Adjusted to pH 7.2	
Triton X	0.5 mL

**0.5% Tween 20 in PBS**

PBS solution	100 mL
Tween 20	0.5 mL

**RIPA lysis buffer**

Water	45 mL
NaCl	0.44 g
TRIZMA® base	0.3 g
Triton X	0.5 mL
Sodium deoxycholate (1%)	0.5 g
SDS (1%)	0.05 g
Make up to 50 mL with water	

***Aqua Regia***

Concentrated nitric acid	10 mL
Concentrated hydrochloric acid	30 mL

## **2.2 Cell Culture**

### **2.2.1 General Protocol**

The hMSCs were cultured in T75 flask with modified alpha-MEM media at 37°C with 5% CO<sub>2</sub>. Once the cells were confluent, the media was removed and the cells were washed with HEPES solution. Cells were detached from the surface using trypsin/versene (2 minutes at 37°C). Fresh media was added to the flask to neutralise the active trypsin, and the cell suspension was centrifuged for 4 minutes at 1400 rpm. After centrifugation, the supernatant was removed leaving a pellet of cells. The cells were re-suspended in fresh media and seeded into appropriate wells for experiments.

The same protocol was followed for other cells types including h-TERT fibroblasts and primary osteoblasts, except using different culture mediums for h-TERTs and primary osteoblasts. H-TERTs were cultured with modified-DMEM whereas, primary osteoblast were cultured with modified alpha-MEM.

### **2.2.2 Bone Marrow extraction**

Each bone marrow sample was divided into two and centrifuged for 10 minutes at 1400 rpm. Any bone chips were placed into flasks containing modified alpha-MEM media. The supernatant was removed and the pellet was re-suspended in 10 mL fresh media; the cell suspension was centrifuged (10 minutes at 1400 rpm). The media was removed and the pellet was re-suspended in 10 mL fresh media; the cell suspension was slowly overlaid onto 7.5 mL Ficoll-Paque™ PREMIUM and then centrifuged for 45 minutes at 1513 rpm. The middle layer was extracted and placed in a new tube containing 10 mL fresh media, which was then centrifuged for 10 minutes at 1400 rpm. The supernatant was removed and the pellet was re-suspended in 10 mL fresh media, followed by centrifugation for 10 minutes at 1400 rpm. The supernatant was removed and the pellet was re-suspended in 10 mL fresh media and then placed in a vented flask at 37°C with 5% CO<sub>2</sub>.

### 2.2.3 CD271 positive selection from bone marrow extracts

The EasySep™ Human CD271 Selection Kit was used to isolate CD271<sup>+</sup> MSCs. Once the cells were confluent, the media was removed and the cells were washed with HEPES solution. Cells were detached using trypsin/versene (2 minutes at 37°C). Fresh media was added to the flask and the cell suspension was centrifuged for 4 minutes at 1400rpm. After centrifugation, the supernatant was removed leaving a pellet of cells. The cells were re-suspended in 500 µL 2% FBS/1xPBS and the mixture was added to a round bottom tube. Fc receptor blocker (12 µL) was added to the tube, followed by the addition of CD271<sup>+</sup> (25 µL) selection cocktail, for 15 minutes at room temperature. 2.5 mL of 2% FBS/1xPBS was thoroughly mixed with the cell solution. The tube was placed in the magnet block for 5 minutes at room temperature and subsequently inverted for 2 seconds. The tube was removed from the magnet block and 2.5 mL of 2% FBS/1xPBS was thoroughly mixed with the cell suspension. The tube was placed in the magnet block for a further 5 minutes at room temperature and inverted for 2 seconds to remove the solution. This process was repeated once more and then the cells were re-suspended in 500 µL of fresh media, before being smeared across the centre of a vented flask. The flask was left for 30 minutes (37°C/5% CO<sub>2</sub>), at which point 10 mL fresh media was added to the flask.

The maximum number of passages used MSCs collected from Southern General Hospital, Glasgow was 3.

## 2.3 Cell Culturing Methods

### 2.3.1 Optimising Magnetic Nanoparticle Uptake into Cells

hMSCs were seeded at a concentration of  $1 \times 10^4$  cells/cm<sup>2</sup> directly onto sterile glass coverslips (13 mm diameter) in a 24 well plate and left overnight to adhere (37°C/5% CO<sub>2</sub>). The media was removed and exchanged for 1 mL of magnetic nanoparticles (mNPs) diluted in fresh alpha-MEM media (0.01 mg/mL or 0.1 mg/mL), and incubated for 15 minutes, 30 minutes or 1 hour in the presence or absence of a magnetic field of 350 mT (24 magnet array from Chemicell, placed beneath the 24 well plate). Cells cultured in media for 1 hour were used as

## Chapter 2 - Material and Methods

control samples. Optimised conditions were 0.1 mg/mL mNPs concentration for 30 minutes with a magnetic field.

### 2.3.2 Type I collagen gel formation

#### 2.3.2.1 Collagen gel formation

The following described preparation allows for three gels. 0.5 mL fresh alpha-MEM media with 0.5 mL 10xDMEM and 0.5 mL FBS added stepwise to each cell suspension. 2.5 mL acetic acid solubilised collagen Type I, and 1 mL 0.1 M NaOH were mixed homogeneously, then added to the cell suspension mixture; 0.1 M NaOH was subsequently added drop wise to the to neutralise the solution, which turned pink (*via* phenol red indicator in the media). The suspension was then added to the appropriate wells and allowed to gel during incubation at 37°C with 5% CO<sub>2</sub> for the required experimental period. Media was changed with fresh media twice weekly.

#### 2.3.2.2 Collagen gel formation with cells

The same procedure described above was followed whereas, 0.5 mL cell suspension in fresh alpha-MEM media was used instead of 0.5 mL fresh alpha-MEM media. Cells were pre-loaded with mNPs as described in Section 2.3.1.

### 2.3.3 Monolayer Culture

hMSCs were seeded at a concentration of  $3 \times 10^4$  cells/cm<sup>2</sup> and left overnight (37°C/5% CO<sub>2</sub>). The media was removed and exchanged for 1 mL of mNPs diluted in fresh alpha-MEM media (0.1 mg/mL), and incubated for 30 minutes in the presence of a magnetic field. Cells were washed with HEPES followed by trypsinisation with trypsin/versene and centrifuged at 1400 rpm for 4 minutes. The supernatant was removed and pellet re-suspended in media, re-seeded onto sterile glass coverslips (13 mm diameter) for the appropriate incubation period. Media was changed twice weekly.

### **2.3.4 Spheroid Culture**

#### **2.3.4.1 MSC Spheroid Culture in Media**

The preparation described below generates two spheroids. Following incubation with the mNPs, the cells ( $1 \times 10^4$  cells/cm<sup>2</sup>) were trypsinised, pooled together and centrifuged at 1400 rpm for 4 minutes. All control cells (i.e. without mNPs) were also pooled together and centrifuged at 1400 rpm for 4 minutes. The cells were re-suspended in 1 mL fresh and 0.5 mL of cell suspension was added to 4 mL fresh media in a well (6 well plate). A single magnet (13 mm diameter, 350 mT) was either placed on the top or the bottom of the well and the plate was incubated at 37°C with 5% CO<sub>2</sub> for the required experimental period.

#### **2.3.4.2 MSC Spheroids in Type I Collagen gels**

Spheroids were prepared as previously discussed in Section 2.3.4.1. After 24 hours, the spheroids were added to the gel mixture described above in section 2.3.2, but without the addition of the cells in the initial stages.

## **2.4 Statistical Analysis**

GenStat software version 15 (VSN International, UK) was used to determine the statistical significance of each statistical analysis. The analysis of variance (ANOVA) was performed using either one-way ANOVA or two-way ANOVA tests depending on the sample set. The statistical significance of the results was determined by calculating the probability of a null hypothesis being true, using a pre-specified threshold (p-value). If the level of confidence was lower than 5% (p-value  $\leq 0.05$ ), the null hypothesis was rejected and the result was classed as being statistically significant. The embedded statistical analysis in Microsoft Office Suite version 2013 (excel) was used to calculate the mean and standard deviation of each experiment.

## **2.5 Research colleagues**

David Stirling, University of West Scotland, operated the equipment to obtain ICP-MS results. TEM samples were sectioned by Margaret Mullin, Electron Microscopy Facility, University of Glasgow. Monolayer samples were stained Oil

## Chapter 2 - Material and Methods

Red O by Lynn Robertson from the Veterinary Diagnostic Services Laboratory, University of Glasgow.

# CHAPTER 3

## **3 The Development of an *In vitro* Mesenchymal Stem Cell Niche Model**

### **3.1 Introduction**

#### **3.1.1 The Bone Marrow Niche Microenvironment**

The bone marrow niche environment has a fundamental role in controlling mesenchymal stem cell behaviour, by either regulating stem cell fate through the promotion of self-renewal or directing stem cell differentiation. The niche dynamically regulates these processes by balancing MSC quiescence, proliferation and differentiation. As described in section 1.4, the MSC niche environment is comprised of various components, including MSC niche cells, support cells (pericytes), growth factors (e.g. FGF, HGF, VEGF and TGF- $\beta$ ), ECM proteins (e.g. collagen, fibronectin, laminin and proteoglycans), signalling molecules (e.g. cytokines, CXCL-12, and SCF), as well as HSCs, endothelial cells, adipocytes and macrophages. The interactions between the cells and the surrounding ECM environment are important in preserving a MSC pool to maintain homeostasis and tissue regeneration, throughout the species lifetime. The ECM is important in maintaining the stem cell niche, because its composition and properties (structural, mechanical, biochemical and physical), allow for signal transmission and interaction with the stem cells. Additionally, the ECM anchors stem cells in the niche and binds growth factors, which diffuse to the stem cells and regulate stemness as well as differentiation.

#### **3.1.2 3D *In Vitro* Bone Marrow Niche Models**

Recently, there has been huge interest in exploiting the MSC niche to develop novel therapeutic regenerative medicines. Harnessing the specialised microenvironment properties and understanding the regulatory signals within the niche may lead to direct manipulation of stem cells, allowing external control over their fate. The knowledge gained from this research is very important because MSCs possess interesting immunomodulatory and differentiation properties. Controlling MSC fate within bone marrow niche models may allow, for example, the creation of a multipotent stem cell bank ready to use for transplants. Additionally, directing the MSCs to differentiate down a specific

lineage, for example towards osteoblasts, to correct bone defects such as osteoporosis or osteoarthritis.

In the past there has been limited research conducted on the MSC niche and there is scant information regarding cellular communication between cells and the extracellular environment (see section 1.4.1). Therefore, creating *in vitro* models of the MSC niche would allow for detailed studies into these processes.

Initially, 2D *in vitro* models have been employed using various substrates, with surfaces coated in ECM proteins including collagen and fibronectin, as well as different growth factors to simulate the *in vivo* niche. However, these models have been described as too simplistic as they lack the 3D niche structure, represented within the bone marrow. Most cell types, including MSCs are known to express different receptors and exhibit different cell morphologies when cultured in 2D models compared to 3D model techniques. Therefore, recently there has been a shift from using 2D to 3D culturing methods, to create a more realistic model.

There are various methods involved in creating 3D MSC niche models however, the use of multicellular spheroids has been described as an effective and efficient technique. Typical protocols for generating spheroids, including hanging drop or mechanical agitation, were summarised in section 1.6.2. This chapter aims to adapt a recently described protocol, which coerces cells to clump together to create spheroids using magnetic nanoparticles (mNPs). The internalisation of mNPs within cells has allowed direct cell manipulation through the application of an external magnetic field. Previous studies have shown the incorporation of iron oxide mNPs within the MSCs does not affect phenotypic and the characteristic behaviour of these cells (Arbab et al., 2005, Farrell et al., 2008). Additionally, increasing the complexity of the model has been achieved by incorporating spheroids into collagen gel scaffolds.

MSCs within the bone marrow niche, express certain phenotypic characteristics. In an unstimulated niche, the MSCs remain in a low metabolic and quiescent state, until they become stimulated by external factors. These MSCs express high multipotency (e.g. STRO-1 and nestin) markers, which are indicative of the cells retaining their stem cell properties. However, upon stimulation *via*

osteogenic and adipogenic induction, the MSCs are directed to differentiate and express osteogenic or adipogenic characteristics. Monitoring these phenotypic characteristics or markers will provide an insight into whether the MSCs within this 3D niche model are mimicking their innate environment.

### 3.2 Objectives

This chapter aims to develop a new 3D MSC niche model *in vitro*, which mimics the native *in vivo* bone marrow niche. The generation of a more physiologically relevant 3D model may allow native cellular responses and will facilitate a detailed study in isolation, to observe cellular events in this milieu. If successful, the model will enable the study of niche regulatory signals, as well as both cell-cell and cell-extracellular matrix signalling. Understanding these processes will further develop the artificial manipulation of niche MSCs to produce the desired response or behaviour.

These objectives will be achieved through the following stages *via*:

- Pre-loading a MSC monolayer with mNPs, assessing mNP uptake and retention, as well as subsequent MSC movement to an external magnetic field.
- The creation of 3D MSC spheroids utilising mNP-loaded cells. MSC viability, phenotypic characteristics, cell cycle state and differentiation capacity will be assessed and compared with monolayer cultures over time.
- The incorporation of MSC spheroids into Type I collagen gel scaffolds to mimic the bone marrow environment, with assessment of the model's mechanical properties.

### 3.3 Materials and Methods

#### 3.3.1 Cell culture and Magnetic Nanoparticle Incubation

All results shown within this thesis used MSCs bought from Promocell, Germany. However, initial data collected but not displayed within the thesis used MSCs from patients at the Southern General Hospital, Glasgow. Cells were cultured as monolayers, spheroids and/or as spheroids encapsulated within Type I collagen gels in all experiments in this chapter. The cells cultured in this way were prepared as previously discussed in Chapter 2, section 2.3.3 and 2.3.4. The mNPs (200 nm) were purchased from Chemicell and they consisted of a magnetite core ( $\text{Fe}_3\text{O}_4$ ) coated in poly (ester amide) (PEA) with a FITC green fluorescent tag (see Figure 3-1).

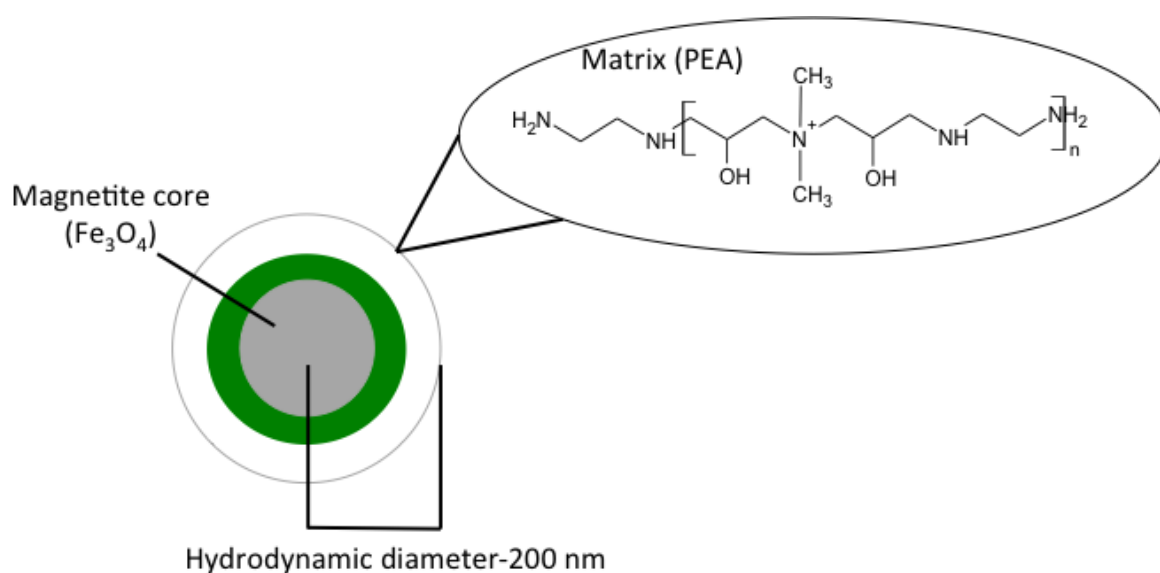


Figure 3-1: Schematic diagram of the fluorescent mNPs employed in the project. (Adapted from Chemicell (Chemicell, 2015)).

#### 3.3.2 Magnetic Nanoparticle Uptake into MSCs

##### 3.3.2.1 Inductively Coupled Plasma-Mass Spectrometry (ICP-MS)

ICP-MS was used to quantitatively assess the uptake of mNPs into MSCs in monolayer culture. The mNPs consisted of an iron oxide core therefore, the ICP-MS elemental analysis of the iron within each sample, served as a direct correlation to the amount of mNPs taken up within the MSCs. This mNP uptake allowed for quantification and optimisation of mNP loading into cells.

Following incubation with the mNPs, cells were washed with 1xPBS. The PBS was then removed and 400  $\mu$ L of RIPA buffer was added for 10 minutes at room temperature. The buffer was removed from the wells, then added to allocated tubes. Each well was washed with 100  $\mu$ L distilled water, then transferred to each relevant tube. Subsequently, 1 mL of *aqua regia* was added to each tube and the tube was incubated at 70°C overnight. The next day, each tube was made up to 50 mL with distilled water ready for analysis by ICP-MS (THERMO X Series III).

### 3.3.2.2 Transmission Electron Microscopy (TEM)

TEM was used to qualitatively verify mNP uptake of MSCs in the monolayer culture, as well as allowing the study the location of nanoparticles within the cells.

Following incubation with the mNPs, the media was removed and cells were fixed in 1.5% glutaraldehyde/0.1M sodium cacodylate (1 hour at 4°C). The wells were subsequently washed with 0.1M sodium cacodylate, post fixed then stained with 1% osmium tetroxide/1xPBS (1 hour at room temperature). The cells were washed with distilled water, stained in 0.5% aqueous uranyl acetate (1 hour at room temperature) then washed with distilled water. The cells were dehydrated using increasing levels of alcohol concentrations (30%, 50%, 70%, 90%, 100% and 100% (absolute)) for 10 minutes at each step. Samples were left in propylene oxide: Epon resin araldite/812 mix (1:1) overnight. The next day, samples were placed into pure resin and cured for 24 hours at 60°C. Ultrathin sections were stained with 2% methanolic uranyl acetate and Reynolds lead citrate, ready for analysis using Leo 912 AB TEM at 120kV.

### 3.3.3 Observing Cells via Fluorescence Microscopy

MSCs were seeded into a 24 well plate, at a concentration of  $1 \times 10^4$  cells/cm<sup>2</sup> and left overnight (37°C/5% CO<sub>2</sub>). The media was removed and 1 mL of 0.1 mg/mL mNPs were added to the wells and incubated for 30 minutes in the presence of a magnetic field (control cells did not contain mNPs).

### 3.3.3.1 Cell viability staining

After the appropriate incubation period the cells, which were either in media or collagen gel, were assessed for cell viability, by preparing 1 mL of fresh alpha-MEM media containing 1  $\mu$ L calcein AM and 1  $\mu$ L ethidium homodimer. This media was added to the cultures then incubated for 1 hour at 37°C. Subsequently, the cells or gels were washed three times with fresh media and analysed immediately using a Zeiss Axiovert 200M fluorescent microscope.

### 3.3.3.2 Actin staining

**Monolayer Cell Cultures:** Following the addition of mNPs and after the appropriate incubation period, the cells were washed with 1xPBS, fixed for 15 minutes at 37°C, permeabilised for 5 minutes at 4°C, then 1% BSA/1xPBS was added to each well for 5 minutes at 37°C. F-actin was stained using rhodamine-phalloidin (1:500 in 1% BSA/1xPBS) for 1 hour at 37°C. The cells were washed with 0.5% Tween 20/1xPBS and mounted onto slides with DAPI (to stain DNA). Images were taken using a Zeiss Axiovert 200M fluorescent microscope.

**Collagen Gel Cell Cultures:** Cell samples, prepared in a gel environment, were treated similarly and images were taken using either a Zeiss Axiovert 200M fluorescent microscope or a Zeiss Axiovert 200M confocal microscope, collecting sequential images every 20  $\mu$ m through the gel, to create a z-stack.

### 3.3.3.3 STRO-1 and nestin staining

Following mNP incubation, the cells were washed with 1xPBS, fixed for 15 minutes at 37°C, permeabilised for 5 minutes at 4°C, then 1% BSA/1xPBS was added to each well for 5 minutes at 37°C. Subsequently, 1 mL of anti-STRO-1 or anti-nestin (1:50 in 1% BSA/1xPBS) was added for 1 hour at 37°C, washed with 0.5% Tween 20/1xPBS, and 1 mL of biotinylated secondary (1:50 in 1% BSA/1xPBS) was added and incubated for 1 hour at 37°C. The cells were washed with 0.5% Tween 20/1xPBS, and finally 1 mL of streptavidin-Texas Red (1:50 in 1% BSA/1xPBS) was added to each well for 30 minutes at 4°C. Following washing in 0.5% Tween 20/1xPBS, cells were mounted with DAPI. Cells were analysed by Zeiss Axiovert 200M fluorescent microscope.

#### **3.3.3.4 BrdU staining**

Following mNP incubation, 6 hours prior to fixing the cells, 1 mM BrdU solution in alpha-MEM was added to each well. The cells were washed with 1xPBS, fixed for 15 minutes at 37°C, permeabilised for 5 minutes at 4°C, then 1% BSA/1xPBS was added to each well for 10 minutes at 37°C. Subsequently, 1 mL of anti-BrdU (1:100 in DNase) was added for 2.5 hours at 37°C, washed with 0.5% Tween 20/1xPBS, and 1 mL of secondary-Texas Red (1:50 in 1% BSA/1xPBS) was added and incubated for 1 hour at 37°C. The cells were washed with 0.5% Tween 20/1xPBS, and finally mounted with DAPI. Cells were analysed using Zeiss Axiovert 200M fluorescent microscope.

#### **3.3.3.5 Calculated Fluorescent Intensity**

All fluorescent images analysed by fluorescent intensity were calculated using ImageJ, which has been created by the National Institute of Health, U.S Department of Human and Health Services.

#### **3.3.4 Rheology analysis of the gels**

Gels were prepared with or without MSC spheroids and analysed after 3 days incubation. Analysis was carried out at 25°C within a heat controlled environment and with a parallel plate (20 mm diameter). Additionally, a solvent trap was used to minimise solvent evaporation thus, creating a saturated internal atmosphere. A strain sweep of the gels was initially used to ensure elastic modulus ( $G'$ ) and viscous modulus ( $G''$ ) measurements were taken within the linear viscoelastic region. Frequency sweeps of the gel were carried out between 0.1 and 40 Hz to determine the dynamic modulus of the gel. All analysis was conducted using a Malvern Kinexus rheometer.

#### **3.3.5 Induced differentiation of MSCs via osteogenesis and adipogenesis**

**Monolayer Cultures:** Following unlabelled mNP incubation, cells were cultured for the first 8 days in modified alpha-MEM. Subsequently, the media was changed to either osteogenic induction media (DMEM, 10% FBS, 2% antibiotics, 350 mM ascorbate-2-phosphate and 0.1  $\mu$ M Dexamethasone) or adipogenic induction

media (DMEM, 10% FBS, 2% antibiotics, 1  $\mu$ M Dexamethasone, 1.7 nM insulin, 200  $\mu$ M indomethacin, 500  $\mu$ M isobutylmethylxanthine)/adipogenic maintenance media (DMEM, 10% FBS, 2% antibiotics, 1.7 nM insulin) and incubated for 28 days. The adipogenic induction media and maintenance media was alternated every 2/3 days. The timeline is depicted in Figure 3-2.

**Spheroid Cultures:** Spheroids were cultured for 7 days in modified alpha-MEM. The spheroids were pooled together and centrifuged for 4 minutes at 1400 rpm, the supernatant was removed and the pellet was re-suspended in modified alpha-MEM. The cells were reseeded as monolayers and left for 72 hours. The media was removed and either osteogenic induction media or adipogenic induction/adipogenic maintenance media was added for 3 times a week for the next 42 days. The timeline is depicted in Figure 3-2.

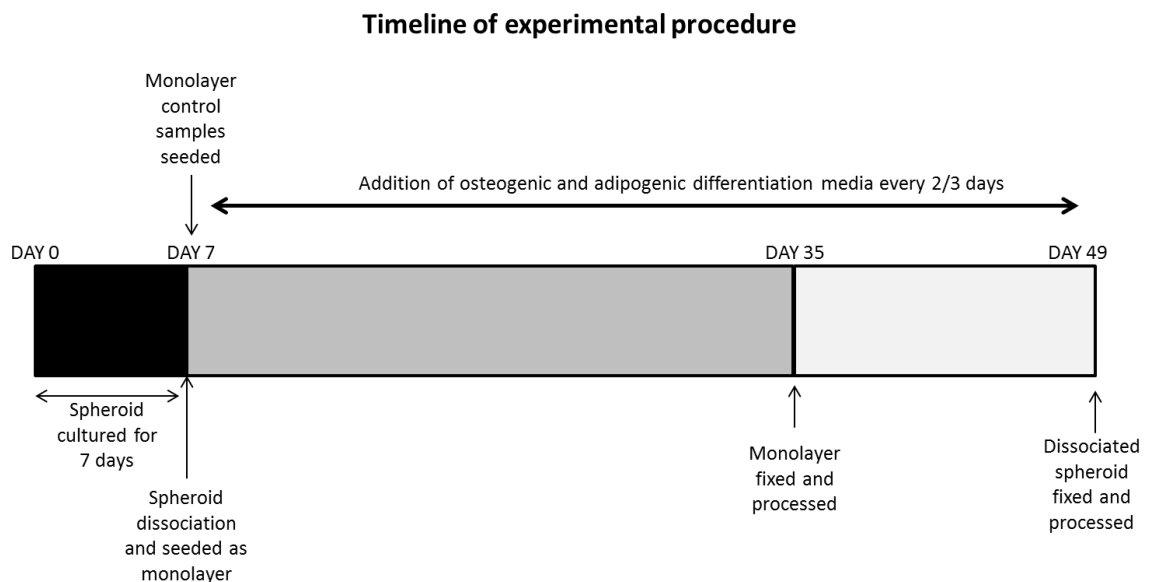


**Figure 3-2: Timeline of experimental procedure used to induce differentiation in MSCs with osteogenic and adipogenic media.**

**Oil Red O stain (assessing adipogenesis):** A solution of 10 mg/mL Oil Red O in 60% triethyl phosphate (aq) was prepared. The cells were washed with 1xPBS, fixed for 15 minutes at 37°C. The fixative was removed and cells rinsed with 60% triethyl phosphate (aq). This solution was removed and Oil Red O solution was added to the cells (room temperature for 10 minutes). Oil Red O was removed and cells rinsed with 60% triethyl phosphate (aq). Filtered Mayer Haematoxylin solution was added (room temperature for 2 minutes) to the cells then rinsed

with tepid tap water. Cells were mounted onto slides and analysed using Zeiss Axiovert 25 light microscope.

**Osteopontin stain (assessing osteogenesis):** Following mNP incubation, the cells were washed with 1xPBS, fixed for 15 minutes at 37°C, permeabilised for 5 minutes at 4°C, 1% BSA/1xPBS was added to each well for 5 minutes at 37°C. Subsequently, 1 mL of anti-osteopontin (1:50 dilution) with phalloidin-rhodamine (1:500 dilution) in 1%BSA/1xPBS was added for 1 hour at 37°C, washed with 0.5% Tween 20/1xPBS, and 1 mL of biotinylated secondary (1:50 in 1% BSA/1xPBS) was added and incubated for 1 hour at 37°C. The cells were washed with 0.5% Tween 20/1xPBS, and finally 1 mL of streptavidin-Fluorescein (1:50 in 1% BSA/1xPBS) was added to each well for 30 minutes at 4°C. Following washing in 0.5% Tween 20/1xPBS, cells were mounted with DAPI. Cells were analysed using Zeiss Axiovert 200M fluorescent microscope.

### 3.3.6 RNA isolation

Analysis was conducted on cells cultured as monolayer or spheroid culture systems for either 1 or 14 days. For the monolayer cultures, three samples were pooled for each replicate (n=3), whereas; for the spheroid cultures, six samples were pooled for each replicate (n=3).

A Qiagen RNeasy micro kit was used during this experimental setup. After the appropriate incubation period, cells were lysed with TRIzol (1 mL) for 10 minutes at room temperature and then centrifuged at 4°C (12 000 g for 15 minutes). The supernatant was transferred and mixed thoroughly with 200 µL chloroform and incubated at room temperature (3 minutes). The mixture was centrifuged at 4°C (12 000 g for 15 minutes) and the aqueous phase was removed, then glycoblue (1 µL) and isopropanol (500 µL) was added to the solution. The Eppendorf tubes were inverted several times, and then incubated at room temperature (10 minutes), followed by centrifugation at 4°C (12 000 g for 20 minutes). The supernatant was removed leaving a blue pellet, which was vortexed with 1 mL ethanol (25% aq), then centrifuged 4°C (7 500 g for 5 minutes). The ethanol was removed to air dry the pellet, then RNase-free water (20 µL) was added and the samples were incubated at 55°C (10 minutes). Each sample was made up to 350 µL with buffer RLT and vortexed then 70% ethanol (350 µL) was added and mixed

thoroughly, then transferred to a spin column for centrifuging at 8 000 g for 15 seconds. Buffer RW1 (350  $\mu$ L) was added to the spin column and centrifuged (8 000 g for 15 seconds), then 80  $\mu$ L DNase I solution in buffer RDD (1:8 dilution) was added at room temperature (15 minutes). Buffer RW1 (350  $\mu$ L) was added to the spin column and centrifuged at 8 000 g for 15 seconds. Buffer RPE (500  $\mu$ L) was added to the spin column, then centrifuged (8 000 g for 15 seconds) followed by 500  $\mu$ L of 80% ethanol and centrifuged at 13 000 g for 2 minutes. The spin column was further centrifuged at 13 000 g for 5 minutes. The dried spin column was placed in a 1.5 mL Eppendorf tube and 14  $\mu$ L RNase-free water was added then centrifuged at full speed for 1 minute.

### 3.3.7 Fluidigm preparation

The RNA was subjected to a reverse transcription using the SuperScript III Reverse Transcriptase. At all stages of the process, reactions were performed at 4°C unless stated. 11  $\mu$ L of each sample was added to 1  $\mu$ L of oligo (dT) and 1  $\mu$ L dNTPmix and then heated to 65°C for 5 minutes. A mixture containing 4  $\mu$ L 5X First Strand buffer, 1  $\mu$ L 0.1M DTT, 1  $\mu$ L RNaseOUT Recombinant RNase inhibitor, 0.5  $\mu$ L SuperScript III RT and 0.5  $\mu$ L water was prepared and added to each sample and left for 5 minutes. The solution was then incubated at 50°C for 30 minutes followed by 70°C for 15 minutes to produce cDNA. All 48 primers (see Table 3-2) were pooled together (1  $\mu$ L from each primer set pooled and 152  $\mu$ L of DNA suspension buffer). A new solution was prepared with 1.25  $\mu$ L from the cDNA of each sample, 2.5  $\mu$ L 2x TaqMan PreAmp Master Mix, 0.5  $\mu$ L pooled primer mix, 0.75  $\mu$ L water. These samples were vortexed, centrifuged and subjected to 22 thermal cycles using the following programme:

**Table 3-1: Thermal cycle conditions used on each sample prior to Fluidigm analysis.**

Condition	Hold	22 Cycles		Hold
Temperature	95°C	95°C	60°C	4°C
Time	10 mins	15 secs	4 mins	$\infty$

After the 22 thermal cycles, 1.4  $\mu$ L water, 0.2  $\mu$ L Exonuclease I Reaction Buffer and 0.4  $\mu$ L Exonuclease were added to each sample and vortexed, centrifuged and incubated at 37°C for 30 minutes and then at 80°C for 15 minutes. After heating, 18  $\mu$ L of TE buffer was added to each sample. The Exonuclease I treated sample (2.7  $\mu$ L) was added to 3.0  $\mu$ L 2x SsoFast EvaGreen Supermix and 0.3  $\mu$ L

20x DNA Binding Dye sample loading reagent. Each sample was vortexed and centrifuged then loaded onto the chip. Additionally, 0.3  $\mu$ L of each individual primer set was added to 3  $\mu$ L 2X assay loading reagent and 2.7  $\mu$ L 1x DNA suspension buffer was vortexed and centrifuged prior to loading on the chip. A 48.48 Dynamic array IFC was used during this analysis.

**Table 3-2: Fluidigm primers designed for human genes.**  
(\*Primers used as housekeeping genes).

Primer	Sequence (5' to 3')
<b>B-Actin*</b>	Forward GTGGGCCGCCCTAGGCACCAG Reverse CACTTTGATGTCACGCACGATTTC
Nestin	Forward GCTCAGGTCCTGGAAGGTC Reverse AAGCTGAGGGAAGTCTTGA
ALCAM	Forward TTCCAGTCCCTCTACTCAGAGC Reverse GCTAAGAAGGACTCGCAGGA
vimentin	Forward GGAGAAATTGCAGGAGGAGA Reverse TGCGTTCAAGGTCAAGACGT
CD63	Forward CCCTTGGAAATTGCTTTTGT Reverse TATCCACTCCCCAGATGA
c-myc	Forward GACTCTGAGGAGGAACAAGA Reverse TTGGCAGCAGGATAGTCCTT
<b>ENOX-2*</b>	Forward GAGCTGGAGGGAACCTGATTT Reverse CACTGGCACTACCAAACCTGCA
RUNX-2	Forward CAGCAGCAGCAACAGCAG Reverse GGCGATGATCTCCACCAT
RUNX1T1	Forward ATCACAACAGAGAGGGCCAA Reverse CTGCAGGTTTCACTCGCTTT
Osterix	Forward TGGGCTCCCAACACTATTTT Reverse GGAAGACTGAAGCCTGGA
BMP2	Forward AGACCTGTATCGCAGGCACT Reverse CCACTCGTTTCTGGTAGTTCTTCC
BMPR2	Forward AGCCTCTCACACCCACTCC Reverse GCAGAACAACCGTGAGAGG
OPN	Forward AGCTGGATGACCAGAGTGCT Reverse TGAAATTCATGGCTGTGGAA
<b>TWY-1*</b>	Forward ATTGTCATCAAGACGCAGGGC Reverse GTTGCGAATCCCTTCGCTGTT
PPAR- $\gamma$	Forward TTGCTGTCATTATTCTCAGTGGA Reverse GAGGACTCAGGGTGGTTTCAG
COL2A1	Forward CTGGGACCCCTGGAAATC Reverse CATCAAATCCTCCAGCCATC
ACAN	Forward TCACGTGTAAAAAGGGCACA Reverse CAGGGAATTGATCTCATACCG
B3-tubulin	Forward GCAACTACGTGGGCGACT Reverse ATGGCTCGAGGCACGTA
CCNA1	Forward TCAGTACCTTAGGGAAGCTGAAA Reverse CCAGTCCACCAGAATCGTG

CCNA2	Forward CCATACCTCAAGTATTTGCCATC Reverse TCCAGTCTTTCGTATTAATGATTCAG
<b>CYCR*</b>	Forward ACTGCGGGAAGGTCTCTACTT Reverse GGGTGCCATCGTCAAACCTCA
CCNB1	Forward ACATGGTGCACCTTTCCTCCT Reverse AGGTAATGTTGTAGAGTTGGTGTCC
CCNB2	Forward GAAGATTGGGAGAACCCTCA Reverse TGTGGGTTTATGGACTGCAA
CCNC	Forward TTTGCTGAGCTTTCTGTGGA Reverse AATGGTTGCCATCTCTTTTCTC
CCND1	Forward TGCATCTACACCGACAACCTCC Reverse CGGATGATCTGTTTGTCTCCG
CCND2	Forward TACACCGACAACCTCCATCAAGC Reverse ATGTGCTCAATGAAGTCATGAGG
CCND3	Forward TACACCGACCACGCTGTCT Reverse GAAGGCCAGGAAATCATGTG
<b>UBE2D2*</b>	Forward CCATGGCTCTGAAGAGAATCC Reverse GATAGGGACTGTCATTTGGCC
CCNE1	Forward ACAGCTTGGATTTGCTGGAC Reverse TCTGCTTCTTACCGCTCTGTG
CCNE2	Forward GCCATTGATTCATTAGAGTTCCA Reverse TGAAATACTGTCCCACTCCAAC
CCNT1	Forward GAACATGTCATCAAGGTAGCACA Reverse AATGACCAGATCTTGAACCTGTTG
CDC2	Forward TGAAATGTTTCATGGGGGAAC Reverse AAAAAGCTCCTGATGCCTTG
CDK1	Forward AACTACAGGTCAAGTGGTAGCC Reverse GGAATCCTGCATAAGCACATCC
CDK2	Forward CCTCCTGGGCTGCAAATA Reverse CAGAATCTCCAGGGAATAGGG
<b>RNF20*</b>	Forward GGTGTCTCTTCAACGGAGGAA Reverse TAGTGAGGCATCATCAGTGGC
CDK4	Forward AGTGTGGCTGTATCTTTGCAG Reverse ATCTCGAGGCCAGTCATCC
CDK5	Forward TCTTTTTCCCGCAATGAT Reverse TCTGGCAGCTTGGTCATAGA
CDK6	Forward GAACTAGGCAAAGACCTACTTCTGA Reverse GGTGGGAATCCAGGTTTTCT
CDKN1A	Forward GTGGACCTGGAGACTCTCAG Reverse CCTCTTGGAGAAGATCAGCCG
CDKN1B	Forward GGCTAACTCTGAGGACACGC Reverse TGAGTAGAAGAATCGTCGGTTGC
<b>B2M*</b>	Forward TTGTCTTTCAGCAAGGACTGG Reverse ATGCGGCATCTTCAAACCTCC
BIRC5	Forward AGAACTGGCCCTTCTTGGA Reverse AACTGGGCCAAGTCTGG
PK1	Forward CACCAAGACCTCGTGTGAG Reverse GCTTCAGGTCTCCTTGGAAAGT
ANLN	Forward ATCTAGCCCTTTGAAAATAACATTG Reverse CACTCATCTCAATTTACGTATCAC
SGOL1	Forward AGAATAAAGCAAGCCCAGCA

	Reverse AAAGGGTCCCCTCTTCTCAG
SOX2	Forward ACAACATGATGGAGACGGAG Reverse GATGCACAACCTCGGAGATCA
WNT3A	Forward GCCCACTCGGATACTTCTTAC Reverse CGAGCCCAGGGAGGAATACA
<b>GAPDH*</b>	Forward TCAAGGCTGAGAACGGGAA Reverse TGGGTGGCAGTGATGGCA

## 3.4 Results

### 3.4.1 Niche Model Development: Stage 1

#### Optimising the mNPs Loading Conditions of the MSCs.

Two different mNP concentrations (0.01 mg/mL and 0.1 mg/mL), alongside three different incubation time periods (15 minutes, 30 minutes and 1 hour) were used to determine the best conditions to pre-load the MSCs in a monolayer culture. All samples were either in the presence or absence of an external magnetic field. The mNP uptake into MSCs was analysed (i) quantitatively by ICP-MS (Figure 3-3), and qualitatively by (ii) fluorescence microscopy (Figure 3-4a and Figure 3-4b) and using (iii) TEM (Figure 3-5).

The MSC samples were lysed to allow quantification of mNP uptake Figure 3-3, prior to analysis by ICP-MS. ANOVA analysis was conducted to determine the statistical differences between each parameter. The mNP uptake increased as the concentration of the mNPs increased, and there was a significant difference ( $p < 0.05$ ) between the two concentrations of mNPs, at all conditions. Additionally, the presence of a magnetic field increased mNPs uptake significantly ( $p < 0.05$ ), compared to the absence of a magnetic field, within all parameters. The highest mNPs uptake occurred after the 1 hour incubation period, using 0.1 mg/mL mNPs concentration and in the presence of an external magnetic field. However, there was no significant difference between each incubation period, irrespective of concentration or magnetic field.

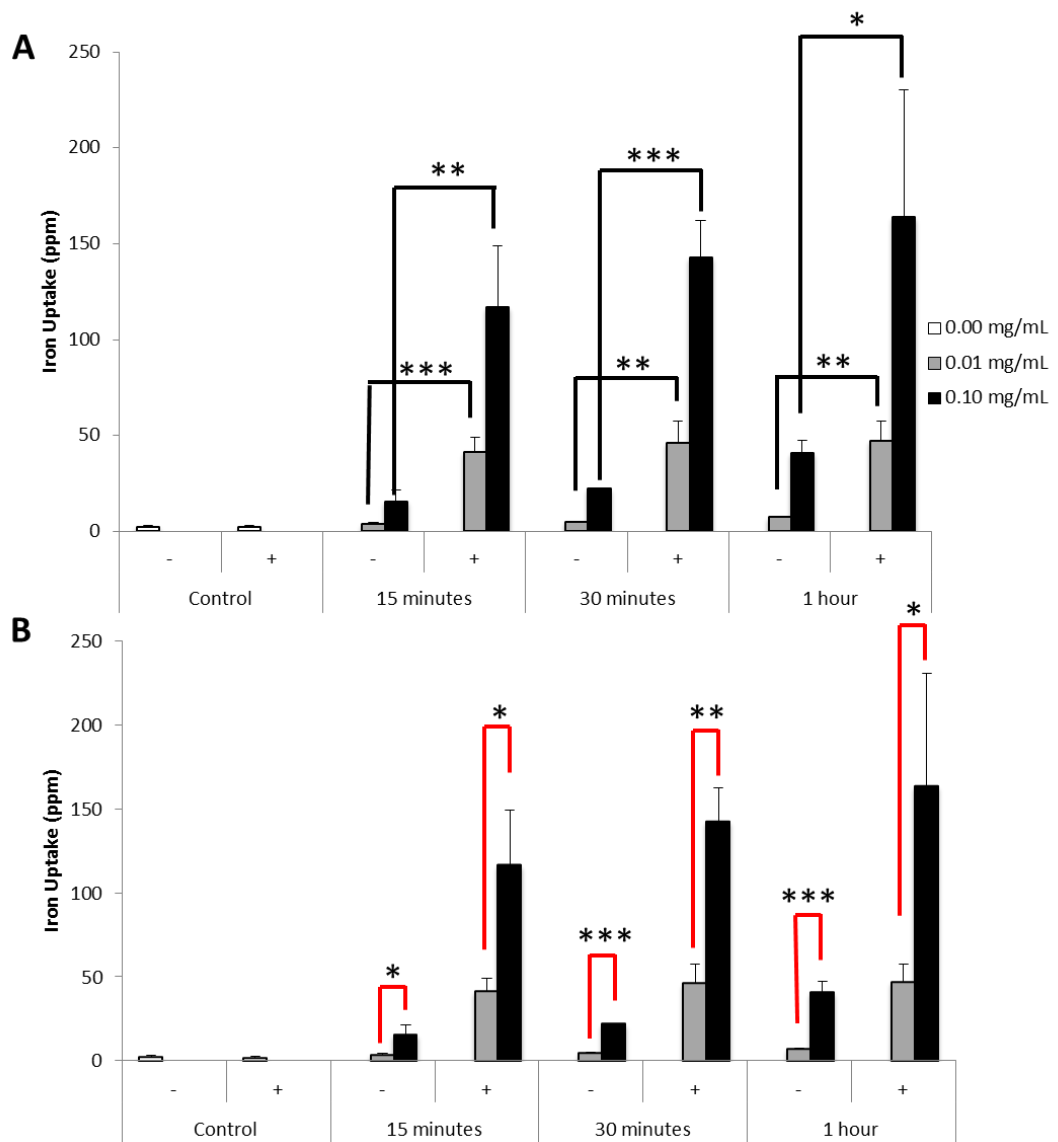


**Figure 3-3: Graph of mNP uptake within MSCs analysed using ICP-MS.**

Analysis was conducted using two different concentrations, three incubation time periods in either the presence or absence of a magnetic field. (n=3, technical replicates); Graph A shows the statistical significance at each concentration and same time point with or without a magnetic field whereas, Graph B shows the statistical significance between concentrations at the same time point and magnetic field environment (Error bars denote standard deviation; \* indicates statistical significance where  $p < 0.05$ , \*\* indicates  $p < 0.01$  and \*\*\* indicates  $p < 0.001$  as calculated using one way ANOVA)).

A FITC fluorescent tag permitted mNP observation, *via* the use of fluorescence microscopy. Conditions were identical to the ICP-MS experiment to determine the mNP uptake into MSC monolayer cultures. The results, depicted in Figure 3-4, mirror the results obtained using ICP-MS, when an increase in green fluorescence (mNPs) was observed at the higher mNPs concentration of 0.1 mg/mL, compared to the lower concentration of 0.01 mg/mL. Quantitative analysis (Figure 3-4b) was conducted on the complete set of fluorescent images obtained for qualitative analysis. There was a significant difference between fluorescent intensity ( $p < 0.001$ ) of mNP presence in the MSCs against mNP

concentration. Also the mNP fluorescence intensity showed a significant increase ( $p < 0.05$ ) in the presence of a magnetic field. However, there was no statistical significant difference between each time period, regardless of concentration or magnetic field. Therefore, these results shown in Figure 3-4 correlate with the ICP-MS data depicted in Figure 3-3.

Analysis was conducted on data collected from both the fluorescence images and ICP-MS. The results indicated the optimal pre-loading conditions of MSCs with mNPs were at a concentration of 0.1 mg/mL over an incubation period of 30 minutes.

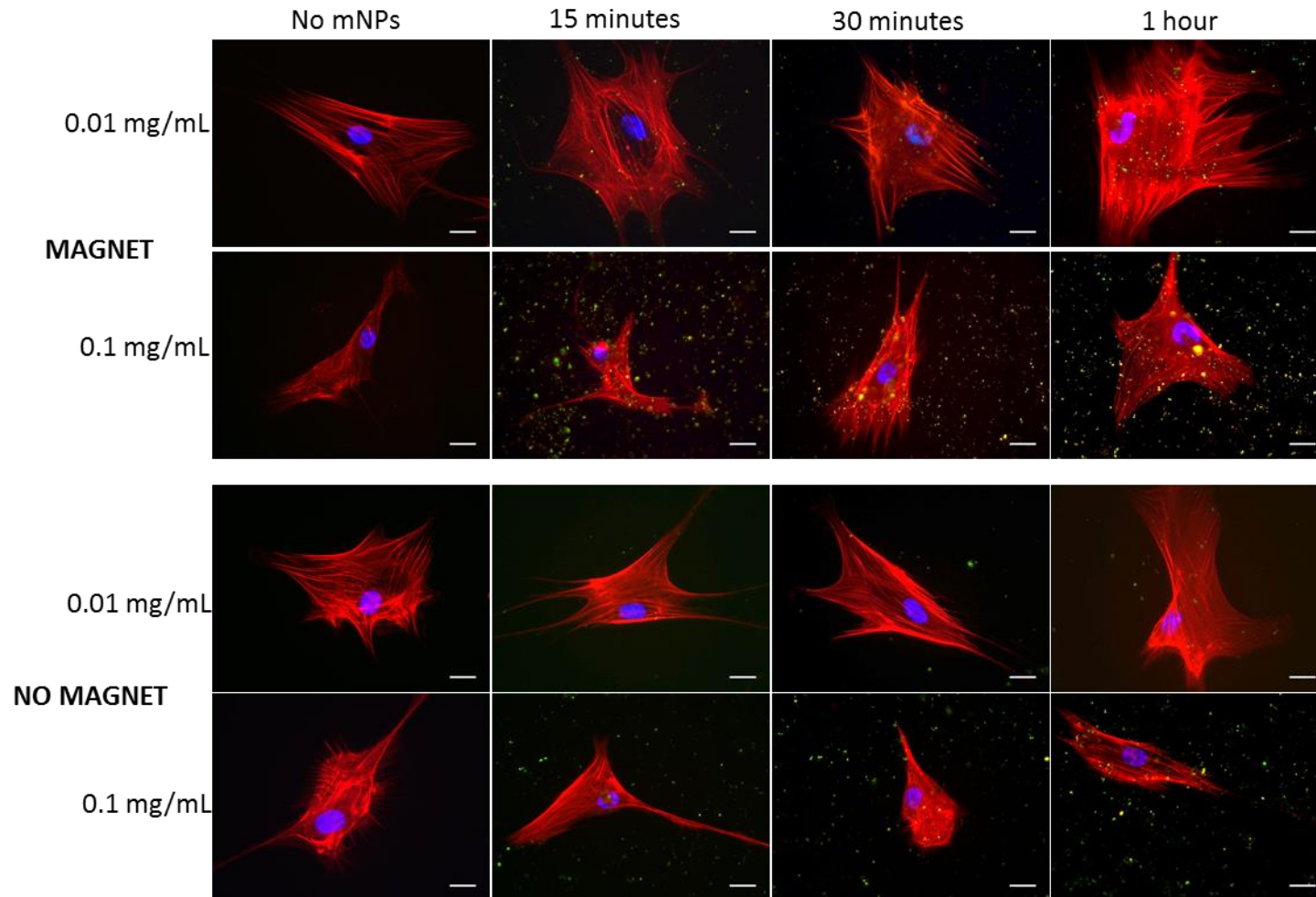
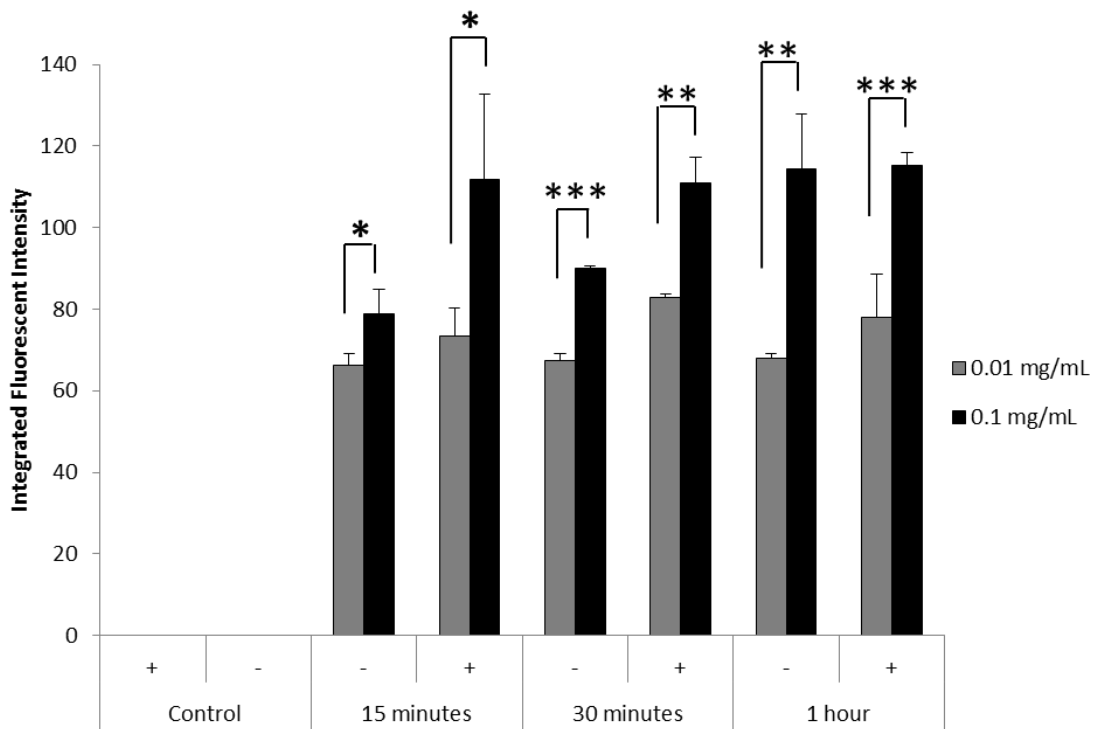


Figure 3-4a: Representative fluorescence images of MSCs incubated with mNPs in the presence or absence of a magnetic field. Two concentrations of mNPs were used, with three incubation periods; in either the presence or absence of a magnetic field. Red=actin, green=nanoparticles, blue=nucleus, 40x objective, scale bar = 20  $\mu$ m. (n=3, three technical replicates)



**Figure 3-4b: Quantitative analysis of the complete immunofluorescent images from Figure 3-4a demonstrating mNP uptake into MSCs.**

Two concentrations of mNPs were used, with three incubation periods; in either the presence or absence of a magnetic field. (Error bars denote standard deviation; \* indicates statistical significance where  $p < 0.05$ , \*\* indicates  $p < 0.01$  and \*\*\* indicates  $p < 0.001$  as calculated using one way ANOVA)

The use of TEM provided a more detailed observation of mNP internalisation; allowing verification of uptake and information on intracellular location of the mNPs. A comparative study on the effect of the presence or absence of a magnetic field on the uptake of mNPs was performed at the optimum condition of a concentration (0.1 mg/mL) and incubated for 30 minutes. The study showed the mNPs were clearly visible on the outer periphery of the cells, as well as internally present within the MSCs (Figure 3-5). The TEM images show a magnetic field enhanced mNP uptake into the cell, with less NPs visible outside the cells (i.e. image B had a higher ratio of NPs out with the cell compared to image C) (see Figure 3-5).

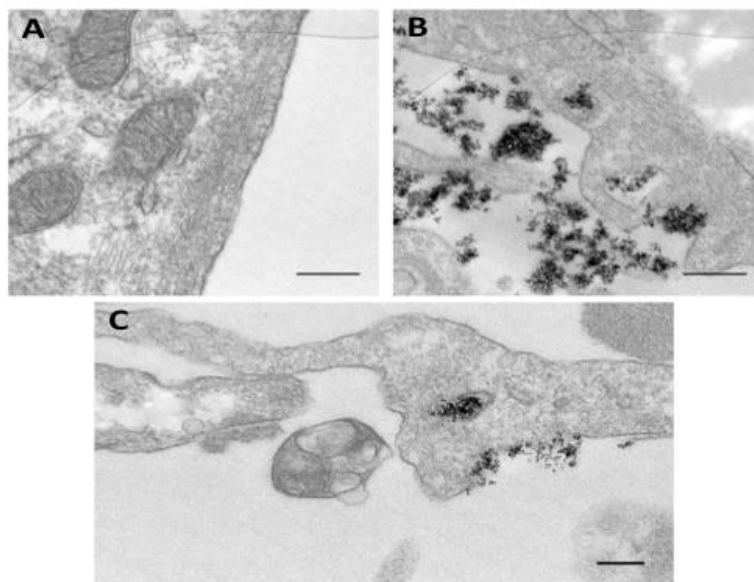


**Figure 3-5: Representative TEM images of MSCs incubated with mNPs.** Cells were incubated without mNPs (A), with 0.1 mg/mL mNPs concentration for 30 minutes (B), and with 0.1 mg/mL mNPs concentration for 30 minutes with an external magnetic field (C), scale bar = 200 nm. (n=3, three technical replicates)

### 3.4.2 Niche Model Development: Stage 2

#### **Assessing mNP Retention Within MSCs Following Trypsinisation.**

In order to generate multicellular MSC spheroids, it is necessary to make the MSCs responsive to a magnetic field following the internalisation of the mNPs. It was vital the mNPs were retained within the cells therefore, to assess mNP retention the MSCs were incubated under the optimised mNPs pre-loading conditions. These cells were subsequently trypsinised off one substrate and re-seeded onto a different substrate, to determine (i) whether the mNPs were retained within the MSCs and (ii) whether the resultant MSCs were responsive to an external magnetic field.

MNP retention was assessed using both light microscopy and fluorescence microscopy. MSCs were seeded onto glass coverslips, for 24 hours, incubated with mNPs for 15, 30 and 60 minutes, followed by washing, trypsinising and seeding onto a new coverslip. Cells were then cultured for 3 hours, prior to being fixed and processed for light and fluorescence microscopy. Fluorescence microscopy clearly demonstrated that the mNPs were retained within the MSCs,

and localised around the nucleus, (Figure 3-6a). Furthermore, these images indicated an almost total absence of mNPs in the surrounding area of the cells. Quantitative results depicted in Figure 3-6b showed there was no statistical difference between mNP up take over the three incubation periods.

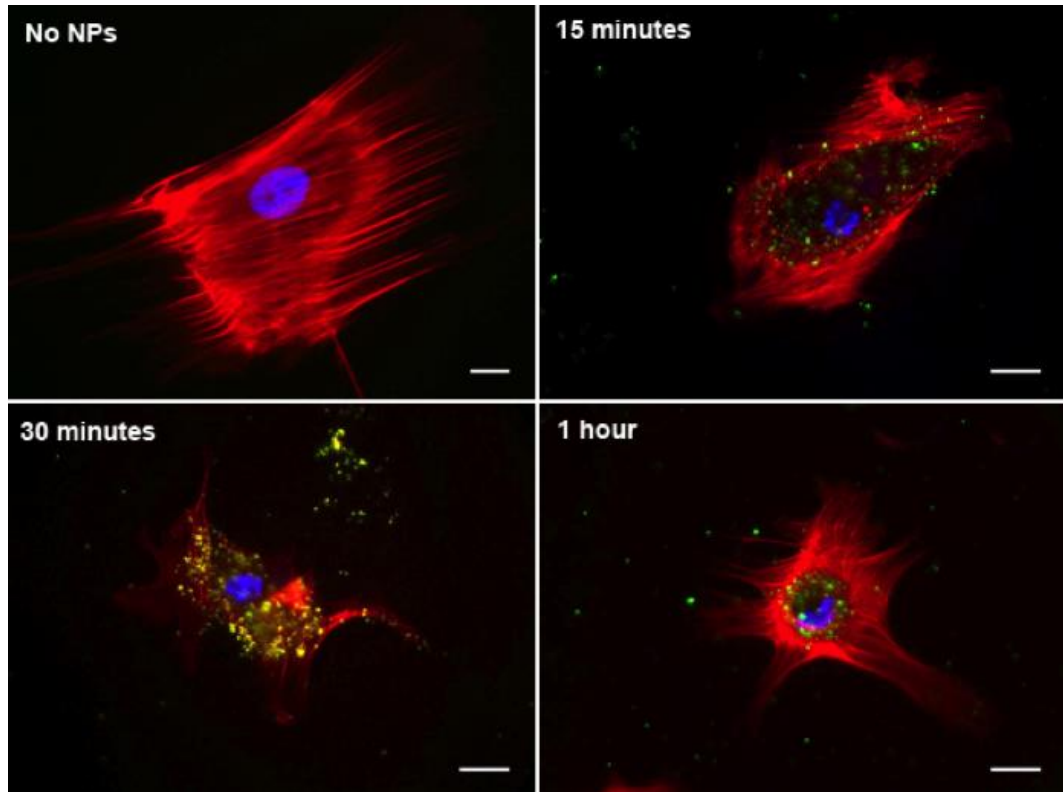


**Figure 3-6a: Fluorescence images of MSCs with and without mNPs (for 15, 30 and 60 minutes) following trypsinisation and re-seeding. Images depicting MSCs post trypsinisation and transferred from one substrate to another substrate. (Red = actin, green = mNPs, blue = nucleus), 40x objective, scale bar = 20  $\mu\text{m}$ . (n=3, three technical replicates)**

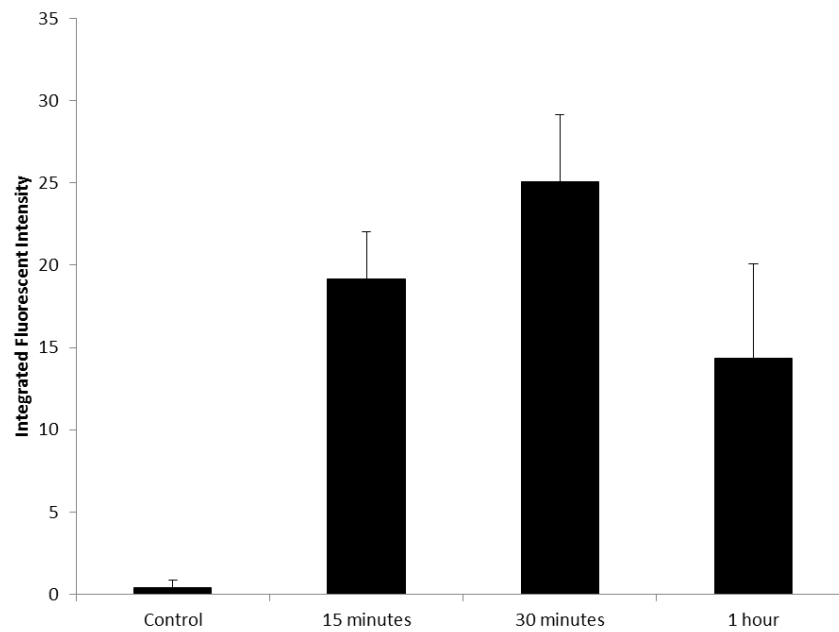


**Figure 3-6b: Quantitative analysis of complete fluorescent images with and without mNPs (for 15, 30 and 60 minutes) following trypsinisation and re-seeding. (Error bars denote standard deviation)**

Additionally, the retention of the mNPs within the cell was confirmed using light microscopy (Figure 3-7), which highlighted the mNPs (brown clusters) within the MSCs. Furthermore, the retention of the mNPs was observed at all three incubation periods, where they were localised around the nucleus. Figure 3-7 shows an image of mNP retention within the MSC after 30 minutes of incubation.

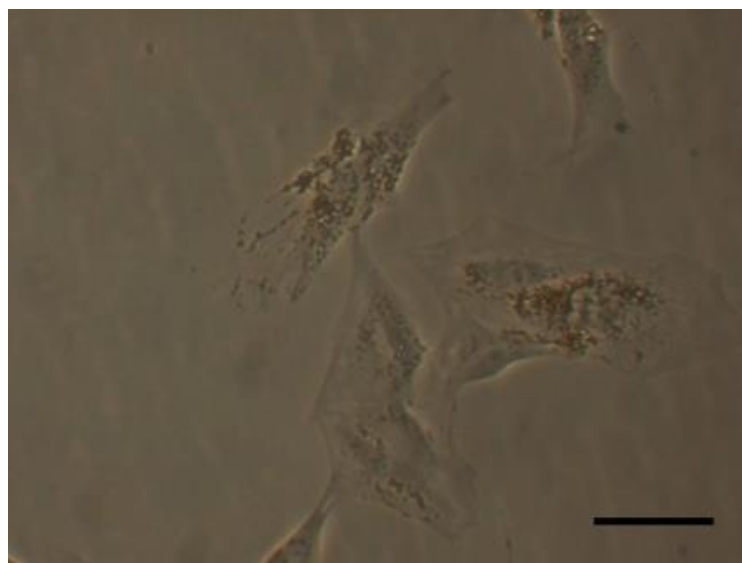


**Figure 3-7: Representative light microscopy image of mNPs residing within MSCs, under optimised pre-loading conditions, following 30 minutes incubation. (Brown = mNPs), 20x objective, scale bar = 50  $\mu$ m.**

### 3.4.3 Niche Model Development: Stage 3

#### Assessing mNP-loaded MSC Response to an External Magnetic Field in Monolayer.

MSCs pre-loaded with mNPs for 30 minutes, were re-seeded as monolayer cultures (as above) and subjected to an external magnetic field, by the placement of a 13 mm diameter magnet below the 6 well plate culture well, over an initial 24 hour culture period. Images showed the majority of cells were all localised within the area of the magnetic field, after the 24 hour incubation period (Figure 3-8). A pattern in the MSC attachment was noted, which corresponded with the magnetic field pattern of the disc magnet. There was a higher concentration of cells at the outer rim of the magnet where the magnet was the strongest with fewer cells in the centre of the magnetic field. Therefore, an assumption may be made that the mNP-loaded MSCs were able to respond positively to the presence of the magnetic field.

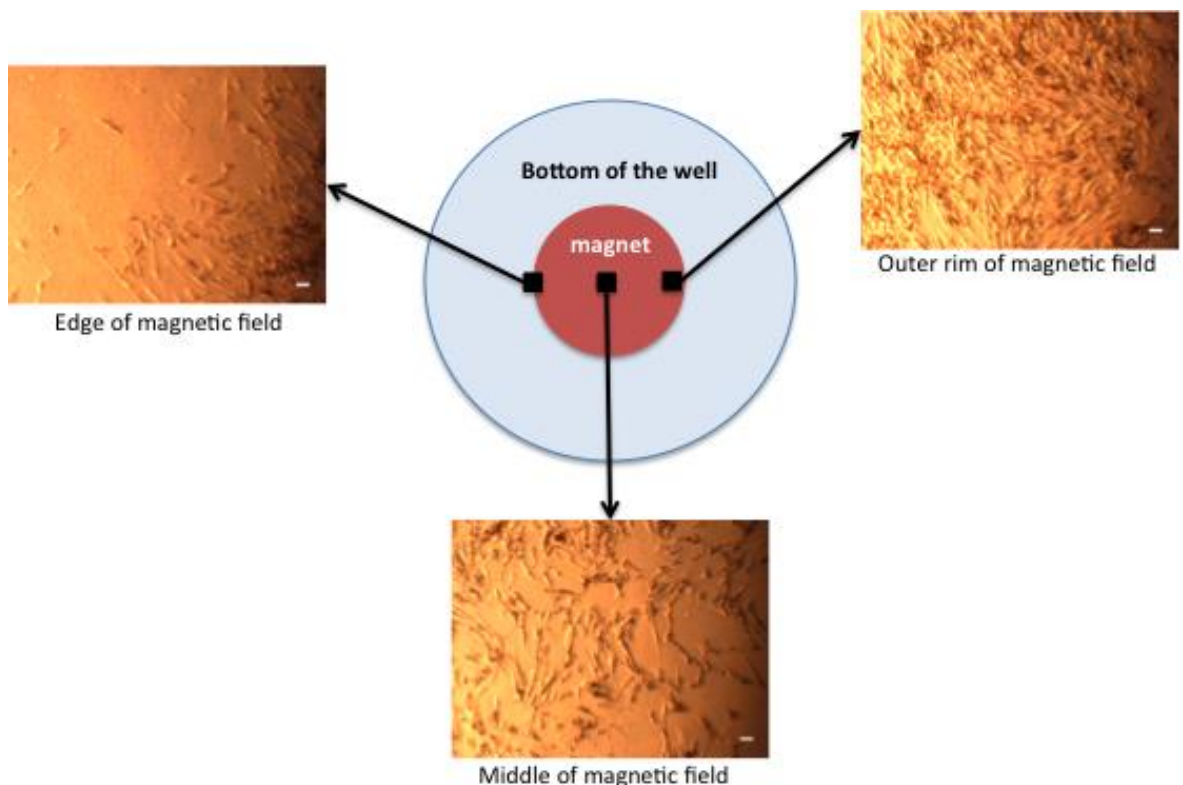


**Figure 3-8: Schematic diagram of 6 well plate design with the magnet beneath the well. Light microscopy images of MSCs incubated for 30 minutes with mNPs and cultured for 24 hours, 5x objective, scale bar = 50  $\mu$ m.**

### 3.4.4 Niche Model Development: Stage 4:

#### **Assessing mNP-loaded MSC Viability and Phenotype in Monolayer Culture and 3D Spheroid Culture.**

MSCs have been traditionally cultured as *in vitro* monolayer systems, to assess niche parameters (Fernandes et al., 2013). Therefore, MSCs pre-loaded with mNPs were cultured as monolayers and assessed for viability and phenotype after 1, 3, 7 and 14 days. The cells were stained for STRO-1 and nestin, which are MSC surface markers, to assess the ability of the MSCs to retain their multipotency properties (Figure 3-9). The fluorescence images depicted in Figure 3-9 show the cells pre-loaded with the mNPs remained viable over the 2 week period. Additionally, cells on day 1 demonstrated a high expression of STRO-1 and nestin. However, cells on day 14 showed a lack of expression of either MSC multipotency markers. During the 2 week incubation period, the presence of both STRO-1 and nestin clearly decreased over time.

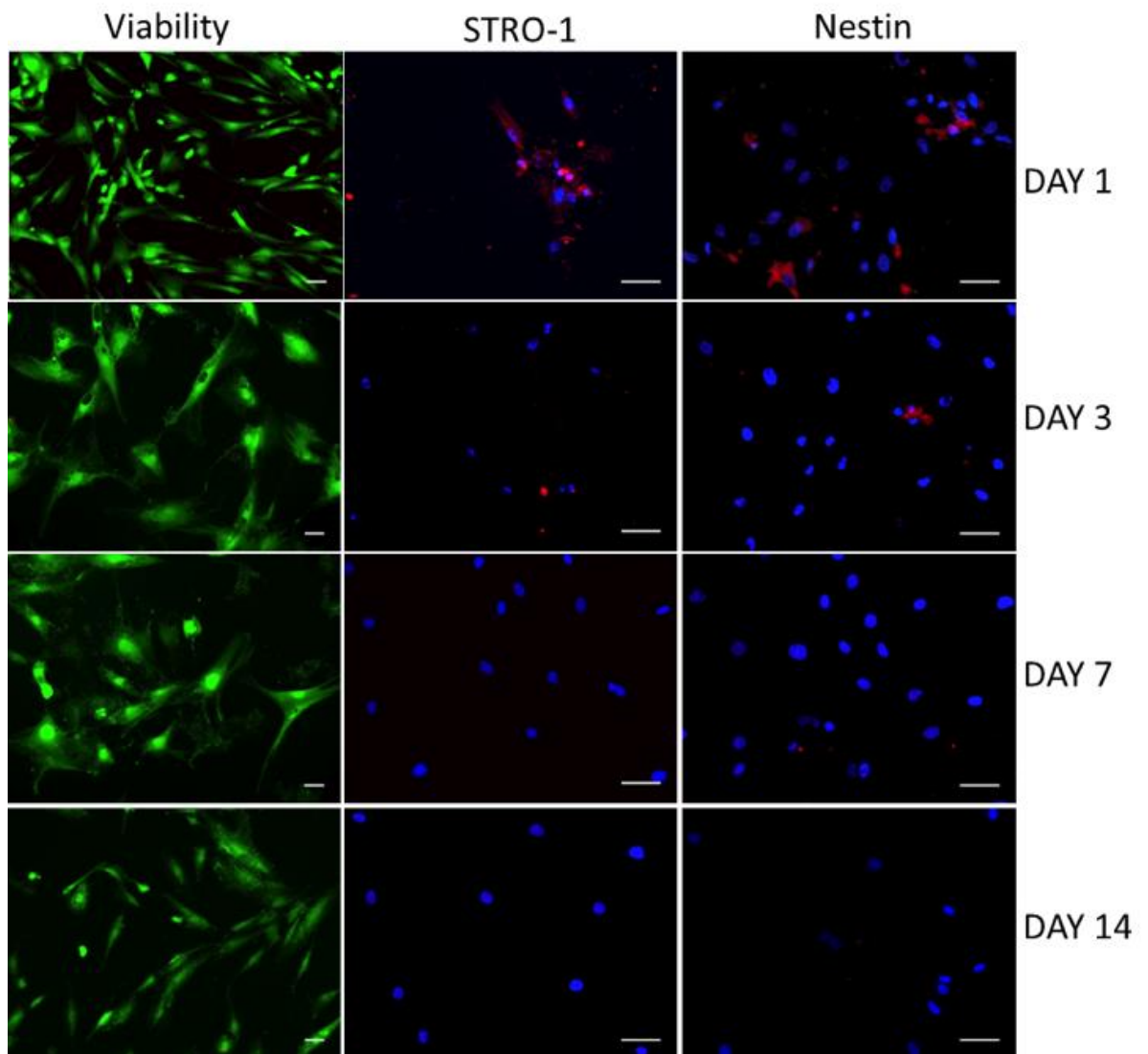


**Figure 3-9: Monolayer culture of mNP-loaded MSCs cultured for up to 14 days.** Fluorescence images were taken at day 1, 3, 7 and 14 assessing cell viability (green=living cells, red=dead cells, 10x objective) and phenotype (red=STRO-1/nestin, blue=nucleus, 20x objective). Scale bar = 50  $\mu$ m. (n=3, three technical replicates)

To generate spheroids, it is important to coerce the MSCs together to create a 3D MSC niche model, which allow the formation of cell-cell and cell-ECM interactions, which are observed *in vivo*. As previously shown, the mNP-loaded MSCs responded to an external magnetic field, when cultured in monolayer (by localising within the magnetic field area). Therefore, the application of an external magnetic field to a cell suspension, should force the MSCs to migrate towards the field and congregate together. The cells natural adherence for survival and close proximity to each other caused by the magnetic field, should encourage cell-cell attachment. Consequently, the mNP-loaded MSCs were added as a cell suspension to a 6 well culture plate well with a magnet located directly above the well, as indicated in Figure 3-10.

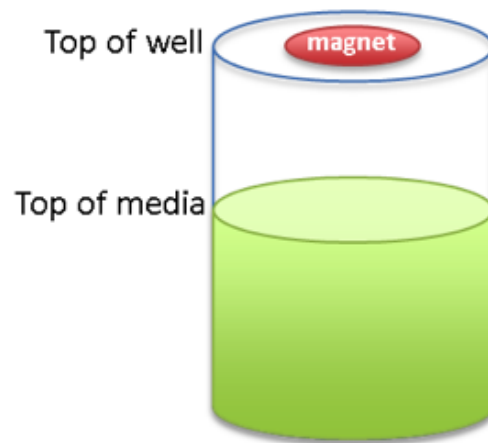


**Figure 3-10: Schematic diagram of 6 well plate design for MSC spheroid formation, with the magnet above the well.**

MSC spheroids were cultured in parallel with monolayer cultures. The spheroids were assessed for viability and phenotype over the same time period of 14 days. It was observed that following only a few hours of incubation, beneath the magnet, the MSCs levitated towards the field and formed a spheroid structure. Within the spheroid structure, the MSCs exhibited high viability over the 14 day culture period Figure 3-11. There was no difference in cell viability between day 1 and day 14. Additionally, the MSCs expressed high levels of STRO-1 and nestin over the 2 week incubation period, at all time points.

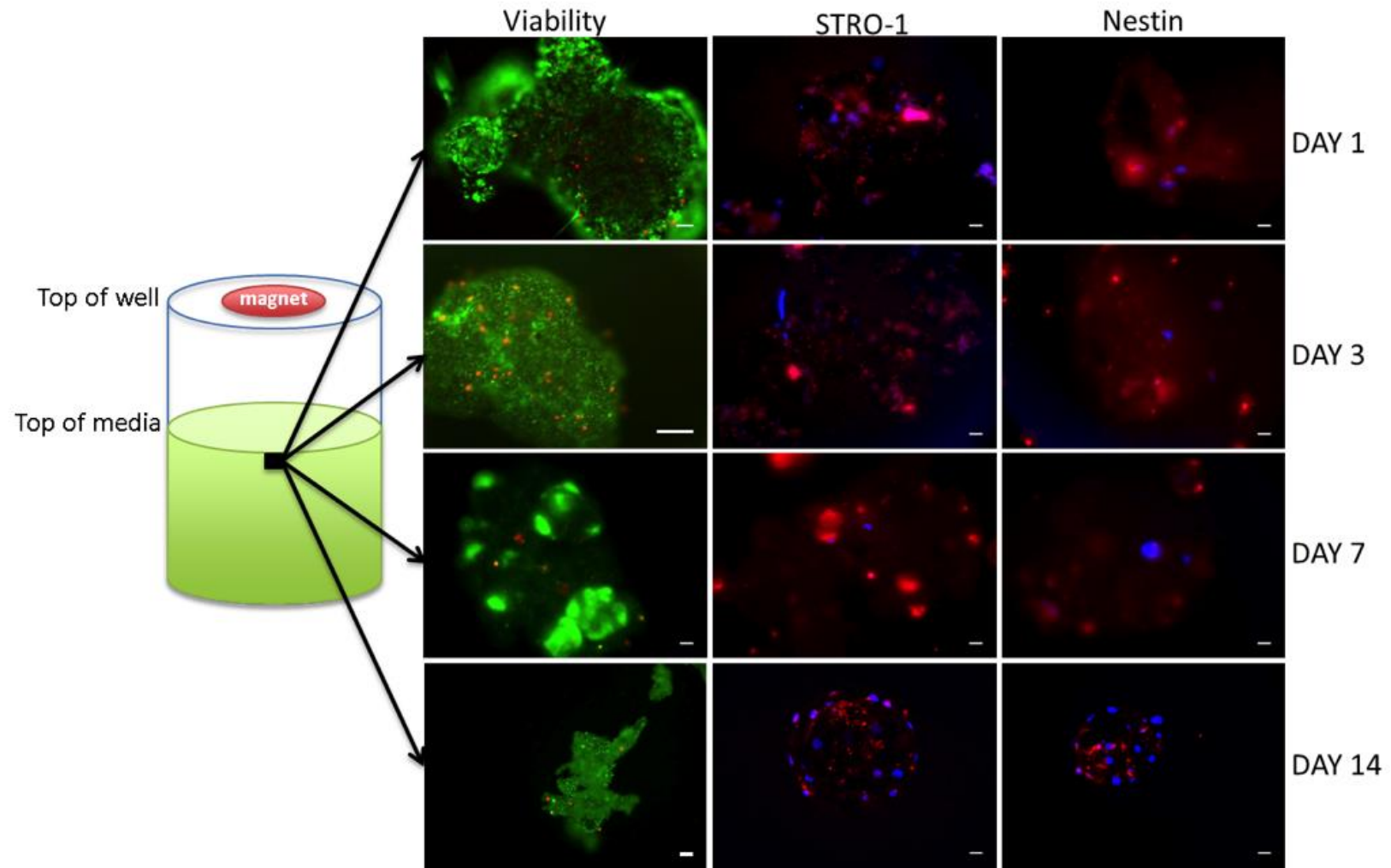


**Figure 3-11: Spheroid culture of MSCs with mNPs incubated for up to 14 days.** Fluorescence image of mNP-loaded MSCs cultured for 1, 3, 7 and 14 days, to assess cell viability (green=living cells, red=dead cells) and phenotype (red=STRO-1/nestin, blue=nucleus). 20x objective, scale bar = 20  $\mu\text{m}$ . (n=3, three technical replicates)

Figure 3-12 shows quantitative analysis of the immuno-fluorescence images (Figure 3-9 and Figure 3-11), which demonstrated there was a highly significant difference in the reduction of STRO-1 and nestin expression in the MSC monolayer cultures over time. However, there was no significant difference in STRO-1 or nestin expression in the MSC spheroids over time.

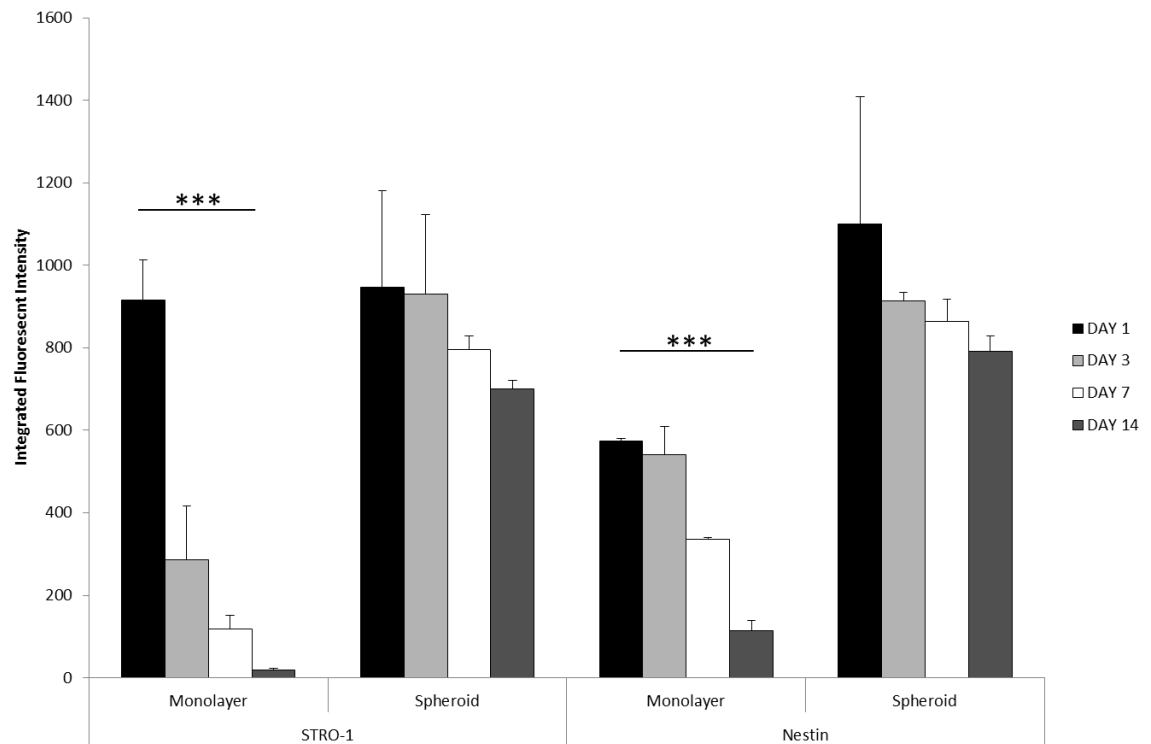


**Figure 3-12: Quantitative analysis of data collected from immuno-fluorescent images depicted in Figure 3-9 and Figure 3-11, which compared monolayer and spheroid culture conditions.**

**(Error bars denote standard deviation; \* indicates statistical significance where  $p < 0.05$ , \*\* indicates  $p < 0.01$  and \*\*\* indicates  $p < 0.001$  as calculated using one way ANOVA))**

Research suggests the diameter size of the spheroid (above 200  $\mu\text{m}$ ) has a detrimental effect on oxygen diffusion to the spheroid centre, creating a hypoxic environment (Curcio et al., 2007, Gatenby et al., 2007). A study by Li et al., suggested cancer stem cells, which reside within a hypoxic secondary niche in tumours, maintain the stem cells in an undifferentiated and quiescent state (Li et al., 2009). Therefore, an environment of low oxygen may allow the stem cells to remain in a dormant condition. Figure 3-13 illustrates the size distribution of a selection of MSC spheroids produced for this thesis and found the mean diameter to be 259  $\mu\text{m}$ .

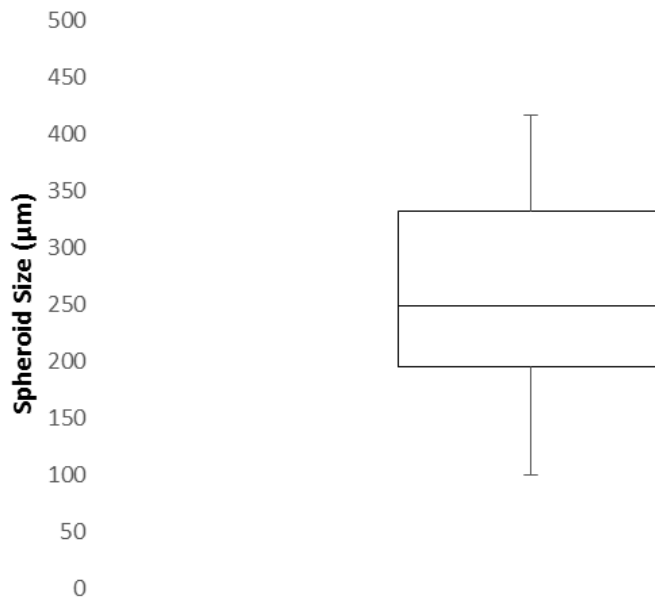


**Figure 3-13: Box plot depicting the size distribution of a sample of MSC spheroids produced in this thesis. (n=15)**

ECM is an important component of the MSC niche and maintains homeostasis. Therefore, it is necessary to determine whether the MSCs in the spheroids produce their own ECM. TEM analysis of spheroids demonstrated areas of cell-cell contact (red arrows) with voids (black arrows) Figure 3-14. The voids between the cells in the spheroids indicate a lack of ECM production as highlighted in Figure 3-14.

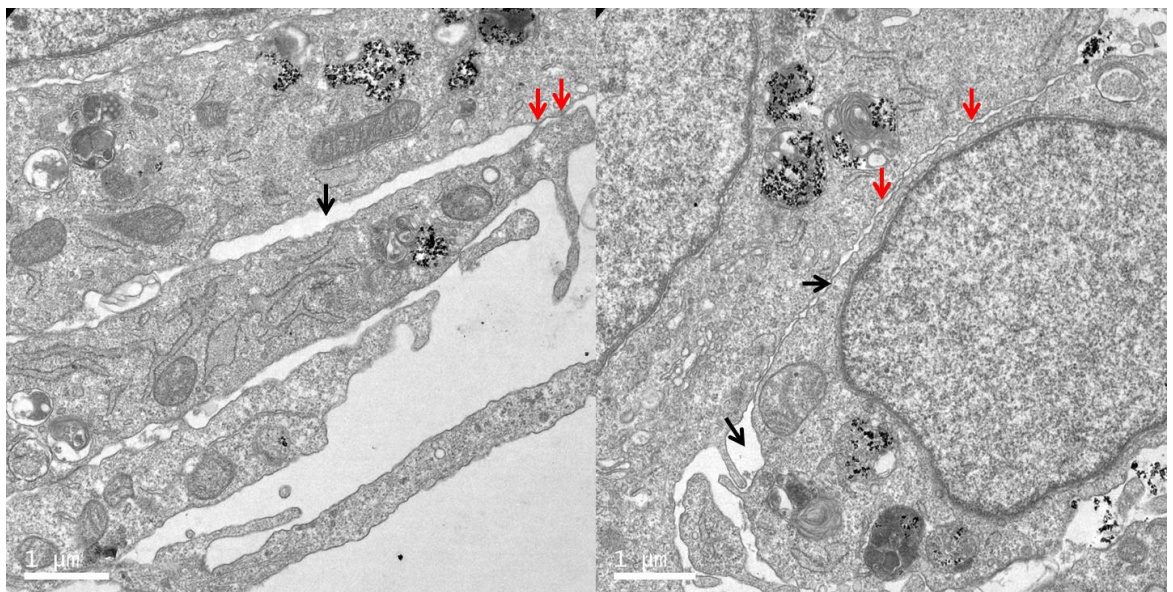


**Figure 3-14: TEM images of cross-sectioned spheroids highlighting areas between MSCs. Black arrows indicate voids between MSCs in the spheroids and red arrows indicate MSC-MSC contacts. Scale bar=1 µm. This work was carried out by Gemma McLelland (honours project student in 2014), University of Glasgow.**

### 3.4.5 Niche Model Development: Stage 5

#### Assessing the Formation of a MSC Spheroid Within a Collagen Gel.

Following the success of the initial experiments, a Type I collagen gel was employed to generate a more complex 3D environment for the MSC spheroid. The gel was designed to be of a similar stiffness and composition of bone marrow (the location of the *in vivo* MSC niche).

Collagen gels were mixed with mNP-loaded MSC suspensions and cast into 24 well plates. Initially, the control MSCs (containing no mNPs) and mNP-loaded MSCs were assessed for viability and morphology in the collagen gels after 24 hours, 72 hours and 1 week incubation periods. To assess whether the fibrous collagen network may inhibit cell mobility, two different magnets were applied to the gel below the well. Both magnets had differing field strengths (350mT and 420 mT) and each measured 13 mm in diameter and were identical to the well diameter. Magnets were placed below the well, to allow the MSCs to migrate through the gel and congregate together to form spheroids (Figure 3-15).

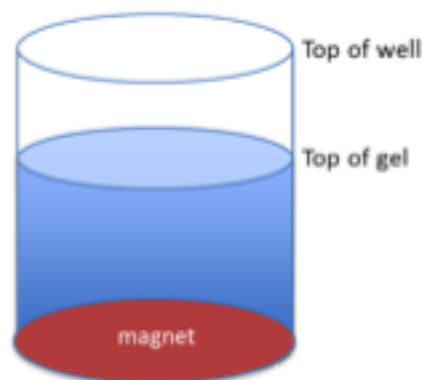


**Figure 3-15: Schematic diagram of one of the wells in the 24 well plate design with the magnet below the well.**

The MSCs remained viable up to one week within the collagen gel, irrespective of the presence of mNPs or magnetic field strength (Figure 3-16 and Figure 3-17). There was no statistical significant difference in cell viability over time in relation to magnetic field strength as depicted in Figure 3-18. Therefore, the presence of the magnetic field did not influence the cells viability over the week incubation period.

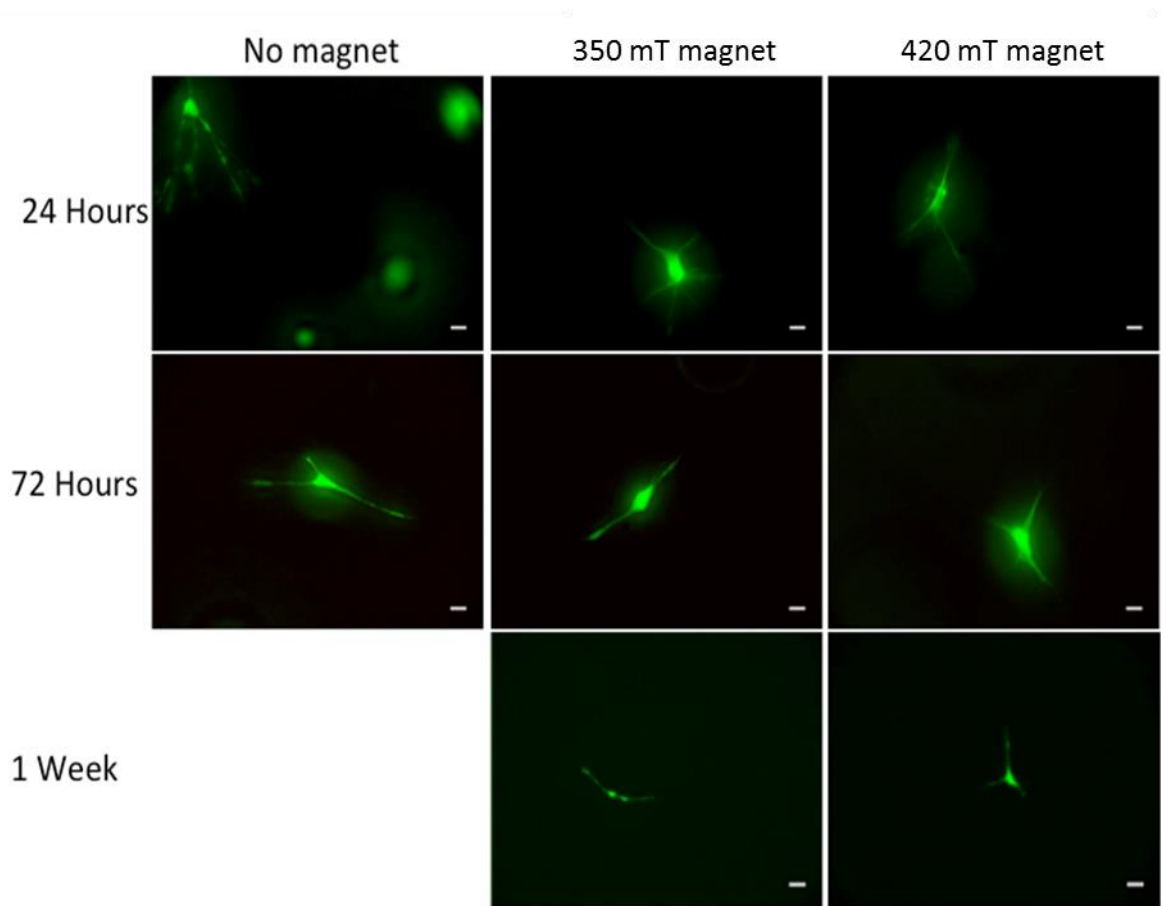


**Figure 3-16: Representative viability images of control MSCs incorporated within a collagen gel.**  
Fluorescence viability images (green=living cells, red=dead cells), 20x objective, scale bar = 20  $\mu\text{m}$ . (n=3, technical replicates)

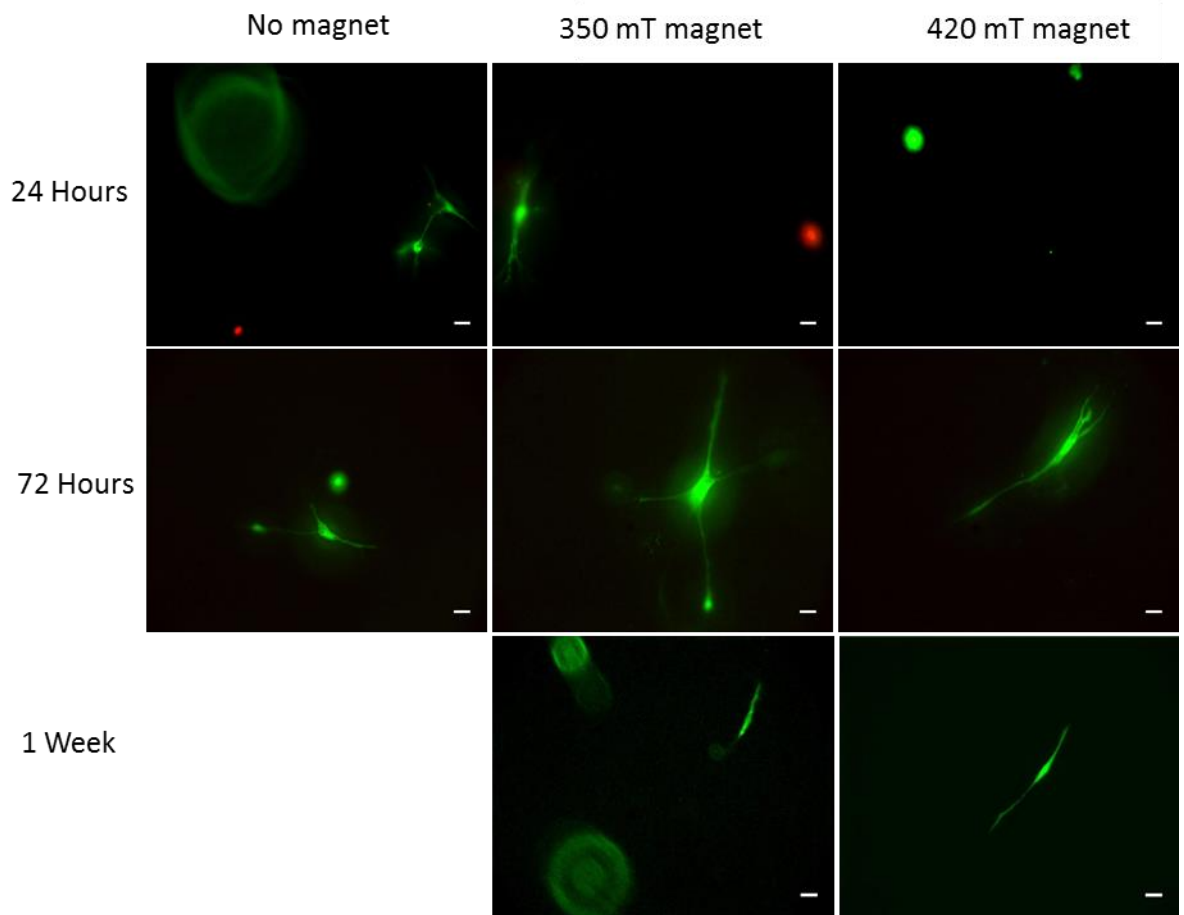


**Figure 3-17: Representative viability images of MSCs pre-loaded with mNPs and incorporated within a collagen gel. Fluorescence viability images (green=living cells, red=dead cells), 20x objective, scale bar = 20  $\mu$ m. (n=3 technical replicates)**

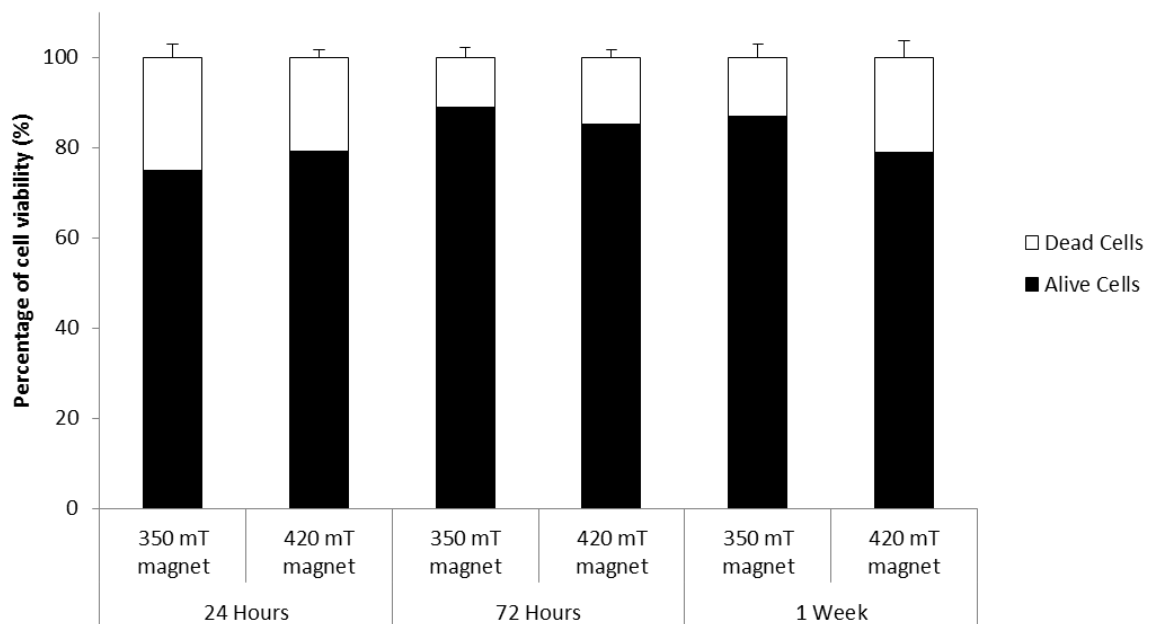


**Figure 3-18: Schematic diagram showing the MSC viability within the gel. MSCs were assessed over 1 week in the presence of two different magnetic fields. (n=3, three technical replicates)**

To assess cell cytoskeleton and mNP retention within the MSCs, the cells were again cultured up to 1 week, stained for F-actin and observed under fluorescence microscopy. Following a 24 hour culture period, the cells began to elongate within the collagen gel. After 72 hours there was minimal difference in cellular morphology, between cells cultured in the absence of an external magnetic field compared to cells exposed to the 350 mT magnet. Control MSCs without mNPs, irrespective of environment exhibited very little difference in cellular morphology, over the week incubation period (Figure 3-19). Moreover, the mNPs were retained within the MSCs irrespective of the different cell environment (no magnet, 350 mT or 420 mT magnet) over a 1 week incubation period (Figure 3-20). The images of the MSCs depicted elongated cytoskeletons, at all time points.

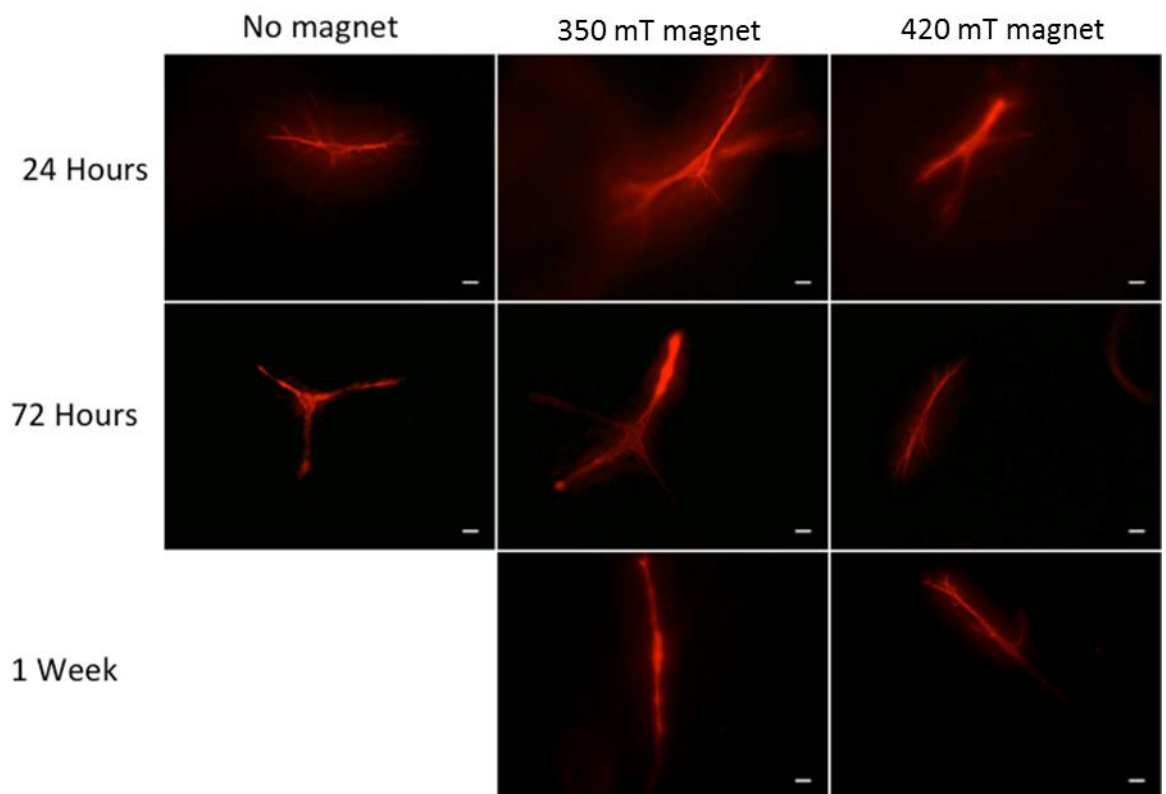


**Figure 3-19: Representative cytoskeleton images of control MSCs incorporated within a collagen gel.** Fluorescence images (red=actin, green=mNPs), 20x objective, scale bar = 20  $\mu\text{m}$ . (n=3, three technical replicates)

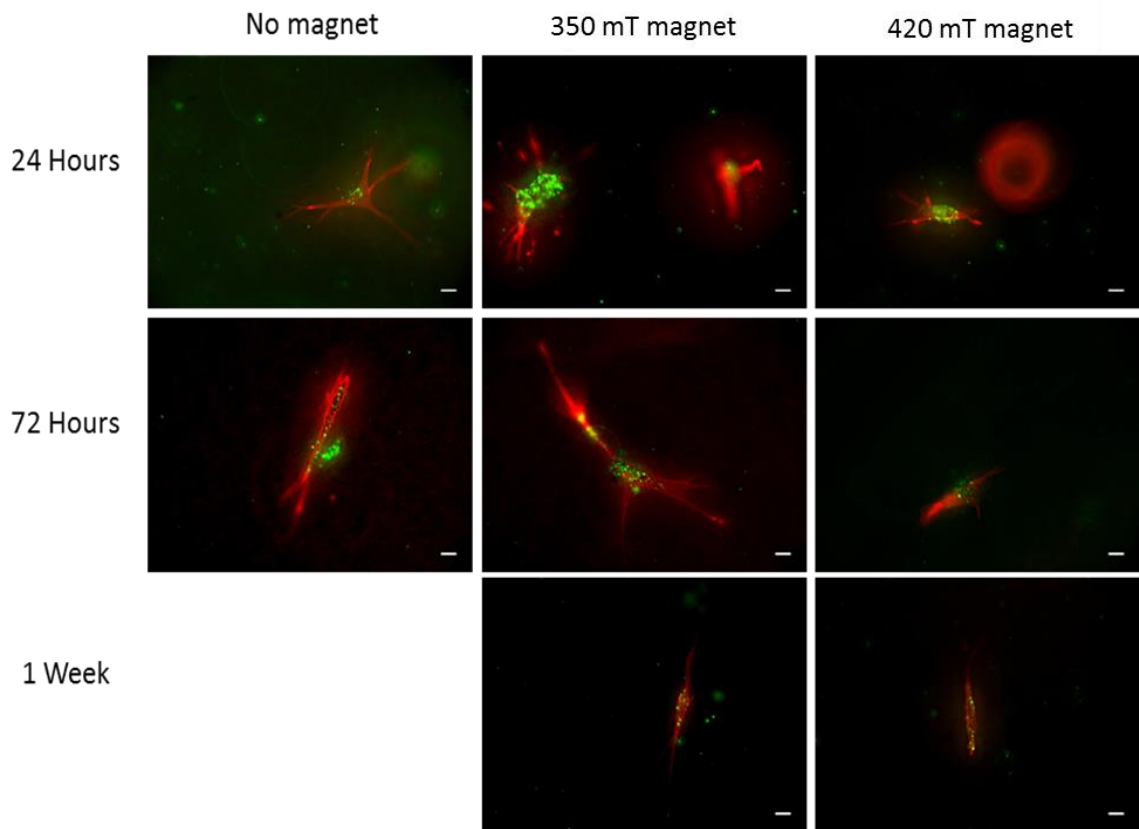


**Figure 3-20: Representative cytoskeleton images of MSCs pre-loaded with mNPs and incorporated within a collagen gel. Fluorescence images (red=actin, green=mNPs), 20x objective, scale bar = 20  $\mu$ m. (n=3, three technical replicates)**

Following verification of cell viability and mNP retention over 1 week, an assessment was made of the cell response to a magnetic field (Figure 3-16-Figure 3-20). Confocal microscopy was used to assess cell location within the collagen gel over 24 and 72 hour incubation periods. A z-stack was taken through the gel to assess the location and distribution of the MSCs, with an expectation of cell mobility towards the bottom of the well (i.e. towards the magnet). The results are shown in Figure 3-21.

The MSCs were mixed homogeneously throughout the gel, prior to setting. Gel observations showed all the control MSCs samples remained homogeneous and evenly distributed throughout the collagen gel. The presence of either a weak or strong magnet caused the mNP-loaded MSCs to congregate to the lower part of the gel and there was a lack of cells present within the top part of the gel. Additionally, the presence of the weaker magnet caused the cells to locate in the lower 60% of the gel over the initial 24 hour incubation period. However, after 72 hours there was significant cellular movement, as all cells were found to reside within the bottom half of the gel. The use of the strong magnet

indicated the mNP-loaded MSCs were distributed within the bottom 80% of the gel after 24 hours. However, after 72 hours in another sample the MSCs resided within the bottom 50% of the gel. Therefore, these results show no statistical difference between the uses of magnets as the MSCs pre-loaded with mNPs were observed within the bottom 50% of the gel and leaving the top 50% free of cells after 72 hours (Figure 3-21). Therefore, both magnetic field strengths (350 mT and 420 mT) resulted in the same MSC distribution in the gel at 72 hours.

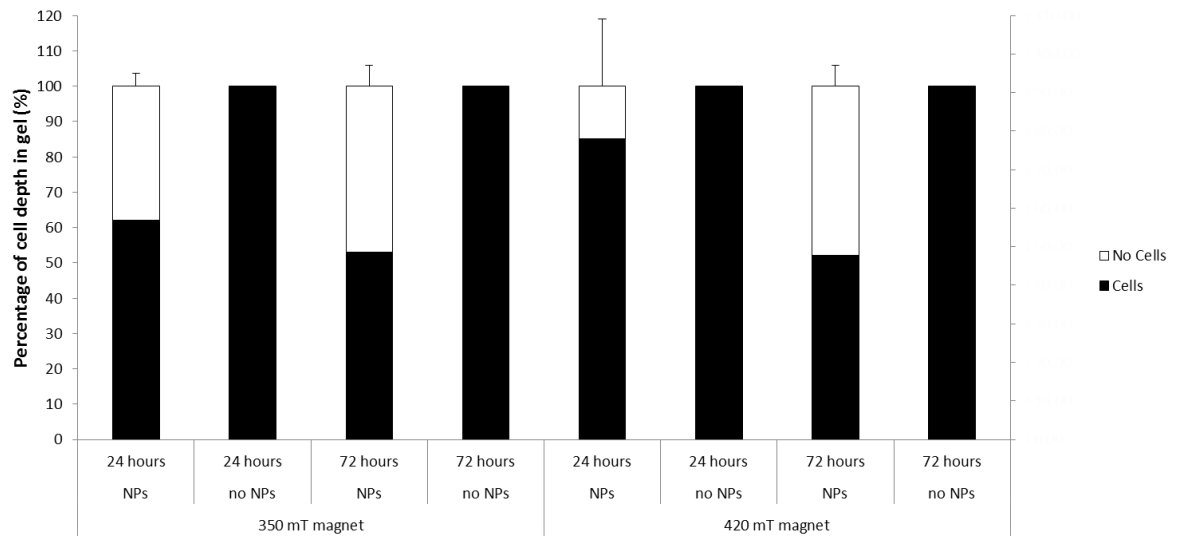


**Figure 3-21: Schematic diagram showing the MSC cell distribution within the gel. MSCs were assessed over 24 and 72 hours in the presence of two different magnetic fields. (n=3, three technical replicates)**

Unfortunately, although the MSCs did respond to the magnetic field by migration through the gel, the MSCs failed to conglomerate to form spheroids within the gel mixture. Therefore, in all further studies, the MSC spheroids were generated in media (as section 2.3.4.1), prior to transplantation into the gel mixture, before setting. The transplanted MSC spheroids were assessed for viability over 2 weeks, as shown in Figure 3-22. The MSCs remained viable over the 2 week incubation period.

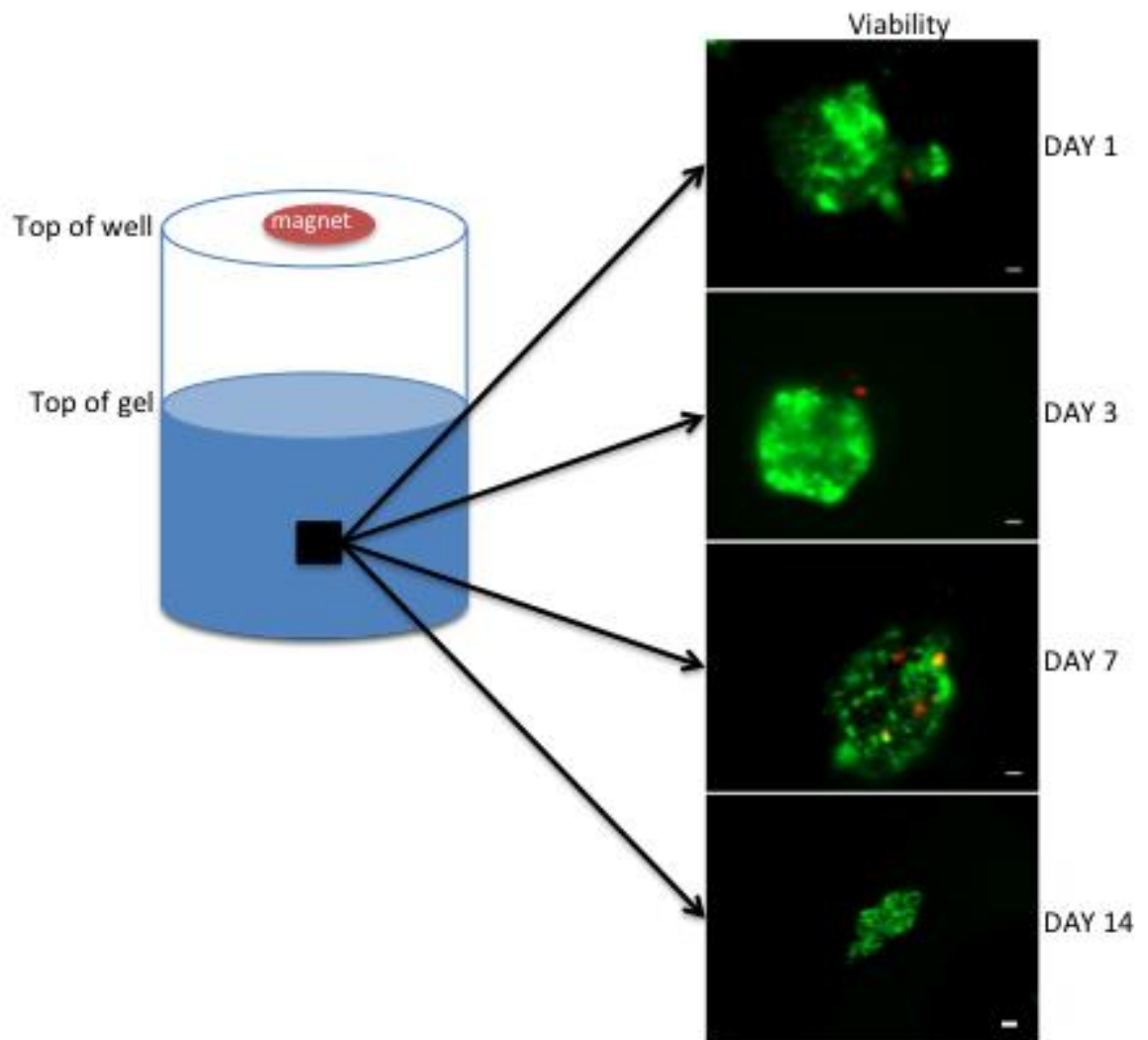


**Figure 3-22: Schematic diagram of MSC spheroids transplanted into a collagen gel. Fluorescence image of spheroids incubated for 1, 3, 7 and 14 days, within collagen gels, assessing cell viability (green=living cells, red=dead cells). 20x objective, scale bar = 20  $\mu$ m. (n=3, three technical replicates)**

### 3.4.6 Niche Model Development: Stage 6

#### **Assessing the Collagen Gel Stiffness (with and without spheroids).**

The bone marrow ECM retains MSCs within the niche microenvironment *via* a supportive ECM scaffold, which anchors the niche. The physical properties (stiffness/rigidity) of the ECM component within the bone marrow has been shown to affect stem cells (Lee et al., 2014). Therefore, it was important to verify the stiffness of the collagen gels used in the study, to ensure they had similar mechanical properties to the bone marrow ECM. The collagen gels, both with and without MSC spheroids, were assessed using rheology to determine

whether the stiffness of the study gels were akin to the *in vivo* bone marrow niche environment.

Collagen gels were prepared either with or without MSC spheroids and cultured for 3 days. The elastic and viscous moduli of the gels were rheology tested to calculate the stiffness of the material (Figure 3-23). The elastic modulus of both the control collagen gels and the gels containing the spheroids was higher than the viscous modulus, when the frequency increased from 0.1 Hz to 10 Hz. Additionally, the elastic modulus of the collagen gels encasing the spheroids was slightly higher (41 Pa) compared the collagen gels without spheroids (36 Pa).

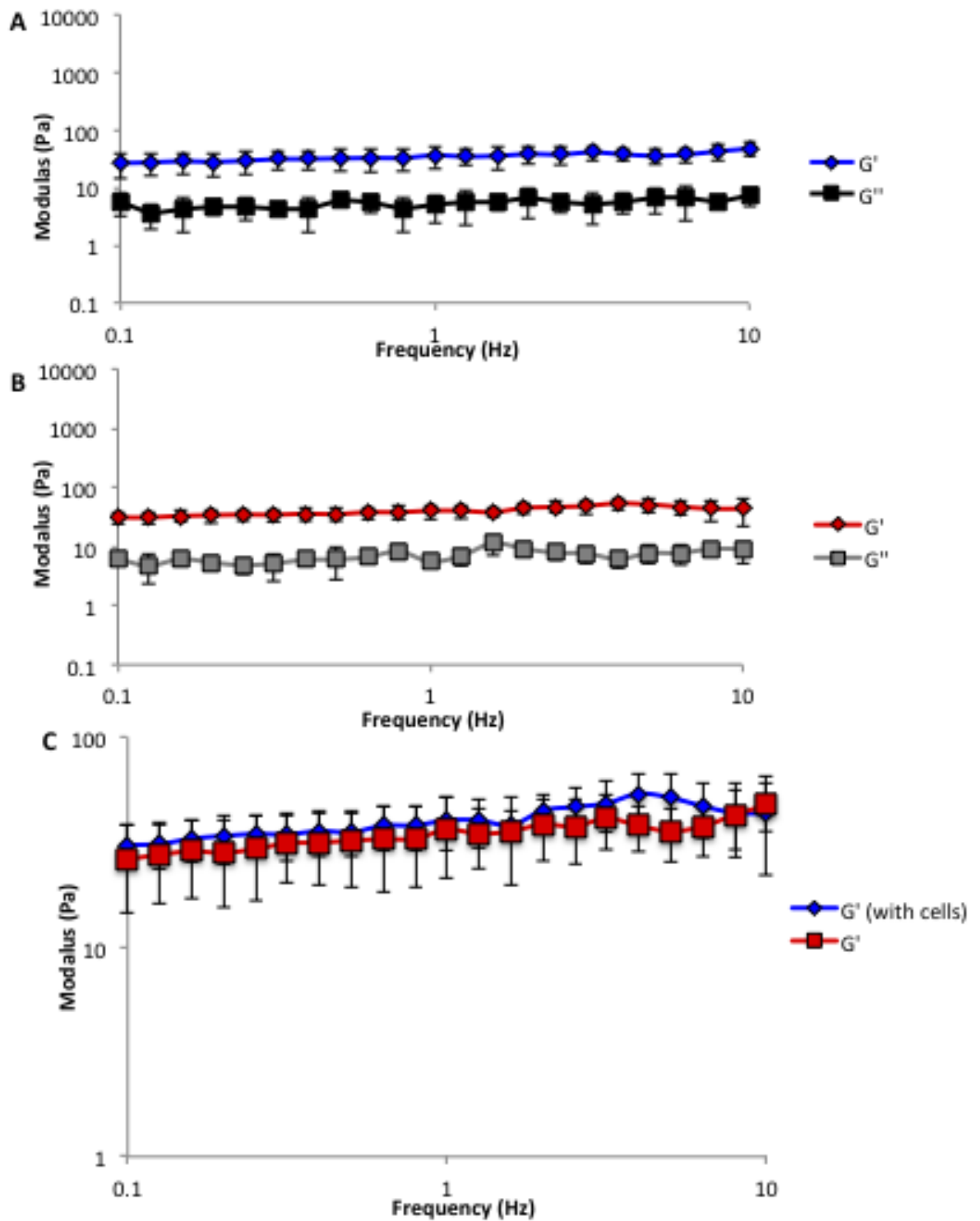


**Figure 3-23: Stiffness of collagen gels, with and without spheroids.** Rheology testing the elastic modulus ( $G'$ ) and viscous modulus ( $G''$ ) of (A) control collagen gels and (B) collagen gels encompassing spheroids. (C) Comparison graph of the elastic modulus of control collagen gels and gels containing spheroids. (n=3, three technical replicates)

### 3.4.7 Niche Model Development: Stage 7

#### **Assessing MSC Proliferation and Cell Cycle Gene Expression in Monolayer and Spheroid Culture Systems.**

The MSC niche is able to uphold stem cell function by retaining the MSCs in a quiescent state, which is regulated by Notch, Wnt, cell-cell and cell-ECM signalling factors as well as a hypoxic environment (Orford and Scadden, 2008). MSCs in the niche may enter the cell cycle through the stimulation of these factors. Therefore, this study was designed to determine whether the cells within the niche model reflected this quiescent state. MSCs, both in monolayer and in spheroid culture, were analysed both using BrdU incorporation (which binds directly to DNA as the cell proliferates), and also *via* cell cycle gene expression.

5-bromo-2'-deoxyuridine (BrdU) was incorporated into the media, during both monolayer and spheroid cell culture. BrdU binds with DNA during the DNA synthesis stage of the cell cycle therefore, its presence denotes a proliferative cell state. Cells were analysed at days 1, 3, 7 and 14. The monolayer cells, shown in Figure 3-24 demonstrated BrdU incorporation at days 1, 3 and 7, indicating the presence of proliferative cells. However, BrdU was not present at day 14 within the monolayer system. Conversely, the MSC spheroid cultures showed there was an absence of BrdU incorporation at any time point.

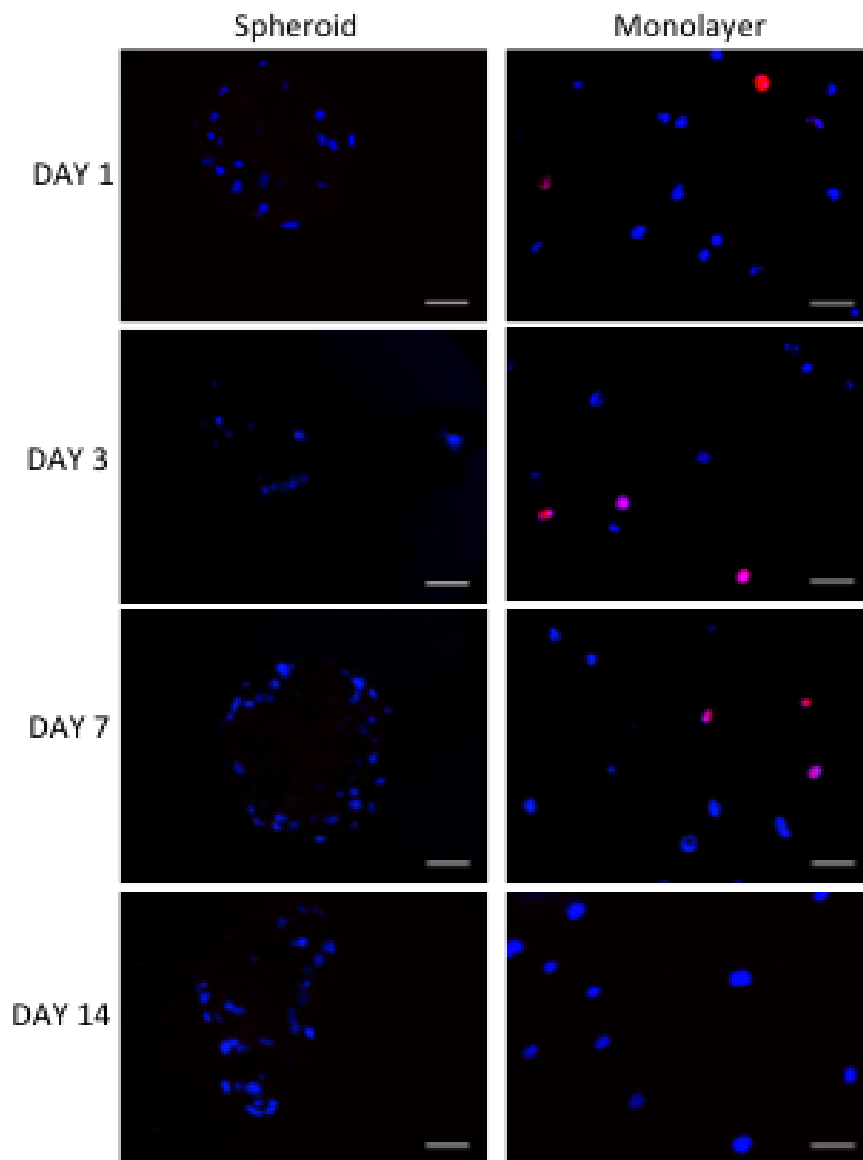


**Figure 3-24: Analysis of MSC proliferation via BrdU incorporation within a monolayer and spheroid culture system.** MSCs were assessed for 1, 3, 7 and 14 days, (purple = proliferating state of nucleus, blue = quiescent state of nucleus), 20x objective, scale bar = 50  $\mu\text{m}$ . (n=3, three technical replicates)

Further genomic analysis was used to assess whether the MSCs were either entering or engaged in the cell cycle in preparation for division within both monolayer and spheroid culture methods after 1 and 14 days. The cell cycle gene analysis is shown in Table 3-2. All data was normalised against the monolayer culture system at day 1 and day 14.

The results depicted in Figure 3-25 showed the MSC spheroids, at both day 1 and day 14 had a reduction in cell cycle gene expression, for 75% of the selected genes analysed, compared to the monolayer culture system (i.e. 18 out of the 24 genes showed a negative fold change in gene regulation). The day 1 and day 14

spheroids showed decreased expression in CCN A2, CCN B1, CCN E2, BIRC5, ANLN and SGOL1 compared to the monolayer cultures. Additionally, only the day 14 spheroids showed an absence of gene expression for cyclin E2, cyclin kinase 2 and ANLN.

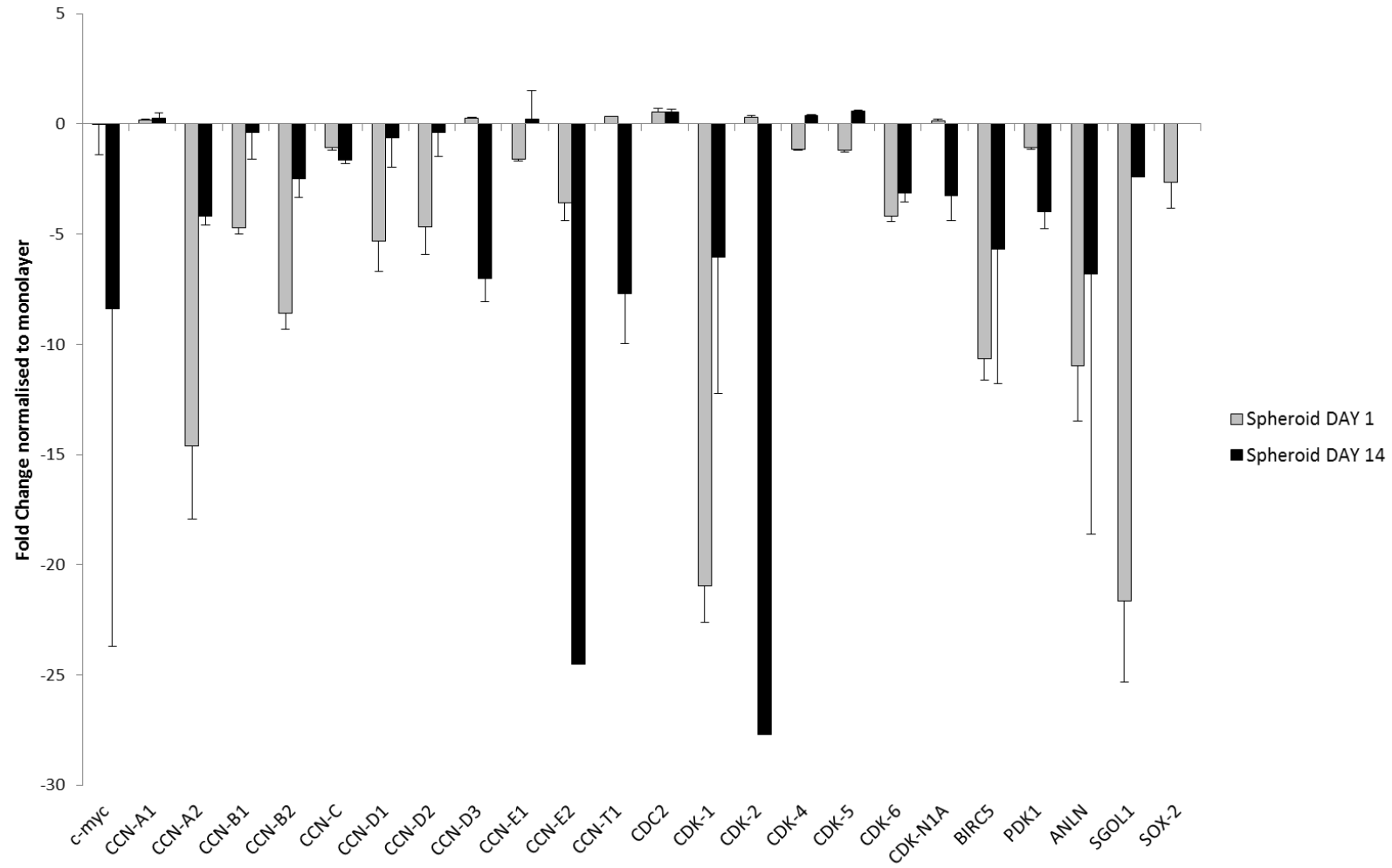


**Figure 3-25: Gene expression analysis of key cell cycle genes from MSCs extracted from spheroid cultures.** Fold change analysis conducted on spheroids at DAY 1 and DAY 14 normalised to the monolayer cultures at the identical time points. (CCN=cyclin and CDK=cyclin dependent kinase) (n=3, technical replicates)

### 3.4.8 Niche Model Development: Stage 8

#### **Assessing MSC Differentiation Potential in Monolayer and Spheroid Culture Systems.**

To assess MSC potency within both 2D and 3D MSC culture systems, the MSCs ability to differentiate was analysed following stimulation by osteogenic and adipogenic factors. Spheroid MSCs were dissociated/fragmented, then seeded as 2D cultures, to assess differentiation potential. Therefore, MSCs were cultured as monolayers over 28 days whereas, the spheroids were cultured for an additional 14 days.

Initially, several methods were applied to determine the optimal approach to dissociate/fragment the spheroids. Four techniques were used: 1) the spheroid was agitated using a pipette tip, 2) a narrow bore needle was slowly plunged up and down into the spheroid, 3) a needle was rapidly plunged up and down into the spheroid and 4) the spheroid was left intact. All the spheroid samples were then transferred onto fresh culture plates and left to incubate for 4 days (Figure 3-26). The images showed the fragmentation process, which used the agitated pipette tip produced the greatest MSC outgrowth and cell coverage in the monolayer culture system. In addition this method left fewer MSCs remaining within the spheroid culture (i.e. the darker concentration of cell stain). Whereas, the use of the rapid agitation process with the needle produced the least amount of MSC outgrowth and cell coverage. The spheroids left intact and seeded onto coverslips showed a continual spread of cells migrating out and dispersing into the surrounding area. However, cells were only present around the spheroid and there was an uneven distribution of cells covering the coverslips.

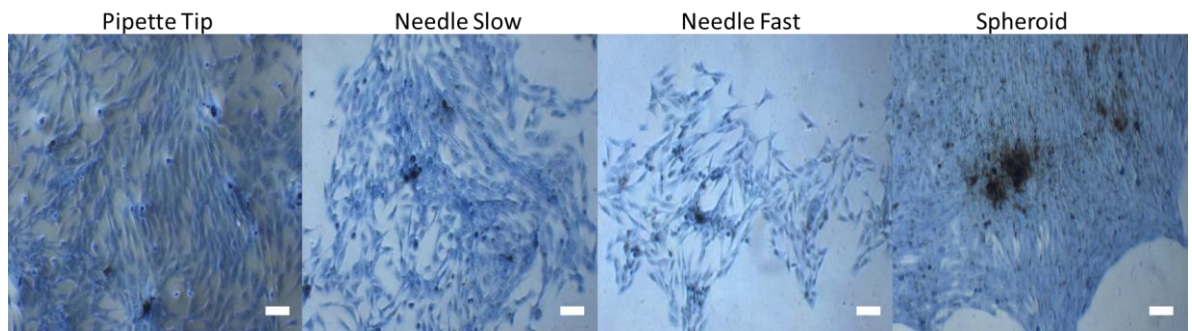


**Figure 3-26: Outgrowth of MSC monolayer from MSC spheroids.** Spheroids were dissociated using four individual techniques, 5x objective, scale bar = 200  $\mu\text{m}$ .

Therefore, the pipette tip method of fragmentation was adopted to grow MSCs in monolayer post-spheroid culture. The MSCs were subsequently induced with osteogenic or adipogenic media for either 28 days (monolayer) or 42 days (spheroids). These cultures were compared with conventional 2D MSC culture systems, to determine whether the stem cells were still able to differentiate (Figure 3-27). Osteopontin staining was evident in both monolayer and spheroid cultures, (Figure 3-27, image A and C) whilst lipid droplets were also evident in both culture systems (Figure 3-27, image B and D). This evidence verified the MSCs cultured under both culture systems were capable of being induced to express osteogenic (osteopontin) and adipogenic (lipids) markers.

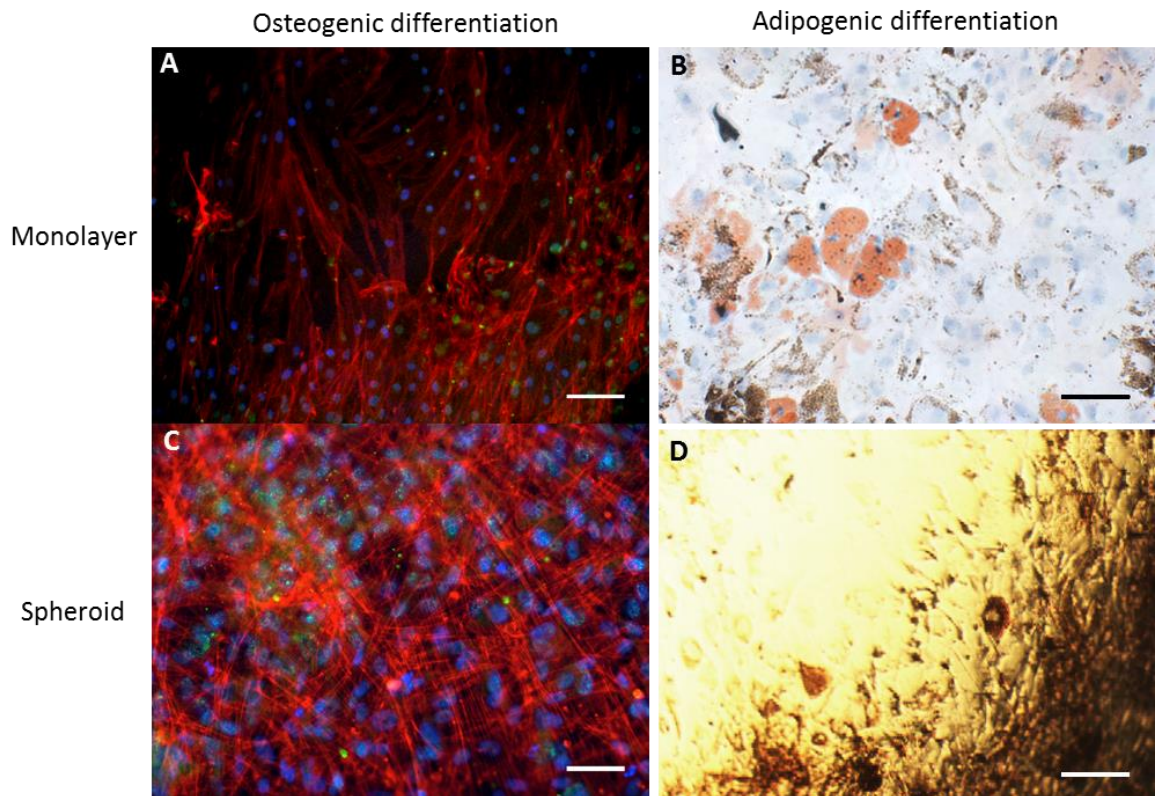


**Figure 3-27: Microscopy images of induced MSCs with osteogenic and adipogenic media. Monolayer cells were seeded and cultured for 28 days. Dissociated spheroids were seeded and cultured for 42 days. (A) Fluorescence image of MSCs cultured as monolayers induced with osteogenic media (red = actin, green = osteopontin, blue = nucleus). (B) Light microscopy image of MSCs cultured as monolayers induced with adipogenic media (red = lipid droplets, blue = nucleus). (C) Fluorescence image of MSCs cultured as dissociated spheroids induced with osteogenic media (red = actin, green = osteopontin, blue = nucleus). (D) Light microscopy image of MSCs cultured as dissociated spheroids induced with adipogenic media (red = lipid droplets, blue = nucleus). 10x objective, scale bar = 50  $\mu\text{m}$ .**

## 3.5 Discussion

### 3.5.1 Niche Model Development: Stage 1

#### Optimising the mNPs Loading Conditions of the MSCs.

The uptake of the mNPs within the MSCs was successfully achieved at both concentrations and either in the presence or absence of an external magnetic field. Cellular uptake of mNPs has been shown to occur *via* a variety of endocytic pathways, including clathrin-dependent endocytosis, caveolae-dependent endocytosis, macropinocytosis or clathrin- and caveolae- independent endocytosis (Kou et al., 2013). The exact pathway by which these mNPs enter the cell is still unclear. However, it is well established that the mNP size affects which cellular uptake pathway may be used by the cell. For example, studies have shown large NPs (500 nm to 5  $\mu$ m) are engulfed through macropinocytosis and smaller NPs (60-80 nm) are internalised by caveolae-dependent endocytosis (Benmerah and Lamaze, 2007). Rejman et al., showed NPs  $\leq$  200 nm in size were internalised by mouse melanoma cells, *via* clathrin mediated endocytosis (Rejman et al., 2004). The mNPs used throughout this thesis had a hydrodynamic diameter of 200 nm, which suggests the clathrin-dependent pathway was the most likely method used by the MSCs to engulf the mNPs.

However, there are other factors influencing which endocytic pathway is employed for NP internalisation within the cell. Surface charge on the mNP affects the rate of cellular uptake. The cytomembrane of the cell possesses an overall net negative charge, so positively (cationic) charged mNPs have a strong electrostatic interaction with the cell membrane, thus leading to rapid internalisation within the cell (Kou et al., 2013). Figure 3-3 shows the mNPs were being taken up by the MSCs, within 15 minutes of being subjected to mNP presence, irrespective of concentration or external magnetic field. The mNPs used in these experiments possessed a cationic surface charge. Therefore, these results correlate with the theory that surface charge plays an important role, in uptake of these mNPs within the MSCs.

Figure 3-3 showed a correlation between mNPs concentration and the level of internalisation. The higher concentration (0.1 mg/mL) allowed for significantly

greater mNP uptake by the MSCs, at all time points and conditions compared to the lower concentration (0.01 mg/mL).

The results depicted in Figure 3-3 and Figure 3-4, demonstrated a significant increase in mNP uptake, within the MSCs when an external static magnetic field was applied below the cells. The concept of applying an external magnetic field to enhance delivery of mNPs was initially applied to target gene delivery in cells, and was termed magnetofection (Plank et al., 2003). Many current pre-loading methods are time consuming and inefficient, with the cells being incubated with the mNPs for upwards of 24 hours. However, research groups have adapted the magnetofection method to show significant differences in mNP uptake when using an external magnetic field (Dejardin et al., 2011, Liu et al., 2012). Studies conducted by Liu et al., found mNP-labelled cancer cells uptake was increased by 40% using a static external magnetic field over a period of 40 minutes compared to labelled cells without a magnetic field (Liu et al., 2012). Additionally, Dejardin et al., demonstrated mNP internalisation within fibroblasts was greatly enhanced in the presence of a magnetic field (Dejardin et al., 2011). Attracting the mNPs towards the magnet located beneath the cells, increases the density of NPs at the cell surface (shown in Figure 3-5) allowing for an increased rate of endocytosis, as shown by ICP-MS (Figure 3-3).

The ICP-MS experimental procedure did not require the use of normalising mNP uptake against either cell number or DNA content. Figure 3-3 reflects the measured amount of mNP uptake in cell lysates, after 24 hours growth (Kim et al., 2010, Janer et al., 2014, Child et al., 2011). However, normalising to cell number (e.g. *via* per cm<sup>2</sup> or counting trypsinised cells) would provide a more accurate recording of mNP uptake in MSCs (Albanese et al., 2012, Suzuki et al., 2014).

### **3.5.2 Niche Model Development: Stage 2**

#### **Assessing mNP Retention Within MSCs Following Trypsinisation.**

In order to use a magnetic field to generate MSC spheroids, the cells must be able to retain the mNPs and respond to an external magnetic field. The images

depicted in Figure 3-6 show retention of the mNPs within the MSCs, after the cells were trypsinised and seeded onto another substrate.

Small particles such as mNPs, which have been internalised within cells, may be readily released from the cell, through a process known as exocytosis. However, the rate of exocytosis and excretion has been shown to be size dependent (Xu et al., 2012). For example, the larger the NP, the slower it is released from the cell. A study conducted by Chithrani and Chan, compared the exocytosis rates of different sized transferrin coated gold NPs (Chithrani and Chan, 2007). The researchers found the exocytosis rate was 2 times higher/faster for 14 nm sized NPs, compared to the 74 nm sized NPs. Additionally, they discovered the rate of exocytosis was linearly related to size of the gold NPs. Furthermore, the researcher assessed whether the shape of the nanoparticle affected the exocytosis rate and they found rod shaped nanoparticles were released faster at a higher rate compared to spherical shaped nanoparticles.

Sarkar et al., studied the exocytosis rate of particles sized 1-2  $\mu\text{m}$  and found particles were retained within MSCs for at least 7 days (Sarkar et al., 2011). Moreover, Guzman et al., pre-loaded neural stem cells with superparamagnetic iron oxide (SPIO) nanoparticles sized between 80-120 nm and took long term observations using MRI (Guzman et al., 2007). The researchers were able to detect the stem cells, labelled with the SPIO nanoparticles for up to 18 weeks post internalisation. Furthermore, Jo et al., labelled MSCs with iron oxide-pullulan NPs sized ~100 nm and found these were retained within the cell for 21 days (Jo et al., 2010).

Collating these studies, it became apparent that both the size and shape of the mNPs are extremely important in the retention within the MSCs. The mNPs used in this study were spherical in shape and 200 nm in diameter. These mNPs were larger than the nanoparticles used by Guzman et al., Chithrani and Chan, and Jo et al. Therefore, the mNPs should remain within the MSCs and not be so readily exocytosed from the cells post manipulation as depicted in Figure 3-6 (Guzman et al., 2007, Jo et al., 2010, Chithrani and Chan, 2007).

### 3.5.3 Niche Model Development: Stage 3

#### **Assessing mNP-loaded MSC Response to an External Magnetic Field in Monolayer.**

When the magnet was placed directly under a mNP-loaded MSC suspension, all the cells attached to the well within the magnetic field area (see Figure 3-8). The magnet used had a magnetic field strength of 350 mT, with the North Pole facing the well and the South Pole positioned below the well (see Figure 3-28). The magnet distributes a non-uniform magnetic field and then induces a force on the mNPs. The distribution of the magnetic field studied by Dejardin et al., and Smith et al., applied similar magnets to cells cultured with mNPs is shown below in Figure 3-28 (Smith et al., 2010b, Dejardin et al., 2011).

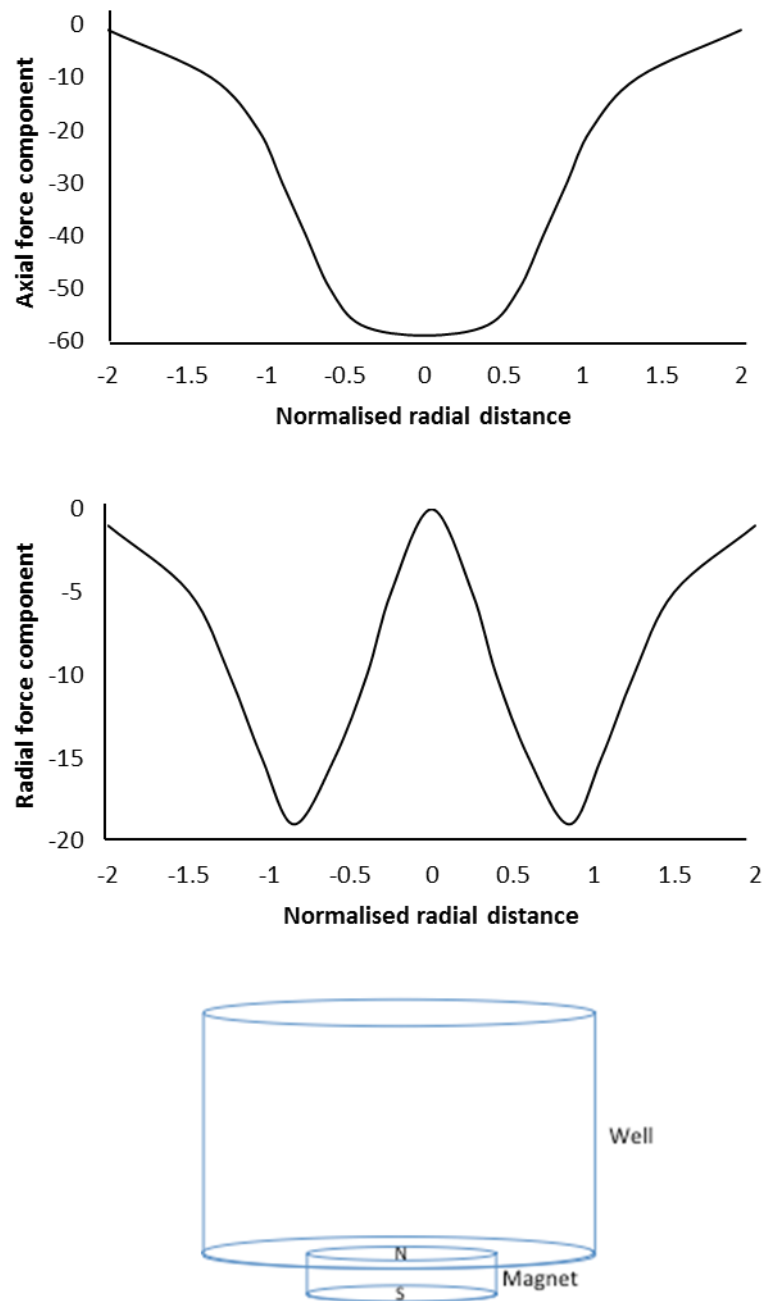


**Figure 3-28: Schematic diagram of magnetic field distribution from 350 mT magnet.** Diagram of the position of the magnetic dipole moments from the 350 mT magnet underneath the well containing a MSC suspension labelled with mNPs. (Adapted from (Dejardin et al., 2011)).

Dejardin et al., calculated the forces and field strength of the magnet on mNPs sized 500 nm. The researchers stated the axial force from the magnet varied radially across the cell culture, attracting mNPs towards the surface of the magnet. The distribution and position of the cells shown in Figure 3-8 correlates with the variation in magnetic forces exerted from the magnet observed and described by Dejardin et al., (Dejardin et al., 2011). These results indicate that the MSCs retained a sufficient number of mNPs to be easily manipulated with a static external magnetic field. Magnetic cell manipulation may be an excellent

tool to influence cell motility. Indeed, in a study conducted by Polyak et al., the authors were able to directly move magnetically labelled endothelial cells, to steel stents *in vivo* using an external magnetic field (Polyak et al., 2008).

### 3.5.4 Niche Model Development: Stage 4:

#### **Assessing mNP-loaded MSC Viability and Phenotype in Monolayer Culture and 3D Spheroid Culture.**

The MSCs were loaded with mNPs and the cell viability was assessed over time, to determine whether these particles were detrimental to cells in culture. Previous research has suggested that the ease at which certain NPs cross the cell membrane barrier may increase their cytotoxic potential (Nel et al., 2006). The viability of the cells containing the mNPs were assessed over 14 days and approximately 100% of the cells remained viable as shown in Figure 3-9. Therefore, the amount of mNPs retained within the MSCs did not appear to cause any cytotoxic effects. Studies have found the internalisation of the iron oxide mNPs do not affect cellular responses or behaviour (Qin et al., 2013, Guzman et al., 2007). Qin et al., compared unlabelled and iron oxide NP labelled ADSCs and found the NPs did not affect cell viability, proliferation, cell cycle or differentiation capability (Qin et al., 2013).

MSCs within the bone marrow niche express characteristic surface markers, which allows for the identification of their differentiation and self-renewal capacity. Therefore, these markers indicate the stem cells multipotency properties. Two distinct MSC surface antigen markers (STRO-1 and nestin), which are highly expressed in bone marrow were used to determine whether the MSCs were retaining their stem cell properties. Over the past 20 years, STRO-1 has been considered as the best-known marker to identify and isolate MSCs (Ning et al., 2011). A review by Lin et al., found over 100 MSC studies used STRO-1 as an identification and isolation marker for MSCs (Lin et al., 2011). Furthermore, MSCs extracted and isolated using STRO-1 possess functional properties akin to those *in vivo* (Kolf et al., 2007).

Historically, nestin has been widely used, as an identification marker of neuronal cells. Recently however, MSCs supporting the HSC niche have shown high nestin antigen expression (Mendez-Ferrer et al., 2010, Svachova et al., 2011).

Furthermore, bone marrow studies reported HSC home towards nestin<sup>+</sup> MSCs (Mendez-Ferrer et al., 2010). Nestin is a characteristic MSC marker of multipotency for cells, which are able to proliferate, migrate and differentiate (i.e. retain their stem cell properties) (Svachova et al., 2011). Therefore, STRO-1 and nestin expression were assessed in the traditional 2D monolayer system over time, to determine whether they correlate with the properties observed within an *in vivo* niche.

Figure 3-9 shows that within the first 3 days of monolayer culture, the MSCs exhibited high STRO-1 and nestin expression. However, between day 3 and day 14, the MSCs showed a significant reduction in STRO-1 and nestin expression. These results indicate the MSCs are losing their “stemness” and starting to differentiate. Research has shown there are clear differences in gene expression between MSCs cultured in 2D and 3D environments, thus leading to overall differences in protein/antigen expression (Pedersen and Swartz, 2005). These differences include alterations in differentiation and self-renewal capabilities, which indicates that cells in 2D culture do not exhibit behaviour shown in the *in vivo* niche (Shen et al., 2013).

Parallel studies have further highlighted issues associated with culturing MSCs within 2D culture environments. MSCs cultured this way exhibit unpredictable behaviours, including enhanced differentiation in response to “rough” handling, overcrowding and stress (Marx, 2013). Once isolated and cultured in 2D systems, MSCs initially maintain their multipotency properties. However, MSCs multipotency reduces over a short culture period (Baer et al., 2010, Baraniak and McDevitt, 2012). This loss of multipotency poses a real difficulty for their use within regenerative medicine, which requires large numbers of MSCs.

A magnet located on top of the culture well, induced magnetic levitation of an MSC suspension towards the magnetic field, causing the MSCs to coerce together and form a 3D multicellular spheroid structure within several hours (Figure 3-11). This time period correlated to the time taken to form a cohesive multicellular spheroid of neural stem cells using mNPs *in vitro* (Souza et al., 2010). As the spheroid was generated at the air-liquid interface within the well, which suggested the magnetic field force was sufficient to overcome the gravitational forces applied on the cells.

The MSCs spheroids were assessed for viability, STRO-1 and nestin at the same time points as the monolayer MSCs studies. The viability images of the spheroids shown in Figure 3-11, depicted high MSC viability. These cells have been described as adherent cells, which require cellular adhesion for survival. Therefore, the cells will have formed cell-cell attachments to maintain survival within the 3D structure. Studies have shown spheroid cultures stabilise cells and prevent apoptosis, as they allow cell-to-cell interactions, which is the minimum requirement for cell survival (Kim et al., 2013). Additionally, spheroid cultures encourage strong cell-cell contacts, which in turn provides a good representation of the natural bone marrow niche environment (Wang et al., 2009). A study conducted by Hildebrandt et al., showed it was possible to maintain the cell viability of MSCs, within a spheroid structure, for a period of 29 days (Hildebrandt et al., 2011).

MSCs within the spheroids clearly retained high STRO-1 and nestin expression profiles over the 2 week incubation period, indicating the MSCs were maintaining their multipotency, within the 3D spheroid structure. A study conducted by Cheng et al., assessed the stemness properties of human adipose stem cells (hASCs) and found significant up regulation of these markers within spheroids, compared to monolayer cultures (Cheng et al., 2012). Stem cell homeostasis is regulated and controlled by the niche, therefore it follows stem cells retention of high self-renewal and multipotency properties when cultured in mimicked environments.

The MSC niche has been found to display low oxygen tensions (hypoxia) and research has suggested hypoxia maintains MSCs in an undifferentiated state (Harrison et al., 2002, Pasarica et al., 2009, Matsumoto et al., 2005). Therefore, MSCs in the hypoxic niche are able to retain their multipotent properties as detected by the expression of multipotency markers e.g. STRO-1 and nestin. Gatenby et al., found multicellular 3D spheroids with a diameter in excess of 200  $\mu\text{m}$  exhibited hypoxic regions (Gatenby et al., 2007). Studies have shown that oxygen is only able to diffuse 50-100  $\mu\text{m}$  into a tumour spheroid, leading to hypoxic conditions occurring within the tumour (Curcio et al., 2007, Bryce et al., 2009). Sun et al., detected regions of hypoxia in the centre of multicellular spheroids (Sun et al., 2015). The researchers observed hypoxia 100  $\mu\text{m}$  from the

outer edge of the spheroid. Therefore, these results suggest the spheroids created in this thesis may exhibit hypoxia, because the average spheroid diameter was 259  $\mu\text{m}$  (Figure 3-13), which may allow the MSCs to remain in an undifferentiated state.

Furthermore, the voids adjoining the MSCs within the spheroids as shown in Figure 3-14 indicated an absence of ECM production from the MSCs, which may be due to the spheroids being in a quiescent state, as a result of hypoxia. A study conducted by Barkan et al., found the creation of ECM, including fibronectin was a result of the transition of quiescence to metastatic growth in mammary cancer cells (Barkan et al., 2010). Furthermore, the authors found a related dormant mammary cancer cell line did not produce fibronectin, indicating ECM production is reliant on active cell proliferation.

### **3.5.5 Niche Model Development: Stage 5**

#### **Assessing the Formation of a MSC Spheroid Within a Collagen Gel.**

The bone marrow niche is a complex environment, comprised of various factors, including numerous cellular compartments, ECM, secreted factors, physical parameters (stiffness and shear force) and metabolic control e.g. glycolysis (Lane et al., 2014). Spheroid cultures allow important cell-cell interactions however, they lack the complexity of the physical and ECM components of the *in vivo* niche. Therefore, to create a more realistic *in vitro* model, the complexity was increased by using collagen Type I gels. Collagen Type I has been described as the most abundant ECM protein within the human body and is the main component of bone and skin (Higuchi et al., 2012). In addition, gel stiffness may be tailored by simply adapting the collagen concentration, to produce the varying mechanical properties of any particular tissue.

Initial experiments homogeneously mixed MSCs within the collagen gel and assessed for viability (see Figure 3-16 and Figure 3-17). The MSCs remained viable up to 1 week in the collagen, irrespective of the presence of magnetic fields or mNPs (Qin et al., 2013, Guzman et al., 2007). Collagen Type I scaffolds have been used extensively in tissue engineering and regenerative medicine studies, without any detrimental influence on cell viability. The MSCs remained

viable in this study, so it may be expected the MSCs formed cell-collagen (matrix) attachments (Glowacki and Mizuno, 2008, Pang and Greisler, 2010, Parenteau-Bareil et al., 2010).

MSC morphology was assessed over a week using different static magnetic field strengths (Figure 3-19 and Figure 3-20). The stronger magnet (420 mT) did affect the mNP-loaded MSC morphology, which indicated the magnetic field was potentially affecting the cells behaviour. Meng et al., studied the morphology of MSCs in the presence of superconductive magnetic field (Meng et al., 2011). The researchers found the magnetic field caused cell shrinkage and disrupted the cytoskeleton (Meng et al., 2011). Therefore, the stronger 420 mT magnet was not used in future experiments because it caused MSC morphological changes.

Both magnetic field strengths influenced the MSC distribution within the collagen gels (shown in Figure 3-21). The magnets were placed at the bottom of the well, whilst the gels were setting. Cell distribution was analysed using confocal microscopy, the results showed the cells containing mNPs responded to the magnets and migrated towards the magnetic field. However, the images in Figure 3-16-Figure 3-20 showed individual MSCs with an absence of spheroid formation. Whilst the mNP-loaded MSCs were clearly attracted by the axial force towards the surface of the magnet, the radial magnetic force did not cause the MSCs to coerce together.

The failure to create a multicellular MSC structure within the gels, led to the generation of spheroids in media. The spheroids were then transferred to gel culture during the gel setting stage. These transferred spheroids/gels were assessed for cell viability, over a two week period showed high MSC viability (Figure 3-22). Furthermore, the collagen gel provided a physical medium, which was mechanically similar to the *in vivo* bone marrow environment.

### **3.5.6 Niche Model Development: Stage 6**

#### **Verifying the Collagen Gel Stiffness (with and without spheroids).**

The native bone marrow is a dynamic environment, within which the MSC niche is anchored and supported by the ECM (Gattazzo et al., 2014). The mechanical

characteristics of the bone marrow ECM have been shown to regulate niche homeostasis, proliferation and differentiation. For example, the ECM's stiffness confers isometric tension within the cells' cytoskeleton, which induces a dynamic response that regulates stem cell behaviour (Engler et al., 2006). The elastic modulus (also known as the Young's modulus) has been used to determine the stiffness of ECM scaffolds and substrates. Several research studies have adjusted the stiffness of their substrates to mimic particular tissues, thus inducing MSC differentiation associated with that specific matrix elasticity (Zhao et al., 2014b, Li et al., 2013, Her et al., 2013, Rasi Ghaemi et al., 2013). For example, Engler et al., showed MSC neuronal differentiation commitment on soft gels (1 kPa), myogenic differentiation on stiffer gels (11 kPa) and osteogenic differentiation on stiff gels (34 kPa) (Engler et al., 2006).

The bone marrow is a soft tissue, which has a reported stiffness of approximately 100 Pa (Metzger et al., 2014, Sobotková et al., 1988). Winer et al., previously analysed the rheology of bovine bone marrow and found the stiffness to be  $220 \pm 50$  Pa (Winer et al., 2009). The authors cultured their MSCs on polyacrylamide gels (250 Pa) and found the cells mimicked *in vivo* niche behaviour by remaining quiescent. Therefore, imitating the elasticity of bone marrow environment allowed the researchers to mimic *in vivo* niche responses.

The results depicted in Figure 3-23 showed the elastic modulus of the collagen gels, containing the MSC spheroids, was slightly higher than the gel without cells. The increased stiffness may be due to the MSCs binding to the collagen, to anchor the spheroid. MSCs attach to collagen via integrins, which are transmembrane proteins. Integrins adhere to specific amino acid sequences on various ECM components, such as collagen. The direct mechanical link between the ECM and the cell cytoskeleton, means any changes in cytoskeleton will directly affect the physical properties of the ECM (Walters and Gentleman, 2015). Therefore, the addition of MSC spheroids may increase tension and alter the collagen gel stiffness. Additionally, the elastic modulus of the newly created model containing spheroids (40 Pa), shown in Figure 3-23 is comparable to the elastic modulus observed within the native bone marrow environment (100 Pa). Therefore, this addition of collagen to the MSC niche model further mimicked the innate MSC niche milieu in the bone marrow.

### 3.5.7 Niche Model Development: Stage 7

#### **Assessing MSC Proliferation and Cell Cycle Gene Expression in Monolayer and Spheroid Culture Systems.**

Stem cells within the bone marrow niche reside in a quiescent (resting) state, when the stem cells do not enter the cell cycle. There are major regulatory events, which occur at the initial phase of the cell cycle ( $G_1$ ) allowing the cell to progress through the S phase. During the S phase, the synthesis and replication of DNA is initiated readily for cell division. BrdU is a synthetic analogue of the nucleoside thymidine, which competes with thymidine, when the cells are in the S phase of the cell cycle. Therefore, BrdU becomes incorporated into the DNA of actively dividing cells (Taupin, 2007, Li et al., 2008).

The images shown in Figure 3-24, show the MSCs in the monolayer culture system incorporated BrdU within the cell nuclei, indicating the MSCs were in or had gone through the S phase of the cell cycle and were actively dividing and proliferating. The cell proliferation correlates with the diminished expression of STRO-1 and nestin over time in monolayer culture supporting the fact that MSCs cultured in 2D systems may lead to undesired differentiation.

Conversely, the corresponding MSC spheroid images in Figure 3-24 indicated a lack of BrdU incorporation within the MSC nuclei, suggesting the cells had not entered the S phase of the cell cycle, but remained within their quiescent state. A study by Cheng et al., found cell proliferation (assessed by alamar blue assay) was inhibited within ASC spheroids, indicating stem cells were in a quiescent state (Cheng et al., 2012).

MSCs in the niche experience a low metabolic rate, which helps to reduce stem cell damage and this effect has been observed in spheroids (Ivanov et al., 2014). The low metabolic rate may slow down cell cycle progression within the MSC spheroids, thus delaying progression of MSCs through to the S phase of the cycle. Therefore, BrdU may not have been incorporated into the MSC DNA, because of the delayed cell cycle progression into the S phase. The BrdU in this experiment was only added 6 hours prior to analysis and therefore, had not sufficient time to become integrated into the MSC DNA. However, if the BrdU had remained in

situ with MSC spheroids for a longer period of time, there may have been incorporation into the DNA.

Cell cycle gene analysis in Figure 3-25, showed a significant number of genes (18 out of 24) were down regulated in spheroid culture, compared to monolayer culture. The cell cycle is regulated by cyclin-cyclin dependent kinase (CCN-CDK) complexes, which control cell cycle progression (Malumbres and Barbacid, 2005). Previous cell cycle observations found variations in gene expressions for CCNs and CDKs, and these changes indicated the location of the cell in the cell cycle (Bertoli et al., 2013). Cell cycle progression is driven by the increased gene expression of certain CCNs and CDKs at specific stages in the cycle. Studies have shown cells undergo three major transitions within the cell cycle ( $G_1$  to S,  $G_2$  to M and M to  $G_1$  phase) and these are triggered by the activity of CDKs, which bind with CCNs depicted in Figure 3-29 (Matsumoto and Nakayama, 2013).

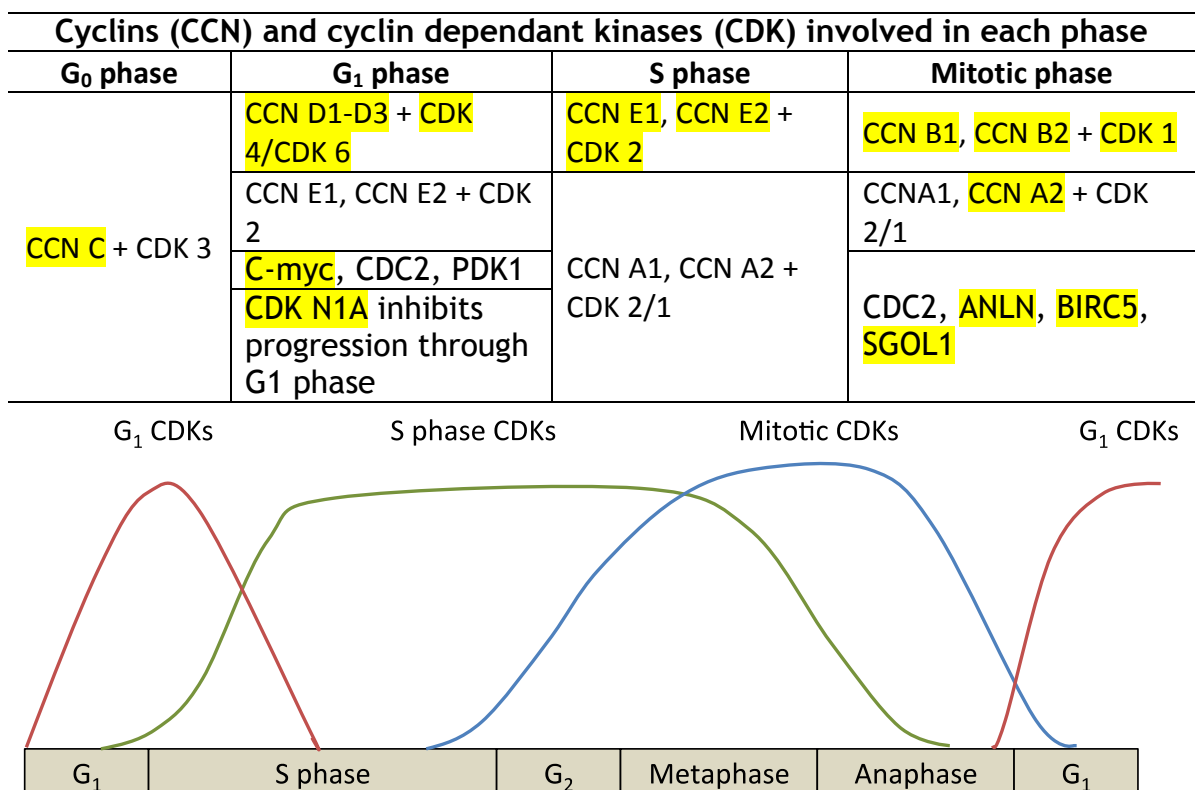


**Figure 3-29: Table and graph depicting cyclins and cyclin dependent kinase expression involved during the different phases of the MSC cell cycle. The graph shows the expression levels of CDKs in cell cycle progression. Yellow highlighted genes were noted to be decreased in spheroid cultures compared to monolayer cultures. (Adapted from Bardin and Amon (Bardin and Amon, 2001)).**

Cells are able to exit the cell cycle during the  $G_1$  phase, to enter a state of physiological arrest, also known as quiescence ( $G_0$ ). Ren and Rollins identified

cyclin C-CDK 3 complex regulated the transition of cells exiting the quiescent state and re-entering  $G_1$  phase and thus, entering the cell cycle (Ren and Rollins, 2004). The graph in Figure 3-25 showed a reduction of cyclin C expression in the spheroids at days 1 and 14, compared to the monolayer system. Therefore, these results indicate the cells within the spheroids were being retained within a quiescent state and had not re-entered the cell cycle.

The transition from  $G_1$  to S phase is initiated by the presence of growth factors. If the cell progresses through the  $G_1$  phase, there is a checkpoint, called the restriction (R) point, which the cell must pass through to continue progression to S phase. Once the cell passes the R point, there is no requirement for growth factors to complete the cell cycle. Therefore, the cell becomes committed to synthesising and replicating new DNA (Blagosklonny and Pardee, 2002). Prior to the R point, D-type cyclins (D1, D2 and D3) mediate progression through the  $G_1$  phase. Figure 3-25 showed a significant decrease in cyclins D1 and D2 expression, within the spheroids at day 1, compared to the equivalent time point in the monolayer system.

All three D-type cyclins form active complexes with CDK 4 and CDK 6, which trigger phosphorylation of retinoblastoma (Rb) protein (Hinds et al., 1992). Additionally, at day 1 there was decreased CDK 4 and CDK 6 expression in the spheroids, compared to the monolayer system (see Figure 3-25). The phosphorylated Rb is unable to bind to E2F, which in turn activates E2F-mediated transcription. E2F-1 transcription factor has been shown to be involved in activating genes that produce products. These products synthesise DNA and drive the cell cycle progression into the S phase (Nevins, 1998). Additionally, the E2F-1 transcription factor, trans-activates cyclins E and cyclins A to form complexes with CDK 2. Cyclin D-CDK 4/6 complexes initiate the phosphorylation of Rb. However, the process is completed by the cyclin E-CDK 2 complex (Blagosklonny and Pardee, 2002). The cyclin E-CDK 2 complex activity is high in the late stages of  $G_1$  and early S phases. Studies have shown cyclin E is accumulated between the R point and the S phase and a threshold is required for cell cycle progression (Dulic et al., 1992, Gong et al., 1995). Therefore, expression of cyclin E and CDK 2 is indicative of a cell committed to cell division.

Figure 3-25 showed a decrease in gene expression of both cyclins E1 and E2 at day 1 in the spheroids examined against monolayer cultures.

As well as a reduction in c-myc expression in spheroids, there was increased expression of CDK N1A in the study samples. Studies have shown CDK N1A acts an inhibitor, which inhibits cell cycle progression through the G<sub>1</sub> phase, by stopping phosphorylation of CDK 2 (Mandal et al., 1998). Whereas, c-myc has been shown to aid cell cycle progression through G<sub>1</sub> and initiate the transition through to the S phase (Schmidt, 2004). The observed reduction in gene expression of the cyclin D-CDK 4/6 complexes in this study may have led to decreased Rb phosphorylation, resulting in a decrease in cyclin E expression and accumulation at the R point. Furthermore, the decrease in c-myc, suggests there was a delay in the G<sub>1</sub> phase, restricting the progression through the cell cycle. Additionally, the increased expression of CDK N1A may suggest cell cycle progression was being inhibited through the G<sub>1</sub> phase. Therefore, all these changes in gene expression may indicate the cells slow the progression through the G<sub>1</sub> phase with a resulting resistance to transfer to the S phase of the cell cycle compared to the monolayer system.

The day 14 spheroids showed a reduction in all three D-type cyclins, CDK 6, c-myc and cyclin A2 expression, compared to the day 14 monolayer culture systems (see Figure 3-25). Moreover, there was no observed gene expression of either cyclin E2 or CDK 2. The decrease in all D-type cyclins expression, may have led to reduced Rb phosphorylation and in turn limited activation of the E2F-1 transcription factor. This reduction in E2F-1 results in a lack of activation of genes involved in triggering cyclin E2 or CDK 2 production. Therefore, the complete absence of the cyclin E2-CDK 2 expression, may suggest the cell cycle had not progressed beyond the R point and arrested in the early stages of the G<sub>1</sub> phase. Furthermore, cyclin A activates CDK 2 and assists with cell cycle progression, by aiding the cell transition between the S and G<sub>2</sub> phases. However, the lack of expression of CDK 2 may indicate the complex with cyclin A had not formed and the cell cycle had arrested at the early G<sub>1</sub> phase.

A study conducted by Cheung and Rando investigated gene expression in quiescent HSCs, muscle stem cells (MuSCs) and hair follicle stem cells (HFSCs) (Cheung and Rando, 2013). The study found a group of genes expressed by all

three cell types unravelled signatures in gene expression. The researchers identified a set of common genes in the quiescent cells, which were down regulated (ANLN, BIRC5, CCN A2, CCN B1, CCN E2 and SGOL1). The spheroid results depicted in Figure 3-25 showed a down regulation in all 6 of the genes identified by Cheung and Rando at day 1 and day 14 compared to the monolayer culture systems. Therefore, the results observed in Figure 3-25 correlated with the observations by Cheung and Rando, indicating the spheroids were in a quiescent and non-proliferating state at both day 1 and day 14. Furthermore, the gene analysis results depicted in Figure 3-25 correlate with the results observed in Figure 3-24.

### **3.5.8 Niche Model Development: Stage 8**

#### **Assessing MSC Differentiation Properties in Monolayer and Spheroid Culture Systems.**

The bone marrow niche protects the stem cells from over stimulation however, when required, external factors may stimulate the stem cells to migrate from the niche and start to differentiate into the desired cell type. Therefore, it was important to determine whether the MSCs retain their multipotency properties, in either monolayer or spheroid culture. Following longer-term culture (14 days) in spheroids, the MSCs were induced to differentiate down both osteogenic and adipogenic lineages and the MSC differential properties were assessed. The 2D and 3D systems depicted in Figure 3-27, showed directed differentiation, by either the expression of osteopontin or presence of lipid droplets in the MSCs. The mNP-loaded MSCs were able to differentiate down the desired lineage, which suggests the mNPs did not have an effect on MSC multipotency. Guzman et al., compared differentiation of neural stem cells with or without SPIO nanoparticles (Guzman et al., 2007). The researchers found no statistical differences between the differential capacity of both groups (Guzman et al., 2007). However, another study suggested high doses of mNPs may influence chondrocytic differentiation (Kostura et al., 2004).

Osteopontin is a protein highly expressed by immature osteoblasts, which are vital for bone development (Komori, 2010). Therefore, osteopontin expression, observed within the MSCs cultured with osteogenic differentiation media,

indicated the cells were differentiating through the osteogenic lineage. Oil Red O has been extensively used to stain lipids thus, labelling cells of adipose origin (Deutsch et al., 2014, Chamberlain et al., 2007, Kim et al., 2012). Therefore, the presence of Oil Red O (stained lipids) within the cells vacuoles, showed the MSCs had differentiated into adipocytes, through the adipogenic lineage. A study conducted by Wang et al., also induced MSCs in spheroids and monolayer systems into adipocytes and osteoblasts (Wang et al., 2009). The researchers found higher differentiation efficiency of MSCs cultured in spheroids compared to the monolayer system (Wang et al., 2009).

The differentiation capacity of MSCs cultured in 2D and 3D were comparable to each other as highlighted in Figure 3-27. However, MSCs cultured as spheroids showed the cells remained quiescent (see Figure 3-24 and Figure 3-25) and retained their stem cell markers (see Figure 3-11) over time, until stimulated to differentiate as shown in Figure 3-27. MSCs cultured in the 2D monolayer system were also able to differentiate within *in vitro* cultures as shown in Figure 3-27. However, these MSCs also started to lose their multipotency properties very rapidly (Figure 3-9). Therefore, theoretically their differentiation capacity was reduced over time. This study did not show this expected reduction in potency.

### 3.6 Summary

The aim in this chapter was to develop a physiologically relevant MSC bone marrow niche model, which was achieved by culturing MSCs in 3D spheroids, within a Type I collagen gel.

Multicellular spheroids may be generated in several ways. However, this study adapted a method by Souza et al., which was published in Nature Nanotechnology in 2010. The MSCs were incubated with 200 nm fluorescently tagged mNPs, under the guiding force of an external magnetic field (optimised for both NP concentration and incubation time). The internalised mNPs did not have any effect on the MSCs viability, stemness, multipotency or cell cycle properties. Once magnetically loaded, the cells were assessed for mNP retention and responsiveness to a magnetic field. The cells were then magnetically levitated to create a multicellular MSC spheroid.

In the monolayer culture system, the MSCs showed significant reductions in STRO-1 and nestin expression over time (2 weeks), which were comparable to other studies culturing MSCs two-dimensionally. Furthermore, the monolayer system exhibited MSC proliferation through the incorporation of BrdU within the nucleus. These results indicated the MSCs were not displaying behaviours observed within the native bone marrow niche and were a poor representation of this environment.

Conversely, the spheroidal MSC structure exhibited high expression of STRO-1 and nestin over the 2 week period, thus showing they retained their multipotency properties. Additionally, MSCs in the spheroid did not show incorporation of BrdU, which indicated the cells had not entered the cell cycle. Gene analysis showed a 75% decrease in the number of genes being expressed in the spheroids compared to the monolayer culture system. Furthermore, the MSCs cultured in the 3D spheroids were induced to differentiate into osteoblasts and adipocytes. These MSC behaviours mimic the innate MSC niche environment.

The complexity of the model was increased by the use of a Type I collagen gel to mimic the physical properties in the bone marrow environment. Initially, the homogeneous mix of gel and MSCs did not lead to the amalgamation of MSCs to

form the necessary cell-cell contacts. Therefore, the spheroids were preliminary created and then transplanted into the collagen gels. Rheology analysis of the gels containing spheroids exhibited similar stiffness properties of a bone marrow environment, thus creating a more realistic *ex vivo* niche model. The functional properties of this newly developed model will be assessed in the following chapter.

# CHAPTER 4

## 4 MSC Spheroid Niche Model Response to Wound Healing

### 4.1 General Introduction

Bone marrow MSCs possess immune-modulatory and wound healing properties, which are beneficial for regenerating damaged tissue or organs (Ma et al., 2014, Anthony and Shiels, 2013). The wound healing process is initiated following injury and involves three distinct overlapping phases; inflammatory, proliferative and remodelling (Häkkinen et al., 2015). In the initial inflammatory stage, chemokines and cytokines are released from cells within the damaged vicinity, creating an attractant concentration gradient in the surrounding area. The MSCs within the bone marrow niche possess numerous chemokine and cytokine receptors on the cell surface. The chemokines/cytokines released post injury, bind to their cognate receptor on the MSCs causing a cascade of events. Once activated, the MSCs proliferate, migrate out from the niche and home to the site of injury *via* chemotaxis and pro-inflammatory cytokines (Rennert et al., 2012). The MSC homing process to the damaged area comprises multiple steps, which include rolling, adhesion and transmigration across the vascular endothelium, followed by migration through tissue to the damaged area (Chen et al., 2011).

Once the MSCs reach the injured site, the cells are known to play an important role in all three phases of wound healing. The inflammatory stage occurs within the first few days of injury, where factors (e.g. platelet-derived growth factor (PDGF), interleukin 1 $\beta$  (IL-1 $\beta$ ), IL-6 and tumour necrosis factor- $\alpha$  (TNF- $\alpha$ )) are released from damaged cells, platelets and mast cells to recruit neutrophils and monocytes to the injured area (Velnar et al., 2009). Re-epithelialisation, ECM deposition and granulation tissue formation occur during the second proliferative phase. The final stage of wound healing involves the remodelling of granulation tissue into scar tissue (Velnar et al., 2009).

MSCs directly suppress the native immune response by secreting anti-inflammatory cytokines, such as IL-10 and IL-4 (Kyurkchiev et al., 2014). Additionally, MSCs prevent proliferation and function of the immune inflammatory cells including monocytes (Zhao et al., 2015). Furthermore, MSCs

possess and secrete antimicrobial factors, which aid the wound healing process (Krasnodembskaya et al., 2010). MSCs use paracrine signalling to regulate local cellular responses, such as local cell proliferation, migration and cell survival. Paracrine signalling from the MSCs have also been shown to recruit specific cell types to the wound. A final role for MSCs in the wound healing process is by directly differentiating into cells of mesenchymal lineages, to repair damaged tissue.

The wound healing response is key to MSC behaviour, and confers one of the main benefits MSCs hold for potential regenerative medicine applications. The aim of this chapter was to determine whether the MSC niche model developed in Chapter 3 is able to express similar *in vivo* responses, in the presence of an artificially created wound. Furthermore, discover whether stimulated MSCs should migrate towards the site of injury and accelerate wound healing, through local cell proliferation, migration and differentiation.

## 4.2 Objectives

In the previous chapter, a 3D *in vitro* MSC niche model was created using MSC spheroids within collagen gel scaffolds. The MSCs in this environment mimicked *in vivo* MSC phenotype and behaviour; by expressing high levels of STRO-1 and nestin. The MSCs retained their multipotency properties and remained quiescent over time, compared to traditional 2D culture methods. It was important to subsequently assess the MSC niche model's functional properties in terms of wound healing, to determine whether they parallel responses observed in an *in vivo* environment.

This evaluation was achieved by subjecting the niche model to numerous wound-healing assays, to assess whether the MSCs migrated out from the spheroid niche towards an artificially created wound. In addition, it was necessary to determine whether these migrated MSCs were actually aiding wound healing, by differentiating into the desired cell types. Assessment of these innate properties, will determine whether the MSCs within the niche model mimic the *in vivo* niche response.

These objectives will be achieved *via*:

- Optimisation of a simple wound healing assay; the study of wound closure of scratched fibroblasts and osteoblasts, over time.
- The assessment of MSC migration from a spheroid niche, in response to an artificial wound.
- The genomic and proteomic investigation of migrating MSCs from the spheroid niche towards the wound, to determine whether the MSCs would trans-differentiate into the local resident cell type.

## **4.3 Materials and Methods**

### **4.3.1 Time-lapse assessment of wound healing assays.**

#### **4.3.1.1 Light microscopy: time course assessment of scratched monolayers with or without overlaid collagen gels**

The wound healing rate of scratched monolayers in the presence or absence of an overlaid collagen gel was determined by culturing either h-TERTs (fibroblasts) or osteoblasts as confluent monolayers on CellBind plates. The monolayers were scratched using a P1000 pipette tip. Osteogenic differentiation media (see Chapter 3, section 3.3.5) was added every 2/3 days for 10 days to the osteoblast monolayer, prior to being scratched by the pipette tip. An artificial wound was created prior the addition of either fresh media or collagen gels. The monolayers were assessed using light microscopy to determine the closure rate of the scratch.

#### **4.3.1.2 Immunofluorescence microscopy: cell viability assessment of scratched monolayers**

To determine whether there was an increased presence of dead cells at the scratched edge, human dermal fibroblasts, h-TERTs, were seeded as a confluent monolayer, which was scratched with a P1000 pipette tip to create a wound. Fresh media was immediately placed directly onto the scratched monolayer and the cells were monitored over the first 24 hour period post scratch. H-TERTs were assessed *via* a live/dead stain (see section 3.3.3.1) and analysed using a Zeiss Axiovert 200M fluorescent microscope.

### **4.3.2 Assessing MSC migration from a spheroid niche in response to an artificial wound.**

#### **4.3.2.1 Immunofluorescence microscopy: cell cytoskeleton (F-actin staining)**

Either h-TERTs or primary osteoblasts were grown as a confluent monolayer on CellBind plates and left either unscratched or scratched using a P1000 pipette tip. The osteoblast monolayer culture cells were seeded and osteogenic differentiation media (see Chapter 3, section 3.3.5) was added every 2/3 days for 10 days, prior to the addition of an MSC spheroid. An artificial wound was created just before the addition of the spheroid/gel (i.e. the niche model).

Cultures were monitored every 24 hours for 3 days. The MSCs and underlying monolayer were fixed and stained with phalloidin-rhodamine and DAPI (see Section 3.3.3.2) and analysed using a Zeiss Axiovert 200M fluorescent microscope.

### **4.3.3 MSC differentiation assessment post migration from the spheroid niche to wound site.**

#### **4.3.3.1 Immunofluorescence microscopy: MSC differentiation (phosphorylated RUNX-2 and osteopontin staining)**

The above mentioned procedure (see Section 4.3.2.1) was followed using fibroblasts and osteoblast cells. The niche model was cultured for either 3 or 14 days with both cell types, to assess migrating MSC staining for early and late osteogenic markers. The media covering the gels was changed twice weekly over the appropriate culture period. MSCs were fixed and stained with phosphorylated RUNX-2 (1:50 dilution), followed by biotinylated secondary (1:50 dilution) and streptavidin-Texas Red (1:50 dilution), then mounted with DAPI on day 3 (see section 3.3.3.3). Whereas, on day 14 the cells were stained for osteopontin (1:50 dilution), followed by biotinylated secondary (1:50 dilution) and streptavidin-Texas Red (1:50 dilution). The cells were then mounted with DAPI (see section 3.3.3.3). Both day 3 and day 14 samples were analysed using a Zeiss Axiovert 200M fluorescent microscope.

#### **4.3.3.2 RNA extraction from the spheroid niche post-exposure to control and wounded osteoblasts**

**Differentiation analysis of migrated MSCs within niche model:** Analysis was conducted on confluent primary osteoblast monolayers, which were either left unscratched or scratched with a P1000 pipette tip. The cells were seeded onto CellBind plates and osteogenic differentiation media (see section 3.3.5) was added for 10 days, prior to the addition of the niche model on top. After 24 hours or 72 hours, the collagen gels containing the spheroids were removed from the wells ready for RNA extraction. Six samples were pooled for each replicate (n=3).

A TRIzol extraction and Qiagen RNeasy micro kit was used as described in Chapter 3, section 3.3.6, to extract the RNA from the MSC spheroids, within the

collagen gels. The RNA was subjected to Fluidigm analysis and prepared by the method described in Chapter 3, section 3.3.7, with a modified primer list (see Table 4-1).

**Table 4-1: Fluidigm primers designed for human genes.**  
(\*Primers used as housekeeping genes).

Primer	Sequence (5' to 3')
<b>β-Actin*</b>	Forward GTGGGCCGCCCTAGGCACCAG Reverse CACTTTGATGTCACGCACGATTTC
RUNX-2	Forward CAGCAGCAGCAACAGCAG Reverse GGCGATGATCTCCACCAT
ACVR1A	Forward GCCAAGGGGACTGGTGTAAC Reverse GAGAATAATGAGGCCAACCTCCA
SMAD1	Forward GCTGCTCTCCAATGTTAACCG Reverse CACTAAGGCATTTCGGCATAAC
SMAD2	Forward CCACGGTAGAAATGACAAGAAGG Reverse GATTACAATTGGGGCTCTGCAC
SMAD3	Forward GTCTGCGTGAATCCCTACCAC Reverse GGGATGGAATGGCTGTAGTCG
<b>ENOX2*</b>	Forward GAGCTGGAGGGAACCTGATTT Reverse CACTGGCACTACCAAACCTGCA
SMAD4	Forward GGGTCAACTCTCCAATGTCCAC Reverse GTCACTAAGGCACCTGACCC
SMAD5	Forward TGGGTCAAGATAATTCCCAGCCT Reverse GGCTCTTCATAGGCAACAGGC
SMAD6	Forward CTCCTACTCTCGGCTGTCT Reverse AGAATTCACCCGGAGCAGTG
SMAD7	Forward CCATCACCTTAGCCGACTCT Reverse CCAGGGGCCAGATAATTCGT
SMAD9	Forward CTTATCATGCCACAGAAGCCTCT Reverse GCTCCTCGTAACAACTGGTCG
BMPR1A	Forward ACGCCGGACAATAGAATGTTGTC Reverse GAGCAAAACCAGCCATCGAATG
<b>TWY1*</b>	Forward ATTGTCATCAAGACGCAGGGC Reverse GTTGCGAATCCCTTCGCTGTT
BMPR1B	Forward GGTTCAACTTCTGCTGATTCAT Reverse CGCAAAGCATGTTATCAAGG
BMP2	Forward CTTCTAGCGTTGCTGCTTCC Reverse AACTCGCTCAGGACCTCGT
BMP2	Forward AGACCTGTATCGCAGGCACT Reverse CCACTCGTTTCTGGTAGTTCTTCC
BMPR2	Forward AGCCTCTCACACCCACTCC Reverse GCAGAACAACCGTGAGAGG

ACVR1B	Forward GACATTGCCCCGAATCAGAGG Reverse GCCCGAGGGCATAAATATCAGC
BMP4	Forward CAGCACTGGTCTTGAGTATCCT Reverse AGCAGAGTTTTCACTGGTCCC
<b>CYCR*</b>	Forward ACTGCGGGAAGGTCTCTACTT Reverse GGGTGCCATCGTCAAACCTCTA
BMP7	Forward CAGGCCTGTAAGAAGCACGA Reverse TGGTTGGTGGCGTTCATGTA
BMP10	Forward ACCCACCAGAGTACATGTTGG Reverse GCCATTAAACTGACCGGC
Nestin	Forward GCTCAGGTCCTGGAAGGTC Reverse AAGCTGAGGGAAGTCTTGGA
CD63	Forward CCCTTGAATTGCTTTTGTT Reverse TATTCCACTCCCCAGATGA
ALCAM	Forward TTCCAGTCCCTCTACTCAGAGC Reverse GCTAAGAAGGACTCGCAGGA
Osterix	Forward TGGGCTCCCAACACTATTTTC Reverse GGAAGACTGAAGCCTGGA
<b>UBE2D2*</b>	Forward CCATGGCTCTGAAGAGAATCC Reverse GATAGGGACTGTCATTTGGCC
RUNX1T1	Forward ATCACAACAGAGAGGGCCAA Reverse CTGCAGGTTTTCACTCGCTTT
SMURF1	Forward ATGCAGTTCGTGGCCAGATA Reverse CAGGCCCGGAGTCTTCATAC
SMURF2	Forward GACAGGATCCTCTCGAGTGC Reverse AGCTTTCATAGGGTGAATGTCT
INHBA	Forward AAGTCGGGGAGAACGGGTAT Reverse GGTCACTGCCTTCCTTGGA
ACVR2A	Forward ACCATGGCTAGAGGATTGGC Reverse GCCAACCCAAAGTCAGCAAT
ACVR2B	Forward CTGCAACGAACGCTTCACTC Reverse CAGGACGATGAGGGAAAGGC
<b>RNF20*</b>	Forward GGTGTCTCTTCAACGGAGGAA Reverse TAGTGAGGCATCATCAGTGGC
TGFB1	Forward CGACTCGCCAGAGTGGTTATC Reverse GTTATCCCTGCTGTACAGGAG
TGFBR1	Forward CGTTCGTGGTTCCGTGAGG Reverse TAATCTGACACCAACCAGAGCTG
TRAF6	Forward CGCACTAGAACGAGCAAGTGA Reverse GCCACACAGCAGTCACTTTCA
SNAIL2	Forward TCCTTCCTGGTCAAGAAGCA Reverse GGTATGACAGGCATGGAGTA
Vimentin	Forward GGAGAAATTGCAGGAGGAGA Reverse TGC GTTCAAGGTCAAGACGT
IL-8	Forward GTGTGAAGGTGCAGTTTTGCC

	Reverse GTGGTCCACTCTCAATCACTC
<b>B2M*</b>	Forward TTGTCTTTCAGCAAGGACTGG Reverse ATGCGGCATCTTCAAACCTCC
CathepsinB	Forward TGTGTATTCCGACTTCCTGC Reverse TTAAAGAAGCCATTGTCACCC
CathepsinD	Forward GGTGCTCAAGAACTACATGG Reverse ATTCTTCACGTAGGTGCTGG
CathepsinG	Forward AACAGATACACTCCGAGAGG Reverse ACGACTTTCATAGGAGACG
CathepsinL	Forward GACTCTGAGGAATCCTATCC Reverse CTTAGGGATGTCCACAAAGC
CathepsinS	Forward GCGTCATCCTTCTTTCTTCC Reverse CCAGCTGTTTTTCACAAGCC
<b>GAPDH*</b>	Forward TCAAGGCTGAGAACGGGAA Reverse TGGGTGGCAGTGATGGCA

Permutmatrix software (Réseau National des plates-formes Bioinformatiques (ReNaBi), France) was used on each cluster gene expression, to convert the numerical values from the collected data into a graduation scale of colours. For example, shades of red were used to represent the degree of up regulated genes, whilst shades of green indicated the degrees of down regulated genes.

## 4.4 Results

### 4.4.1 Time-lapse assessment of wound healing assays.

Confluent monolayer culture systems were scratched (to create an artificial wound) and time-lapse experiments were conducted, to assess the ability of the monolayer to repair and close the scratch/wound. Two different cell models were employed; (i) a connective tissue model using fibroblasts (h-TERTS) and (ii) a bone matrix model using primary osteoblasts. The cell models were grown in either the presence or absence of overlaid collagen gels (Figure 4-1). It was necessary to assess whether the presence of collagen gels altered the rate of wound closure.

Figure 4-1 demonstrated both fibroblasts and osteoblasts directionally migrated from the edge of the wound inwards, across the scratch to close the wound. However, in the absence of a collagen gel, fibroblasts closed the wound much quicker, (after only 24 hours) whereas, the osteoblasts took 5 days to close the wound.

However, the scratch (wound) healed slower in the presence of the collagen gel, in both the connective tissue and bone matrix models (Figure 4-1). The connective tissue model, took an extra 5 days for the scratch to close in the presence of collagen gels. Whereas, the bone matrix model took an extra 2 days for the wound to fully heal and close.

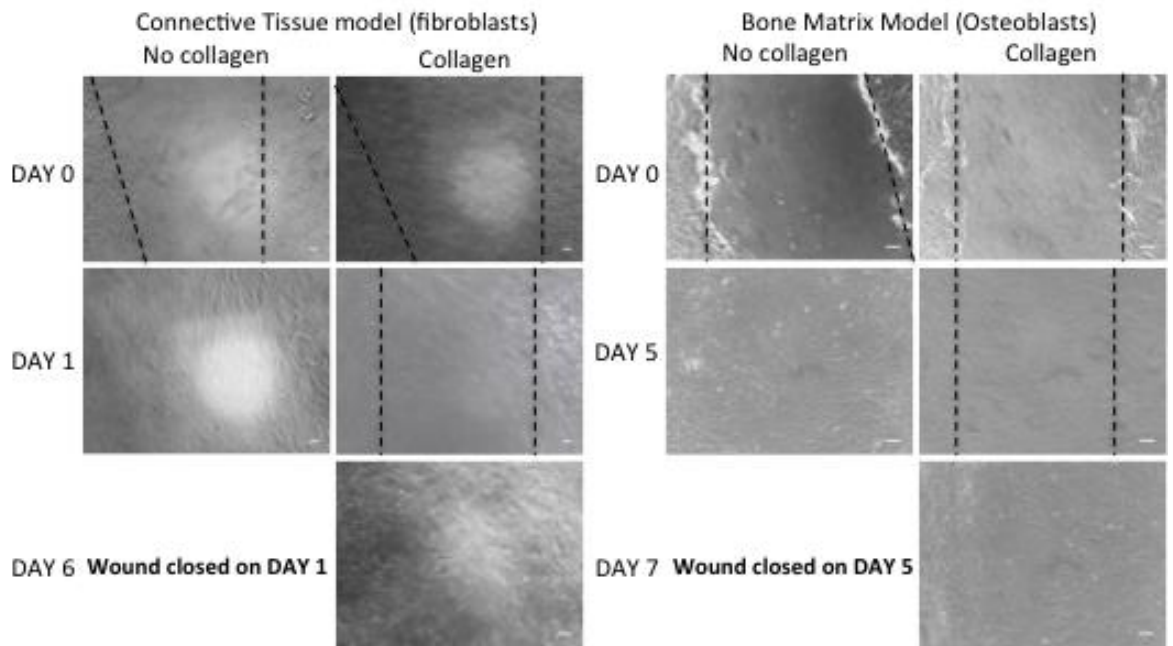


**Figure 4-1: Light microscopy time lapse images assessing the wound healing process. Two different cell models were used; connective tissue (fibroblasts) and bone matrix (osteoblasts) models, in the presence and absence of an overlaid collagen gel. 10x objective, scale bar = 50  $\mu$ m.**

Subsequently, a viability assessment of the scratched fibroblast monolayer control was carried out. MSCs are known to migrate out of the niche and are guided to the wound, following the release of chemokines and cytokines from the site of injury. Therefore, it was necessary to assess the presence of dead cells at the wound edges, as damaged or dying cells release danger-associated molecular patterns (DAMPs), as part of the pro-inflammatory response by the wound (Tolle and Standiford, 2013).

Figure 4-2 demonstrated there were limited dead cells in the control, non-scratched samples, which were not localised within a specific area but distributed throughout the control samples (highlighted with the white arrows). However, the scratched samples clearly showed a higher concentration of dead cells at the edge of the scratch 24 hours post injury, (highlighted by white arrows in Figure 4-2). Despite this finding, it was noted that the presence of dead cells only comprised a very small percentage, compared to the percentage of living cells at the wound edge.

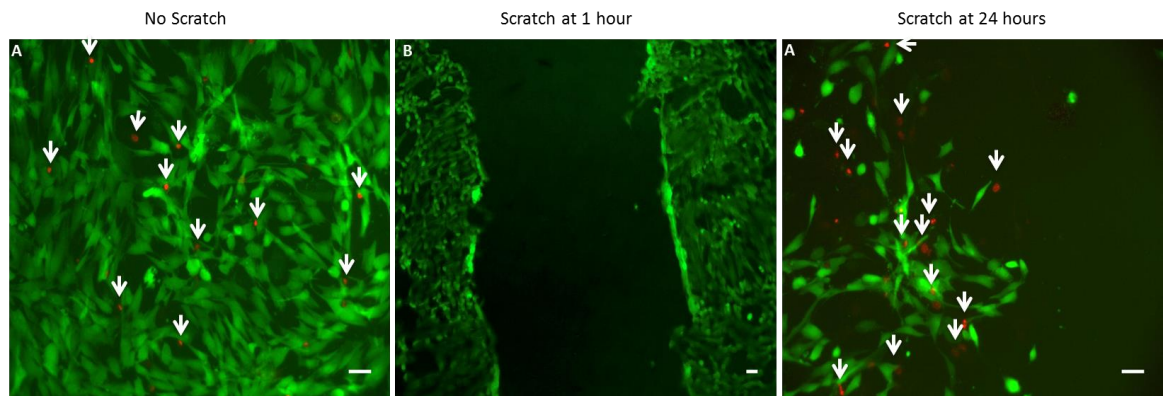


**Figure 4-2: Fibroblast viability assessed over 24 hours, in the presence or absence of a scratch.**

Live/dead stain green = living cells, red = dead cells and highlighted with white arrows. (A) 10x objective and (B) 5x objective. Scale bar = 50  $\mu\text{m}$

Soluble factors including cytokines, released from MSCs following injury, stimulate proliferation and migration of other cell types, to enhance and accelerate wound healing (Hocking and Gibran, 2010). Therefore, further research was conducted to assess whether the MSCs within the spheroid niche model were able to migrate out of the niche, upon injury stimulation.

#### 4.4.2 Assessing MSC migration from a spheroid niche, in response to an artificial wound.

Chapter 3 demonstrated the absence of external stimulation allows the MSCs to remain quiescent and *in situ* within the spheroid niche (Chapter 3, Figure 3-24 and Figure 3-25). However, the presence of stimulation, which in this case was a scratched monolayer, should initiate the migration of MSCs out of the niche, towards the wound. Further studies were conducted using both fibroblast and osteoblast scratched monolayer cultures, to investigate potential MSC migration from the niche model over time in co-culture.

Scratched and unscratched (control) fibroblast and osteoblast monolayers were overlaid the with MSC spheroid niche model. Light micrographs were taken alongside fluorescent images (with F-actin stained monolayers (red) and mNP fluorescently tagged MSC spheroids (green)). Figure 4-3 showed the MSCs in the unscratched control samples remained within the niche during all time points in both fibroblast and osteoblast monolayers. These results verified that a confluent cell monolayer co-cultured beneath the MSC niche model failed to stimulate MSC migration.

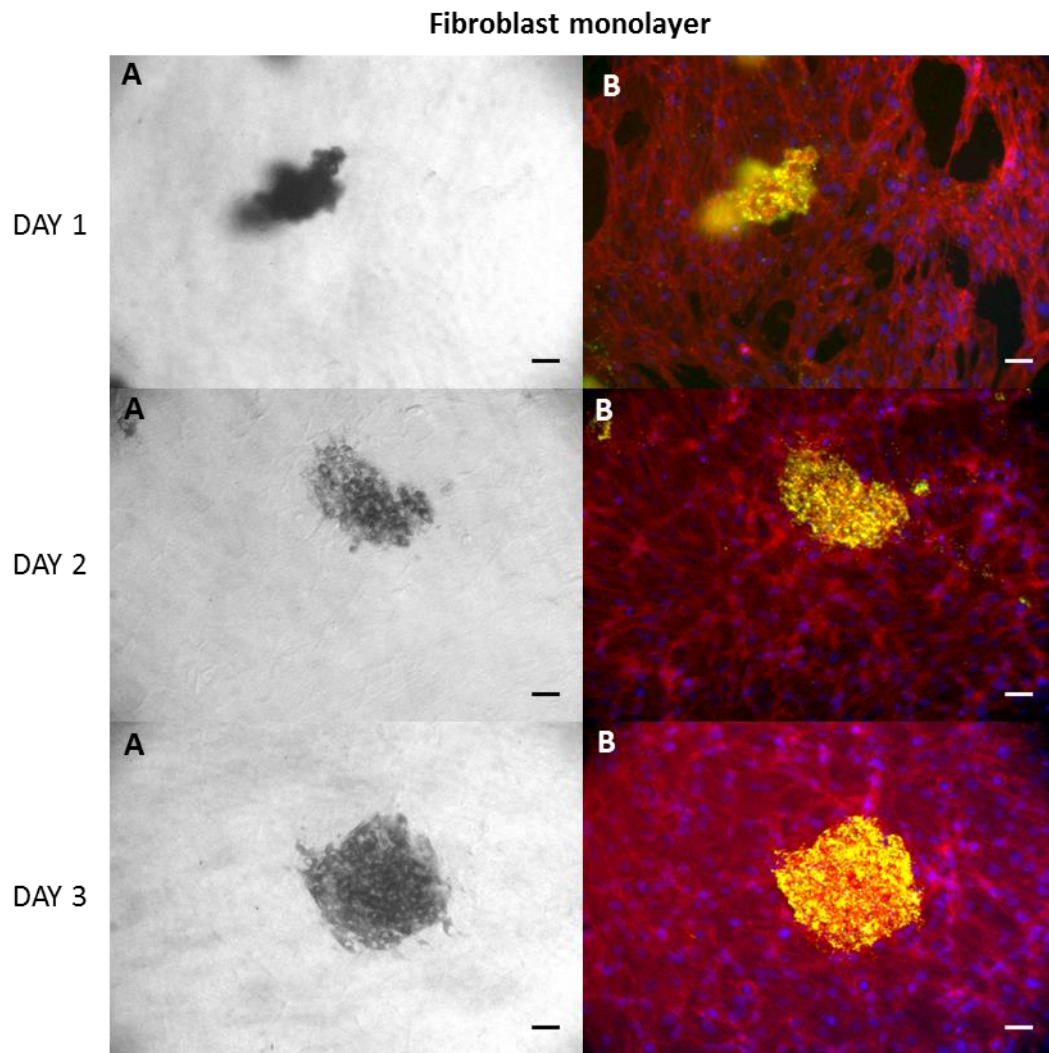


**Figure 4-3a: MSC spheroid niche co-cultured with control (unscratched) fibroblast monolayers assessed over 3 days.**

MSC spheroid niche cultured over an unscratched fibroblast monolayer. (A) Light microscopy image, (B) Fluorescence image (red = actin, green = mNPs, blue = nucleus). 10x objective, scale bar = 50  $\mu\text{m}$ .

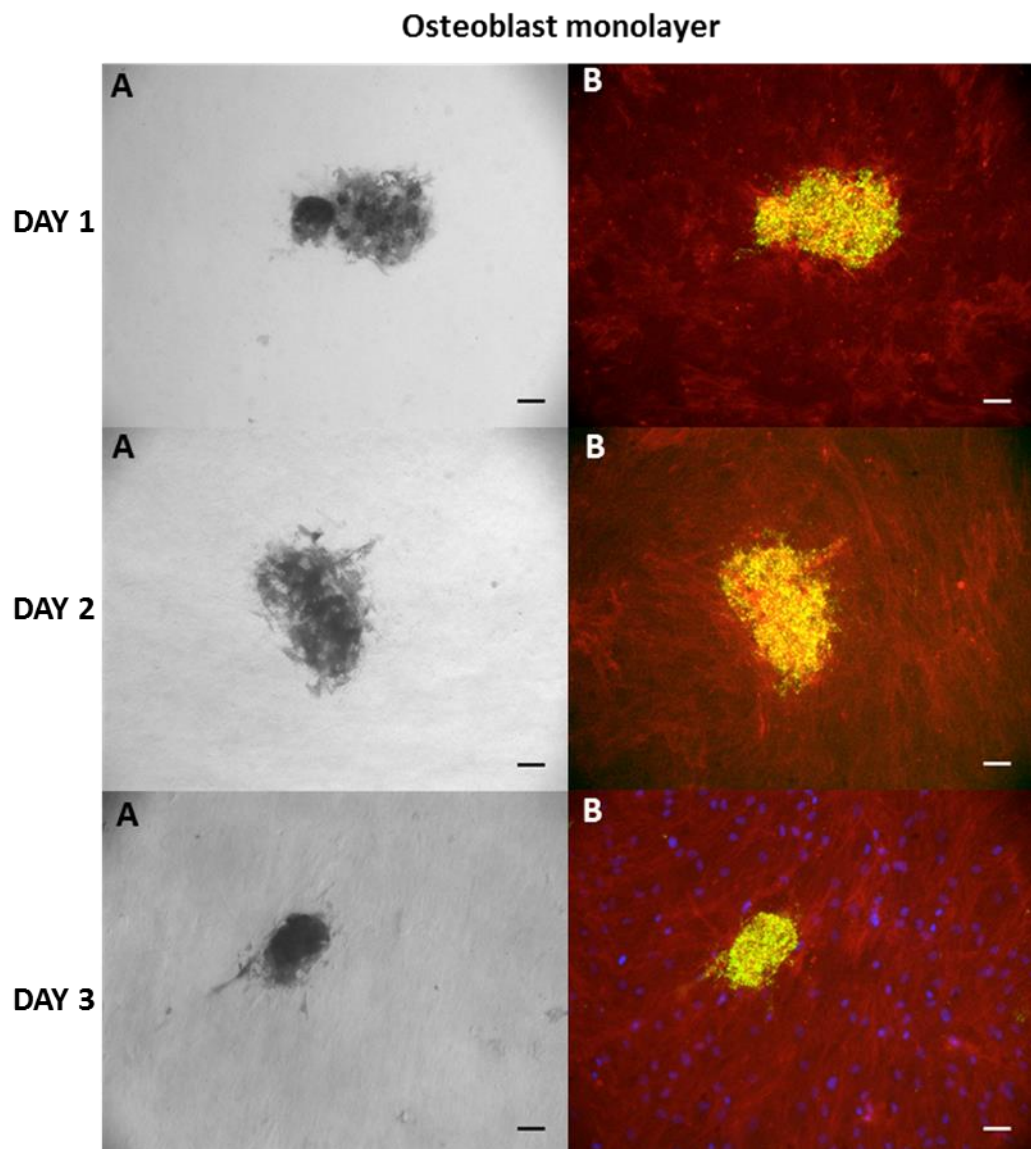


**Figure 4-3b: MSC spheroid niche co-cultured with control (unscratched) osteoblast monolayer assessed over 3 days.**

MSC spheroid niche cultured over an unscratched osteoblast monolayer. (A) Light microscopy image, (B) Fluorescence image (red = actin, green = mNPs, blue = nucleus). 10x objective, scale bar = 50  $\mu\text{m}$ .

Conversely, when MSC niche models were co-cultured above scratched monolayers, the MSCs clearly migrated out of the niche after 1 day in both osteoblast and fibroblast models (Figure 4-4). MSC migration from the niche increased over time following exposure to the scratch, with more cells exiting the niche at day 3 compared to day 1. Moreover, at all time points, the images showed directional MSC migration towards the scratch, as indicated in the image. However, if the niche was positioned above the middle of the scratch all peripheral MSCs migrated out of the niche (see Figure 4-4). It was noted that only the niche MSCs exposed nearest to the wound became stimulated and migrated towards the wound site.

Following MSC migration, the cells were also observed to integrate within the wound (scratch) area therefore, these results show MSCs appear to play a role in wound healing (Figure 4-4). Figure 4-1 demonstrated wound closure using both fibroblasts and osteoblasts at days 6 and 7 respectively, when overlaid with a collagen gel. However, when the wound was overlaid with the MSC spheroid niche model (within a collagen gel), both wounds closed much earlier, by day 3.

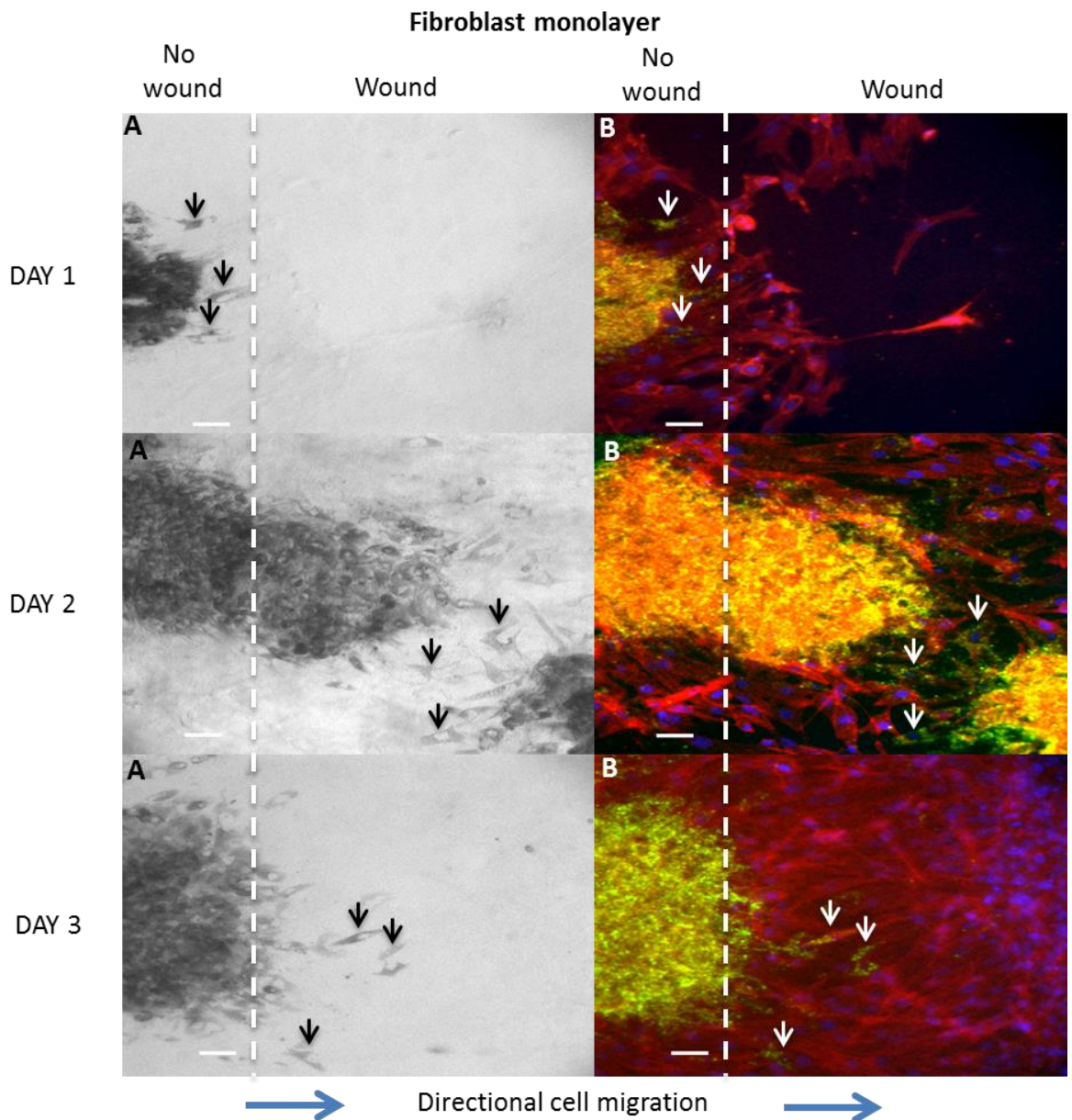


**Figure 4-4a: MSC migration from the spheroid niche when co-cultured with scratched fibroblast monolayers, assessed over 3 days.**

MSC spheroid niche depicting migration of MSCs towards a scratch on a fibroblast monolayer (black and white arrows indicate migrating MSCs). (A) Light microscopy image, (B) Fluorescence image (red = actin, green = mNPs, blue = nucleus), edge of scratch/wound (dashed white line), 10x objective, scale bar = 50  $\mu\text{m}$ .

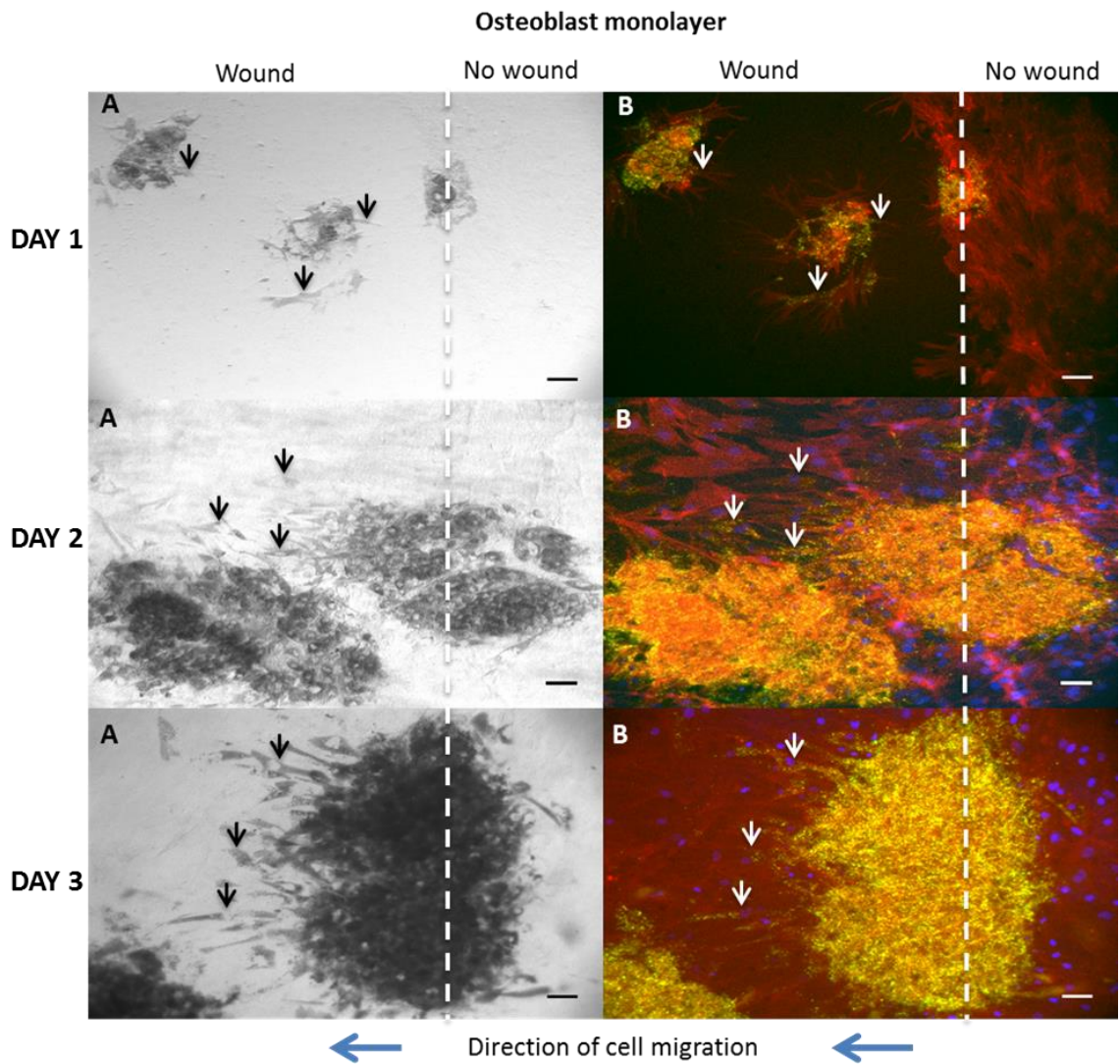


**Figure 4-4b: MSC migration from the spheroid niche when co-cultured with scratched osteoblast monolayers, assessed over 3 days.**

MSC spheroid niche depicting migration of MSCs towards a scratch on an osteoblast monolayer (black and white arrows indicate migrating MSCs). (A) Light microscopy image, (B) Fluorescence image (red = actin, green = mNPs, blue = nucleus), edge of scratch/wound (dashed white line), 10x objective, scale bar = 50  $\mu\text{m}$ .

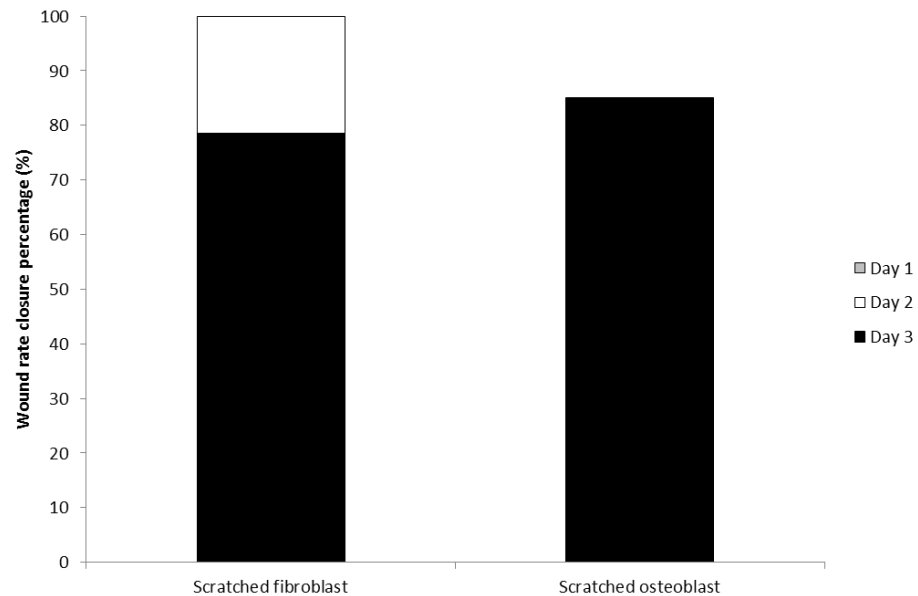


**Figure 4-4c: Quantitative analysis showing percentage rate of wound closure over a period of 3 days with MSC spheroids cultured with scratched fibroblast and osteoblast monolayers.**

#### **4.4.3 MSC differentiation assessment post migration from spheroid niche to wound site.**

Figure 4-4 showed the directional migration of MSCs from the niche, in the presence of a scratch/wound. *In vivo* studies have shown, following MSC arrival at the wound site, the cells begin to differentiate into the desired cell type and encourage cell proliferation within the affected area, leading to improved tissue repair (Maxson et al., 2012). Therefore in this study, a series of wound healing assays were initiated, to determine whether, following migration, the MSCs differentiate into the scratched (wounded) monolayer cells.

The connective tissue (fibroblast) and bone matrix (osteoblast) scratched models were employed to assess potential MSC differentiation into osteoblasts. All MSC cultures were assessed for early and late stage bone markers, to verify differentiation into osteoblasts over a period of 3 to 14 days (Figure 4-5).

The images in Figure 4-5 showed the control MSC samples without a scratch/wound did not cause the MSC migration, in either the osteoblast or fibroblast models. Furthermore, these samples showed no expression of phosphorylated RUNX-2 after 3 days or osteopontin on day 14. The osteoblast model showed osteopontin expression on day 14. However, these stained cells

corresponded with cells from the monolayer and not from the MSC niche cells (Figure 4-5b upper panel).

Conversely, MSCs in the scratched fibroblast samples started to migrate out of the niche and incorporate into the scratched area by day 3, with evidence of more MSC migration after 14 days (Figure 4-5a). There was no observed phosphorylated RUNX-2 expression on day 3 or osteopontin expression after day 14.

Similarly, MSCs in the scratched osteoblast samples also migrated out of the niche by day 3 and were fully incorporated within the wound area by 14 days (Figure 4-5b). The migrated MSCs were shown to express phosphorylated RUNX-2 after 3 days, following exposure to the scratch (see Figure 4-5b and Figure 4-6), and clear expression of osteopontin after 14 days (Figure 4-5b).

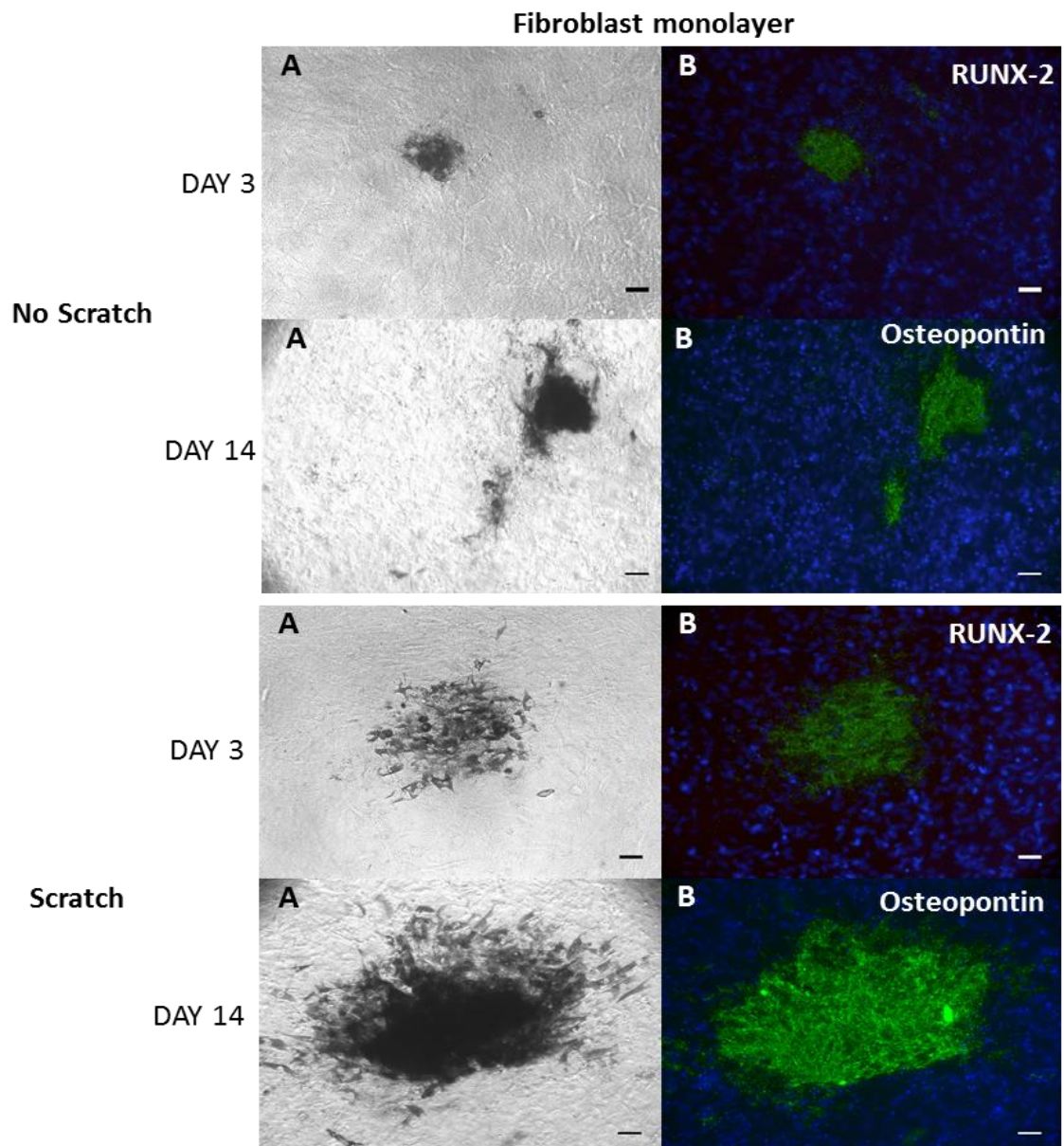


**Figure 4-5a: Wound healing assay assessing the presence of MSC niche models. Fibroblast monolayer assessed at DAY 3 and DAY 14 with or without a scratch. (A) Light microscopy image and (B) fluorescent image, red = phosphorylated RUNX-2 (DAY3)/osteopontin (DAY 14), green = mNPs, blue = nucleus. 10x objective, scale bar = 50  $\mu$ m.**

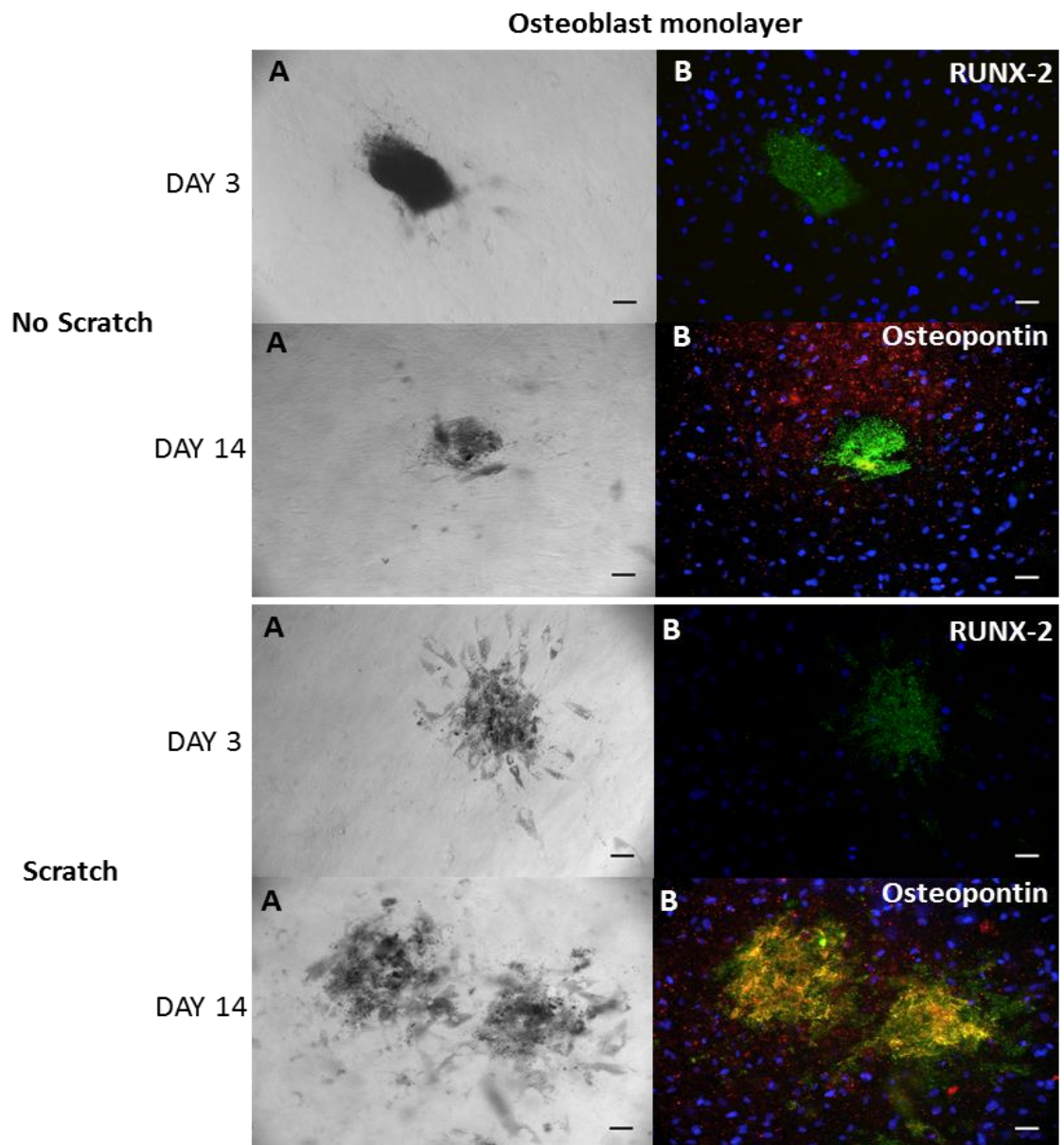


**Figure 4-5b: Wound healing assay assessing the presence of MSC niche models.** Osteoblast monolayer assessed at DAY 3 and DAY 14 with or without a scratch. (A) Light microscopy image and (B) fluorescent image, red = phosphorylated RUNX-2 (DAY3)/osteopontin (DAY 14), green = mNPs, blue = nucleus. 10x objective, scale bar = 50  $\mu$ m.

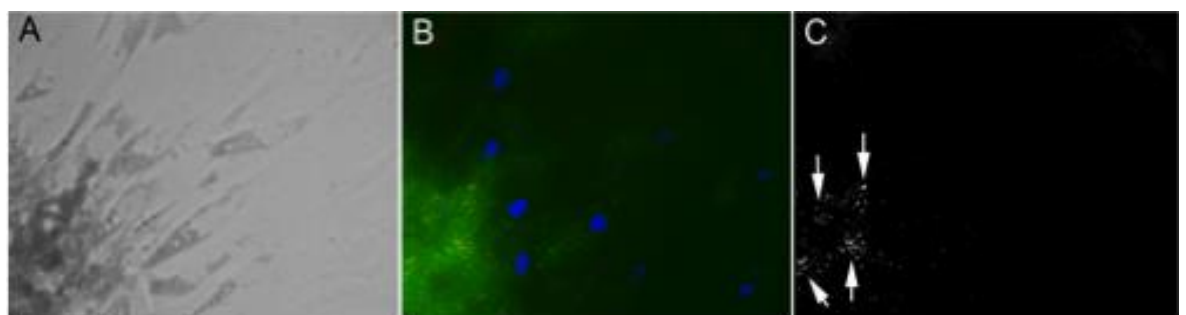


**Figure 4-6: High magnification images of MSCs migrating towards a scratched osteoblast monolayer expressing phosphorylated RUNX-2 after 3 days.** (A) Light microscopy image, (B) fluorescent image, red = phosphorylated RUNX-2, green = mNPs, blue = nucleus. (C) Fluorescent image highlighting phosphorylated RUNX-2. 20x objective.

Further analysis was conducted on the migrated MSCs, to identify any osteoblastic gene expression. This analysis would complement the results depicted in Figure 4-5 (i.e. RUNX-2 and osteopontin staining). The osteoblast monolayer was scratched (or left unscratched) and MSC spheroid gene expression was assessed, following exposure to a scratch either over a period of 1 day or 3 days (see Figure 4-7 and Figure 4-8). Specific genes, involved in osteogenesis and stemness, were analysed *via* fluidigm to confirm whether the MSCs were differentiating in the presence of the osteoblast wound. All data was normalised against the corresponding unscratched wound assay, which was processed on the same day.

After 3 days, there was high expression of nestin and ALCAM in both scratched and unscratched osteoblast models, further confirming the MSC phenotype in spheroid culture. There was a significant increase in RUNX-2 expression within the scratched model at day 3, compared to all other conditions ( $p < 0.001$ ), supporting the RUNX-2 staining observed at day 3 in Figure 4-6. There was no RUNX-2 expression after 3 days in the absence of a wound.

An increased in the expression levels of osteoblast markers- BMP-2, SMAD-2, SMAD-4, and SMAD-5 was recorded at both time points in the scratched assay, compared to the unscratched assay.

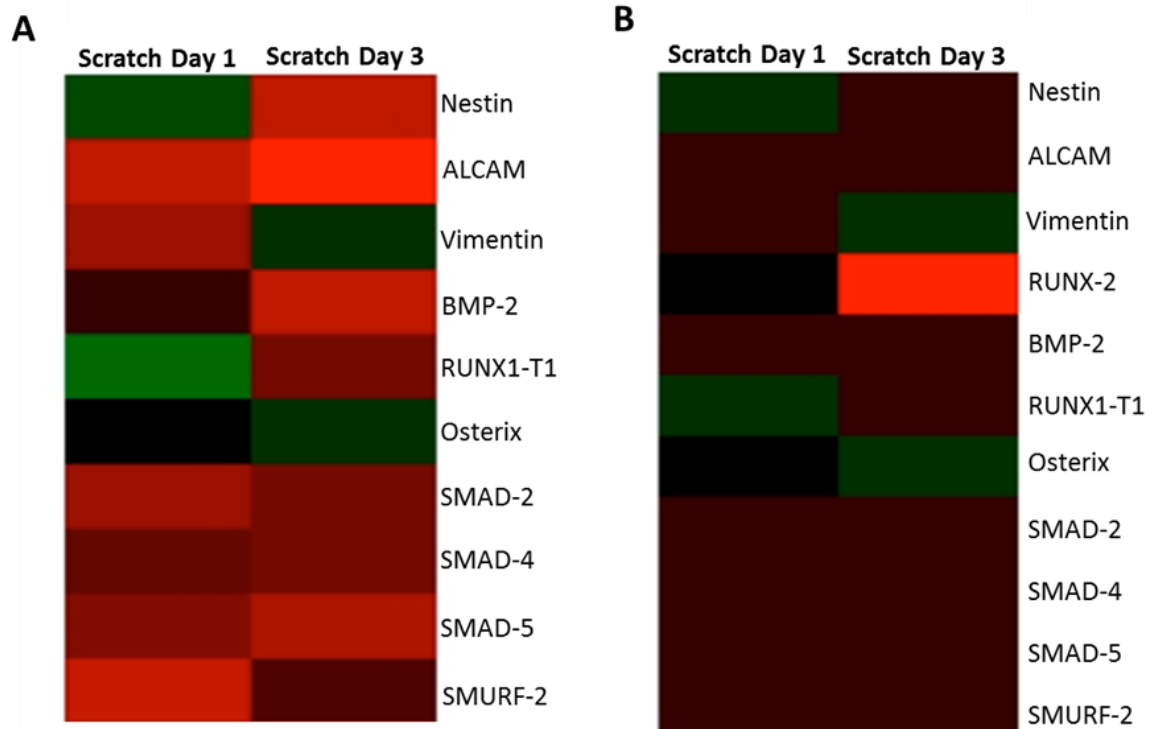


**Figure 4-7: Heat map depicting MSC gene expression profiles extracted from the spheroid niche model.**

MSC spheroids were co-cultured with unscratched or scratched primary osteoblast monolayer cultures, for 1 day and 3 days. (A) Heat map of MSC gene expression without RUNX-2, (B) heat map of MSC gene expression including RUNX-2. MSC Gene expression was depicted relative to the unscratched assay at the same time point, (red = up regulation, green = down regulation).

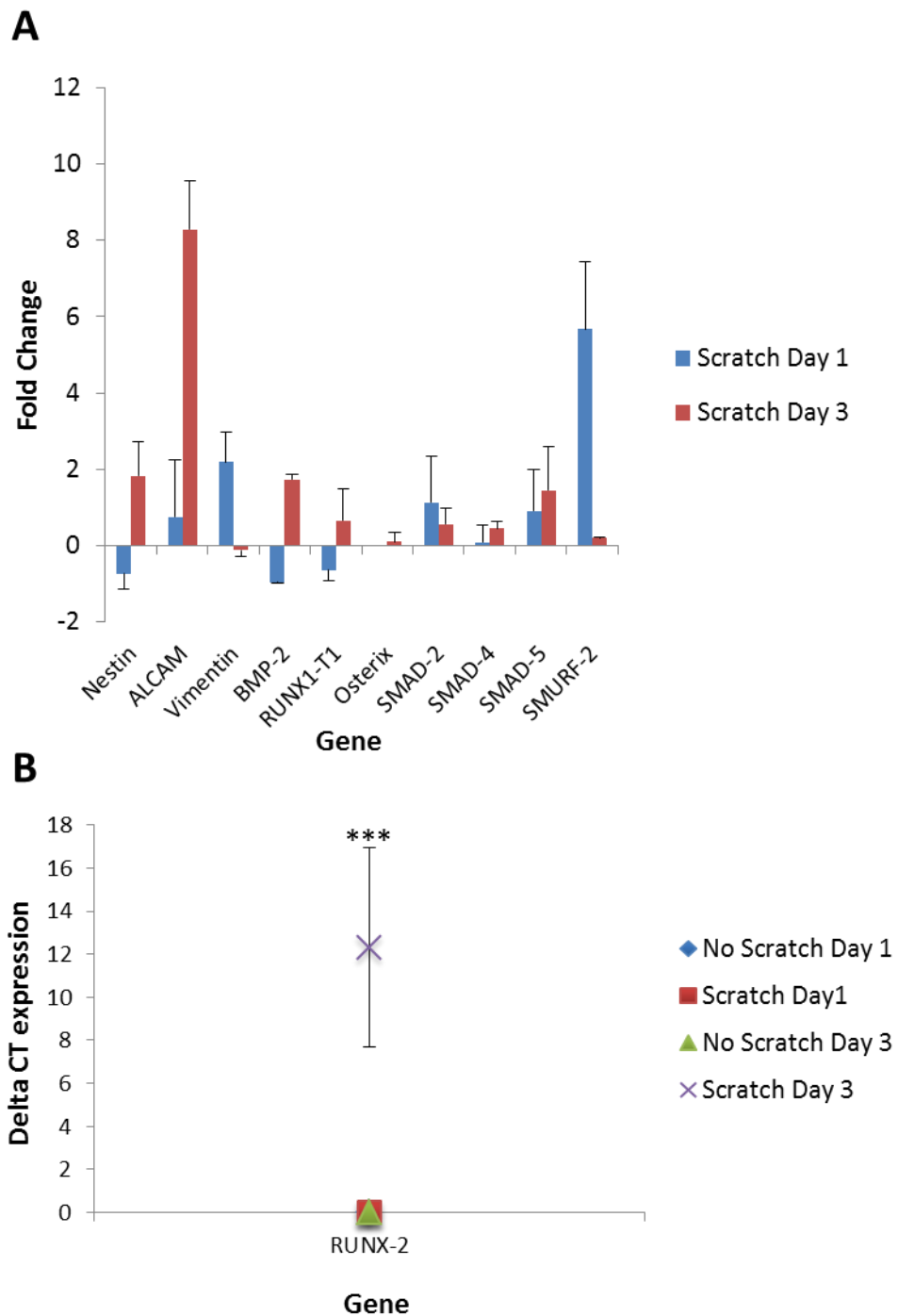


**Figure 4-8: Gene expression analysis of MSCs extracted from the spheroid niche model after co-culture with an unscratched and scratched osteoblast monolayer.** The gel containing the MSC spheroid/niche was cultured over unscratched or scratched primary osteoblast monolayers, for 1 day and 3 days. MSC gene expression was conveyed as a fold change, relative to the unscratched assay, at the same time point.

## 4.5 Discussion

### 4.5.1 Time lapse assessment of wound healing assays.

The images in Figure 4-1 showed the scratch healed greater rate in the absence of a collagen gel. This rapid healing process was observed in both the connective and bone matrix models. In order for the scratch to close and heal, cells neighbouring the scratched edge, appeared to migrate and proliferate within the damaged area. Scratched monolayers, in the presence of a collagen gel, required a longer healing rate. This prolonged healing rate, in both models, may be due to a greater resistance to cell mobility, caused by the fibrous network of the collagen. Another factor prolonging the healing rate may be caused by more resistance to cell signalling molecule transmission through the collagen gel.

Collagen molecules consist of three polypeptide chains, which entwine with each other to form a three stranded rope structure. The strands are held together by hydrogen and covalent bonds. These stranded structures self-assemble into fibrils (10 - 300 nm in diameter), which group together to form collagen fibres (0.5 - 3  $\mu\text{m}$  wide). These fibres cross-link together to form a fibrous network within the gel (Parenteau-Bareil et al., 2010, Lee et al., 2001). Therefore, when cells migrate across the scratch to heal the wound, there may be a greater movement resistance compared to the control, without collagen gel. The fibrous collagen gel network meant the scratch sample cells took 5 times and 0.5 times longer respectively to heal compared to the controls, without collagen gel.

Cellular migration through the collagen may occur *via* two processes. Cells may distort their morphology to migrate through the pores between the collagen fibres (Charras and Sahai, 2014). However, this migration process is limited by the pore size. Another way the cells may migrate through the collagen gel is by the release of proteolytic enzymes, matrix metalloproteinases (MMPs), which degrade the surrounding collagen fibres (Wolf et al., 2013, Ozeki et al., 2014, Zhang et al., 2014). These enzymes widen the pores by cleaving the fibres within the matrix thus, allowing greater motility of the cells. The cells then use integrin-mediated binding to the collagen and actomyosin-mediated contraction to propel the cell in the desired direction (Chi et al., 2014). The osteoblasts and fibroblasts used within these models have been shown to be able to remodel the

collagen gels to allow migration to the injured/scratched site (Alves et al., 2015). Studies have shown collagen is highly dynamic as the surrounding cells constantly remodel it, particularly during the wound healing process (Schultz and Wysocki, 2009).

Figure 4-1 also showed the connective tissue model scratch, took less time to heal compared to the bone matrix model, irrespective of the presence of a collagen gel. *In vivo* healing rates vary depending upon the position of the wound within the body; for example, connective tissue heals extremely rapidly compared to bone regeneration (LaStayo et al., 2003). A study conducted by Kawase et al., assessed cell proliferation abilities of mouse fibroblast-like cells compared to mouse osteoblast-like cells (Kawase et al., 2014). The researchers seeded both cells at the same concentration and assessed the time taken for the cells to reach 100% confluence. The osteoblast-like cells took twice as long to reach full confluence compared to the fibroblast-like cells. These results indicated osteoblast-like cells have a much lower proliferation rate compared the fibroblast-like cells. The results depicted in Figure 4-1 correlate with this observation, with a slower proliferation and healing rate within the bone matrix model.

Following verification of wound closure, it was important to identify whether there were potential dead cells at the scratch edge. Damaged, stressed or injured cells are known to release danger signals in the form of danger associated molecule patterns (DAMPs), which stimulate neighbouring cell migration (Kato and Svensson, 2015). Damaged or injured cells, which occur during injury lose their structural membrane integrity and release intracellular contents into the surrounding area e.g. DAMPs (Rosin and Okusa, 2011). These molecules initiate an inflammation response and recruit dendritic cells, macrophages, T cells and neutrophils, by binding to pattern recognition receptors (PPRs) on these particular cells. Therefore, DAMPs initiate the tissue repair process *via* the recruitment of the innate immune cells, which in turn release cytokines and chemokines to attract other wound healing cells to the area (Bianchi, 2007). The live/dead images depicted in Figure 4-2 showed limited dead cells at the scratched edge, 1-hour post injury. Therefore, the migration response of the fibroblasts and osteoblasts may partly be due to

DAMPs being released from damaged cells to the surrounding area. Other soluble factors may also have been released from the live cells at the edge of the wound, to encourage cell migration and ultimately wound closure.

#### **4.5.2 Assessing MSC migration from a spheroid niche in response to an artificial wound**

MSCs which were co-cultured with a control (unscratched) monolayer, Figure 4-3 showed a failure to migrate from the niche spheroids at all-time points. These results suggest the MSCs in the niche model remained unstimulated by the presence of the underlying cell monolayer. The innate bone marrow niche maintains MSCs in a quiescent state, and regulates the stem cell quiescence by numerous factors, including cell-cell contacts, intrinsic factors and the creation of a hypoxic environment. These MSC bone marrow niche cells remain in this quiescent state, until stimulated; e.g. when stem cells are required to regenerate damaged tissue, which has occurred as a result of injury (Wang et al., 2010). The results in Figure 4-3, Figure 3-24 and Figure 3-25, imply the spheroid MSCs were in a quiescent state, suggesting the stem cells were not within the proliferating cell cycle, but resting in the G<sub>0</sub> phase outside of the cell cycle (Spencer et al., 2013).

Research has shown that within the vascular neural stem cell niche, cell-cell contacts are extremely important in maintaining neural stem cell quiescence (Ottone et al., 2014). Furthermore, Ottone et al., found direct neural stem cell contact with endothelial cells led to stem cell quiescence, *via* ephrinB2 and Jagged1 pathway activation (Ottone et al., 2014). Within the bone marrow niche, a study by Yang et al., found Cdc42 expression maintained HSC quiescence and retained the stem cells in the correct location, by regulating the expression of cell adhesion molecules, including  $\beta$ 1-integrin and N-cadherin (Yang et al., 2007). The niche spheroids have been shown to mimic the cell-cell and cell-ECM interactions observed within the *in vivo* niche, *via* the creation of a multicellular three dimensional structure (Fennema et al., 2013, Pampaloni et al., 2007).

Another crucial niche component, in the maintenance of quiescence is a hypoxic environment. Studies have shown hypoxia greatly affects embryonic and adult

stem cell metabolic processes (Silván et al., 2009, Eliasson and Jonsson, 2010). Researchers have suggested that stem cells residing within a hypoxic milieu, decrease the rate of DNA mutations and activate signalling pathways (Notch and Oct4) associated with maintaining stemness (Simon and Keith, 2008). MSCs residing within the bone marrow niche environment, experience hypoxic conditions and exhibit increased Oct4 expression, which maintains stemness and quiescence (Mohyeldin et al., 2010). The MSC spheroid niche resides within a collagen gel, which is known to possess oxygen gradients creating hypoxic environments. These hypoxic environments are similar to those observed in the native niche (Mohyeldin et al., 2010, Bhang et al., 2011). Cells within the spheroids have exhibited quiescence and maintenance of stemness, when compared to parallel 2D monolayer cultures, which may in part be due to the hypoxic milieu (Hirschhaeuser et al., 2010, Saleh and Genever, 2011). Additionally, a study conducted by Ong et al., analysed oxygen gradients in spheroid cultures and assessed quiescence *via* BrdU labelling of the cells (Ong et al., 2010). The researchers observed hypoxic environments, as well as cell quiescence in the spheroids.

Conversely, the results from Figure 4-4 demonstrated the MSC migration from the spheroid niche towards the wound site when co-cultured with scratched monolayers. Previous studies have shown MSCs migrate and home towards injured sites, in the presence of chemoattractant molecules released from the damaged area (da Silva Meirelles et al., 2009). The homing and migration process of the MSCs is greatly enhanced by their expression of many receptors, which interact with molecules released from the site of injury. Several receptors have been identified, which are involved in the migration and homing process, including chemokine receptors; CXCR4, CCR1, CCR4, CCR7, CCR9, CCR10, CXCR5 and CXCR6 (Ryu et al., 2010, Honczarenko et al., 2006, Von Luttichau et al., 2005).

Chemokine receptor expression, such as CXCR4 are influenced by the Notch signalling pathway (Xie et al., 2013). Notch is an essential gene, which encodes a transmembrane signalling receptor, which in turn regulates cell fate outcomes e.g. cell migration. Notch signalling is a cell communication mechanism, which involves an interaction between a Notch receptor expressed on a membrane of

one cell (Cell 1) and Notch ligands attached to the membrane of a neighbouring cell (notch extracellular domain (NECD) on Cell 2, see Figure 4-9) (Guruharsha et al., 2012). Following the binding of the receptor and the ligand, the S2 cleavage site of the receptor on Cell 2 is exposed and proteolysis occurs by the action of the TNF- $\alpha$  converting enzyme (TACE). A second cleavage at the S3 site occurs through the effect of  $\gamma$ -secretase. This subsequent cleavage causes the Notch intracellular domain (NICD) to translocate into the nucleus of Cell 2. The NICD binds with CBF1/RBP-J $\kappa$ /suppressor of Hairless/Lag1 (CSL) to form a complex, which recruits other co-activators to induce transcriptional expression of downstream target genes (Seke Etet et al., 2012).

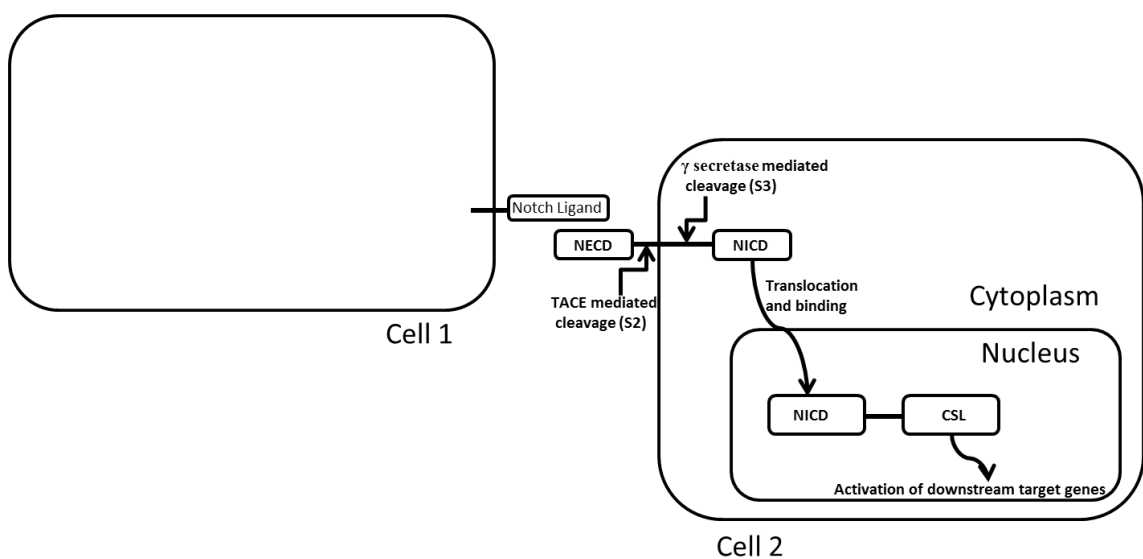


**Figure 4-9: Simplified diagram of Notch signalling pathway.**

The binding of Notch ligand and receptor between cell 1 and cell 2 causes breakdown at S2 and S3 of Notch receptor cleavage sites, leading to the release of the receptor's intracellular domain, which trans-locates to the cell 2 nucleus, leading to the activation of downstream target genes. (NECD-Notch extracellular domain, NICD-Notch intracellular domain, TACE-TNF- $\alpha$  converting enzyme, CSL-CBF1/RBP-J $\kappa$ /suppressor of Hairless/Lag1). (Adapted from (Seke Etet et al., 2012)).

A study by Xie et al., suggested inhibition of Notch signalling improved MSC migration, as a result of increased receptor CXCR4 expression (Xie et al., 2013). Furthermore, a study by Williams et al., showed Notch signalling activation down regulated CXCR4 expression in endothelial cells, which in turn led to reduced cell migration (Williams et al., 2008). Therefore, it may be suggested that the observed migration of the MSCs from the niche, shown in Figure 4-4 is due to the interruption in the Notch signalling with a subsequent increase in cytokine receptor expression, causing the migration of MSCs to the wound site.

The MSC *in vivo* homing process requires multiple steps, initiated by the rolling process. Low affinity interactions occur until the cell tethers *via* E-selectin receptors onto the cell using selectins, which allows the cell to transmigrate as depicted in Figure 4-10. This process causes integrin expression activation within the MSC, leading to firm cell adhesion, and thus, the cell is able to transmigrate to the desired location by the release of MMPs (see Figure 4-10) (Kholodenko et al., 2013, Khaldoyanidi, 2008, Karp and Leng Teo, 2009). Whilst the spheroid niche model is a very simplistic version of the *in vivo* environment, it is possible that the spheroid MSCs may adopt this *in vivo* migration process, in addition to MMP release, to migrate through the collagen gel to the monolayer site of injury.

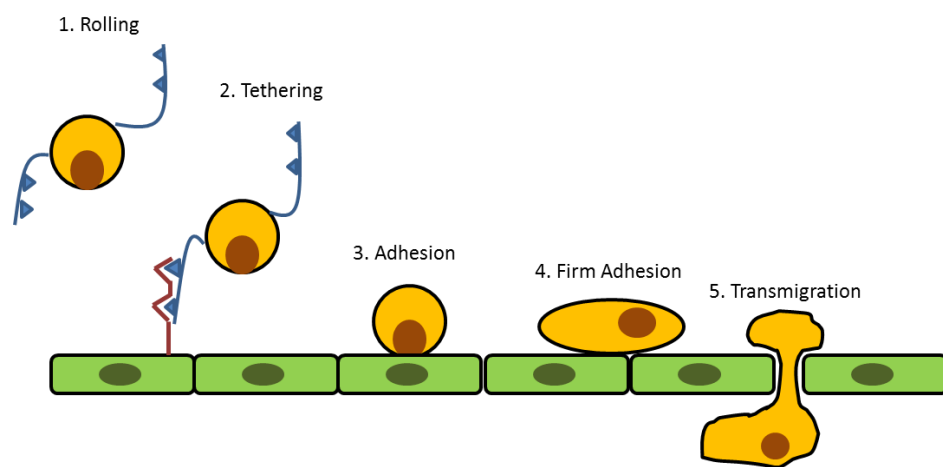


**Figure 4-10: Illustration of MSC migration and homing *in vivo*.**  
(Image adapted from (Khaldoyanidi, 2008))

In Figure 4-1 showed the fibroblasts, in the absence of a MSC niche, took 6 days to heal the wound. However, the images in Figure 4-4 showed the fibroblasts in the presence of a MSC niche spheroid closed the scratch within 3 days. Therefore, these results indicate the presence of a MSC niche, greatly increased the healing rate. Studies have shown MSCs enhance wound repair, *via* paracrine signalling to cells surrounding the affected area. Previous research has found that media collected from MSC monolayers contained chemoattractant molecules, recruited epidermal keratinocytes, as well as dermal fibroblasts at the wound site (Chen et al., 2008, Gurtner et al., 2008). Another study found the presence of MSCs within a wound, regulated dermal fibroblast migration, which in turn led to accelerated wound closure (Smith et al., 2010a). This study agreed with research by Hocking and Gibran, who found MSCs affected the regulation of fibroblast proliferation, thus accelerating wound healing (Hocking and Gibran, 2010).

In summary, the images in Figure 4-4 showed an increased MSC migration out of the niche over time. These results suggest attractant mechanisms were utilised within this niche model system. Chapter 5 describes further research, which studied the potential attractant molecules released from an injured monolayer site.

### **4.5.3 MSC differentiation assessment post migration from spheroid niche to wound site.**

Figure 4-5 indicated the MSCs, within the scratched models were migrating out of the spheroid and incorporating in the scratched area. Numerous studies have shown MSCs enhance wound healing *via* paracrine signalling mechanisms, as discussed in Section 4.5.2. However, MSCs may also enhance this healing process by differentiating into resident cells, which surround the injured site.

Researchers have established that MSCs migrate to the wound site and transdifferentiate into cells of the surrounding area (Sasaki et al., 2008, Wu et al., 2007). Sasaki et al., found MSCs were recruited to the damaged skin and these cells aided wound repair, by transdifferentiating into multiple skin cell types (Sasaki et al., 2008). However, research studies have shown conflicting evidence that MSCs may not differentiate into resident cutaneous cells (Javazon et al., 2007). Therefore, it was important to determine whether the MSCs, which had migrated out of the spheroid niche, were differentiating into the local cells.

Extensive research has shown MSCs differentiate into cells of osteogenic lineages. Therefore, osteogenic markers (phosphorylated runt-related transcription factor-2 (RUNX-2) and osteopontin) were used to assess MSC differentiation, in both fibroblast (control) and osteoblast scratched monolayer models. RUNX-2 is an important transcription factor, which is known to induce MSC osteoblast differentiation (Tai et al., 2014). RUNX-2 has also been shown to be involved in the regulation of bone-related genes. Phosphorylation of RUNX-2 is a post translational modification, which regulates RUNX-2 activity. During MSC osteogenic differentiation, key residues on RUNX-2 become phosphorylated, leading to increased RUNX-2 activity, which drives the differentiation process. RUNX-2 expression by MSCs, indicates the early onset of osteogenesis (Yang et al., 2014). Osteopontin is a marker associated with maturing osteoblasts and has

been used to identify MSCs, which have become further committed into osteogenic differentiation (Rust et al., 2007). Therefore, either phosphorylated RUNX-2 or osteopontin expression, within the migrating MSCs in the scratched models would indicate these cells were differentiating, into the resident osteoblastic cells.

The control fibroblast model images depicted in Figure 4-5a, showed an absence of expression of phosphorylated RUNX-2 or osteopontin released from the migrating MSCs and/or spheroids. This result would suggest the MSCs within this model, were not spontaneously differentiating into cells of osteoblastic origin. Whereas, the presence of a scratched osteoblast monolayer led to the expression of both phosphorylated RUNX-2 (Figure 4-5b and Figure 4-6) and osteopontin (Figure 4-5b) in the migrating MSCs. Therefore, this novel experiment proved the MSCs migrating from the niche spheroids, into the scratched osteoblast area were differentiating into the resident osteoblasts.

Fluidigm was subsequently used to compare gene expression of a selection of MSC and osteoblast markers, from RNA isolated from MSC spheroids co-cultured with scratched and unscratched osteoblast monolayers. Nestin and ALCAM are MSC surface markers used to characterise multipotency. High expression of nestin and ALCAM, after 3 days in the scratched model suggested the MSCs in the niche were retaining their stemness. Therefore, the MSCs were potentially able to self-renew and replace migrating MSCs, mimicking the bone marrow niche response.

Bone morphogenetic proteins (BMPs) are essential for skeletal development and regeneration, particularly BMP-2, which interacts and induces RUNX-2, which in turn promotes osteoblast differentiation (Song et al., 2009). Furthermore, SMAD proteins are intracellular proteins, which regulate certain gene expression and are recruited by RUNX-2 to form an activator complex. These SMAD proteins initiate the responsive gene transcription of BMPs and are important in the initial processes of osteogenic differentiation. Figure 4-8 showed increased gene expressions of BMP-2, SMAD-2, SMAD-4 and SMAD-5 following a three day co-culture period in the MSC scratched samples, suggesting the MSCs were beginning to differentiate down through the osteogenic lineage.

Previous studies indicate that whilst mature osteoblasts down regulate RUNX-2, it is up regulated in pre-osteoblasts and immature osteoblasts (Komori, 2010). MSCs have been shown to differentiate into immature osteoblasts, *via* the expression of RUNX-2. The day 3 scratched osteoblast samples showed high RUNX-2 expression, indicating the MSCs were starting to differentiate into pre-osteoblasts or immature osteoblasts post 3 days. These results suggest the MSCs were migrating out of the niche, towards the scratch and starting the osteogenesis differentiation process.

Additionally, BMP-2 is known to control osterix, which regulates another vital transcription factor for osteogenesis (Lai et al., 2011). Osterix has been shown to be involved in inducing pre-osteoblasts into mature osteoblasts. Therefore, osterix acts further along the differentiation process and downstream of RUNX-2 (Lee et al., 2011a). The small amount of fold change of osterix expression, over a period of 3 days of the scratched osteoblasts, supports the theory the MSCs were at the initial stages of osteogenesis.

## 4.6 Summary

This chapter aimed to further study the MSC niche model developed in Chapter 3, by determining whether the MSCs could be stimulated, by co-culture with a wounded cell monolayer, to migrate towards the wound and aid wound healing, as observed *in vivo*.

Initial studies on the wound healing model (i.e. scratched monolayers) demonstrated that the resident monolayer cells (fibroblasts or osteoblasts), directionally migrated perpendicular to the scratch edge, closing the site of injury. Furthermore, the presence of a collagen gel prolonged the healing rate in both scratched fibroblast and osteoblast monolayer models.

The co-culture of the MSC spheroid niches placed directly on top of the unscratched fibroblast and osteoblast monolayers, demonstrated the MSCs failed to migrate out of the niche into the surrounding area over three days. This result supported the data from Chapter 3, which demonstrated that the MSCs within the spheroids were in a quiescent state, and remained unstimulated by the presence of the monolayer. However, when the underlying monolayer was scratched, the MSCs directionally migrated out the spheroid, towards the scratched area. The addition of the MSC spheroid, accelerated the wound healing rate by 100%, compared to scratched models without MSC spheroids. Therefore, the MSCs appeared to encourage the proliferation of the local resident cell type to close the wound. Furthermore, following migration towards the wound, the MSCs became fully incorporated within the scratched area. This finding mimicked the *in vivo* niche response, where MSCs remain in a quiescent state when unstimulated, but in the presence of injury, they migrate out of the niche and accelerate the wound healing process.

The migrated MSCs exhibited phosphorylated RUNX-2 and osteopontin expression, in the presence of the scratched osteoblast monolayer. Therefore, these results suggest the MSCs were differentiating *via* osteogenesis, into the resident cell type. Furthermore, RUNX-2 expression was observed at the gene level in MSCs extracted from the scratched osteoblast monolayer at day 3. Not only were the MSCs starting to differentiate, but there was also an increased nestin and STRO-1 expression, which indicated there was increased MSC

proliferation in the spheroid, in anticipation of the need to replace the migrated MSCs.

These results suggest the MSC spheroid niche model is capable of mimicking the native bone marrow niche responses therefore, creating a responsive biomimetic model. The signals causing the MSCs to migrate out of the niche, towards site of injury, will be assessed in the following chapter.

# CHAPTER 5

## 5 Assessment of paracrine cell signalling within the induced MSC spheroid niche

### 5.1 General Introduction

During the wound healing process, MSCs migrate to the site of injury through a process of paracrine signalling. Small biologically active molecules, termed cytokines, assist in cell-cell communication in immune responses (Zhang and An, 2007). Cytokines are released from cells in the injured area, which stimulate the movement of MSCs towards sites of trauma, inflammation and infection (Lin et al., 2003). Cytokines have various modes of action, which are able to affect neighbouring injured cells (autocrine), nearby cells (paracrine) or distant cells (endocrine) (Dembic, 2015). Various cells in the body produce a large variety of cytokines, including the interleukin, chemokine, interferon, transforming growth factor (TGF) and tumour necrosis factor (TNF) sub-families (Dinarello, 2007). Cytokines may be classified into various functional classes dependent on their primary properties. The table below (Table 5-1) lists a selection of cytokines and their mode of action in the body.

**Table 5-1: Functional classes of selected cytokines.**  
(Adapted from (Dinarello, 2007)).

Functional Class	Primary Property	Examples
Chemokines	Cellular emigration	MCP-1, MIP-1 $\alpha$
Interleukins	Stimulation of T cells, synergistic effects, chemo-attracts neutrophils	IL-1, IL-6, IL-8
Interferons I and II	Macrophage activation, anti-viral	IFN- $\alpha$ , IFN- $\beta$ , IFN- $\gamma$
Tumour necrosis factor	Induces cytolysis and cytostasis, enhances proliferation of T cells	TNF- $\alpha$ , TNF- $\beta$
Colony stimulating factors	Haematopoietic differentiation, proliferation of neutrophilic, eosinophilic and monocytic lineages	GM-CFS, M-CFS, G-CFS

Cytokines are further categorised by their properties, including pro-inflammatory and anti-inflammatory. During the initial inflammatory stage of the wound healing process, cells release pro-inflammatory cytokines including IL-6, IL-1 $\beta$  and TNF- $\alpha$  (Yagi et al., 2012). Following initial inflammatory

response, the chemokines subsequently induce chemotaxis. This process involves a directional cell migration, or homing, into the surrounding matrix.

MSC/cytokine interaction causes an intracellular cascade of events, which induces MSC migration from the niche. These MSCs are further attracted to the injured area, due to the cytokine concentration gradient, caused by the event. The homing capacity of MSCs is dependent on the type of chemokine receptors present on the cells (Sohni and Verfaillie, 2013). Studies have identified specific cytokine receptors which aid MSC migration and homing, including CXCR4, CCR1, CCR4, CCR7, CXCR5 and CXCR6 (Sordi et al., 2005). The most studied chemokine and chemokine receptor associated with MSC homing and migration have been stromal derived factor-1 (SDF-1)/CXCL12 (chemokine) and CXCR4 (receptor). However, a number of studies have shown MSCs possess other cytokine receptors, including IL-1R, IL-6R and TNFI and aid MSC migration (Minguell et al., 2001).

Osteoblasts, under stressed conditions, have been shown to express and secrete IL-1, IL-6, IL-12, IL-18 and TNF- $\alpha$ , during the inflammatory response (Bost et al., 1999, Udagawa et al., 1997). Another study found that 36 hours after injury, there were significantly increased levels of cytokine IL-2, suggesting this cytokine was involved in the initial pro-inflammatory response (Kowal-Vern et al., 1994). Furthermore, following skin trauma, researchers found significant increased levels of a few cytokines (IL-1 $\beta$ , IL-6, and TNF- $\alpha$ ), which were also determined as pro-inflammatory mediators (Kubo et al., 2014, Grellner et al., 2000). Therefore, in the present study, IL-1 $\beta$ , IL-2, IL-6, IL-12p70 and TNF- $\alpha$  were selected for analysis, from the scratched osteoblast and fibroblast monolayer cultures, during the first 72 hours following injury.

## 5.2 Objectives

Chapter 4 adopted the 3D MSC niche model and assessed the functional properties of the model, in relation to wound healing. The MSCs were found to directionally migrate from the spheroid niche, towards the site of monolayer culture injury. Subsequently, the MSCs integrated with the scratch-wound and advanced the healing rate. In this chapter, further investigations aim to establish the MSC migration cues, which trigger the cells to travel from the niche

to the site of injury. Cytokine analysis from the underlying scratched monolayers, would determine which biologically active molecules may be stimulating the MSCs, to home and migrate to the damaged area. Identification of specific cytokines would enable further analysis of the stimulatory effect of the identified cytokine(s) on MSCs within the niche model.

These objectives will be achieved by:

- The analysis and identification of secreted cytokines from scratched and unscratched monolayers, over various time periods.
- The addition of identified cytokines to the niche model, in the absence of other stimuli.

## 5.3 Materials and Methods

### 5.3.1 Cytokine Analysis

#### 5.3.1.1 Luminex assay

Either osteoblast cells or h-TERTs were seeded onto CellBind plates. The osteoblast monolayer culture cells were cultured with osteogenic differentiation media (see Chapter 3, section 3.3.5), which was changed every 2/3 days, over a 10 day period. The monolayer was either scratched or left unscratched followed by the immediate addition of fresh media. The supernatant was removed after 3 hours, 12 hours, 24 hours and 72 hours and the Bio-Rad Bio-Plex Pro cytokine assay protocol was used to analyse the cytokines.

All solutions were prepared from the Bio-Rad Pro Human Cytokine Group I, 5-plex assay kit, except for the modified media, which was prepared in house. Each supernatant was centrifuged at 1000 g at 4°C for 15 minutes and the media was removed, in preparation for processing. The cytokine standard was reconstituted with modified media and 8 serial dilutions (1:4) were followed with the addition of modified media, to create a standard curve. A control blank was prepared with modified media. Each sample was further diluted (1:4) with modified media. Stock solutions (10x) of conjugated coupled magnetic beads were pooled together with assay buffer, to make a single 1x solution. The plate was pre-wetted with 100 µL of assay buffer, which was removed and 50 µL of the 1x magnetic beads solution was added.

Prior to the removal of each solution from the plate, a magnetic plate was applied to retain the beads within the wells. The solution was removed and the plate was washed twice with 100 µL of wash buffer. The standards, samples and blanks (50 µL) were added to the appropriate wells and left covered and shaken at room temperature for 30 minutes. After the appropriate incubation period, the solution was removed and the wells were washed thrice with wash buffer (100 µL). Stock solutions (10x) of detection antibodies were mixed together and diluted, to create a 1x solution with detection antibody diluent. The 1x solution was added to the wells (25 µL), left covered and shaken at room temperature for 30 minutes. After the appropriate incubation period, the solution was removed and the wells were washed thrice with wash buffer (100 µL). Stock solution

(100x) of streptavidin-PE was diluted to create a 1x solution with assay buffer. The 1x solution was added to the wells (50  $\mu$ L), left covered and shaken at room temperature for 10 minutes. After the appropriate incubation period, the solution was removed and the wells were washed thrice with wash buffer (100  $\mu$ L). The beads were re-suspended with assay buffer (125  $\mu$ L), in preparation for analysis using the Bio-Rad Bio-Plex Luminex 100 plate reader.

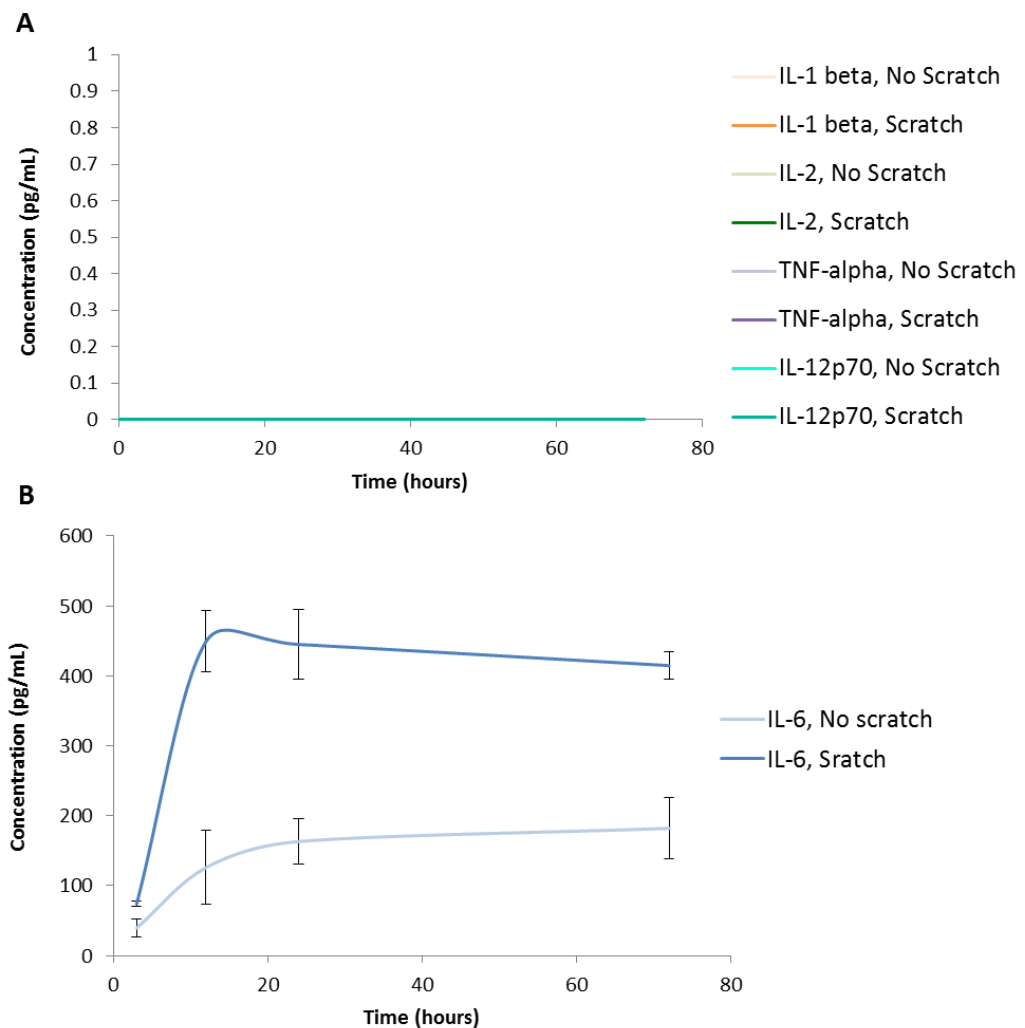
### **5.3.2 IL-6 Addition assay**

Media (1 mL) containing IL-6 (450 pg/mL) was added to MSC niche models (within collagen gels, prepared as previously described in section 2.3.4.2), for either 3 hour, 12 hour, 24 hour or 48 hour incubation periods. Controls were prepared using fresh media, which was added to MSC niche models for up to 48 hours. Following each incubation period, test and control samples were fixed with 4% formaldehyde. These samples were stained for actin and analysed using a Zeiss Axiovert 200M fluorescent microscope.

## 5.4 Results

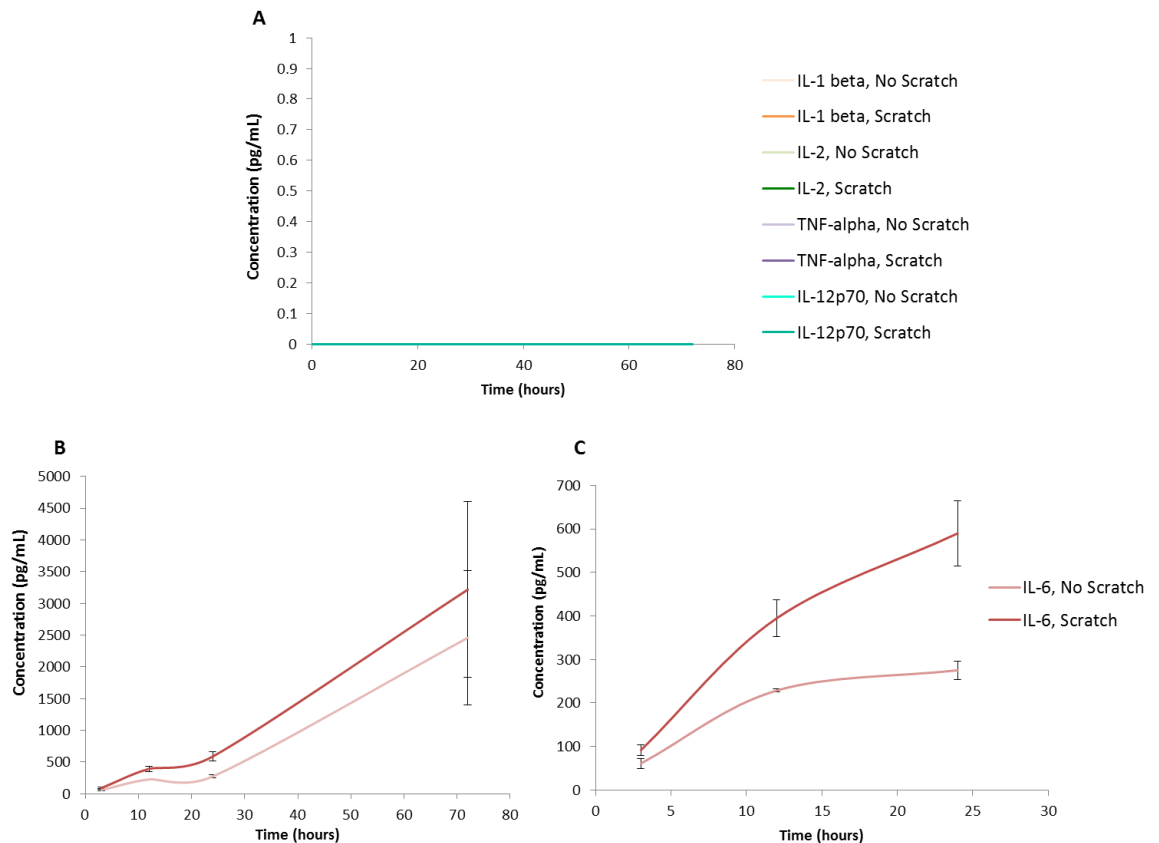
### 5.4.1 Identification of cytokine secretion from scratched models.

Figure 5-1 showed the absence of IL-1 $\beta$ , IL-2, IL-12p70 and TNF- $\alpha$  cytokines in the osteoblast cultures (Figure 5-1, image A). However, there was a significant increase of IL-6 in the presence of a scratch, compared to the unscratched model (Figure 5-1, image B). The control, unscratched samples, indicate a background level of IL-6 over the 72 hours (180 pg/mL). However, there was a significantly increased level of IL-6 between 3 hours and 12 hours in the scratched samples (an increase from 74 pg/mL to 450 pg/mL). IL-6 levels in the scratched osteoblasts remained constant between 12 hours and 72 hours post scratch.



**Figure 5-1: Quantitative analysis of cytokines secreted, from unscratched and scratched osteoblast monolayer after, 3 hours, 12 hours, 24 hours and 72 hours. (A) Graph depicting the concentration of secreted IL-1 $\beta$ , IL-2, TNF- $\alpha$  and IL-12p70 from scratched and unscratched osteoblast monolayers over 72 hours. (B) Concentration of secreted IL-6 from scratched and unscratched osteoblast monolayers over 72 hours.**

Similarly, Figure 5-2 illustrated the lack of IL-1 $\beta$ , IL-2, IL-12p70 or TNF- $\alpha$  cytokine secretion in the fibroblast monolayer cultures (Figure 5-2, image A), with a significant increase of IL-6 in the presence of a scratch, compared to the unscratched model, up to and including the 24 hour sample period (Figure 5-2, image B and C). However, post 24 hours, there was a significant increase in IL-6 concentration in both scratched and unscratched models. At 72 hours there was no significant difference between either models.



**Figure 5-2: Quantitative analysis of cytokines secreted, from unscratched and scratched fibroblast monolayer after, 3 hours, 12 hours, 24 hours and 72 hours.**

**(A)** Depicts the concentration of secreted IL-1 $\beta$ , IL-2, TNF- $\alpha$  and IL-12p70 from scratched and unscratched fibroblast monolayers over 72 hours. **(B)** Concentration of secreted IL-6 after 3 hours, 12 hours, 24 hours and 72 hours and **(C)** without 72 hours time point.

#### 5.4.2 MSC niche model response to IL-6.

Results from both Figure 5-1 and Figure 5-2 identified cytokine IL-6, as one of the signalling molecules secreted from the scratched osteoblast and fibroblast monolayer cultures. Therefore, IL-6 was deemed a potential candidate in the induction of MSC migration from the niche model. Therefore, IL-6 (at 450 pg/mL

concentration) was added to MSC niche models, in the absence of osteoblast and fibroblast monolayers, and assessed over a 48 hour period. Additionally, control gels in the absence of IL-6 were assessed over the same period of time (Figure 5-3).

The images depicted in Figure 5-3 showed a lack of MSC migration from the control samples, over the 48 hour period. Conversely, within 3 hours of the addition of IL-6 to the gels, there were MSC cellular protrusions from the spheroid into the surrounding collagen gel. At 12 hours, individual MSCs were noted to migrate from the spheroid niche, into the local vicinity of the gel. As time progressed, from 12 hours to 24 hours, there was a marked increase in the number of MSCs migrating out and exiting the niche. By 48 hours, migration was evident throughout the niche cultures. These results demonstrated a clear relationship between IL-6 exposure and MSC migration out of the spheroid niche model.

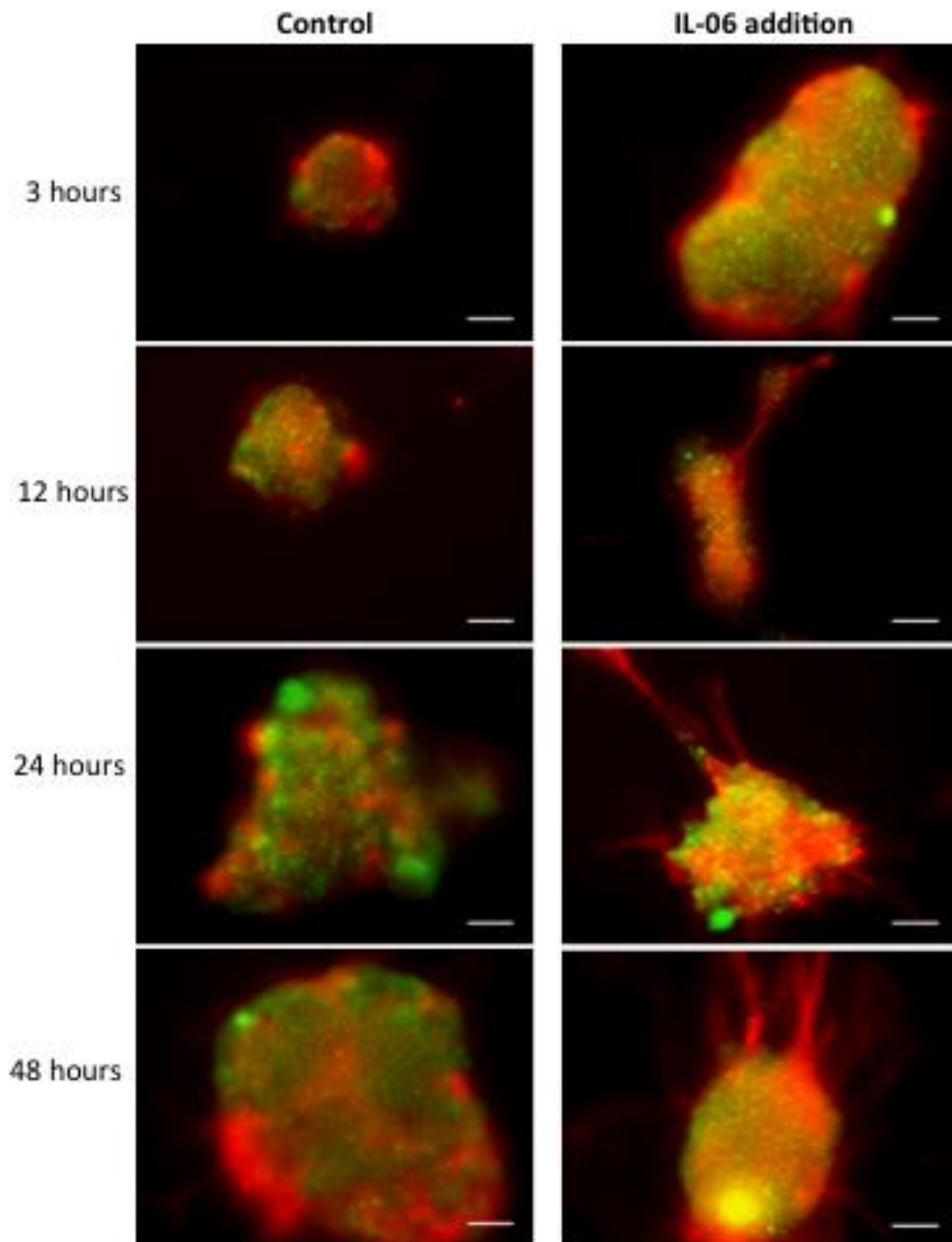


**Figure 5-3: Niche model response to IL-6 addition over time.**

The MSC niche model was assessed with and without the addition of IL-6 to media over time (3 hours, 12 hours, 24 hours and 48 hours), in the absence of co-cultured monolayers. 20x objective, scale bar=50  $\mu\text{m}$ .

## 5.5 Discussion

### 5.5.1 Identification of cytokine secretion from scratched models.

The cytokine IL-6 was the only identified secreted cytokine from the candidate panel in both osteoblast and fibroblast monolayers (Figure 5-1 and Figure 5-2). Various cells produce and secrete cytokine IL-6 to regulate numerous processes, including immune responses and bone homeostasis. Additionally, observations have shown that osteoblasts produce IL-6 (Marriott et al., 2004, Grellner et al., 2000). IL-6 is known to regulate the differentiation of osteoblasts and osteoclasts. Osteoblasts secrete IL-6 to induce osteoclast differentiation and osteoclast-mediated bone demineralisation (Ishimi et al., 1990, Yoshitake et al., 2008, Liu et al., 2006). IL-6 from osteoblasts stimulates osteoclast differentiation, by inducing the expression of the NF- $\kappa$ B ligand (RANKL) on osteoblasts, which in turn interacts with RANK expressed on osteoclast progenitors (Liu et al., 2006). During the bone remodelling cycle, osteoclast precursors fuse and become mature osteoclasts, allowing them to attach to the bone (Figure 5-4). These mature osteoclasts resorb bone to form Howship's lacuna (Novack and Teitelbaum, 2008).

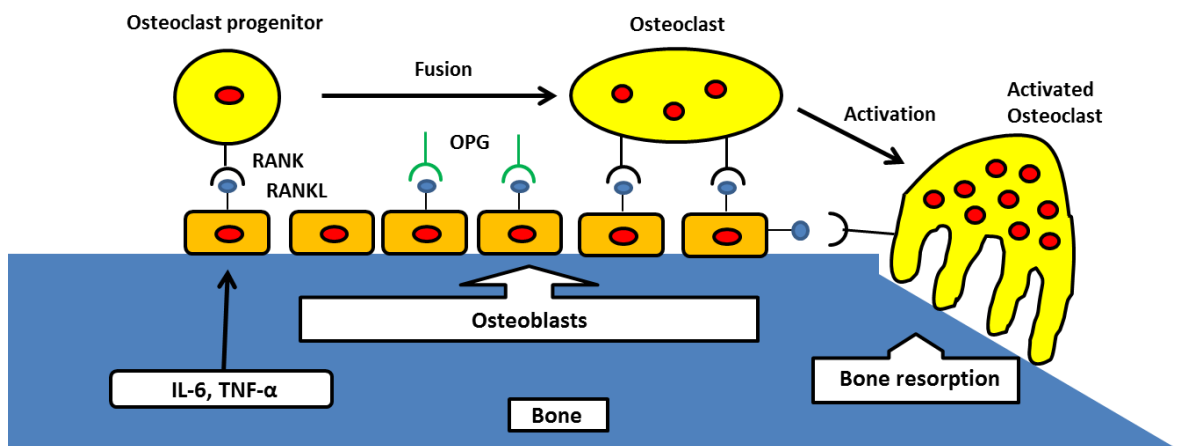


**Figure 5-4: Diagram demonstrating the bone remodelling process.**

IL-6 and TNF- $\alpha$  stimulate osteoblasts to express RANKL, which interacts with RANK receptors on the osteoclast progenitors causing them to fuse together to form osteoclasts. These osteoclasts are activated and become mature osteoclasts, which attach to the bone and initiate bone resorption process. (Adapted from (Meikle, 2006)).

These cells are instrumental in the repair of damaged bone, *via* the bone healing process. A study showed osteoclasts were extremely important in the very early stages of bone healing, in the remodelling and resorption of bone (Schell et al., 2006).

This study demonstrated that IL-6 was highly secreted, within the scratched osteoblast model during the initial 12 hours. These findings may therefore, suggest that the osteoblasts were being activated to initiate bone regeneration. An increased production of the cytokine from the osteoblasts, may lead to the potential differentiation of osteoblasts into osteoclasts.

Following the initial increase in IL-6 secretion (during the first 12 hours), the IL-6 levels remained at least double that of control unscratched cultures, subsequently, the levels of IL-6 plateaued over the next 60 hours. A study conducted by Kondo and Ohshima found IL-6 peaked at 12 hours, post wound induction of mouse skin (Kondo and Ohshima, 1996). These results correlate with the findings from this study in relation to the osteoblast samples. Kondo and Ohshima, suggest the initial significant increase in IL-6 concentration secreted by scratched models may be produced at this time to induce B-cell, T cell and macrophage differentiation, as well as stimulate keratinocyte growth to accelerate wound healing. Therefore, the observed increase of IL-6 in the media, within the scratched models, may stimulate cell growth and hasten the wound healing process.

Other cells, including fibroblasts have been shown to produce and secrete IL-6, during the pro-inflammatory phase of wound healing post injury (Akira and Kishimoto, 1992). A study conducted by Lin et al., found IL-6 was critical in the healing of mouse skin excisions (Lin et al., 2003). Mice deficient in IL-6 displayed reduced wound healing rates, compared to normal wild mice. IL-6 deficiency in the mice affected all three phases of wound healing process thus, increasing the time taken to close the skin excisions (Lin et al., 2003).

The scratched fibroblast monolayers also showed significantly increased levels of IL-6, compared to the unscratched sample, but only over the initial 24 hour period (Figure 5-2). After this time point, both unscratched and scratched models showed parallel increased levels of IL-6, with no significant differences between either model. These results may be due to the fibroblast cells becoming over-confluent and inducing a false positive response. The fibroblasts were seeded as a confluent monolayer and have a much higher proliferation rate, compared to osteoblasts (Fedarko et al., 1995). Therefore, when the fibroblasts were assessed over a period of 72 hours, the cells may have become

over-confluent. Over-confluent fibroblasts have previously been used as positive controls, for detecting matrix metalloproteinases and tissue inhibitors of metalloproteinases. A study by Cook et al., found fibroblasts over-expressed these molecules in this environment (Cook et al., 2000). Similarly, high secretion levels of IL-6 at 72 hours may not be a true representation of the fibroblast response, within the scratched and unscratched models.

### **5.5.2 MSC niche model response to IL-6.**

In the initial stages of wound healing following injury, the surrounding cells within the damaged tissue release pro-inflammatory signals. Cytokine analysis highlighted IL-6 release in the scratched bone and connective tissue models. Cytokines are small proteins, which have various modes of action on numerous cell types. Cytokines diffuse into the surrounding area of injury, creating a concentration gradient. MSCs express numerous receptors, which interact with the cytokines. This interaction causes the MSCs to exit the bone marrow niche and migrate to the site of injury, *via* the cytokine concentration gradient. The exact homing mechanisms of MSCs to site of injury are poorly understood. However, studies identified numerous MSC chemokine homing receptors including: - CXCR4, CXCL12, CCR1, CCR7, CXCR5 and CXCR6 (Abumaree et al., 2013).

Additional studies have shown that damaged tissue in the initial inflammatory stage releases an influx of cytokines, including IL-6 (Spaeth et al., 2008). The increased circulation of IL-6 at the site of injury plays an active role in the recruitment of MSC migration to the wound (Yagi et al., 2012, Tondreau et al., 2009). An *in vitro* study conducted by Shi et al., observed improved MSC migration and increased CXCR4 receptor expression, when the cells were pre-treated with IL-6 (Shi et al., 2007). Moreover, Rattigan et al., demonstrated hypoxic breast cancer cells enhanced IL-6 production, thus increasing MSC recruitment to the tumour, *via* IL-6 interaction with its cognate IL-6 receptor (Rattigan et al., 2010). The authors stated the IL-6 released from the cancer cells acted in a paracrine fashion on nearby MSCs. The researchers were able to identify signalling pathways Janus kinase (JAK)/signal transducer and activator of transcription 3 (STAT3) and Mitogen-activated protein kinase (MAPK) involvement, in MSC migration/homing (Rattigan et al., 2010).

The JAK/STAT signalling pathway is the main signalling pathway utilised by numerous cytokines, including IL-6 to enter the cell and influence cell behaviour (e.g. cell proliferation, differentiation, migration and apoptosis) (Rawlings et al., 2004). MSCs are known to possess IL-6 receptors (IL-6R). Studies have shown that IL-6 utilises the classical signalling pathway, when IL-6 binds to its membrane bound IL-6 receptor (IL-6R), together with the signal-transducing protein, glycoprotein 130 (gp 130) (Luu et al., 2013, Heinrich et al., 1998). This binding causes the receptor to dimerise and activate the associated JAK tyrosine kinases attached to the receptor. The activated JAKs produce phosphotyrosine docking sites for STAT3 (a latent cytoplasmic transcription factor). The STAT3 is phosphorylated by the JAKs and leaves the receptor to dimerise and translocates to the nucleus. Once in the nucleus, the STAT3 dimer activates specific gene transcription (see Figure 5-5) (Aaronson and Horvath, 2002).

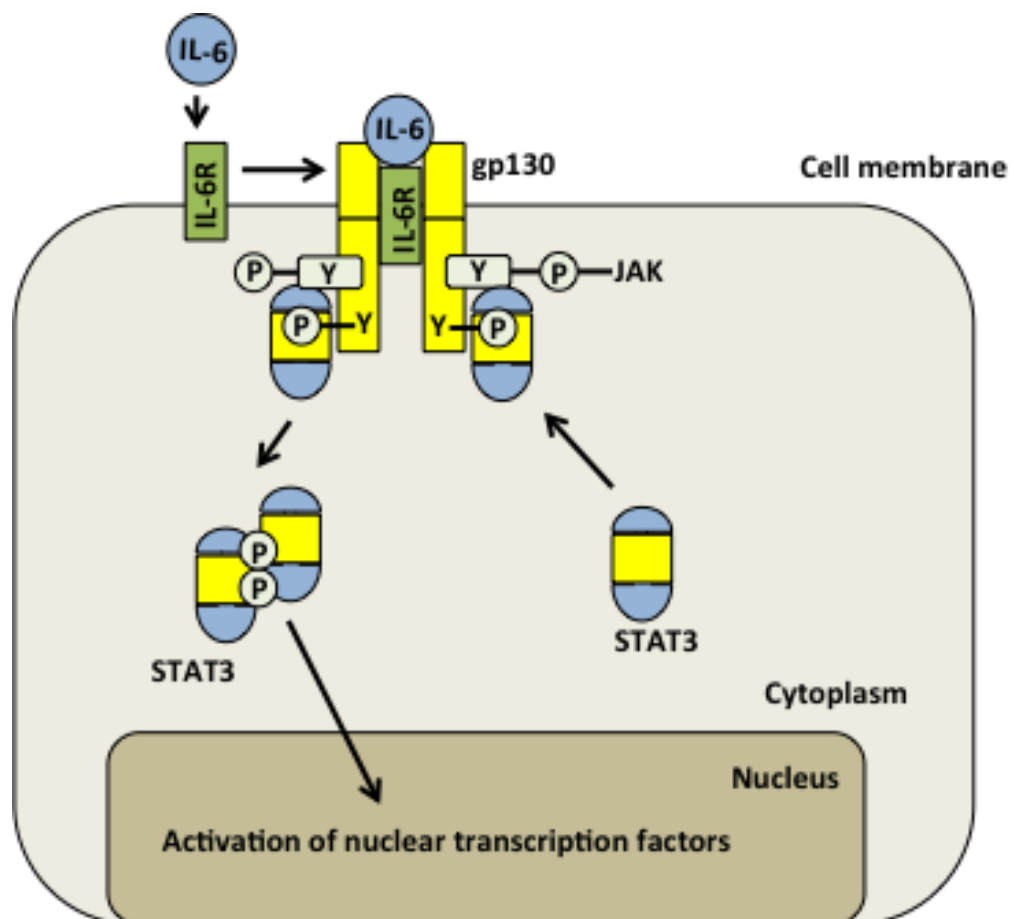


**Figure 5-5: IL-6 signalling via the gp130/JAK/STAT pathway.**

IL-6 dimerises gp 130 molecules and activates the associated JAK, which phosphorylates the gp 130 part inside the cell. This creates docking sites for STAT3, which become phosphorylated and form homo-dimers and translocate to the nucleus to activate gene transcription. Abbreviations used: gp 130 = glycoprotein 130, encircled Y = tyrosine, encircled P = phosphate. (Adapted from (Nishimoto and Kishimoto, 2006)).

A study by Takeda and Akira, found phosphorylated STAT3 accelerated cell cycle progression and promoted cellular differentiation, by regulating expression of Cyclin D1 and c-myc (Takeda and Akira, 2000). Additionally, researchers have found the JAK/STAT signalling pathway to be extremely important in the stem cell and stem cell niche interaction. A study by Leatherman et al., found stem cell adhesion (cadherins) was influenced by the JAK/STAT signalling pathway (Leatherman and DiNardo, 2010). The reduction of STAT92E affected DE-cadherin binding between the stem cells causing the cells to detach and migrate from the niche.

Furthermore, JAK/STAT has been shown to integrate with the BMP and growth hormone signalling pathway, to aid stem cell differentiation (Huang et al., 2012). The growth hormone binds to its receptor which activates the JAK/STAT pathway. Further analysis has shown the growth hormone (GH) is a direct target of the BMP9/SMAD pathway and induces early and late osteogenic marker expression, causing osteogenic differentiation (Lamplot et al., 2013).

The images depicted in Figure 5-3 clearly demonstrate that IL-6 addition to the MSC niche model instigated MSC migration from the spheroid niche into the surrounding collagen. Whereas, the absence of IL-6 allowed the MSCs to remain within the spheroids. These results verify IL-6 as a migratory cue for MSCs within the niche model. Therefore, the secreted IL-6 may have activated MSC recruitment, *via* JAK/STAT3 and MAPK signalling pathways, as highlighted by Rattigan et al (Rattigan et al., 2010).

These studies suggest IL-6 secretion by the scratched monolayers, activated the JAK/STAT3 pathway to initiate MSC migration (see Figure 4-4 and Figure 5-3) by affecting the cadherin adhesion within the niche. The change in cadherin adhesion may initiate MSC detachment and migration from the niche, to the site of injury, *via* the IL-6 concentration gradient created by the damaged cells at the scratched site. Additionally, the JAK/STAT3 pathway may induce MSC osteogenic differentiation by also directly affecting the BMP/GH signalling pathway (see Figure 4-5).

## 5.6 Summary

The study identified IL-6 as a contributory MSC migratory signal, from a panel of five cytokines candidates (IL-1 $\beta$ , IL-2, IL-6, IL-12p70, TNF- $\alpha$ ), in both the fibroblast and osteoblast models. The scratched model showed a significant increase in IL-6 secretion into the surrounding area, compared to the unscratched model. This study highlights the importance of IL-6 secretion within both bone and connective tissue models in the initiation of the wound healing process.

During the initial stage of wound healing, the site of injury induces a pro-inflammatory response, *via* the release of cytokines. These small biologically active molecules, which include IL-6, enable the recruitment of various specialised cells, such as MSCs, to the injury site. This recruitment of cells occurs by a concentration gradient, which triggers wound regeneration and accelerates the rate of wound healing. In addition, IL-6 is a fundamental factor in the regeneration and remodelling of bone. Therefore, the significant increase of IL-6 in the scratched osteoblast model, may indicate IL-6 is being secreted to induce the bone healing process and thus, corroborates previous researchers' findings.

The isolated IL-6 cytokine was clearly shown to stimulate MSC migration out of the niche model into the surrounding area, without the presence of an injury. This finding verified the involvement of IL-6 in the initial stages of wound healing.

# CHAPTER 6

## 6 Concluding remarks: MSC *in vitro* niche model

### 6.1 General Discussion

Mesenchymal stem cell properties, including self-renewal, proliferation and differentiation, are crucial in the regeneration of damaged tissue. This area of study holds great future potential in the field of regenerative medicine. *In vivo* MSCs reside within a niche microenvironment in the bone marrow, which comprises of stem cells, differentiating progenitors, non-stem support cells and ECM. The interactions within this niche environment regulate maintenance, division and fate of the stem cell, throughout the whole lifespan of the organism.

The bone marrow niche is able to integrate signals from soluble and surface-bound factors, cell-cell contacts and mechanical properties of the surrounding environment, to influence stem cell fate. In the absence of such external cues, MSCs remain in an un-stimulated and quiescent state. However, the niche is able to respond rapidly to stimulating factors, resulting in stem cell proliferation and differentiation. Scientific consideration of MSC niche regulation has increased worldwide over the last decade. This interest has led to the exploration of niche interactions, by the recreation of the niche in an *in vitro* environment.

Although the work in this thesis was unable to produce consistently sized MSC spheroids, the project was able to create MSC spheroids, which were all able to exhibit identical functionality; expressing high multipotency markers (STRO-1 and nestin), a reduction in cell cycle progression and an improvement in the wound healing process. The inability to reproduce consistently sized spheroids may affect the reproducibility of research data in future experimentation. However, the use of a precise method to localise the magnetic field may benefit the production of uniform sized spheroids.

The MSC niche is a complex and dynamic system, so the creation of a bio-responsive *in vitro* niche model is extremely ambitious. Building an *in vitro* niche model requires 1) a fundamental understanding of the MSC niche biology and 2) the ability to create the desired 3D structures, which may simulate relevant physicochemical and biological properties. The resultant niche model should

prove to be an improvement on current *in vitro* stem cell culture, thus reducing spontaneous cell differentiation. In addition, the model would provide an opportunity for detailed studies into MSC behaviour and regulation, within their niche environment. The overarching aim of the study would be to improve the retention of MSC multipotency properties, thus extending the time they may be used in clinical trials. Additionally, studying the signalling pathways and cell interactions within the MSC niche may aid artificial differentiation and the regeneration of diseased tissue.

## **6.2 *In vitro* niche models compared to *in vivo* niche behaviours**

Results from *in vitro* niche studies do not always correlate with observations from the *in vivo* niche microenvironment. *In vitro* studies by Reya et al., and Willert et al., demonstrated Notch and Wnt signalling in the hematopoietic system was sufficient to promote HSC self-renewal (Reya et al., 2003, Willert et al., 2003). However, a study of the HSC niche *in vivo*, showed conditional deletion of the Notch receptor and ligand did not affect HSC maintenance and self-renewal (Mancini et al., 2005). Therefore, the *in vivo* results indicate more than one signal may be affecting this behaviour (Morrison and Spradling, 2008). These studies suggest the *in vitro* model was too simplistic in design to allow observation and interplay of the regulatory signals, involved in the *in vivo* HSC maintenance.

Additionally, studies of neural stem cells by Gabay et al., and Stiles et al., showed a disparity between the *in vitro* reactions, compared to the normal *in vivo* neural stem cell niche (Stiles, 2003, Gabay et al., 2003). Canalia et al., concluded *in vitro* neural stem cell niche models should retain the intricate microenvironment, as well as cell-cell interactions, which are observed in the *in vivo* neural stem cell niche (Canalia et al., 2007).

An interesting study, by Jones et al., proposed that MSCs may undergo phenotypic rearrangements, within *in vitro* modelling causing changes in MSC cell surface marker expression, compared to the natural *in vivo* bone marrow environment (Jones et al., 2002). Similarly, Marquez-Curtis and Janowska-Wieczorek stated MSCs, which had been manipulated *ex vivo*, exhibited

phenotypic rearrangements (Marquez-Curtis and Janowska-Wieczorek, 2013). Additionally, Eggenhofer et al., postulated differences in migratory behaviour between cultured and non-cultured MSCs, may be due to *in vitro* induced phenotypic changes of the MSCs (Eggenhofer et al., 2014).

The models described above do not replicate the true *in vivo* niche microenvironment, as highlighted by the outlined discrepancies. Although, there are known inconsistencies between *in vitro* models and native niche behaviours; the MSC spheroid niche model created in this project is an improvement, on previous and current niche models. The spheroid model was a better representation of an *in vivo* MSC niche, through the retention of MSC quiescence and multipotency properties. The model also demonstrated a wound healing response similar to *in vivo* observations.

### **6.3 Applications of the MSC spheroid niche model**

*In vitro* models have major advantages over *in vivo* studies as they allow analysis, without the dilemmas associated with *in vivo* experimentation. At the present time, the complexity of observing intricate behaviours of the niche *in vivo* is restricted by the current limitations of medical techniques. The MSC spheroid model presented by this study allows the isolated investigation of MSC behaviour in a simplistic, yet physiologically relevant model system, which may be adopted for various applications.

#### **6.3.1 MSC regulation within the niche**

The MSC spheroid niche model provides an excellent tool to investigate the mechanisms controlling MSC proliferation and differentiation, within a controlled environment. The model was able to exhibit some cell-cell contacts, which are found in the *in vivo* bone marrow, allowing the study of MSC motility and response to artificial regulation and signalling.

Future studies may include the exploration of asymmetric stem cell division. In the niche stem cells divide into two daughter cells; one which remains in the niche, and when required, one which exits the niche and differentiates. Morrison and Spradling reported on issues, which occurred when directly imaging stem

cell divisions within *in vivo* adult niches, because only a small percentage (2%) of the stem cells are actively dividing at any given time (Morrison and Spradling, 2008). The MSCs within the bone marrow, constitutes only 0.01% of the cell population, which creates difficulties during the study of *in vivo* MSC divisions. Therefore, the ability to analyse MSC division *in vitro*, using a niche model, may allow a major breakthrough in scientific investigation.

Another application of the model may permit in depth investigation of intercellular signals involved in regulating in the niche. Nystul and Spradling have studied the *in vivo* intercellular communication in the *Drosophila* follicle stem cell (FSC) niche (Nystul and Spradling, 2007). However, the authors were unable to elucidate the molecular mechanisms, involved in the prevention of external cells gaining entry to and displacing resident stem cells in the niche. The author's stated it was important to understand these mechanisms, as external cells replacing niche stem cells, may cause the spread of precancerous mutations. Therefore, the MSC niche model may allow improved analysis of these mechanisms, which are involved in niche stem cell displacement, by labelling the MSCs within the niche with either radioactive isotopes or fluorescence tags to detect cell movement. On the other hand, the cells displacing the MSCs may also be labelled with either of the afore mentioned tags to assess cellular movement. The displacement mechanisms may then be investigated using antagonists to achieve a greater understanding of the processes, which protect the niche from cell infiltration.

A further research area of interest would be the assessment and quantification of cell-cell and cell-ECM adhesion mechanisms, within the MSC niche. It would be impossible to quantify specific adhesion distances between cells *in vivo* whereas, *in vitro* modelling would provide a feasible alternative method of analysis. Adhesion within the niche is tightly regulated and integral to MSC differentiation and self-renewal. Understanding of these processes would allow direct manipulation of the MSCs, to promote either self-renewal or differentiation, within the niche. A recent study conducted by Burk et al., utilised a bone marrow niche model, which assessed N-cadherin and SDF-1 $\alpha$  adhesion mechanisms in the HSC niche (Burk et al., 2015). The researchers were able to identify the mechanism of HSC adhesion, *via* N-cadherin homophilic

interactions and SDF-1 $\alpha$  heterophilic interactions. Additionally, Burk et al., was able to measure the distances between the ligand molecules in the HSC niche using reflection interference contrast microscopy. These changes in ligand distances are detected by the HSCs, which in turn may influence HSC ability to either differentiate or self-renew. The niche model in this thesis, may similarly be used to quantify and assess adhesion mechanisms and junctions within the MSC niche. Therefore, controlling these distances may allow direct manipulation of the MSC niche to either maintain stasis of the quiescent MSCs, or initiate MSC migration from the niche and promote cell differentiation.

### **6.3.2 Creation of a MSC bank**

Mesenchymal stromal cells are the most widely used cell type in cell therapy clinical trials at this time. Current trends indicate MSC use in clinical applications will continue to rapidly increase. However, clinical applications typically require the use of large numbers of MSCs, ideally in an off-the-shelf format (Thirumala et al., 2013). This requirement necessitates extensive MSC expansion *ex vivo* and storage, which promotes MSC multipotency (Carmelo et al., 2015, dos Santos et al., 2014). At present, MSCs are cryopreserved and banked however, this treatment leads to cell shock and loss of viability on cell recovery, resulting in reduced numbers of functional cells. Existing *in vitro* MSC culturing techniques are only able to maintain the stem cells for short periods of time, before they spontaneously differentiate. The work described in this project, prepares the foundation for the production of a viable and multipotent population of MSCs, which may be used to create a clinical bank of quiescent stem cells. Such an MSC bank would allow the long-term storage of undifferentiated MSCs, which may limit the need for invasive extractions from human sources.

### **6.3.3 Modelling disease states**

#### **6.3.3.1 Osteoporosis**

Interactions between adipose and bone tissue is affected by the stimulation or deactivation of transcription factors, signalling molecules and genes. The interruption of these interactions is known to be involved in various bone disorders including osteoporosis. Osteoporosis is a disease characterised by

systemic bone loss and destruction of the bone microstructure, causing fragility of the bone mass (Savopoulos et al., 2011). People with osteoporosis have an increased risk of low-traumatic fractures (Muschitz et al., 2015). Studies by Burkhardt et al., and Meunier et al., found osteoporotic patients showed an increased incidence of adipose tissue, within their bone marrow (Burkhardt et al., 1987, Meunier et al., 1971). Osteoporosis is linked to a shift in MSC differentiation from osteoblasts towards adipocyte formation in the bone marrow. This shift is caused by the activation of the proliferative activated receptor (PPAR)  $\gamma$ 2 pathway, rather than the RUNX-2 pathway, in MSC differentiation (Rosen and Buxsein, 2006). Correction of this pathway disorder, may help rectify this imbalance, thus redirecting MSC differentiation towards osteogenesis. Isolated studies utilising the MSC niche model, for example to block adipogenic differentiation of the MSCs and encourage osteogenesis, would provide useful information in the research of this topical area.

### **6.3.3.2 Osteoarthritis**

Osteoarthritis occurs when the chondrocytes, within the synovial joint (cartilage, synovium and underlying bone) respond to injury leading to the degradation of cartilage within the joint. There are two phases in the osteoarthritis process: 1) the biosynthetic phase when the chondrocytes endeavour to repair damaged ECM and 2) degradative phase, when the MMPs, released by the chondrocytes, break down the matrix and inhibit matrix synthesis (Sandell and Aigner, 2001). This dual process leads to accelerated cartilage erosion, causing chronic pain in the joint.

Kraus et al., suggests the identification of biomarkers using 'omics technologies (genomics, proteomics, transcriptomics and metabolomics), may be used to detect early onset molecular abnormalities in osteoarthritis (Kraus et al., 2015). In normal physiology, chondrocytes maintain a balance between synthesis and degradation of MMPs. However, when the joint is subjected to abnormal loading, there is shift in this balance, leading to increased MMP levels and in turn increased degeneration of matrix. The MSC niche model may benefit such studies. MSC migration from the spheroids towards the damaged area, in this case scratched chondrocytes, may be monitored and assessed, to determine whether the cells may differentiate into chondrocytes. These migratory MSCs

will restore the balance of MMP synthesis and degradation, and therefore prevent further destruction of the matrix. Knowledge gained from the *in vitro* model experimentation may be transposed to *in vivo*, which both assists an early diagnosis (*via* biomarkers) and treatment to prevent osteoarthritis.

#### **6.3.4 Scar healing**

Following injury, the body initiates the wound healing response, to close the wound as rapidly as possible. The initial healing stage involves the pro-inflammatory response, when cytokines are released from neutrophils (Maxson et al., 2012). This process causes fibroblasts to migrate towards the wound site and leads to excessive secretion of collagen, to enable closure of the wound (Huang et al., 2015). This collagen deposition leads to a loss of normal epithelial formation, resulting in the formation of fibrous scar tissue. Tissue fibrosis restricts natural movement, as well as contractures of the joint (Fourie, 2012). Furthermore, the fibrous scar tissue lacks the tensile strength or structure of normal skin, so the scar is vulnerable to further injury.

The MSC niche model may be used to investigate MSC signalling mechanisms, which encourage proliferation of local resident epithelial cells in the prevention of fibroblastic granulation of the scar tissue. The signalling pathways may be transposed to any *in vivo* injury, to allow regrowth of normal epithelial tissue and thus, reduce the inherent movement restrictions associated with scar tissue. This newly created epithelial tissue will possess normal function and reduce the need for surgical interventions in the future.

#### **6.3.5 Aging of the MSC niche**

Problems associated with lack of efficient tissue repair in the aging population, have a major impact in the cost of medical care. Therefore, investigations into the maintenance of MSC 'stemness', through the analysis of intrinsic and extrinsic factors of the niche are essential to the understanding of the niche functions, in relation to an individual's aging process (Silva and Conboy, 2008). A study on rats conducted by Carlson and Faulkner, showed the age of an individual rat was the sole factor in the success of muscle graft transplantation (Carlson and Faulkner, 1989). Young rats were able to accept both old and young

transplanted muscle grafts. However, old rats were unable to accept either old or young transplanted muscles grafts (Carlson and Faulkner, 1989). Therefore, the identification of age-specific factors from a range of different aged niches, may determine the underlying mechanisms, involved in the process of stem cell deterioration, over time (Silva and Conboy, 2008).

The MSC niche model may be used to study the mechanisms and signalling pathways, involved in the aging process of the MSCs. This information may have considerable impact on regenerating damaged tissue in the aging population. Knowledge gained from this research may benefit post-operative elderly patients' recovery, by accelerating the healing processes.

### **6.3.6 Pharmacology Assessments**

The pharmaceutical industry extensively uses a process known as high throughput screening (HTS), to rapidly identify potential chemical targets or leads for the development of new drugs for the future. The HTS process has been characterised by its high efficiency, rapidness, simplicity, and low cost, which is able to screen >100 000 samples per day (Mayr and Bojanic, 2009). Recently, the HTS process has been applied to creating cell culture platforms for the use in the study of stem cell biology. There has been a vast amount of interest in the use of this process to reduce reagent consumption, increase throughput, and shorten analysis times (Maerkl, 2009). Kobel and Lutolf suggest there are three applications areas in the use of HTS to study stem cell niches, which include; i) creating platforms to screen various different niche factors and their combinations; ii) creating *in vitro* niche models to assess key aspects of natural niches; and iii) in depth single stem cell analysis (Kobel and Lutolf, 2010). However, there has been limited work into the creation of HT tests, involving realistic *in vitro* stem cell niche models (Kitambi and Chandrasekar, 2011). There have been difficulties in creating cellular- or subcellular-scale approaches, to simplify this spatially complex system and to study structural aspects of the niche.

The MSC spheroid niche model may hold wide pharmacological implications. It shows promise of a human cell-based model platform, which acts as a high throughput, cost effective and reproducible assay, as well as mimicking the *in*

*vivo* niche microenvironment. Therefore, the model may be used to rapidly screen a multitude of drugs, for disease states including those highlighted above (as a 'disease-in-a-dish' models), as well as allowing toxicity testing thus, enhancing the scope for novel drug screening.

## 6.4 Conclusion

The research encompassed in this thesis, primarily described the developmental stages of creating a physiologically relevant MSC *in vitro* niche model (Chapter 3). This work has demonstrated the incorporation of mNPs within MSCs, enabled the creation of multicellular spheroids, in the presence of an external magnetic field. The maintenance of cell contacts, MSC behaviour and response, mimicked an *in vivo* MSC niche environment through the high expression of STRO-1 and nestin, as well as exhibiting multipotency. The MSCs remained in a dormant, quiescent state over time within the spheroid culture, compared to traditional 2D culturing techniques. Increasing the complexity of the model using Type I collagen introduced cell-ECM contacts, and enhanced the *in vitro* model's representation of a natural *in vivo* niche. The 3D collagen gels created an environment akin to *in vivo* bone marrow, demonstrating similar stiffness and ECM properties.

Chapters 4 and 5 assessed the bio-responsive properties of the MSC spheroid model, to determine whether the MSCs, within the spheroids, were capable of detection, homing and migration towards a wound site, with consequent integration and differentiation. Exposure to a scratch-wounded monolayer, induced the MSCs to directionally migrate towards to the scratch and become incorporated in the wound area. Additionally, the presence of the MSC spheroid accelerated the wound-healing rate. However, the main finding of the study, was the trans-differentiation of the spheroid MSCs into the local resident cell type. MSCs expressing osteogenic markers, identified IL-6 as a potential MSC migratory signal in the wound healing process.

This newly created *in vitro* MSC niche model exhibited native *in vivo* behaviours and responses in an environment, similar to natural bone marrow milieu. These findings indicate this model may be highly valuable in the exploration and *in vitro* study of intricate MSC niche processes.

### 6.4.1 Recommendation for Future work

The research performed during the course of this project, has raised unexplored areas of interest and it may be advantageous to investigate further ways of improving the *in vitro* model. Particular areas of interest requiring further study are described and summarised below.

- Investigations into additional bio-responsive behaviours of the niche model.
- Assessment of MSC signalling pathways involved in MSC migration and niche homeostasis.
- Improve the niche model through the incorporation of support cells i.e. pericytes, osteocytes and HSCs.
- Cell cycle investigation of migrating MSCs from the niche to a wounded site.
- Increase complexity of the wound healing assay by the introduction of neutrophils into the niche model.
- Identify the presence of additional cytokines and chemokines released by wounds.
- Assess the level of hypoxia within the MSC spheroids.
- Improve localisation of the magnetic field to produce uniform sized spheroids.

## References:

- AARONSON, D. S. & HORVATH, C. M. 2002. A road map for those who don't know JAK-STAT. *Science*, 296, 1653-5.
- ABUMAREE, M. H., AL JUMAH, M. A., KALIONIS, B., JAWDAT, D., AL KHALDI, A., ALTALABANI, A. A. & KNAWY, B. A. 2013. Phenotypic and Functional Characterization of Mesenchymal Stem Cells from Chorionic Villi of Human Term Placenta. *Stem Cell Reviews and Reports*, 9, 16-31.
- AGGARWAL, S. & PITTENGER, M. F. 2005. Human mesenchymal stem cells modulate allogeneic immune cell responses. *Blood*, 105, 1815-22.
- AKIRA, S. & KISHIMOTO, T. 1992. IL-6 and NF-IL6 in acute-phase response and viral infection. *Immunol Rev*, 127, 25-50.
- ALBANESE, A., TSOI, K. M. & CHAN, W. C. W. 2012. Simultaneous Quantification of Cells and Nanomaterials by Inductive-Coupled Plasma Techniques. *Journal of Laboratory Automation*.
- ALIMPERTI, S., LEI, P., WEN, Y., TIAN, J., CAMPBELL, A. M. & ANDREADIS, S. T. 2014. Serum-free spheroid suspension culture maintains mesenchymal stem cell proliferation and differentiation potential. *Biotechnology Progress*, 30, 974-983.
- ALVES, L. B., MARIGUELA, V. C., GRISI, M. F. D. M., DE SOUZA, S. L. S., NOVAES, A. B., TABA, M., DE OLIVEIRA, P. T. & PALIOTO, D. B. 2015. Expression of osteoblastic phenotype in periodontal ligament fibroblasts cultured in three-dimensional collagen gel. *Journal of Applied Oral Science*, 23, 206-214.
- ANTHONY, D. F. & SHIELS, P. G. 2013. Exploiting paracrine mechanisms of tissue regeneration to repair damaged organs. *Transplantation Research*, 2, 10-10.
- ARBAB, A. S., WILSON, L. B., ASHARI, P., JORDAN, E. K., LEWIS, B. K. & FRANK, J. A. 2005. A model of lysosomal metabolism of dextran coated superparamagnetic iron oxide (SPIO) nanoparticles: implications for cellular magnetic resonance imaging. *NMR in Biomedicine*, 18, 383-389.
- BAER, P. C., GRIESCHE, N., LUTTMANN, W., SCHUBERT, R., LUTTMANN, A. & GEIGER, H. 2010. Human adipose-derived mesenchymal stem cells in vitro: evaluation of an optimal expansion medium preserving stemness. *Cytotherapy*, 12, 96-106.
- BARANIAK, P. R., COOKE, M. T., SAEED, R., KINNEY, M. A., FRIDLEY, K. M. & MCDEVITT, T. C. 2012. Stiffening of human mesenchymal stem cell spheroid microenvironments induced by incorporation of gelatin microparticles. *Journal of the Mechanical Behavior of Biomedical Materials*, 11, 63-71.
- BARANIAK, P. R. & MCDEVITT, T. C. 2012. Scaffold-free culture of mesenchymal stem cell spheroids in suspension preserves multilineage potential. *Cell and Tissue Research*, 347, 701-11.
- BARDIN, A. J. & AMON, A. 2001. MEN and SIN: what's the difference? *Nat Rev Mol Cell Biol*, 2, 815-826.
- BARKAN, D., GREEN, J. E. & CHAMBERS, A. F. 2010. Extracellular Matrix: A Gatekeeper in the Transition from Dormancy to Metastatic Growth. *European journal of cancer (Oxford, England : 1990)*, 46, 1181-1188.
- BARKER, R. A. & DE BEAUFORT, I. 2013. Scientific and ethical issues related to stem cell research and interventions in neurodegenerative disorders of the brain. *Progress in Neurobiology*, 110, 63-73.

- BARTOSH, T. J., YLÖSTALO, J. H., MOHAMMADIPOOR, A., BAZHANOV, N., COBLE, K., CLAYPOOL, K., LEE, R. H., CHOI, H. & PROCKOP, D. J. 2010. Aggregation of human mesenchymal stromal cells (MSCs) into 3D spheroids enhances their antiinflammatory properties. *Proceedings of the National Academy of Sciences*, 107, 13724-13729.
- BECKER, A. J., MCCULLOCH, E. A. & TILL, J. E. 1963. Cytological Demonstration of the Clonal Nature of Spleen Colonies Derived from Transplanted Mouse Marrow Cells. *Nature*, 197, 452-454.
- BENMERAH, A. & LAMAZE, C. 2007. Clathrin-coated pits: vive la difference? *Traffic*, 8, 970-82.
- BENVENUTO, F., FERRARI, S., GERDONI, E., GUALANDI, F., FRASSONI, F., PISTOIA, V., MANCARDI, G. & UCCELLI, A. 2007. Human Mesenchymal Stem Cells Promote Survival of T Cells in a Quiescent State. *STEM CELLS*, 25, 1753-1760.
- BERRY, C. C. 2009. Progress in functionalization of magnetic nanoparticles for applications in biomedicine. *Journal of Physics D: Applied Physics*, 42, 224003.
- BERTOLI, C., SKOTHEIM, J. M. & DE BRUIN, R. A. M. 2013. Control of cell cycle transcription during G1 and S phases. *Nat Rev Mol Cell Biol*, 14, 518-528.
- BHANG, S. H., CHO, S. W., LA, W. G., LEE, T. J., YANG, H. S., SUN, A. Y., BAEK, S. H., RHIE, J. W. & KIM, B. S. 2011. Angiogenesis in ischemic tissue produced by spheroid grafting of human adipose-derived stromal cells. *Biomaterials*, 32, 2734-47.
- BIANCHI, M. E. 2007. DAMPs, PAMPs and alarmins: all we need to know about danger. *Journal of Leukocyte Biology*, 81, 1-5.
- BIANCO, P., CAO, X., FRENETTE, P. S., MAO, J. J., ROBEY, P. G., SIMMONS, P. J. & WANG, C.-Y. 2013. The meaning, the sense and the significance: translating the science of mesenchymal stem cells into medicine. *Nat Med*, 19, 35-42.
- BLAGOSKLONNY, M. V. & PARDEE, A. B. 2002. The Restriction Point of the Cell Cycle. *Cell Cycle*, 1, 102-109.
- BOIDO, M., GARBOSSA, D., FONTANELLA, M., DUCATI, A. & VERCELLI, A. 2014. Mesenchymal Stem Cell Transplantation Reduces Glial Cyst and Improves Functional Outcome After Spinal Cord Compression. *World Neurosurgery*, 81, 183-190.
- BOST, K. L., RAMP, W. K., NICHOLSON, N. C., BENTO, J. L., MARRIOTT, I. & HUDSON, M. C. 1999. Staphylococcus aureus infection of mouse or human osteoblasts induces high levels of interleukin-6 and interleukin-12 production. *J Infect Dis*, 180, 1912-20.
- BRATT-LEAL, A. M., CARPENEDO, R. L., UNGRIN, M., ZANDSTRA, P. W. & MCDEVITT, T. C. 2011. Incorporation of Biomaterials in Multicellular Aggregates Modulates Pluripotent Stem Cell Differentiation. *Biomaterials*, 32, 48-56.
- BRESLIN, S. & O'DRISCOLL, L. 2013. Three-dimensional cell culture: the missing link in drug discovery. *Drug Discovery Today*, 18, 240-249.
- BRYCE, N. S., ZHANG, J. Z., WHAN, R. M., YAMAMOTO, N. & HAMBLEY, T. W. 2009. Accumulation of an anthraquinone and its platinum complexes in cancer cell spheroids: the effect of charge on drug distribution in solid tumour models. *Chem Commun (Camb)*, 2673-5.
- BUITENHUIS, M. 2011. The role of PI3K/protein kinase B (PKB/c-akt) in migration and homing of hematopoietic stem and progenitor cells. *Curr Opin Hematol*, 18, 226-30.

- BURK, A. S., MONZEL, C., YOSHIKAWA, H. Y., WUCHTER, P., SAFFRICH, R., ECKSTEIN, V., TANAKA, M. & HO, A. D. 2015. Quantifying Adhesion Mechanisms and Dynamics of Human Hematopoietic Stem and Progenitor Cells. *Sci. Rep.*, 5.
- BURKHARDT, R., KETTNER, G., BOHM, W., SCHMIDMEIER, M., SCHLAG, R., FRISCH, B., MALLMANN, B., EISENMENGER, W. & GILG, T. 1987. Changes in trabecular bone, hematopoiesis and bone marrow vessels in aplastic anemia, primary osteoporosis, and old age: a comparative histomorphometric study. *Bone*, 8, 157-64.
- CAMPBELL, A. & WICHA, M. 1988. Extracellular matrix and the hematopoietic microenvironment. *Journal of Laboratory and Clinical Medicine*, 112, 140.
- CANALIA, N., ARMENTANO, M., PONTI, G. & BONFANTI, L. 2007. In vivo and in vitro Approaches for the Study of Adult Neurogenesis in Light, Confocal, and Electron Microscopy. *Modern Research and Educational Topics in Microscopy*, 1, 100-110.
- CAPLAN, A. I. 1991. Mesenchymal stem cells. *Journal of Orthopaedic Research*, 9, 641-650.
- CAPLAN, A. I. & BRUDER, S. P. 2001. Mesenchymal stem cells: building blocks for molecular medicine in the 21st century. *Trends Mol Med*, 7, 259-64.
- CARLSON, B. M. & FAULKNER, J. A. 1989. Muscle transplantation between young and old rats: age of host determines recovery. *Am J Physiol*, 256, C1262-6.
- CARMELO, J., FERNANDES-PLATZGUMMER, A., CABRAL, J. S. & DA SILVA, C. 2015. Scalable Ex Vivo Expansion of Human Mesenchymal Stem/Stromal Cells in Microcarrier-Based Stirred Culture Systems. In: TURKSEN, K. (ed.) *Stem Cells and Good Manufacturing Practices*. Springer New York.
- CASADO-DÍAZ, A., PÉREZ, G. D. & QUESADA-GÓMEZ, J. M. 2011. Stem Cell Research and Molecular Markers in Medicine. In: MOO-YOUNG, M. (ed.) *Comprehensive Biotechnology*. Second Edition ed. Burlington: Academic Press.
- CHAMBERLAIN, G., FOX, J., ASHTON, B. & MIDDLETON, J. 2007. Concise Review: Mesenchymal Stem Cells: Their Phenotype, Differentiation Capacity, Immunological Features, and Potential for Homing. *STEM CELLS*, 25, 2739-2749.
- CHANG, Y., LEE, G. H., KIM, T. J. & CHAE, K. S. 2013. Toxicity of magnetic resonance imaging agents: small molecule and nanoparticle. *Curr Top Med Chem*, 13, 434-45.
- CHAROEN, K. M., FALLICA, B., COLSON, Y. L., ZAMAN, M. H. & GRINSTAFF, M. W. 2014. Embedded multicellular spheroids as a biomimetic 3D cancer model for evaluating drug and drug-device combinations. *Biomaterials*, 35, 2264-2271.
- CHARRAS, G. & SAHAI, E. 2014. Physical influences of the extracellular environment on cell migration. *Nat Rev Mol Cell Biol*, 15, 813-824.
- CHEMICELL. 2015. *nano-screenMAG* [Online]. Available: <http://www.chemicell.com/products/magneticfluorescent/index.html> [Accessed 02/07/2015].
- CHEN, F.-M., WU, L.-A., ZHANG, M., ZHANG, R. & SUN, H.-H. 2011. Homing of endogenous stem/progenitor cells for in situ tissue regeneration: Promises, strategies, and translational perspectives. *Biomaterials*, 32, 3189-3209.
- CHEN, G. D., ALBERTS, C. J., RODRIGUEZ, W. & TONER, M. 2009a. Concentration and Purification of Human Immunodeficiency Virus Type 1 Virions by

- Microfluidic Separation of Superparamagnetic Nanoparticles. *Analytical Chemistry*, 82, 723-728.
- CHEN, L., TREDGET, E. E., WU, P. Y. G. & WU, Y. 2008. Paracrine Factors of Mesenchymal Stem Cells Recruit Macrophages and Endothelial Lineage Cells and Enhance Wound Healing. *PLoS ONE*, 3, e1886.
- CHEN, T., ZHOU, Y. & TAN, W.-S. 2009b. Effects of low temperature and lactate on osteogenic differentiation of human amniotic mesenchymal stem cells. *Biotechnology and Bioprocess Engineering*, 14, 708-715.
- CHEN, Y., BAI, B., ZHANG, S., YE, J., CHEN, Y. & ZENG, Y. 2014. Effects of Parathyroid Hormone on Calcium Ions in Rat Bone Marrow Mesenchymal Stem Cells. *BioMed Research International*, 2014, 6.
- CHEN, Y., GAO, D., LIU, H., LIN, S. & JIANG, Y. 2015. Drug cytotoxicity and signaling pathway analysis with three-dimensional tumor spheroids in a microwell-based microfluidic chip for drug screening. *Analytica Chimica Acta*, 898, 85-92.
- CHENG, N.-C., WANG, S. & YOUNG, T.-H. 2012. The influence of spheroid formation of human adipose-derived stem cells on chitosan films on stemness and differentiation capabilities. *Biomaterials*, 33, 1748-1758.
- CHEUNG, T. H. & RANDO, T. A. 2013. Molecular regulation of stem cell quiescence. *Nat Rev Mol Cell Biol*, 14, 329-340.
- CHI, Q., YIN, T., GREGERSEN, H., DENG, X., FAN, Y., ZHAO, J., LIAO, D. & WANG, G. 2014. Rear actomyosin contractility-driven directional cell migration in three-dimensional matrices: a mechano-chemical coupling mechanism. *Journal of the Royal Society Interface*, 11, 20131072.
- CHILD, H. W., DEL PINO, P. A., DE LA FUENTE, J. M., HURSTHOUSE, A. S., STIRLING, D., MULLEN, M., MCPHEE, G. M., NIXON, C., JAYAWARNA, V. & BERRY, C. C. 2011. Working Together: The Combined Application of a Magnetic Field and Penetratin for the Delivery of Magnetic Nanoparticles to Cells in 3D. *ACS Nano*, 5, 7910-7919.
- CHITHRANI, B. D. & CHAN, W. C. W. 2007. Elucidating the Mechanism of Cellular Uptake and Removal of Protein-Coated Gold Nanoparticles of Different Sizes and Shapes. *Nano Letters*, 7, 1542-1550.
- CHITHRANI, B. D., GHAZANI, A. A. & CHAN, W. C. W. 2006. Determining the Size and Shape Dependence of Gold Nanoparticle Uptake into Mammalian Cells. *Nano Letters*, 6, 662-668.
- CHO, P. S., MESSINA, D. J., HIRSH, E. L., CHI, N., GOLDMAN, S. N., LO, D. P., HARRIS, I. R., POPMA, S. H., SACHS, D. H. & HUANG, C. A. 2008. Immunogenicity of umbilical cord tissue-derived cells. *Blood*, 111, 430-438.
- COOK, H., DAVIES, K. J., HARDING, K. G. & THOMAS, D. W. 2000. Defective extracellular matrix reorganization by chronic wound fibroblasts is associated with alterations in TIMP-1, TIMP-2, and MMP-2 activity. *J Invest Dermatol*, 115, 225-33.
- CORCIONE, A., BENVENUTO, F., FERRETTI, E., GIUNTI, D., CAPPIELLO, V., CAZZANTI, F., RISSO, M., GUALANDI, F., MANCARDI, G. L., PISTOIA, V. & UCCELLI, A. 2006. Human mesenchymal stem cells modulate B-cell functions. *Blood*, 107, 367-72.
- CURCIO, E., SALERNO, S., BARBIERI, G., DE BARTOLO, L., DRIOLI, E. & BADER, A. 2007. Mass transfer and metabolic reactions in hepatocyte spheroids cultured in rotating wall gas-permeable membrane system. *Biomaterials*, 28, 5487-5497.

- DA SILVA MEIRELLES, L., FONTES, A. M., COVAS, D. T. & CAPLAN, A. I. 2009. Mechanisms involved in the therapeutic properties of mesenchymal stem cells. *Cytokine Growth Factor Rev*, 20, 419-27.
- DALBY, M. J., GADEGAARD, N., TARE, R., ANDAR, A., RIEHLE, M. O., HERZYK, P., WILKINSON, C. D. W. & OREFFO, R. O. C. 2007. The control of human mesenchymal cell differentiation using nanoscale symmetry and disorder. *Nat Mater*, 6, 997-1003.
- DAMDIMOPOULOU, P., RODIN, S., STENFELT, S., ANTONSSON, L., TRYGGVASON, K. & HOVATTA, O. 2015. Human embryonic stem cells. *Best Practice & Research Clinical Obstetrics & Gynaecology*, In Press.
- DAZZI, F. & KRAMPERA, M. 2011. Mesenchymal stem cells and autoimmune diseases. *Best Practice & Research Clinical Haematology*, 24, 49-57.
- DE BANK, P. A., HOU, Q., WARNER, R. M., WOOD, I. V., ALI, B. E., MACNEIL, S., KENDALL, D. A., KELLAM, B., SHAKESHEFF, K. M. & BUTTERY, L. D. 2007. Accelerated formation of multicellular 3-D structures by cell-to-cell cross-linking. *Biotechnol Bioeng*, 97, 1617-25.
- DEJARDIN, T., DE LA FUENTE, J., DEL PINO, P., FURLANI, E. P., MULLIN, M., SMITH, C. A. & BERRY, C. C. 2011. Influence of both a static magnetic field and penetratin on magnetic nanoparticle delivery into fibroblasts. *Nanomedicine*, 6, 1719-1731.
- DELLATORE, S. M., GARCIA, A. S. & MILLER, W. M. 2008. Mimicking stem cell niches to increase stem cell expansion. *Current Opinion in Biotechnology*, 19, 534-540.
- DEMBIC, Z. 2015. Chapter 1 - Introduction—Common Features About Cytokines. In: DEMBIC, Z. (ed.) *The Cytokines of the Immune System*. Amsterdam: Academic Press.
- DEUTSCH, M. J., SCHRIEVER, S. C., ROSCHER, A. A. & ENSENAUER, R. 2014. Digital image analysis approach for lipid droplet size quantitation of Oil Red O-stained cultured cells. *Analytical Biochemistry*, 445, 87-89.
- DINARELLO, C. A. 2007. Historical Review of Cytokines. *European journal of immunology*, 37, S34-S45.
- DOMINICI, M., LE BLANC, K., MUELLER, I., SLAPER-CORTENBACH, I., MARINI, F., KRAUSE, D., DEANS, R., KEATING, A., PROCKOP, D. & HORWITZ, E. 2006. Minimal criteria for defining multipotent mesenchymal stromal cells. The International Society for Cellular Therapy position statement. *Cytotherapy*, 8, 315-7.
- DONG, J.-D., GU, Y.-Q., LI, C.-M., WANG, C.-R., FENG, Z.-G., QIU, R.-X., CHEN, B., LI, J.-X., ZHANG, S.-W., WANG, Z.-G. & ZHANG, J. 2009. Response of mesenchymal stem cells to shear stress in tissue-engineered vascular grafts. *Acta Pharmacologica Sinica*, 30, 530-536.
- DOS SANTOS, F., CAMPBELL, A., FERNANDES-PLATZGUMMER, A., ANDRADE, P. Z., GIMBLE, J. M., WEN, Y., BOUCHER, S., VEMURI, M. C., DA SILVA, C. L. & CABRAL, J. M. S. 2014. A xenogeneic-free bioreactor system for the clinical-scale expansion of human mesenchymal stem/stromal cells. *Biotechnology and Bioengineering*, 111, 1116-1127.
- DULIC, V., LEES, E. & REED, S. 1992. Association of human cyclin-E with a periodic G(1)-S phase protein kinase. *Science*, 257, 1958-1961.
- DUPONT, S., MORSUT, L., ARAGONA, M., ENZO, E., GIULITTI, S., CORDENONSI, M., ZANCONATO, F., LE DIGABEL, J., FORCATO, M., BICCIATO, S.,

- ELVASSORE, N. & PICCOLO, S. 2011. Role of YAP/TAZ in mechanotransduction. *Nature*, 474, 179-183.
- EDMONDSON, R., BROGLIE, J. J., ADCOCK, A. F. & YANG, L. 2014. Three-Dimensional Cell Culture Systems and Their Applications in Drug Discovery and Cell-Based Biosensors. *Assay and Drug Development Technologies*, 12, 207-218.
- EGGENHOFER, E., LUK, F., DAHLKE, M. H. & HOOGDUIJN, M. J. 2014. The Life and Fate of Mesenchymal Stem Cells. *Frontiers in Immunology*, 5.
- EHNINGER, A. & TRUMPP, A. 2011. The bone marrow stem cell niche grows up: mesenchymal stem cells and macrophages move in. *The Journal of Experimental Medicine*, 208, 421-428.
- ELIASSON, P. & JONSSON, J. I. 2010. The hematopoietic stem cell niche: low in oxygen but a nice place to be. *J Cell Physiol*, 222, 17-22.
- EMA, H. & SUDA, T. 2012. Two anatomically distinct niches regulate stem cell activity. *Blood*, 120, 2174-2181.
- ENGLER, A. J., SEN, S., SWEENEY, H. L. & DISCHER, D. E. 2006. Matrix Elasticity Directs Stem Cell Lineage Specification. *Cell*, 126, 677-689.
- ENGLISH, K. & WOOD, K. J. 2011. Immunogenicity of embryonic stem cell-derived progenitors after transplantation. *Curr Opin Organ Transplant*, 16, 90-5.
- ENNIS, W. J., SUI, A. & BARTHOLOMEW, A. 2013. Stem Cells and Healing: Impact on Inflammation. *Adv Wound Care (New Rochelle)*, 2, 369-378.
- FARRELL, E., WIELOPOLSKI, P., PAVLJASEVIC, P., VAN TIEL, S., JAHR, H., VERHAAR, J., WEINANS, H., KRESTIN, G., O'BRIEN, F. J., VAN OSCH, G. & BERNSEN, M. 2008. Effects of iron oxide incorporation for long term cell tracking on MSC differentiation in vitro and in vivo. *Biochemical and Biophysical Research Communications*, 369, 1076-1081.
- FEDARKO, N. S., D'AVIS, P., FRAZIER, C. R., BURRILL, M. J., FERGUSON, V., TAYBACK, M., SPONSELLER, P. D. & SHAPIRO, J. R. 1995. Cell proliferation of human fibroblasts and osteoblasts in osteogenesis imperfecta: influence of age. *J Bone Miner Res*, 10, 1705-12.
- FENNEMA, E., RIVRON, N., ROUWKEMA, J., VAN BLITTERSWIJK, C. & DE BOER, J. 2013. Spheroid culture as a tool for creating 3D complex tissues. *Trends in Biotechnology*, 31, 108-115.
- FERNANDES, T. G., DIOGO, M. M. & CABRAL, J. M. S. 2013. 2 - Stem cell culture: mimicking the stem cell niche in vitro. In: FERNANDES, T. G., DIOGO, M. M. & CABRAL, J. M. S. (eds.) *Stem Cell Bioprocessing*. Woodhead Publishing.
- FISCHER, J., KOLK, A., WOLFART, S., PAUTKE, C., WARNKE, P. H., PLANK, C. & SMEETS, R. 2011. Future of local bone regeneration - Protein versus gene therapy. *Journal of Cranio-Maxillofacial Surgery*, 39, 54-64.
- FISCHER, U. M., HARTING, M. T., JIMENEZ, F., MONZON-POSADAS, W. O., XUE, H., SAVITZ, S. I., LAINE, G. A. & COX JR., C. S. 2009. Pulmonary Passage is a Major Obstacle for Intravenous Stem Cell Delivery: The Pulmonary First-Pass Effect. *Stem Cells and Development*, 18, 683-692.
- FOURIE, W. J. 2012. 7.17 - Surgery and scarring. In: HUIJING, R. S. W. F. C. A. (ed.) *Fascia: The Tensional Network of the Human Body*. Oxford: Churchill Livingstone.
- FRIEDENSTEIN, A. 1989. Stromal-Hematopoietic Interrelationships: Maximov's Ideas and Modern Models. In: NETH, R., GALLO, R., GREAVES, M., GAEDICKE, G., GOHLA, S., MANNWEILER, K. & RITTER, J. (eds.) *Modern Trends in Human Leukemia VIII*. Springer Berlin Heidelberg.

- FRIEDENSTEIN, A. J., CHAILAKHYAN, R. K., LATSINIK, N. V., PANASYUK, A. F. & KEILISS-BOROK, I. V. 1974. STROMAL CELLS RESPONSIBLE FOR TRANSFERRING THE MICROENVIRONMENT OF THE HEMOPOIETIC TISSUES: Cloning In Vitro and Retransplantation In Vivo. *Transplantation*, 17, 331-340.
- GABAY, L., LOWELL, S., RUBIN, L. L. & ANDERSON, D. J. 2003. Deregulation of dorsoventral patterning by FGF confers trilineage differentiation capacity on CNS stem cells in vitro. *Neuron*, 40, 485-99.
- GATENBY, R. A., SMALLBONE, K., MAINI, P. K., ROSE, F., AVERILL, J., NAGLE, R. B., WORRALL, L. & GILLIES, R. J. 2007. Cellular adaptations to hypoxia and acidosis during somatic evolution of breast cancer. *Br J Cancer*, 97, 646-653.
- GATTAZZO, F., URUIOLO, A. & BONALDO, P. 2014. Extracellular matrix: A dynamic microenvironment for stem cell niche. *Biochimica et Biophysica Acta (BBA) - General Subjects*, 1840, 2506-2519.
- GEBLER, A., ZABEL, O. & SELIGER, B. The immunomodulatory capacity of mesenchymal stem cells. *Trends in Molecular Medicine*, 18, 128-134.
- GERDONI, E., GALLO, B., CASAZZA, S., MUSIO, S., BONANNI, I., PEDEMONTE, E., MANTEGAZZA, R., FRASSONI, F., MANCARDI, G., PEDOTTI, R. & UCCELLI, A. 2007. Mesenchymal stem cells effectively modulate pathogenic immune response in experimental autoimmune encephalomyelitis. *Ann Neurol*, 61, 219-27.
- GERLACH, J. C., LIN, Y. C., BRAYFIELD, C. A., MINTEER, D. M., LI, H., RUBIN, J. P. & MARRA, K. G. 2012. Adipogenesis of human adipose-derived stem cells within three-dimensional hollow fiber-based bioreactors. *Tissue Eng Part C Methods*, 18, 54-61.
- GLAVASKI-JOKSIMOVIC, A. & BOHN, M. C. 2013. Mesenchymal stem cells and neuroregeneration in Parkinson's disease. *Experimental Neurology*, 247, 25-38.
- GLOWACKI, J. & MIZUNO, S. 2008. Collagen scaffolds for tissue engineering. *Biopolymers*, 89, 338-344.
- GÓMEZ-BARRENA, E., ROSSET, P., LOZANO, D., STANOVICI, J., ERMTHALLER, C. & GERBHARD, F. 2015. Bone fracture healing: Cell therapy in delayed unions and nonunions. *Bone*, 70, 93-101.
- GONG, J., TRAGANOS, F. & DARZYNKIEWICZ, Z. 1995. Threshold expression of cyclin E but not D-type cyclins characterizes normal and tumour cells entering S phase. *Cell Prolif*, 28, 337-346.
- GRELLNER, W., GEORG, T. & WILSKE, J. 2000. Quantitative analysis of proinflammatory cytokines (IL-1beta, IL-6, TNF-alpha) in human skin wounds. *Forensic Sci Int*, 113, 251-64.
- GRIFFITH, L. G. & SWARTZ, M. A. 2006. Capturing complex 3D tissue physiology in vitro. *Nat Rev Mol Cell Biol*, 7, 211-224.
- GURSKI L., PETRELLI N., JIA X. & M, F.-C. 2010. Three-dimensional matrices for anti-cancer drug testing and development. *Oncology Issues*, 25, 20-25.
- GURTNER, G. C., WERNER, S., BARRANDON, Y. & LONGAKER, M. T. 2008. Wound repair and regeneration. *Nature*, 453, 314-321.
- GURUHARSHA, K. G., KANKEL, M. W. & ARTAVANIS-TSAKONAS, S. 2012. The Notch signalling system: recent insights into the complexity of a conserved pathway. *Nat Rev Genet*, 13, 654-666.
- GUZMAN, R., UCHIDA, N., BLISS, T. M., HE, D., CHRISTOPHERSON, K. K., STELLWAGEN, D., CAPELA, A., GREVE, J., MALENKA, R. C., MOSELEY, M. E., PALMER, T. D. & STEINBERG, G. K. 2007. Long-term monitoring of

- transplanted human neural stem cells in developmental and pathological contexts with MRI. *Proceedings of the National Academy of Sciences*, 104, 10211-10216.
- HÄKKINEN, L., KOIVISTO, L., HEINO, J. & LARJAVA, H. 2015. Chapter 50 - Cell and Molecular Biology of Wound Healing. In: RAMALINGAM, A. V. S. S. (ed.) *Stem Cell Biology and Tissue Engineering in Dental Sciences*. Boston: Academic Press.
- HALDER, G., DUPONT, S. & PICCOLO, S. 2012. Transduction of mechanical and cytoskeletal cues by YAP and TAZ. *Nat Rev Mol Cell Biol*, 13, 591-600.
- HARRISON, J. S., RAMESHWAR, P., CHANG, V. & BANDARI, P. 2002. Oxygen saturation in the bone marrow of healthy volunteers. *Blood*, 99, 394.
- HEINRICH, P. C., BEHRMANN, I., MULLER-NEWEN, G., SCHAPER, F. & GRAEVE, L. 1998. Interleukin-6-type cytokine signalling through the gp130/Jak/STAT pathway. *Biochem J*, 334 ( Pt 2), 297-314.
- HER, G. J., WU, H.-C., CHEN, M.-H., CHEN, M.-Y., CHANG, S.-C. & WANG, T.-W. 2013. Control of three-dimensional substrate stiffness to manipulate mesenchymal stem cell fate toward neuronal or glial lineages. *Acta Biomaterialia*, 9, 5170-5180.
- HIGUCHI, A., LING, Q.-D., CHANG, Y., HSU, S.-T. & UMEZAWA, A. 2013. Physical Cues of Biomaterials Guide Stem Cell Differentiation Fate. *Chemical Reviews*, 113, 3297-3328.
- HIGUCHI, A., LING, Q.-D., HSU, S.-T. & UMEZAWA, A. 2012. Biomimetic Cell Culture Proteins as Extracellular Matrices for Stem Cell Differentiation. *Chemical Reviews*, 112, 4507-4540.
- HILDEBRANDT, C., BÜTH, H. & THIELECKE, H. 2011. A scaffold-free in vitro model for osteogenesis of human mesenchymal stem cells. *Tissue and Cell*, 43, 91-100.
- HINDS, P. W., MITTNACHT, S., DULIC, V., ARNOLD, A., REED, S. I. & WEINBERG, R. A. 1992. Regulation of retinoblastoma protein functions by ectopic expression of human cyclins. *Cell*, 70, 993-1006.
- HIRSCHHAEUSER, F., MENNE, H., DITTFELD, C., WEST, J., MUELLER-KLIESER, W. & KUNZ-SCHUGHART, L. A. 2010. Multicellular tumor spheroids: An underestimated tool is catching up again. *Journal of Biotechnology*, 148, 3-15.
- HOCKING, A. M. & GIBRAN, N. S. 2010. Mesenchymal stem cells: Paracrine signaling and differentiation during cutaneous wound repair. *Experimental Cell Research*, 316, 2213-2219.
- HONCZARENKO, M., LE, Y., SWIERKOWSKI, M., GHIRAN, I., GLODEK, A. M. & SILBERSTEIN, L. E. 2006. Human bone marrow stromal cells express a distinct set of biologically functional chemokine receptors. *STEM CELLS*, 24, 1030-41.
- HORWITZ, E. M., LE BLANC, K., DOMINICI, M., MUELLER, I., SLAPER-CORTENBACH, I., MARINI, F. C., DEANS, R. J., KRAUSE, D. S. & KEATING, A. 2005. Clarification of the nomenclature for MSC: The international society for cellular therapy position statement. *Cytotherapy*, 7, 393-395.
- HSU, S.-H. & HUANG, G.-S. 2013. Substrate-dependent Wnt signaling in MSC differentiation within biomaterial-derived 3D spheroids. *Biomaterials*, 34, 4725-4738.
- HUANG, E., ZHU, G., JIANG, W., YANG, K., GAO, Y., LUO, Q., GAO, J.-L., KIM, S. H., LIU, X., LI, M., SHI, Q., HU, N., WANG, L., LIU, H., CUI, J., ZHANG, W., LI, R., CHEN, X., KONG, Y.-H., ZHANG, J., WANG, J., SHEN, J., BI, Y., STATZ, J., HE, B.-C., LUO, J., WANG, H., XIONG, F., LUU, H. H., HAYDON,

- R. C., YANG, L. & HE, T.-C. 2012. Growth hormone synergizes with BMP9 in osteogenic differentiation by activating the JAK/STAT/IGF1 pathway in murine multilineage cells. *Journal of Bone and Mineral Research*, 27, 1566-1575.
- HUANG, G.-S., DAI, L.-G., YEN, B. L. & HSU, S.-H. 2011. Spheroid formation of mesenchymal stem cells on chitosan and chitosan-hyaluronan membranes. *Biomaterials*, 32, 6929-6945.
- HUANG, S., WU, Y., GAO, D. & FU, X. 2015. Paracrine action of mesenchymal stromal cells delivered by microspheres contributes to cutaneous wound healing and prevents scar formation in mice. *Cytotherapy*, 17, 922-931.
- ISHIMI, Y., MIYAURA, C., JIN, C. H., AKATSU, T., ABE, E., NAKAMURA, Y., YAMAGUCHI, A., YOSHIKI, S., MATSUDA, T., HIRANO, T. & ET AL. 1990. IL-6 is produced by osteoblasts and induces bone resorption. *J Immunol*, 145, 3297-303.
- IVANOV, D. P., PARKER, T. L., WALKER, D. A., ALEXANDER, C., ASHFORD, M. B., GELLERT, P. R. & GARNETT, M. C. 2014. Multiplexing Spheroid Volume, Resazurin and Acid Phosphatase Viability Assays for High-Throughput Screening of Tumour Spheroids and Stem Cell Neurospheres. *PLoS ONE*, 9, e103817.
- JANER, G., MAS DEL MOLINO, E., FERNÁNDEZ-ROSAS, E., FERNÁNDEZ, A. & VÁZQUEZ-CAMPOS, S. 2014. Cell uptake and oral absorption of titanium dioxide nanoparticles. *Toxicology Letters*, 228, 103-110.
- JAVAZON, E. H., KESWANI, S. G., BADILLO, A. T., CROMBLEHOLME, T. M., ZOLTICK, P. W., RADU, A. P., KOZIN, E. D., BEGGS, K., MALIK, A. A. & FLAKE, A. W. 2007. Enhanced epithelial gap closure and increased angiogenesis in wounds of diabetic mice treated with adult murine bone marrow stromal progenitor cells. *Wound Repair and Regeneration*, 15, 350-359.
- JIANG, X.-X., ZHANG, Y., LIU, B., ZHANG, S.-X., WU, Y., YU, X.-D. & MAO, N. 2005. *Human mesenchymal stem cells inhibit differentiation and function of monocyte-derived dendritic cells.*
- JO, C. H., LEE, Y. G., SHIN, W. H., KIM, H., CHAI, J. W., JEONG, E. C., KIM, J. E., SHIM, H., SHIN, J. S., SHIN, I. S., RA, J. C., OH, S. & YOON, K. S. 2014. Intra-Articular Injection of Mesenchymal Stem Cells for the Treatment of Osteoarthritis of the Knee: A Proof-of-Concept Clinical Trial. *STEM CELLS*, 32, 1254-1266.
- JO, J.-I., AOKI, I. & TABATA, Y. 2010. Design of iron oxide nanoparticles with different sizes and surface charges for simple and efficient labeling of mesenchymal stem cells. *Journal of Controlled Release*, 142, 465-473.
- JODDAR, B. & ITO, Y. 2013. Artificial niche substrates for embryonic and induced pluripotent stem cell cultures. *Journal of Biotechnology*, 168, 218-228.
- JONES, E. A., KINSEY, S. E., ENGLISH, A., JONES, R. A., STRASZYNSKI, L., MEREDITH, D. M., MARKHAM, A. F., JACK, A., EMERY, P. & MCGONAGLE, D. 2002. Isolation and characterization of bone marrow multipotential mesenchymal progenitor cells. *Arthritis & Rheumatism*, 46, 3349-3360.
- KAGAMI, H., AGATA, H. & TOJO, A. 2011. Bone marrow stromal cells (bone marrow-derived multipotent mesenchymal stromal cells) for bone tissue engineering: Basic science to clinical translation. *The International Journal of Biochemistry & Cell Biology*, 43, 286-289.
- KARP, J. M. & LENG TEO, G. S. 2009. Mesenchymal Stem Cell Homing: The Devil Is in the Details. *Cell Stem Cell*, 4, 206-216.

- KARUSSIS, D., KASSIS, I., KURKALLI, B. G. S. & SLAVIN, S. 2008. Immunomodulation and neuroprotection with mesenchymal bone marrow stem cells (MSCs): A proposed treatment for multiple sclerosis and other neuroimmunological/neurodegenerative diseases. *Journal of the Neurological Sciences*, 265, 131-135.
- KATO, J. & SVENSSON, C. I. 2015. Chapter Nine - Role of Extracellular Damage-Associated Molecular Pattern Molecules (DAMPs) as Mediators of Persistent Pain. In: THEODORE, J. P. & GREGORY, D. (eds.) *Progress in Molecular Biology and Translational Science*. Academic Press.
- KAWASE, M., HAYASHI, T., ASAKURA, M., MIEKI, A., FUYAMADA, H., SASSA, M., NAKANO, S., HAGIWARA, M., SHIMIZU, T. & KAWAI, T. 2014. Cell Proliferation Ability of Mouse Fibroblast-Like Cells and Osteoblast-Like Cells on a Ti-6Al-4V Alloy Film Produced by Selective Laser Melting. *Materials Sciences and Applications*, 5, 475-483.
- KEAN, T. J., LIN, P., CAPLAN, A. I. & DENNIS, J. E. 2009. MSCs: Delivery Routes and Engraftment, Cell-Targeting Strategies, and Immune Modulation. *Stem Cells International*, 2013, 1-13.
- KEATING, A. 2012. Mesenchymal Stromal Cells: New Directions. *Cell Stem Cell*, 10, 709-716.
- KELF, T. A., SREENIVASAN, V. K. A., SUN, J., KIM, E. J., GOLDYS, E. M. & ZVYAGIN, A. V. 2010. Non-specific cellular uptake of surface-functionalized quantum dots. *Nanotechnology*, 21, 285105.
- KHALDOYANIDI, S. 2008. Directing Stem Cell Homing. *Cell Stem Cell*, 2, 198-200.
- KHOLODENKO, I. V., KONIEVA, A. A., KHOLODENKO, R. V. & YARYGIN, K. N. 2013. Molecular mechanisms of migration and homing of intravenously transplanted mesenchymal stem cells. *Journal of Regenerative Medicine and Tissue Engineering*, 2.
- KIEL, M. J., YILMAZ, O. H., IWASHITA, T., TERHORST, C. & MORRISON, S. J. 2005. SLAM family receptors distinguish hematopoietic stem and progenitor cells and reveal endothelial niches for stem cells. *Cell*, 121, 1109-21.
- KIM, C., AGASTI, S. S., ZHU, Z., ISAACS, L. & ROTELLO, V. M. 2010. Recognition-mediated activation of therapeutic gold nanoparticles inside living cells. *Nat Chem*, 2, 962-966.
- KIM, J. A., CHOI, J.-H., KIM, M., RHEE, W. J., SON, B., JUNG, H.-K. & PARK, T. H. 2013. High-throughput generation of spheroids using magnetic nanoparticles for three-dimensional cell culture. *Biomaterials*, 34, 8555-8563.
- KIM, M.-H. & KINO-OKA, M. 2014. Switching between self-renewal and lineage commitment of human induced pluripotent stem cells via cell-substrate and cell-cell interactions on a dendrimer-immobilized surface. *Biomaterials*, 35, 5670-5678.
- KIM, M., KIM, C., CHOI, Y. S., KIM, M., PARK, C. & SUH, Y. 2012. Age-related alterations in mesenchymal stem cells related to shift in differentiation from osteogenic to adipogenic potential: Implication to age-associated bone diseases and defects. *Mechanisms of Ageing and Development*, 133, 215-225.
- KIM, S.-A., LEE, E. K. & KUH, H.-J. 2015. Co-culture of 3D tumor spheroids with fibroblasts as a model for epithelial-mesenchymal transition in vitro. *Experimental Cell Research*, 335, 187-196.
- KIM, Y. & RAJAGOPALAN, P. 2010. 3D Hepatic Cultures Simultaneously Maintain Primary Hepatocyte and Liver Sinusoidal Endothelial Cell Phenotypes. *PLoS ONE*, 5, e15456.

- KITAMBI, S. S. & CHANDRASEKAR, G. 2011. Stem cells: a model for screening, discovery and development of drugs. *Stem Cells and Cloning : Advances and Applications*, 4, 51-59.
- KOBEL, S. & LUTOLF, M. 2010. High-throughput methods to define complex stem cell niches. *Biotechniques*, 48, ix-xxii.
- KOLF, C. M., CHO, E. & TUAN, R. S. 2007. Mesenchymal stromal cells. Biology of adult mesenchymal stem cells: regulation of niche, self-renewal and differentiation. *Arthritis Research & Therapy*, 9, 204-204.
- KOMORI, T. 2010. Regulation of Osteoblast Differentiation by Runx2. In: CHOI, Y. (ed.) *Osteoimmunology*. Springer US.
- KON, E., FILARDO, G., ROFFI, A., DI MARTINO, A., HAMDAN, M., DE PASQUAL, L., MERLI, M. L. & MARCACCI, M. 2012. Bone regeneration with mesenchymal stem cells. *Clin Cases Miner Bone Metab*, 9, 24-7.
- KONDO, T. & OHSHIMA, T. 1996. The dynamics of inflammatory cytokines in the healing process of mouse skin wound: a preliminary study for possible wound age determination. *Int J Legal Med*, 108, 231-6.
- KOSTURA, L., KRAITCHMAN, D. L., MACKAY, A. M., PITTENGER, M. F. & BULTE, J. W. M. 2004. Feridex labeling of mesenchymal stem cells inhibits chondrogenesis but not adipogenesis or osteogenesis. *NMR in Biomedicine*, 17, 513-517.
- KOU, L., SUN, J., ZHAI, Y. & HE, Z. 2013. The endocytosis and intracellular fate of nanomedicines: Implication for rational design. *Asian Journal of Pharmaceutical Sciences*, 8, 1-10.
- KOWAL-VERN, A., WALENGA, J. M., HOPPENSTEADT, D., SHARP-PUCCI, M. & GAMELLI, R. L. 1994. Interleukin-2 and interleukin-6 in relation to burn wound size in the acute phase of thermal injury. *J Am Coll Surg*, 178, 357-62.
- KRASNODEMBSKAYA, A., SONG, Y., FANG, X., GUPTA, N., SERIKOV, V., LEE, J.-W. & MATTHAY, M. A. 2010. Antibacterial Effect of Human Mesenchymal Stem Cells Is Mediated in Part from Secretion of the Antimicrobial Peptide LL-37. *Stem Cells (Dayton, Ohio)*, 28, 2229-2238.
- KRAUS, V. B., BLANCO, F. J., ENGLUND, M., KARSDAL, M. A. & LOHMANDER, L. S. 2015. Call for standardized definitions of osteoarthritis and risk stratification for clinical trials and clinical use. *Osteoarthritis and Cartilage*, 23, 1233-1241.
- KUBO, H., HAYASHI, T., AGO, K., AGO, M., KANEKURA, T. & OGATA, M. 2014. Temporal expression of wound healing-related genes in skin burn injury. *Leg Med (Tokyo)*, 16, 8-13.
- KURTH, T. B., DELL'ACCIO, F., CROUCH, V., AUGELLO, A., SHARPE, P. T. & DE BARI, C. 2011. Functional mesenchymal stem cell niches in adult mouse knee joint synovium in vivo. *Arthritis Rheum*, 63, 1289-300.
- KYRTATOS, P. G., LEHTOLAINEN, P., JUNEMANN-RAMIREZ, M., GARCIA-PRIETO, A., PRICE, A. N., MARTIN, J. F., GADIAN, D. G., PANKHURST, Q. A. & LYTHGOE, M. F. 2009. Magnetic Tagging Increases Delivery of Circulating Progenitors in Vascular Injury. *JACC: Cardiovascular Interventions*, 2, 794-802.
- KYURKCHIEV, D., BOCHEV, I., IVANOVA-TODOROVA, E., MOURDJEVA, M., ORESHKOVA, T., BELEMEZOVA, K. & KYURKCHIEV, S. 2014. Secretion of immunoregulatory cytokines by mesenchymal stem cells. *World Journal of Stem Cells*, 6, 552-570.
- LAI, Q. G., YUAN, K. F., XU, X., LI, D. R., LI, G. J., WEI, F. L., YANG, Z. J., LUO, S. L., TANG, X. P. & LI, S. 2011. Transcription factor osterix modified

- bone marrow mesenchymal stem cells enhance callus formation during distraction osteogenesis. *Oral Surg Oral Med Oral Pathol Oral Radiol Endod*, 111, 412-9.
- LAINE, S. K., HENTUNEN, T. & LAITALA-LEINONEN, T. 2012. Do microRNAs regulate bone marrow stem cell niche physiology? *Gene*, 497, 1-9.
- LAMPLOT, J. D., QIN, J., NAN, G., WANG, J., LIU, X., YIN, L., TOMAL, J., LI, R., SHUI, W., ZHANG, H., KIM, S. H., ZHANG, W., ZHANG, J., KONG, Y., DENDULURI, S., ROGERS, M. R., PRATT, A., HAYDON, R. C., LUU, H. H., ANGELES, J., SHI, L. L. & HE, T. C. 2013. BMP9 signaling in stem cell differentiation and osteogenesis. *Am J Stem Cells*, 2, 1-21.
- LANE, S. W., WILLIAMS, D. A. & WATT, F. M. 2014. Modulating the stem cell niche for tissue regeneration. *Nat Biotech*, 32, 795-803.
- LASTAYO, P. C., WINTERS, K. M. & HARDY, M. 2003. Fracture healing: bone healing, fracture management, and current concepts related to the hand. *Journal of hand therapy : official journal of the American Society of Hand Therapists*, 16, 81-93.
- LEATHERMAN, J. L. & DINARDO, S. 2010. Germline self-renewal requires cyst stem cells and stat regulates niche adhesion in Drosophila testes. *Nat Cell Biol*, 12, 806-811.
- LEE, C. H., HUANG, Y. L., LIAO, J. F. & CHIOU, W. F. 2011a. Ugonin K promotes osteoblastic differentiation and mineralization by activation of p38 MAPK- and ERK-mediated expression of Runx2 and osterix. *Eur J Pharmacol*, 668, 383-9.
- LEE, C. H., SINGLA, A. & LEE, Y. 2001. Biomedical applications of collagen. *International Journal of Pharmaceutics*, 221, 1-22.
- LEE, J.-H., CHUNG, W.-H., KANG, E.-H., CHUNG, D.-J., CHOI, C.-B., CHANG, H.-S., LEE, J.-H., HWANG, S.-H., HAN, H., CHOE, B.-Y. & KIM, H.-Y. 2011b. Schwann cell-like remyelination following transplantation of human umbilical cord blood (hUCB)-derived mesenchymal stem cells in dogs with acute spinal cord injury. *Journal of the Neurological Sciences*, 300, 86-96.
- LEE, J., ABDEEN, A. A. & KILIAN, K. A. 2014. Rewiring mesenchymal stem cell lineage specification by switching the biophysical microenvironment. *Sci. Rep.*, 4.
- LEE, R. H., PULIN, A. A., SEO, M. J., KOTA, D. J., YLOSTALO, J., LARSON, B. L., SEMPRUN-PRIETO, L., DELAFONTAINE, P. & PROCKOP, D. J. 2009. Intravenous hMSCs Improve Myocardial Infarction in Mice because Cells Embolized in Lung Are Activated to Secrete the Anti-inflammatory Protein TSG-6. *Cell Stem Cell*, 5, 54-63.
- LEGATE, K. R., WICKSTRÖM, S. A. & FÄSSLER, R. 2009. Genetic and cell biological analysis of integrin outside-in signaling. *Genes & Development*, 23, 397-418.
- LEUSCHNER, C., KUMAR, C. S., HANSEL, W., SOBOYEJO, W., ZHOU, J. & HORMES, J. 2006. LHRH-conjugated magnetic iron oxide nanoparticles for detection of breast cancer metastases. *Breast Cancer Res Treat*, 99, 163-76.
- LI, N., YANG, H., LU, L., DUAN, C., ZHAO, C. & ZHAO, H. 2008. Comparison of the labeling efficiency of BrdU, Dil and FISH labeling techniques in bone marrow stromal cells. *Brain Research*, 1215, 11-19.
- LI, Z., BAO, S., WU, Q., WANG, H., EYLER, C., SATHORNSUMETEE, S., SHI, Q., CAO, Y., LATHIA, J., MCLENDON, R. E., HJELMELAND, A. B. & RICH, J. N. 2009. Hypoxia-Inducible Factors Regulate Tumorigenic Capacity of Glioma Stem Cells. *Cancer Cell*, 15, 501-513.

- LI, Z., GONG, Y., SUN, S., DU, Y., LÜ, D., LIU, X. & LONG, M. 2013. Differential regulation of stiffness, topography, and dimension of substrates in rat mesenchymal stem cells. *Biomaterials*, 34, 7616-7625.
- LIAO, S., CHAN, C. K. & RAMAKRISHNA, S. 2008. Stem cells and biomimetic materials strategies for tissue engineering. *Materials Science and Engineering: C*, 28, 1189-1202.
- LIEN, W.-H., POLAK, L., LIN, M., LAY, K., ZHENG, D. & FUCHS, E. 2014. In vivo transcriptional governance of hair follicle stem cells by canonical Wnt regulators. *Nature cell biology*, 16, 179-190.
- LIN, G., LIU, G., BANIE, L., WANG, G., NING, H., LUE, T. F. & LIN, C.-S. 2011. Tissue Distribution of Mesenchymal Stem Cell Marker Stro-1. *Stem Cells and Development*, 20, 1747-1752.
- LIN, H.-T., OTSU, M. & NAKAUCHI, H. 2013. *Stem cell therapy: an exercise in patience and prudence*.
- LIN, P., CORREA, D., KEAN, T. J., AWADALLAH, A., DENNIS, J. E. & CAPLAN, A. I. 2014. Serial Transplantation and Long-term Engraftment of Intra-arterially Delivered Clonally Derived Mesenchymal Stem Cells to Injured Bone Marrow. *Mol Ther*, 22, 160-168.
- LIN, Z. Q., KONDO, T., ISHIDA, Y., TAKAYASU, T. & MUKAIDA, N. 2003. Essential involvement of IL-6 in the skin wound-healing process as evidenced by delayed wound healing in IL-6-deficient mice. *J Leukoc Biol*, 73, 713-21.
- LIU, C., XIA, Z. & CZERNUSZKA, J. T. 2007. Design and Development of Three-Dimensional Scaffolds for Tissue Engineering. *Chemical Engineering Research and Design*, 85, 1051-1064.
- LIU, Q., ZHANG, J., XIA, W. & GU, H. 2012. Magnetic field enhanced cell uptake efficiency of magnetic silica mesoporous nanoparticles. *Nanoscale*, 4, 3415-21.
- LIU, X. H., KIRSCHENBAUM, A., YAO, S. & LEVINE, A. C. 2006. The Role of the Interleukin-6/gp130 Signaling Pathway in Bone Metabolism. In: GERALD, L. (ed.) *Vitamins & Hormones*. Academic Press.
- LIU, Y., GUAN, Y. & ZHANG, Y. 2015. Chitosan as inter-cellular linker to accelerate multicellular spheroid generation in hydrogel scaffold. *Polymer*, 77, 366-376.
- LO, B. & PARHAM, L. 2009. Ethical issues in stem cell research. *Endocr Rev*, 30, 204-13.
- LOYA, K. 2014. Chapter 11 - Stem Cells. In: PADMANABHAN, S. (ed.) *Handbook of Pharmacogenomics and Stratified Medicine*. San Diego: Academic Press.
- LUU, N. T., MCGETTRICK, H. M., BUCKLEY, C. D., NEWSOME, P. N., RAINGER, G. E., FRAMPTON, J. & NASH, G. B. 2013. Crosstalk between mesenchymal stem cells and endothelial cells leads to downregulation of cytokine-induced leukocyte recruitment. *Stem Cells*, 31, 2690-702.
- MA, S., XIE, N., LI, W., YUAN, B., SHI, Y. & WANG, Y. 2014. Immunobiology of mesenchymal stem cells. *Cell Death Differ*, 21, 216-225.
- MAERKL, S. J. 2009. Integration column: Microfluidic high-throughput screening. *Integrative Biology*, 1, 19-29.
- MALTMAN, D. J., HARDY, S. A. & PRZYBORSKI, S. A. 2011. Role of mesenchymal stem cells in neurogenesis and nervous system repair. *Neurochemistry International*, 59, 347-356.
- MALUMBRES, M. & BARBACID, M. 2005. Mammalian cyclin-dependent kinases. *Trends in Biochemical Sciences*, 30, 630-641.
- MANCINI, S. J., MANTEI, N., DUMORTIER, A., SUTER, U., MACDONALD, H. R. & RADTKE, F. 2005. Jagged1-dependent Notch signaling is dispensable for

- hematopoietic stem cell self-renewal and differentiation. *Blood*, 105, 2340-2.
- MANDAL, M., BANDYOPADHYAY, D., GOEPFERT, T. M. & KUMAR, R. 1998. Interferon-induces expression of cyclin-dependent kinase-inhibitors p21WAF1 and p27Kip1 that prevent activation of cyclin-dependent kinase by CDK-activating kinase (CAK). *Oncogene*, 16, 217-25.
- MARQUEZ-CURTIS, L. A. & JANOWSKA-WIECZOREK, A. 2013. Enhancing the Migration Ability of Mesenchymal Stromal Cells by Targeting the SDF-1/CXCR4 Axis. *BioMed Research International*, 2013, 1-15.
- MARRIOTT, I., GRAY, D. L., TRANGUCH, S. L., FOWLER, V. G., JR., STRYJEWSKI, M., SCOTT LEVIN, L., HUDSON, M. C. & BOST, K. L. 2004. Osteoblasts express the inflammatory cytokine interleukin-6 in a murine model of *Staphylococcus aureus* osteomyelitis and infected human bone tissue. *Am J Pathol*, 164, 1399-406.
- MARX, V. 2013. Cell culture: A better brew. *Nature*, 496, 253-258.
- MASON, C. & DUNNILL, P. 2008. A brief definition of regenerative medicine. *Regenerative Medicine*, 3, 1-5.
- MATSUMOTO, A., MATSUMOTO, S., SOWERS, A. L., KOSCIELNIAK, J. W., TRIGG, N. J., KUPPUSAMY, P., MITCHELL, J. B., SUBRAMANIAN, S., KRISHNA, M. C. & MATSUMOTO, K. 2005. Absolute oxygen tension (pO<sub>2</sub>) in murine fatty and muscle tissue as determined by EPR. *Magn Reson Med*, 54, 1530-5.
- MATSUMOTO, A. & NAKAYAMA, K. I. 2013. Role of key regulators of the cell cycle in maintenance of hematopoietic stem cells. *Biochimica et Biophysica Acta (BBA) - General Subjects*, 1830, 2335-2344.
- MAXSON, S., LOPEZ, E. A., YOO, D., DANILKOVITCH-MIAGKOVA, A. & LEROUX, M. A. 2012. Concise review: role of mesenchymal stem cells in wound repair. *Stem Cells Transl Med*, 1, 142-9.
- MAYR, L. M. & BOJANIC, D. 2009. Novel trends in high-throughput screening. *Current Opinion in Pharmacology*, 9, 580-588.
- MCCLURE, K. D. & SCHUBIGER, G. 2007. Transdetermination: *Drosophila* imaginal disc cells exhibit stem cell-like potency. *The International Journal of Biochemistry & Cell Biology*, 39, 1105-1118.
- MCMURRAY, R. J., GADEGAARD, N., TSIMBOURI, P. M., BURGESS, K. V., MCNAMARA, L. E., TARE, R., MURAWSKI, K., KINGHAM, E., OREFFO, R. O. C. & DALBY, M. J. 2011. Nanoscale surfaces for the long-term maintenance of mesenchymal stem cell phenotype and multipotency. *Nat Mater*, 10, 637-644.
- MEIKLE, M. C. 2006. *The tissue, cellular, and molecular regulation of orthodontic tooth movement: 100 years after Carl Sandstedt*.
- MENDEZ-FERRER, S., MICHURINA, T. V., FERRARO, F., MAZLOOM, A. R., MACARTHUR, B. D., LIRA, S. A., SCADDEN, D. T., MA'AYAN, A., ENIKOLOPOV, G. N. & FRENETTE, P. S. 2010. Mesenchymal and haematopoietic stem cells form a unique bone marrow niche. *Nature*, 466, 829-834.
- MENG, R., XU, H. Y., DI, S. M., SHI, D. Y., QIAN, A. R., WANG, J. F. & SHANG, P. 2011. Human mesenchymal stem cells are sensitive to abnormal gravity and exhibit classic apoptotic features. *Acta Biochim Biophys Sin (Shanghai)*, 43, 133-42.
- METZGER, T. A., SHUDICK, J. M., SEEKELL, R., ZHU, Y. & NIEBUR, G. L. 2014. Rheological behavior of fresh bone marrow and the effects of storage. *Journal of the Mechanical Behavior of Biomedical Materials*, 40, 307-313.

- MEUNIER, P., AARON, J., EDOUARD, C. & VIGNON, G. 1971. Osteoporosis and the replacement of cell populations of the marrow by adipose tissue. A quantitative study of 84 iliac bone biopsies. *Clin Orthop Relat Res*, 80, 147-54.
- MINGUELL, J. J., ERICES, A. & CONGET, P. 2001. Mesenchymal Stem Cells. *Experimental Biology and Medicine*, 226, 507-520.
- MITSIADIS, T. A., BARRANDON, O., ROCHAT, A., BARRANDON, Y. & DE BARI, C. 2007. Stem cell niches in mammals. *Experimental Cell Research*, 313, 3377-3385.
- MOHYELDIN, A., GARZÓN-MUVDI, T. & QUIÑONES-HINOJOSA, A. 2010. Oxygen in Stem Cell Biology: A Critical Component of the Stem Cell Niche. *Cell Stem Cell*, 7, 150-161.
- MOORE, K. A. & LEMISCHKA, I. R. 2006. Stem Cells and Their Niches. *Science*, 311, 1880-1885.
- MORRISON, S. J. & SCADDEN, D. T. 2014. The bone marrow niche for haematopoietic stem cells. *Nature*, 505, 327-334.
- MORRISON, S. J. & SPRADLING, A. C. 2008. Stem Cells and Niches: Mechanisms That Promote Stem Cell Maintenance throughout Life. *Cell*, 132, 598-611.
- MUSCHITZ, C., KOCIJAN, R., HASCHKA, J., PAHR, D., KAIDER, A., PIETSCHMANN, P., HANS, D., MUSCHITZ, G. K., FAHRLEITNER-PAMMER, A. & RESCH, H. 2015. TBS reflects trabecular microarchitecture in premenopausal women and men with idiopathic osteoporosis and low-traumatic fractures. *Bone*, 79, 259-266.
- NEL, A., XIA, T., MADLER, L. & LI, N. 2006. Toxic potential of materials at the nanolevel. *Science*, 311, 622-7.
- NEVINS, J. 1998. Toward an understanding of the functional complexity of the E2F and retinoblastoma families. *Cell Growth Diff*, 9, 585-593.
- NING, H., LIN, G., LUE, T. F. & LIN, C.-S. 2011. Mesenchymal stem cell marker Stro-1 is a 75kd endothelial antigen. *Biochemical and Biophysical Research Communications*, 413, 353-357.
- NISHIMOTO, N. & KISHIMOTO, T. 2006. Interleukin 6: from bench to bedside. *Nat Clin Pract Rheum*, 2, 619-626.
- NOVACK, D. V. & TEITELBAUM, S. L. 2008. The osteoclast: friend or foe? *Annu Rev Pathol*, 3, 457-84.
- NYSTUL, T. & SPRADLING, A. 2007. An Epithelial Niche in the Drosophila Ovary Undergoes Long-Range Stem Cell Replacement. *Cell Stem Cell*, 1, 277-285.
- OBERLENDER, S. A. & TUAN, R. S. 1994. Expression and functional involvement of N-cadherin in embryonic limb chondrogenesis. *Development*, 120, 177-187.
- ONG, S.-M., ZHAO, Z., AROOZ, T., ZHAO, D., ZHANG, S., DU, T., WASSER, M., VAN NOORT, D. & YU, H. 2010. Engineering a scaffold-free 3D tumor model for in vitro drug penetration studies. *Biomaterials*, 31, 1180-1190.
- ORFORD, K. W. & SCADDEN, D. T. 2008. Deconstructing stem cell self-renewal: genetic insights into cell-cycle regulation. *Nat Rev Genet*, 9, 115-128.
- OTTONE, C., KRUSCHE, B., WHITBY, A., CLEMENTS, M., QUADRATO, G., PITULESCU, M. E., ADAMS, R. H. & PARRINELLO, S. 2014. Direct cell-cell contact with the vascular niche maintains quiescent neural stem cells. *Nat Cell Biol*, 16, 1045-1056.
- OZAWA, K., SATO, K., OH, I., OZAKI, K., UCHIBORI, R., OBARA, Y., KIKUCHI, Y., ITO, T., OKADA, T., URABE, M., MIZUKAMI, H. & KUME, A. 2008. Cell and

- gene therapy using mesenchymal stem cells (MSCs). *Journal of Autoimmunity*, 30, 121-127.
- OZEKI, N., KAWAI, R., YAMAGUCHI, H., HIYAMA, T., KINOSHITA, K., HASE, N., NAKATA, K., KONDO, A., MOGI, M. & NAKAMURA, H. 2014. IL-1 $\beta$ -induced matrix metalloproteinase-13 is activated by a disintegrin and metalloprotease-28-regulated proliferation of human osteoblast-like cells. *Experimental Cell Research*, 323, 165-177.
- PAGE, H., FLOOD, P. & REYNAUD, E. 2013. Three-dimensional tissue cultures: current trends and beyond. *Cell and Tissue Research*, 352, 123-131.
- PAMPALONI, F., REYNAUD, E. G. & STELZER, E. H. K. 2007. The third dimension bridges the gap between cell culture and live tissue. *Nat Rev Mol Cell Biol*, 8, 839-845.
- PANG, Y. & GREISLER, H. P. 2010. Using a type 1 collagen-based system to understand cell-scaffold interactions and to deliver chimeric collagen-binding growth factors for vascular tissue engineering. *J Investig Med*, 58, 845-8.
- PARENTEAU-BAREIL, R., GAUVIN, R. & BERTHOD, F. 2010. Collagen-Based Biomaterials for Tissue Engineering Applications. *Materials*, 3, 1863-1887.
- PASARICA, M., SEREDA, O. R., REDMAN, L. M., ALBARADO, D. C., HYMEL, D. T., ROAN, L. E., ROOD, J. C., BURK, D. H. & SMITH, S. R. 2009. Reduced adipose tissue oxygenation in human obesity: evidence for rarefaction, macrophage chemotaxis, and inflammation without an angiogenic response. *Diabetes*, 58, 718-25.
- PEDERSEN, J. A. & SWARTZ, M. A. 2005. Mechanobiology in the third dimension. *Annals of Biomedical Engineering*, 33, 1469-90.
- PENNOCK, R., BRAY, E., PRYOR, P., JAMES, S., MCKEEGAN, P., STURMEY, R. & GENEVER, P. 2015. Human cell dedifferentiation in mesenchymal condensates through controlled autophagy. *Scientific Reports*, 5, 13113.
- PLANK, C., SCHERER, F., SCHILLINGER, U., BERGEMANN, C. & ANTON, M. 2003. Magnetofection: Enhancing and Targeting Gene Delivery with Superparamagnetic Nanoparticles and Magnetic Fields. *Journal of Liposome Research*, 13, 29-32.
- POLYAK, B., FISHBEIN, I., CHORNY, M., ALFERIEV, I., WILLIAMS, D., YELLEN, B., FRIEDMAN, G. & LEVY, R. J. 2008. High field gradient targeting of magnetic nanoparticle-loaded endothelial cells to the surfaces of steel stents. *Proceedings of the National Academy of Sciences*, 105, 698-703.
- PRIJIC, S. & SERSA, G. 2011. Magnetic nanoparticles as targeted delivery systems in oncology. *Radiology and Oncology*, 45, 1-16.
- QIN, J., LI, K., PENG, C., LI, X., LIN, J., YE, K., YANG, X., XIE, Q., SHEN, Z., JIN, Y., JIANG, M., ZHANG, G. & LU, X. 2013. MRI of iron oxide nanoparticle-labeled ADSCs in a model of hindlimb ischemia. *Biomaterials*, 34, 4914-4925.
- RAFFAGHELLO, L., BIANCHI, G., BERTOLOTTI, M., MONTECUCCO, F., BUSCA, A., DALLEGRI, F., OTTONELLO, L. & PISTOIA, V. 2008. Human Mesenchymal Stem Cells Inhibit Neutrophil Apoptosis: A Model for Neutrophil Preservation in the Bone Marrow Niche. *STEM CELLS*, 26, 151-162.
- RAGHAVAN, S., WARD, M. R., ROWLEY, K. R., WOLD, R. M., TAKAYAMA, S., BUCKANOVICH, R. J. & MEHTA, G. 2015. Formation of stable small cell number three-dimensional ovarian cancer spheroids using hanging drop arrays for preclinical drug sensitivity assays. *Gynecologic Oncology*, 138, 181-189.

- RAGNI, E., MONTEMURRO, T., MONTELATICI, E., LAVAZZA, C., VIGANÒ, M., REBULLA, P., GIORDANO, R. & LAZZARI, L. 2013. Differential microRNA signature of human mesenchymal stem cells from different sources reveals an “environmental-niche memory” for bone marrow stem cells. *Experimental Cell Research*, 319, 1562-1574.
- RAMASAMY, R., FAZEKASOVA, H., LAM, E. W., SOEIRO, I., LOMBARDI, G. & DAZZI, F. 2007. Mesenchymal stem cells inhibit dendritic cell differentiation and function by preventing entry into the cell cycle. *Transplantation*, 83, 71-6.
- RASI GHAEMI, S., HARDING, F. J., DELALAT, B., GRONTHOS, S. & VOELCKER, N. H. 2013. Exploring the mesenchymal stem cell niche using high throughput screening. *Biomaterials*, 34, 7601-7615.
- RATTIGAN, Y., HSU, J.-M., MISHRA, P. J., GLOD, J. & BANERJEE, D. 2010. Interleukin 6 mediated recruitment of mesenchymal stem cells to the hypoxic tumor milieu. *Experimental Cell Research*, 316, 3417-3424.
- RAWLINGS, J. S., ROSLER, K. M. & HARRISON, D. A. 2004. The JAK/STAT signaling pathway. *Journal of Cell Science*, 117, 1281-1283.
- REJMAN, J., OBERLE, V., ZUHORN, I. S. & HOEKSTRA, D. 2004. Size-dependent internalization of particles via the pathways of clathrin- and caveolae-mediated endocytosis. *Biochemical Journal*, 377, 159-169.
- REN, S. & ROLLINS, B. J. 2004. Cyclin C/Cdk3 Promotes Rb-Dependent G0 Exit. *Cell*, 117, 239-251.
- RENNERT, R. C., SORKIN, M., GARG, R. K. & GURTNER, G. C. 2012. Stem cell recruitment after injury: lessons for regenerative medicine. *Regenerative medicine*, 7, 833-850.
- REYA, T., DUNCAN, A. W., AILLES, L., DOMEN, J., SCHERER, D. C., WILLERT, K., HINTZ, L., NUSSE, R. & WEISSMAN, I. L. 2003. A role for Wnt signalling in self-renewal of haematopoietic stem cells. *Nature*, 423, 409-414.
- RODGERS, J. T., KING, K. Y., BRETT, J. O., CROMIE, M. J., CHARVILLE, G. W., MAGUIRE, K. K., BRUNSON, C., MASTHEY, N., LIU, L., TSAI, C.-R., GOODELL, M. A. & RANDO, T. A. 2014. mTORC1 controls the adaptive transition of quiescent stem cells from G0 to GAlert. *Nature*, 510, 393-396.
- ROEDER, I., LOEFFLER, M. & GLAUCHE, I. 2011. Towards a quantitative understanding of stem cell-niche interaction: Experiments, models, and technologies. *Blood Cells, Molecules, and Diseases*, 46, 308-317.
- ROMPOLAS, P., MESA, K. R. & GRECO, V. 2013. Spatial organization within a niche as a determinant of stem-cell fate. *Nature*, 502, 513-518.
- ROSEN, C. J. & BOUXSEIN, M. L. 2006. Mechanisms of Disease: is osteoporosis the obesity of bone? *Nat Clin Pract Rheum*, 2, 35-43.
- ROSIN, D. L. & OKUSA, M. D. 2011. Dangers Within: DAMP Responses to Damage and Cell Death in Kidney Disease. *Journal of the American Society of Nephrology*, 22, 416-425.
- RUST, P. A., KALSI, P., BRIGGS, T. W., CANNON, S. R. & BLUNN, G. W. 2007. Will mesenchymal stem cells differentiate into osteoblasts on allograft? *Clin Orthop Relat Res*, 457, 220-6.
- RYU, C. H., PARK, S. A., KIM, S. M., LIM, J. Y., JEONG, C. H., JUN, J. A., OH, J. H., PARK, S. H., OH, W.-I. & JEUN, S.-S. 2010. Migration of human umbilical cord blood mesenchymal stem cells mediated by stromal cell-derived factor-1/CXCR4 axis via Akt, ERK, and p38 signal transduction pathways. *Biochemical and Biophysical Research Communications*, 398, 105-110.

- SACCHETTI, B., FUNARI, A., MICHIEZI, S., DI CESARE, S., PIERSANTI, S., SAGGIO, I., TAGLIAFICO, E., FERRARI, S., ROBEY, P. G., RIMINUCCI, M. & BIANCO, P. 2007. Self-Renewing Osteoprogenitors in Bone Marrow Sinusoids Can Organize a Hematopoietic Microenvironment. *Cell*, 131, 324-336.
- SAHAY, G., ALAKHOVA, D. Y. & KABANOV, A. V. 2010. Endocytosis of nanomedicines. *Journal of Controlled Release*, 145, 182-195.
- SALEH, F. A. & GENEVER, P. G. 2011. Turning round: multipotent stromal cells, a three-dimensional revolution? *Cytotherapy*, 13, 903-12.
- SAMADIKUCHAKSARAEI, A., LECHT, S., LELKES, P. I., MANTALARIS, A. & POLAK, J. M. 2014. Chapter 4 - Stem Cells as Building Blocks. In: LANZA, R., LANGER, R. & VACANTI, J. (eds.) *Principles of Tissue Engineering (Fourth Edition)*. Boston: Academic Press.
- SANDELL, L. J. & AIGNER, T. 2001. Articular cartilage and changes in Arthritis: Cell biology of osteoarthritis. *Arthritis Research & Therapy*, 3, 107-113.
- SARKAR, D., ANKRUM, J. A., TEO, G. S. L., CARMAN, C. V. & KARP, J. M. 2011. Cellular and extracellular programming of cell fate through engineered intracrine-, paracrine-, and endocrine-like mechanisms. *Biomaterials*, 32, 3053-3061.
- SASAKI, M., ABE, R., FUJITA, Y., ANDO, S., INOKUMA, D. & SHIMIZU, H. 2008. Mesenchymal Stem Cells Are Recruited into Wounded Skin and Contribute to Wound Repair by Transdifferentiation into Multiple Skin Cell Type. *The Journal of Immunology*, 180, 2581-2587.
- SAVOPOULOS, C., DOKOS, C., KAIAPA, G. & HATZITOLIOS, A. 2011. Adipogenesis and osteoblastogenesis: trans-differentiation in the pathophysiology of bone disorders. *Hippokratia*, 15, 18-21.
- SCHELL, H., LIENAU, J., EPARI, D. R., SEEBECK, P., EXNER, C., MUCHOW, S., BRAGULLA, H., HAAS, N. P. & DUDA, G. N. 2006. Osteoclastic activity begins early and increases over the course of bone healing. *Bone*, 38, 547-54.
- SCHMIDT, E. V. 2004. The role of c-myc in regulation of translation initiation. *Oncogene*, 23, 3217-3221.
- SCHULTZ, G. S. & WYSOCKI, A. 2009. Interactions between extracellular matrix and growth factors in wound healing. *Wound Repair Regen*, 17, 153-62.
- SEKE ETET, P. F., VECCHIO, L. & NWABO KAMDJE, A. H. 2012. Interactions between bone marrow stromal microenvironment and B-chronic lymphocytic leukemia cells: Any role for Notch, Wnt and Hh signaling pathways? *Cellular Signalling*, 24, 1433-1443.
- SELMANI, Z., NAJI, A., ZIDI, I., FAVIER, B., GAIFFE, E., OBERT, L., BORG, C., SAAS, P., TIBERGHEN, P., ROUAS-FREISS, N., CAROSELLA, E. D. & DESCHASEAUX, F. 2008. Human Leukocyte Antigen-G5 Secretion by Human Mesenchymal Stem Cells Is Required to Suppress T Lymphocyte and Natural Killer Function and to Induce CD4<sup>+</sup>CD25<sup>high</sup>FOXP3<sup>+</sup> Regulatory T Cells. *STEM CELLS*, 26, 212-222.
- SHEN, F. H., WERNER, B. C., LIANG, H., SHANG, H., YANG, N., LI, X., SHIMER, A. L., BALIAN, G. & KATZ, A. J. 2013. Implications of adipose-derived stromal cells in a 3D culture system for osteogenic differentiation: an in vitro and in vivo investigation. *The Spine Journal*, 13, 32-43.
- SHI, M., LI, J., LIAO, L., CHEN, B., LI, B., CHEN, L., JIA, H. & ZHAO, R. C. 2007. Regulation of CXCR4 expression in human mesenchymal stem cells by cytokine treatment: role in homing efficiency in NOD/SCID mice. *Haematologica*, 92, 897-904.

- SHI, Y., SU, J., ROBERTS, A. I., SHOU, P., RABSON, A. B. & REN, G. 2012. How mesenchymal stem cells interact with tissue immune responses. *Trends in Immunology*, 33, 136-143.
- SHIN, J., YOO, C.-H., LEE, J. & CHA, M. 2012. Cell response induced by internalized bacterial magnetic nanoparticles under an external static magnetic field. *Biomaterials*, 33, 5650-5657.
- SHIOZAWA, Y., HAVENS, A. M., PIENTA, K. J. & TAICHMAN, R. S. 2008. The bone marrow niche: habitat to hematopoietic and mesenchymal stem cells, and unwitting host to molecular parasites. *Leukemia*, 22, 941-950.
- SILVA, H. & CONBOY, I. M. 2008. Aging and stem cell renewal. *StemBook*. StemBook ed.: The Stem Cell Research Community.
- SILVÁN, U., DÍEZ-TORRE, A., ARLUZZA, J., ANDRADE, R., SILIÓ, M. & ARÉCHAGA, J. 2009. Hypoxia and pluripotency in embryonic and embryonal carcinoma stem cell biology. *Differentiation*, 78, 159-168.
- SIMON, M. C. & KEITH, B. 2008. The role of oxygen availability in embryonic development and stem cell function. *Nat Rev Mol Cell Biol*, 9, 285-296.
- SLACK, J. M. W. 2012. *Stem Cells: A Very Short Introduction*, New York, Oxford University Press Inc.
- SMITH, A. N., WILLIS, E., CHAN, V. T., MUFFLEY, L. A., ISIK, F. F., GIBRAN, N. S. & HOCKING, A. M. 2010a. Mesenchymal stem cells induce dermal fibroblast responses to injury. *Experimental Cell Research*, 316, 48-54.
- SMITH, C.-A. M., FUENTE, J. D. L., PELAZ, B., FURLANI, E. P., MULLIN, M. & BERRY, C. C. 2010b. The effect of static magnetic fields and tat peptides on cellular and nuclear uptake of magnetic nanoparticles. *Biomaterials*, 31, 4392-4400.
- SOBOTKOVÁ, E., HRUBÁ, A., KIEFMAN, J. & SOBOTKA, Z. 1988. Rheological behaviour of bone marrow. In: GIESEKUS, H. & HIBBERD, M. (eds.) *Progress and Trends in Rheology II*. Steinkopff.
- SOENEN, S. J. H., HIMMELREICH, U., NUYTTEN, N. & DE CUYPER, M. 2011. Cytotoxic effects of iron oxide nanoparticles and implications for safety in cell labelling. *Biomaterials*, 32, 195-205.
- SOHNI, A. & VERFAILLIE, C. M. 2013. Mesenchymal Stem Cells Migration Homing and Tracking. *Stem Cells International*.
- SONG, B., ESTRADA, K. D. & LYONS, K. M. 2009. Smad signaling in skeletal development and regeneration. *Cytokine and Growth Factor Reviews*, 20, 379-388.
- SORDI, V., MALOSIO, M. L., MARCHESI, F., MERCALLI, A., MELZI, R., GIORDANO, T., BELMONTE, N., FERRARI, G., LEONE, B. E., BERTUZZI, F., ZERBINI, G., ALLAVENA, P., BONIFACIO, E. & PIEMONTI, L. 2005. Bone marrow mesenchymal stem cells express a restricted set of functionally active chemokine receptors capable of promoting migration to pancreatic islets. *Blood*, 106, 419-27.
- SORRELL, J. M., BABER, M. A. & CAPLAN, A. I. 2009. Influence of adult mesenchymal stem cells on in vitro vascular formation. *Tissue Eng Part A*, 15, 1751-61.
- SOUZA, G. R., MOLINA, J. R., RAPHAEL, R. M., OZAWA, M. G., STARK, D. J., LEVIN, C. S., BRONK, L. F., ANANTA, J. S., MANDELIN, J., GEORGESCU, M.-M., BANKSON, J. A., GELOVANI, J. G., KILLIAN, T. C., ARAP, W. & PASQUALINI, R. 2010. Three-dimensional tissue culture based on magnetic cell levitation. *Nat Nano*, 5, 291-296.

- SPAETH, E., KLOPP, A., DEMBINSKI, J., ANDREEFF, M. & MARINI, F. 2008. Inflammation and tumor microenvironments: defining the migratory itinerary of mesenchymal stem cells. *Gene Ther*, 15, 730-8.
- SPAGGIARI, G. M., CAPOBIANCO, A., BECCHETTI, S., MINGARI, M. C. & MORETTA, L. 2006. Mesenchymal stem cell-natural killer cell interactions: evidence that activated NK cells are capable of killing MSCs, whereas MSCs can inhibit IL-2-induced NK-cell proliferation. *Blood*, 107, 1484-90.
- SPENCER, S. L., CAPPELL, S. D., TSAI, F.-C., OVERTON, K. W., WANG, C. L. & MEYER, T. 2013. The Proliferation-Quiescence Decision Is Controlled by a Bifurcation in CDK2 Activity at Mitotic Exit. *Cell*, 155, 369-383.
- STILES, C. D. 2003. Lost in space: misregulated positional cues create tripotent neural progenitors in cell culture. *Neuron*, 40, 447-9.
- SUN, C., LEE, J. S. H. & ZHANG, M. 2008. Magnetic nanoparticles in MR imaging and drug delivery. *Advanced Drug Delivery Reviews*, 60, 1252-1265.
- SUN, L., LI, G., CHEN, X., CHEN, Y., JIN, C., JI, L. & CHAO, H. 2015. Azo-Based Iridium(III) Complexes as Multicolor Phosphorescent Probes to Detect Hypoxia in 3D Multicellular Tumor Spheroids. *Scientific Reports*, 5, 14837.
- SUN, Y., CHEN, C. S. & FU, J. 2012. Forcing Stem Cells to Behave: A Biophysical Perspective of the Cellular Microenvironment. *Annual Review of Biophysics*, 41, 519-542.
- SUZUKI, Y., TADA-OIKAWA, S., ICHIHARA, G., YABATA, M., IZUOKA, K., SUZUKI, M., SAKAI, K. & ICHIHARA, S. 2014. Zinc oxide nanoparticles induce migration and adhesion of monocytes to endothelial cells and accelerate foam cell formation. *Toxicology and Applied Pharmacology*, 278, 16-25.
- SVACHOVA, H., POUR, L., SANA, J., KOVAROVA, L., RAJA, K. R. M. & HAJEK, R. 2011. Stem cell marker nestin is expressed in plasma cells of multiple myeloma patients. *Leukemia Research*, 35, 1008-1013.
- SWIFT, J., IVANOVSKA, I. L., BUXBOIM, A., HARADA, T., DINGAL, P. C. D. P., PINTER, J., PAJEROWSKI, J. D., SPINLER, K. R., SHIN, J.-W., TEWARI, M., REHFELDT, F., SPEICHER, D. W. & DISCHER, D. E. 2013. Nuclear Lamin-A Scales with Tissue Stiffness and Enhances Matrix-Directed Differentiation. *Science*, 341.
- TAI, P. W. L., WU, H., GORDON, J. A. R., WHITFIELD, T. W., BARUTCU, A. R., VAN WIJNEN, A. J., LIAN, J. B., STEIN, G. S. & STEIN, J. L. 2014. Epigenetic landscape during osteoblastogenesis defines a differentiation-dependent Runx2 promoter region. *Gene*, 550, 1-9.
- TAKAHASHI, K. & YAMANAKA, S. 2006. Induction of Pluripotent Stem Cells from Mouse Embryonic and Adult Fibroblast Cultures by Defined Factors. *Cell*, 126, 663-676.
- TAKEDA, K. & AKIRA, S. 2000. STAT family of transcription factors in cytokine-mediated biological responses. *Cytokine and Growth Factor Reviews*, 11, 199-207.
- TAUPIN, P. 2007. BrdU immunohistochemistry for studying adult neurogenesis: Paradigms, pitfalls, limitations, and validation. *Brain Research Reviews*, 53, 198-214.
- THIRUMALA, S., GOEBEL, W. S. & WOODS, E. J. 2013. Manufacturing and banking of mesenchymal stem cells. *Expert Opin Biol Ther*, 13, 673-91.
- TIBBITT, M. W. & ANSETH, K. S. 2009. Hydrogels as Extracellular Matrix Mimics for 3D Cell Culture. *Biotechnology and Bioengineering*, 103, 655-663.
- TILL, J. E. & MCCULLOCH, E. A. 1961. A direct measurement of the radiation sensitivity of normal mouse bone marrow cells. *Radiat Res*, 14, 213-22.

- TOLLE, L. B. & STANDIFORD, T. J. 2013. Danger-associated molecular patterns (DAMPs) in acute lung injury. *The Journal of Pathology*, 229, 145-156.
- TONDREAU, T., MEULEMAN, N., STAMATOPOULOS, B., DE BRUYN, C., DELFORGE, A., DEJENEFFE, M., MARTIAT, P., BRON, D. & LAGNEAUX, L. 2009. In vitro study of matrix metalloproteinase/tissue inhibitor of metalloproteinase production by mesenchymal stromal cells in response to inflammatory cytokines: the role of their migration in injured tissues. *Cytotherapy*, 11, 559-569.
- TURGUT, M. & LU, I. M. 2007. Mature teratoma associated with an interparietal encephalocele. *Journal of Neurosurgery: Pediatrics*, 106, 305-307.
- UCCELLI, A., MORETTA, L. & PISTOIA, V. 2008. Mesenchymal stem cells in health and disease. *Nat Rev Immunol*, 8, 726-736.
- UDAGAWA, N., HORWOOD, N. J., ELLIOTT, J., MACKAY, A., OWENS, J., OKAMURA, H., KURIMOTO, M., CHAMBERS, T. J., MARTIN, T. J. & GILLESPIE, M. T. 1997. Interleukin-18 (Interferon- $\gamma$ -inducing Factor) Is Produced by Osteoblasts and Acts Via Granulocyte/Macrophage Colony-stimulating Factor and Not Via Interferon- $\gamma$  to Inhibit Osteoclast Formation. *The Journal of Experimental Medicine*, 185, 1005-1012.
- VELNAR, T., BAILEY, T. & SMRKOLJ, V. 2009. The Wound Healing Process: An Overview of the Cellular and Molecular Mechanisms. *Journal of International Medical Research*, 37, 1528-1542.
- VON LUTTICHAU, I., NOTOHAMIPRODJO, M., WECHSELBERGER, A., PETERS, C., HENGER, A., SELIGER, C., DJAFARZADEH, R., HUSS, R. & NELSON, P. J. 2005. Human adult CD34- progenitor cells functionally express the chemokine receptors CCR1, CCR4, CCR7, CXCR5, and CCR10 but not CXCR4. *Stem Cells Dev*, 14, 329-36.
- WAGERS, A. J. 2012. The Stem Cell Niche in Regenerative Medicine. *Cell Stem Cell*, 10, 362-369.
- WALTERS, N. J. & GENTLEMAN, E. 2015. Evolving insights in cell-matrix interactions: Elucidating how non-soluble properties of the extracellular niche direct stem cell fate. *Acta Biomaterialia*, 11, 3-16.
- WAN, D. C., WONG, V. W. & LONGAKER, M. T. 2012. Craniofacial Reconstruction with Induced Pluripotent Stem Cells. *The Journal of craniofacial surgery*, 23, 623-626.
- WANG, C. Q., JACOB, B., NAH, G. S. S. & OSATO, M. 2010. Runx family genes, niche, and stem cell quiescence. *Blood Cells, Molecules, and Diseases*, 44, 275-286.
- WANG, W., ITAKA, K., OHBA, S., NISHIYAMA, N., CHUNG, U.-I., YAMASAKI, Y. & KATAOKA, K. 2009. 3D spheroid culture system on micropatterned substrates for improved differentiation efficiency of multipotent mesenchymal stem cells. *Biomaterials*, 30, 2705-2715.
- WATT, F. M. & HUCK, W. T. S. 2013. Role of the extracellular matrix in regulating stem cell fate. *Nat Rev Mol Cell Biol*, 14, 467-473.
- WEAVER, V. M., PETERSEN, O. W., WANG, F., LARABELL, C. A., BRIAND, P., DAMSKY, C. & BISSELL, M. J. 1997. Reversion of the Malignant Phenotype of Human Breast Cells in Three-Dimensional Culture and In Vivo by Integrin Blocking Antibodies. *The Journal of Cell Biology*, 137, 231-245.
- WEBER, J. M. & CALVI, L. M. 2010. Notch signaling and the bone marrow hematopoietic stem cell niche. *Bone*, 46, 281-285.
- WEN, J. H., VINCENT, L. G., FUHRMANN, A., CHOI, Y. S., HRIBAR, K. C., TAYLOR-WEINER, H., CHEN, S. & ENGLER, A. J. 2014. Interplay of matrix stiffness and protein tethering in stem cell differentiation. *Nat Mater*, 13, 979-987.

- WILLERT, K., BROWN, J. D., DANENBERG, E., DUNCAN, A. W., WEISSMAN, I. L., REYA, T., YATES, J. R. & NUSSE, R. 2003. Wnt proteins are lipid-modified and can act as stem cell growth factors. *Nature*, 423, 448-452.
- WILLIAMS, A. R., SUNCION, V. Y., MCCALL, F., GUERRA, D., MATHER, J., ZAMBRANO, J. P., HELDMAN, A. W. & HARE, J. M. 2013. Durable scar size reduction due to allogeneic mesenchymal stem cell therapy regulates whole-chamber remodeling. *J Am Heart Assoc*, 2, e000140.
- WILLIAMS, C. K., SEGARRA, M., SIERRA MDE, L., SAINSON, R. C., TOSATO, G. & HARRIS, A. L. 2008. Regulation of CXCR4 by the Notch ligand delta-like 4 in endothelial cells. *Cancer Res*, 68, 1889-95.
- WILSON, J. L. & MCDEVITT, T. C. 2013. Stem Cell Microencapsulation for Phenotypic Control, Bioprocessing, and Transplantation. *Biotechnology and Bioengineering*, 110, 667-682.
- WINER, J. P., JANMEY, P. A., MCCORMICK, M. E. & FUNAKI, M. 2009. Bone Marrow-Derived Human Mesenchymal Stem Cells Become Quiescent on Soft Substrates but Remain Responsive to Chemical or Mechanical Stimuli. *Tissue Engineering Part A*, 15, 147-154.
- WOLF, K., TE LINDERT, M., KRAUSE, M., ALEXANDER, S., TE RIET, J., WILLIS, A. L., HOFFMAN, R. M., FIGDOR, C. G., WEISS, S. J. & FRIEDL, P. 2013. Physical limits of cell migration: Control by ECM space and nuclear deformation and tuning by proteolysis and traction force. *The Journal of Cell Biology*, 201, 1069-1084.
- WU, Y., CHEN, L., SCOTT, P. G. & TREDGET, E. E. 2007. Mesenchymal Stem Cells Enhance Wound Healing Through Differentiation and Angiogenesis. *STEM CELLS*, 25, 2648-2659.
- XIE, J., WANG, W., SI, J.-W., MIAO, X.-Y., LI, J.-C., WANG, Y.-C., WANG, Z.-R., MA, J., ZHAO, X.-C., LI, Z., YI, H. & HAN, H. 2013. Notch signaling regulates CXCR4 expression and the migration of mesenchymal stem cells. *Cellular Immunology*, 281, 68-75.
- XU, C., MIRANDA-NIEVES, D., ANKRUM, J. A., MATTHIESEN, M. E., PHILLIPS, J. A., ROES, I., WOJTKIEWICZ, G. R., JUNEJA, V., KULTIMA, J. R., ZHAO, W., VEMULA, P. K., LIN, C. P., NAHRENDORF, M. & KARP, J. M. 2012. Tracking mesenchymal stem cells with iron oxide nanoparticle loaded poly(lactide-co-glycolide) microparticles. *Nano Lett*, 12, 4131-9.
- YAGI, H., SOTO-GUTIERREZ, A., KITAGAWA, Y. & YARMUSH, M. 2012. Mesenchymal Stem Cell Therapy: Immunomodulation and Homing Mechanisms. In: HAYAT, M. A. (ed.) *Stem Cells and Cancer Stem Cells, Volume 8*. Springer Netherlands.
- YAMAMOTO, M., KAWASHIMA, N., TAKASHINO, N., KOIZUMI, Y., TAKIMOTO, K., SUZUKI, N., SAITO, M. & SUDA, H. 2014. Three-dimensional spheroid culture promotes odonto/osteoblastic differentiation of dental pulp cells. *Archives of Oral Biology*, 59, 310-317.
- YANG, J., MCNAMARA, L. E., GADEGAARD, N., ALAKPA, E. V., BURGESS, K. V., MEEK, R. M. D. & DALBY, M. J. 2014. Nanotopographical Induction of Osteogenesis through Adhesion, Bone Morphogenic Protein Cosignaling, and Regulation of MicroRNAs. *ACS Nano*, 8, 9941-9953.
- YANG, L., WANG, L., GEIGER, H., CANCELAS, J. A., MO, J. & ZHENG, Y. 2007. Rho GTPase Cdc42 coordinates hematopoietic stem cell quiescence and niche interaction in the bone marrow. *Proceedings of the National Academy of Sciences of the United States of America*, 104, 5091-5096.

- YOSHITAKE, F., ITOH, S., NARITA, H., ISHIHARA, K. & EBISU, S. 2008. Interleukin-6 directly inhibits osteoclast differentiation by suppressing receptor activator of NF-kappaB signaling pathways. *J Biol Chem*, 283, 11535-40.
- YU, J. & THOMSON, J. A. 2014. Chapter 30 - Induced Pluripotent Stem Cells. In: VACANTI, R. L. L. (ed.) *Principles of Tissue Engineering (Fourth Edition)*. Boston: Academic Press.
- ZAPPIA, E., CASAZZA, S., PEDEMONTE, E., BENVENUTO, F., BONANNI, I., GERDONI, E., GIUNTI, D., CERAVOLO, A., CAZZANTI, F., FRASSONI, F., MANCARDI, G. & UCCELLI, A. 2005. Mesenchymal stem cells ameliorate experimental autoimmune encephalomyelitis inducing T-cell anergy. *Blood*, 106, 1755-61.
- ZHANG, D. & KILIAN, K. A. 2013. The effect of mesenchymal stem cell shape on the maintenance of multipotency. *Biomaterials*, 34, 3962-3969.
- ZHANG, H., LEE, M.-Y., HOGG, M. G., DORDICK, J. S. & SHARFSTEIN, S. T. 2010. Gene Delivery in Three-Dimensional Cell Cultures by Superparamagnetic Nanoparticles. *ACS Nano*, 4, 4733-4743.
- ZHANG, J. M. & AN, J. 2007. Cytokines, inflammation, and pain. *Int Anesthesiol Clin*, 45, 27-37.
- ZHANG, W., DE ALMEIDA, P. & WU, J. 2008. StemBook. *Teratoma formation: A tool for monitoring pluripotency in stem cell research*. Cambridge (MA): Harvard Stem Cell Institute.
- ZHANG, Y., LIN, Z., FOOLEN, J., SCHOEN, I., SANTORO, A., ZENOBI-WONG, M. & VOGEL, V. 2014. Disentangling the multifactorial contributions of fibronectin, collagen and cyclic strain on MMP expression and extracellular matrix remodeling by fibroblasts. *Matrix Biology*, 40, 62-72.
- ZHAO, H., FENG, J., SEIDEL, K., SHI, S., KLEIN, O., SHARPE, P. & CHAI, Y. 2014a. Secretion of shh by a neurovascular bundle niche supports mesenchymal stem cell homeostasis in the adult mouse incisor. *Cell Stem Cell*, 14, 160-73.
- ZHAO, Q., REN, H. & HAN, Z. 2015. Mesenchymal stem cells: Immunomodulatory capability and clinical potential in immune diseases. *Journal of Cellular Immunotherapy*.
- ZHAO, T., ZHANG, Z.-N., RONG, Z. & XU, Y. 2011. Immunogenicity of induced pluripotent stem cells. *Nature*, 474, 212-215.
- ZHAO, W., LI, X., LIU, X., ZHANG, N. & WEN, X. 2014b. Effects of substrate stiffness on adipogenic and osteogenic differentiation of human mesenchymal stem cells. *Materials Science and Engineering: C*, 40, 316-323.